



Universidad  
Carlos III de Madrid

# Human Inspired Humanoid Robot Control Architecture

Santiago Martínez de la Casa Díaz

PhD Thesis

Department of Systems Engineering and Automation  
Leganés, July 2012



# **Human Inspired Humanoid Robot Architecture**

**Candidate**  
**Santiago Martínez de la Casa Díaz**

**Advisers**  
**Carlos Balaguer Bernaldo de Quirós**  
**Alberto Jardón Huete**

## **Review Committee**

**Presidente (Chair): Miguel Ángel Salichs Sanchez-Caballero**

**Vocal (Member): Karsten Berns**

**Vocal (Member): Manuel Ángel Armada Rodríguez**

**Vocal (Member): Pedro José Sanz Valero**

**Secretario (Secretary): Ramón Barber Castaño**

**Grade:**

Leganés, July 13rd, 2012



# ABSTRACT

This PhD Thesis tries to present a different point of view when talking about the development of control architectures for humanoid robots. Specifically, this Thesis is focused on studying the human postural control system as well as on the use of this knowledge to develop a novel architecture for postural control in humanoid robots. The research carried on in this thesis shows that there are two types of components for postural control: a reactive one, and other predictive or anticipatory. This work has focused on the development of the second component through the implementation of a predictive system complementing the reactive one.

The anticipative control system has been analysed in the human case and it has been extrapolated to the architecture for controlling the humanoid robot TEO. In this way, its different components have been developed based on how humans work without forgetting the tasks it has been designed for. This control system is based on the composition of sensorial perceptions, the evaluation of stimulus through the use of the psychophysics theory of the surprise, and the creation of events that can be used for activating some reaction strategies (synergies)

The control system developed in this Thesis, as well as the human being does, processes information coming from different sensorial sources. It also composes the named perceptions, which depend on the type of task the postural control acts over. The value of those perceptions is obtained using bio-inspired evaluation techniques of sensorial inference.

Once the sensorial input has been obtained, it is necessary to process it in order to foresee possible disturbances that may provoke an incorrect performance of a task. The system developed in this Thesis evaluates the sensorial information, previously transformed into perceptions, through the use of the “Surprise Theory”, and it generates some events called “surprises” used for predicting the evolution of a task.

Finally, the anticipative system for postural control can compose, if necessary, the proper reactions through the use of predefined movement patterns called synergies. Those reactions can complement or substitute completely the normal performance of a task.

The performance of the anticipative system for postural control as well as the performance of each one of its components have been tested through simulations and the application of the results in the humanoid robot TEO from the RoboticsLab research group in the Systems Engineering and Automation Department from the Carlos III University of Madrid.



# RESUMEN

Esta Tesis Doctoral pretende aportar un punto de vista diferente en el desarrollo de arquitecturas de control para robots humanoides. En concreto, esta Tesis se centra en el estudio del sistema de control postural humano y en la aplicación de este conocimiento en el desarrollo de una nueva arquitectura de control postural para robots humanoides. El estudio realizado en esta Tesis pone de manifiesto la existencia de una componente de control postural reactiva y otra predictiva o anticipativa. Este trabajo se ha centrado en el desarrollo de la segunda componente mediante la implementación de un sistema predictivo que complementa al sistema reactivo.

El sistema de control anticipativo ha sido estudiado en el caso humano y extrapolado para la arquitectura de control del robot humanoide TEO. De este modo, sus diferentes componentes han sido desarrollados inspirándose en el funcionamiento humano y considerando las tareas para las que dicho robot ha sido concebido. Dicho sistema está basado en la composición de percepciones sensoriales, la evaluación de los estímulos mediante el uso de la teoría psicofísica de la sorpresa y la generación de eventos que sirvan para activar estrategias de reacción (sinergias).

El sistema de control desarrollado en esta Tesis, al igual que el ser humano, procesa información de múltiples fuentes sensoriales y compone las denominadas percepciones, que dependen del tipo de tarea sobre la que actúa el control postural. El valor de estas percepciones es obtenido utilizando técnicas de evaluación bio-inspiradas de inferencia sensorial.

Una vez la entrada sensorial ha sido obtenida, es necesario procesarla para prever posibles perturbaciones que puedan ocasionar una incorrecta realización de una tarea. El sistema desarrollado en esta Tesis evalúa la información sensorial, previamente transformada en percepciones, mediante la ‘Teoría de la Sorpresa’ y genera eventos llamados ‘sorpresa’ que sirven para predecir la evolución de una tarea.

Por último, el sistema anticipativo de control postural puede componer, si fuese necesario, las reacciones adecuadas mediante el uso de patrones de movimientos predefinidos llamados sinergias. Dichas reacciones pueden complementar o sustituir por completo la ejecución normal de una tarea.

El funcionamiento del sistema anticipativo de control postural y de cada uno de sus componentes ha sido probado tanto por medio de simulaciones como por su aplicación en el robot humanoide TEO del grupo de investigación RoboticsLab en el Departamento de Ingeniería de Sistemas y Automática de la Universidad Carlos III de Madrid.



## **AGRADECIMIENTOS**

Largo y difícil ha sido el camino recorrido hasta llegar a este punto de mi vida y de mi carrera. Y todo esto no hubiera sido posible sin toda esa gente que siempre me ha apoyado tanto en los momentos buenos como en los malos.

En primer lugar, quiero expresar mi más profundo agradecimiento a mi familia, que me lo ha dado todo. Agradecer a mis padres, Adrián y María, todo su esfuerzo para que yo pudiese llegar hasta donde he llegado; mis hermanos, Adrián y Mª Asunción que siempre me han ayudado; mis cuñados Caty y Marce; y todos mis sobrinos: Sergio, Aitor y David.

A Patricia que me ha echado tantas manos como ha podido para darle forma a esta Tesis y, por supuesto, a Josu por su simpatía y el apoyo que me ha transmitido. Muchísimas gracias!!!

Ángela, tu que me has animado, que has soportado mi buen y mi mal humor, que me has elevado cuando más bajo estaba y me has sostenido para no caer en los malos momentos, que has reído y llorado conmigo, gracias de todo corazón.

Además de la familia también hay otras personas que considero como mi familia. Mis amigos Oscar, Dany, Rodo y Helen, Félix y Gema, Manolo, Tommy y Paloma, Jorge y Vero siempre han estado ahí cuando los he necesitado. También, muy especialmente, quiero agradecer su apoyo y ayuda a Sonia, con la que siempre me he reído desde que nos conocimos allá por cuarto de Ingeniería Industrial. Y gracias a Edu, que no me olvido de ti!

Por último, quiero agradecer a mis directores de Tesis, Carlos Balaguer y Alberto Jardón, sus consejos y apoyo para lograr llevar a cabo esta Tesis.

A todos, muchas gracias.



# CONTENTS

ABSTRACT .....	i
RESUMEN .....	iii
AGRADECIMIENTOS .....	v
CONTENTS .....	vii
LIST OF TABLES .....	xi
LIST OF FIGURES .....	xiii
LIST OF ABBREVIATIONS .....	17
CHAPTER 1 .....	19
1.1 The Motivation and Origin of the Thesis .....	19
1.2 Objectives of the Thesis .....	21
1.3 Contributions of the Thesis .....	22
1.4 Guide to the Thesis .....	23
CHAPTER 2 .....	25
2.1 Introduction to Human Posture Control .....	25
2.1.1 Manipulation Problem .....	26
2.1.2 Locomotion Problem .....	27
2.2 Physiology of the Postural Control System .....	28
2.2.1 Sensorial System: Receptor .....	29
2.2.1.1 Exoceptive Sensation Systems .....	29
2.2.1.2 Proprioceptive Sensation Systems .....	31
2.2.2 Integration centres: Processor .....	33
2.2.2.1 Spinal cord .....	33
2.2.2.2 Cerebral trunk .....	33
2.2.2.3 Cortical .....	34
2.2.2.4 Associated areas: Cerebellum, Basal ganglia .....	34
2.2.3 Action System: Effector .....	35
2.2.4 Communication channels .....	36
2.2.4.1 Afferent system .....	36
2.2.4.2 Efferent system .....	36
2.3 Foundations of Postural Control .....	37
2.3.1 Levels of Reaction of the Postural Control System .....	38
2.3.2 Psychophysics and Postural Control .....	39
2.3.3 Sensorimotor Integration in Postural Control .....	42
2.3.3.1 Motor Strategies to Control Balance .....	42

2.3.4 Basic Postural Control System Schemes .....	44
2.4 The Human Postural Control System .....	46
CHAPTER 3.....	49
3.1 Introduction to Humanoid Posture Control.....	49
3.2 Performing Humanoid Tasks .....	52
3.3 Human Inspired Postural Control Architecture .....	53
3.4 Perceptual Evaluation.....	56
3.4.1 Sensation Detection.....	57
3.4.2 Perception Evaluation.....	58
3.4.2.1 Proprioceptive Perception Evaluation .....	59
3.4.2.2 Exoceptive Perception Evaluation .....	60
3.5 Surprise Generation.....	62
3.5.1 Passive Expectation Failure .....	64
3.5.2 Active Expectation Failure .....	65
3.6 Behaviour Decision System.....	66
CHAPTER 4.....	70
4.1 Basic Principles of Humanoid Postural Control .....	70
4.2 Human Dynamics Foundations.....	71
4.2.1 Human Dynamics Simplified Models .....	71
4.2.1.1 The Simple Inverted Pendulum.....	72
4.2.1.2 The Double Inverted Pendulum .....	73
4.2.2 Reference Points .....	74
4.2.2.1 The Centre of Mass (CoM) .....	74
4.2.2.2 The Zero Moment Point (ZMP) .....	75
4.3 Human Inspired Soft Computing.....	77
4.3.1 Evolutionary Computation.....	78
4.3.2 Bayesian Networks .....	79
4.3.3 Neural Networks .....	80
4.3.4 Fuzzy Systems .....	82
4.3.5 Hybrid Systems.....	83
4.3.5.1 Fuzzy-Neuro Systems.....	84
4.3.5.2 Neuro-Fuzzy Systems.....	85
CHAPTER 5.....	88
5.1 Physiology of Humanoid Control System .....	88
5.2 Sensorial System.....	89
5.2.1 Exoceptive Perception .....	89

5.2.1.1 Inertial System .....	94
5.2.1.2 Force/Torque Sensor System.....	97
5.2.1.3 Visual System .....	98
5.2.2 Proprioceptive Perception.....	99
5.2.2.1 Joint/Muscles .....	101
5.2.2.2 Cutaneous .....	102
5.3 Integration Centres .....	102
5.3.1 CPU's.....	104
5.3.2 ISCM8005 Intelligent Drives .....	105
5.4 Action System.....	105
5.4.1 Motor and Transmission .....	107
5.5 Communication Channels.....	108
5.5.1 CANBus .....	109
5.5.2 Ethernet .....	110
5.5.3 USB serial bus .....	110
CHAPTER 6.....	112
6.1 Low Level Postural Control Architecture.....	112
6.2 Sensorial Evaluation.....	115
6.2.1 Proprioceptive perception .....	115
6.2.1.1 Lower body proprioception modelling .....	118
6.2.1.2 Upper body proprioception modelling .....	121
6.2.2 Exoceptive perception .....	122
6.2.2.1 Force/Torque system.....	124
6.2.2.2 Inertial system.....	128
6.2.2.3 Vision system.....	131
6.3 Surprise Generation.....	132
6.3.1 Passive Expectation Failure .....	133
6.3.1.1 Manipulation Tasks.....	133
6.3.1.2 Locomotion Tasks.....	134
6.3.2 Active Expectation Failure .....	137
6.3.2.1 Manipulation Tasks.....	137
6.3.2.2 Locomotion Tasks.....	138
6.4 Behaviour Decision System.....	143
6.4.1 Manipulation Tasks.....	143
6.4.2 Locomotion Tasks.....	145

CHAPTER 7.....	149
7.1 Task Frame Overview.....	149
7.1.1 Locomotion Framework .....	150
7.1.2 Manipulation Framework .....	151
7.2 The Human Inspired Postural Control System .....	153
7.2.1 Neuro-Fuzzy Modules Development Procedure .....	154
7.2.2 Perceptions Development Results.....	158
7.2.2.1 Proprioceptive Perception Results.....	158
7.2.2.2 Exoceptive Perception Results .....	165
7.2.3 Surprise Development .....	177
7.2.3.1 Passive Surprise .....	177
7.2.3.2 Active Surprise.....	180
7.2.4 Decision System Development.....	186
7.2.4.1 Manipulation Tasks.....	187
7.2.4.2 Locomotion Tasks.....	190
CHAPTER 8.....	195
8.1 Conclusions .....	195
8.2 Future Works .....	197
REFERENCES .....	201

## LIST OF TABLES

Table 1 Properties of the three motor systems in balance movement control.....	38
Table 2 Human vs. humanoid exoceptive perception.....	55
Table 3 Human vs. humanoid proprioceptive perception .....	55
Table 4 Rate of turn and angular acceleration thresholds from vestibular system .....	90
Table 5 Linear acceleration thresholds of the vestibular system .....	91
Table 6 IMU sensing thresholds .....	96
Table 7 JR3 Force/Torque sensors characteristics .....	97
Table 8 Comparison between human and artificial vision systems .....	99
Table 9 Human skin proprioceptors.....	100
Table 10 Human articular proprioceptors .....	100
Table 11 Comparison between human brain and CPU processing capacities.....	104
Table 12 TEO robot joints features.....	107
Table 13 Comparison of the reflex arc latency .....	110
Table 14 Sub-problem division .....	117
Table 15 Lower body joint angle limits.....	119
Table 16 Lower body datasets.....	120
Table 17 Upper body joint angle limits.....	121
Table 18 Upper body datasets.....	122
Table 19 Robot support phase obtained from force evaluation .....	125
Table 20 ZMP F/T exoception input/output datasets .....	127
Table 21 Wrists F/T exoception input/output datasets.....	128
Table 22 IMU rotational tendency evaluation input/output datasets .....	129
Table 23 IMU linear movement tendency evaluation input/output datasets .....	130
Table 24 Rotational tendency .....	136
Table 25 Linear tendency .....	137
Table 26 Locomotive reaction decision chart .....	146
Table 27 Datasets for right hand 'X' coordinate neuro-fuzzy network development...	155
Table 28 Rule parameters for combination.....	156
Table 29 Example of right hand parameters genfis1 .....	156
Table 30 Training parameters of right hand X coordinate FIS.....	157
Table 31 Example training error evolution .....	157
Table 32 Initial and final commanded configurations of the right arm .....	159
Table 33 Initial and final measured configurations of the right arm .....	160
Table 34 Final evaluated right hand location.....	161
Table 35 Initial and final commanded configurations of the flying leg .....	163
Table 36 Initial and final measured configurations of the right leg.....	163
Table 37 Final computed vs. inferred right leg location .....	164
Table 38 Exoceptive outcomes summary.....	166
Table 39 Object locations to Kinect reference frame.....	167
Table 40 Results from evaluation of the hand-object relative position .....	168
Table 41 Wrist F/T sensors measurements.....	169
Table 42 Force FIS evaluation results .....	170
Table 43 Torque FIS evaluation results.....	170
Table 44 Linear motion tendency test datasets .....	171
Table 45 Linear tendency results comparison (values in m/s <sup>2</sup> ) .....	172
Table 46 Rotational motion tendency test datasets.....	172

Table 47 Rotational tendency results comparison.....	173
Table 48 Evaluated feet angles .....	174
Table 49 Data comparison for $X_{ZMP}$ .....	176
Table 50 Data comparison for $Y_{ZMP}$ .....	176
Table 51 Manipulation passive expectation surprise levels.....	178
Table 52 Locomotion rotational passive expectation surprise levels.....	179
Table 53 Locomotion linear passive expectation surprise levels.....	180
Table 54 Manipulation active surprise levels.....	182
Table 55 Manipulation active surprise evaluation.....	183
Table 56 Manipulation active surprise levels.....	185
Table 57 Locomotion active surprise evaluation.....	186
Table 58 Manipulative decision output chart .....	188
Table 59 Locomotive decision output chart (X coordinate).....	190
Table 60 Locomotive decision output chart (Y coordinate).....	191

# LIST OF FIGURES

Figure 1 Robot TEO.....	20
Figure 2 Basic human postural control system components .....	25
Figure 3 Manipulation task postural control: (a) Normal behaviour. (b) Task deviation corrected by postural control system .....	26
Figure 4 Locomotion task postural control.....	28
Figure 5 Motor neural control hierarchical structure .....	29
Figure 6 Semicircular Canals (adapted from Encyclopaedia Britannica, Inc.) .....	30
Figure 7 The maculae (adapted from Encyclopaedia Britannica, Inc.) .....	30
Figure 8 Articular sensor receptors.....	32
Figure 9 Muscle spindles .....	32
Figure 10 Central Nervous System (Adapted from Kopp Illustration, Inc.) .....	33
Figure 11 Motor Cortex Areas .....	34
Figure 12 Cerebellum and Basal Ganglia functions .....	35
Figure 13 Multisensory integration systems(Ting & McKay, 2007).....	36
Figure 14 Feed-forward and feedback postural adjustment from (Kejonen, 2002) .....	37
Figure 15 Postural control (PC) is influenced by factors related to the individual, the task, and the environment adapted from (Shumway-Cook et al., 1995).....	42
Figure 16 Strategy trigger modification influenced by environment conditions.....	43
Figure 17 Balance strategies .....	44
Figure 18 Feedback control scheme (Kandel et al., 2000) .....	45
Figure 19 Feedforward control scheme (Kandel et al., 2000).....	45
Figure 20 Human postural control architecture adapted from (Massion, 1998).....	46
Figure 21 Human postural control scheme.....	47
Figure 22 Humanoid task modules .....	53
Figure 23 RH-1 Control architecture.....	53
Figure 24 TEO Control architecture.....	54
Figure 25 Perception evaluation .....	57
Figure 26 Sensations pathway .....	57
Figure 27 Sensation Thresholds.....	58
Figure 28 Components of the proprioceptive perception.....	59
Figure 29 Body limbs location evaluation .....	60
Figure 30 Components of the exoceptive perception .....	60
Figure 31 Inertial measurements evaluation.....	61
Figure 32 Wrists forces and torque measurements evaluation .....	61
Figure 33 Ankles forces and torque measurements evaluation.....	62
Figure 34 Objects movement evaluation .....	62
Figure 35 Normal 'throwing a ball and catch it' task .....	63
Figure 36 Deviated 'throwing a ball and catch it' task.....	64
Figure 37 Surprise generation modules.....	64
Figure 38 Passive expectation failure.....	65
Figure 39 Active expectation failure.....	66
Figure 40 Behaviour decision module .....	67
Figure 41 2D simple inverted pendulum .....	72
Figure 42 2D double inverted pendulum.....	73
Figure 43 Reference Points .....	74

Figure 44 Model for ZMP computation using F/T sensor measurements .....	76
Figure 45 Bayesian Network example .....	79
Figure 46 Multilayer Neural Network .....	81
Figure 47 Fuzzy vs. non-fuzzy membership functions.....	82
Figure 48 Mamdani fuzzy inference system .....	83
Figure 49 Sugeno fuzzy inference system.....	83
Figure 50 Model of fuzzy-neural system (adapted from (Fuller, 1995)) .....	85
Figure 51 Fuzzy driven neural network system (adapted from (Fuller, 1995)) .....	85
Figure 52 Anfis Model Structure (adapted from (Jang, 1993)) .....	86
Figure 53 Semicircular canals detection scheme .....	90
Figure 54 Otolith organ detection scheme.....	91
Figure 55 Human sensor fusión scheme (from (Mergner & Glasauer, 1999)).....	91
Figure 56 Human reflex arc .....	103
Figure 57 TEO robot reflex arc .....	105
Figure 58 Human joints lever: (a) Class I, (b) Class II and (c) Class III .....	106
Figure 59 Lower limbs joint (1) and upper limbs joints (2) design .....	107
Figure 60 Human reaction time .....	108
Figure 61 TEO robot communication architecture .....	109
Figure 62 CAN Message Frame .....	110
Figure 63 Feedforward module low level architecture .....	113
Figure 64 TEO robot kinematic chain .....	116
Figure 65 Feet location ( $X_F$ , $Y_F$ , $Z_F$ ) and waist location ( $X_w$ , $Y_w$ , $Z_w$ ) .....	118
Figure 66 Roll (a) and pitch (b) Z axis possible deviations .....	119
Figure 67 Lower body proprioceptive perception evaluation scheme.....	120
Figure 68 Torso location ( $X_T$ , $Y_T$ , $Z_T$ ) and hand location ( $X_H$ , $Y_H$ , $Z_H$ ).....	121
Figure 69 Upper body proprioceptive perception evaluation scheme.....	122
Figure 70 Force frames (a) and torque frames (b) of the F/T sensors .....	124
Figure 71 Ankle pitch ( $\alpha$ ) and roll ( $\beta$ ) .....	125
Figure 72 Virtual Horizontal Plane: projected support convex hull and ZMP.....	126
Figure 73 ZMP F/T sensors exoception scheme .....	126
Figure 74 Wrist F/T sensors .....	127
Figure 75 Wrists F/T sensors exoception scheme.....	127
Figure 76 Inertial exoceptive output.....	128
Figure 77 Robot body rotational tendency.....	129
Figure 78 Robot body linear movement tendency .....	130
Figure 79 IMU outputs for ZMP prediction.....	131
Figure 80 Model for visual perception.....	131
Figure 81 Objects movement evaluation .....	132
Figure 82 Object location reference frame transformation .....	133
Figure 83 Manipulation passive expectation failure.....	134
Figure 84 Rotational surprise evaluations .....	135
Figure 85 Linear surprise evaluations.....	136
Figure 86 Manipulation active expectation failure inference system .....	137
Figure 87 Object landing location prediction module.....	138
Figure 88 Distance from hand to grasping location .....	138
Figure 89 Manipulation active surprise inference module .....	138
Figure 90 Locomotion active expectation failure inference system .....	139
Figure 91 ZMP prediction module.....	139

Figure 92 Reaction Boundaries .....	140
Figure 93 Leak Point evaluation .....	141
Figure 94 Double support phase .....	141
Figure 95 Single support phase.....	142
Figure 96 LP to boundaries distance evaluation.....	142
Figure 97 Active surprise inference module .....	142
Figure 98 Manipulation behaviour decision process .....	144
Figure 99 Manipulation synergies.....	145
Figure 100 Locomotion behaviour decision process .....	146
Figure 101 Locomotion synergies.....	147
Figure 102 Locomotion perturbation sources .....	151
Figure 103 Manipulation task phases .....	152
Figure 104 Development of the postural control architecture .....	153
Figure 105 FIS development workflow .....	154
Figure 106 Proprioceptive system structure .....	159
Figure 107 Manipulation task sequence .....	160
Figure 108 Right hand location inference surfaces .....	161
Figure 109 Right hand position kinematic evaluation error.....	161
Figure 110 Right hand position fuzzy inference error .....	162
Figure 111 Locomotion task sequence.....	163
Figure 112 Right foot location inference surfaces .....	164
Figure 113 Right foot position kinematic evaluation error.....	165
Figure 114 Right foot position fuzzy inference error .....	165
Figure 115 Waist-Kinect-object system (a) and waist-hand-object system (b).....	166
Figure 116 Object location and movement tracking .....	167
Figure 117 Hand-object distance inference surfaces .....	168
Figure 118 Wrists Force FIS inference surfaces .....	168
Figure 119 Wrists Torque FIS inference surfaces .....	169
Figure 120 F/T Sensor validation system .....	169
Figure 121 Evaluation surfaces from linear motion tendency FIS .....	171
Figure 122 Evaluation surfaces from rotational motion tendency FIS .....	173
Figure 123 Foot angles $F_{X-Y}$ vs. $F_Z$ inference surface .....	174
Figure 124 Simple inverted pendulum mock-up (a), simple inverted pendulum virtual model (b) and TEO lower-body (c) .....	175
Figure 125 $T_Y$ vs. $F_Z$ inference surface for $X_{ZMP}$ (a) and $T_X$ vs. $F_Z$ inference surface for $Y_{ZMP}$ (b) .....	175
Figure 126 Pendulum movement task: (a) Initial position, (b) left movement and (c) final position .....	176
Figure 127 $X_{ZMP}$ (a) and $Y_{ZMP}$ (b) evolution during the pendulum movement .....	177
Figure 128 Horizontal plane (a) and vertical plane (b) hand-object components .....	178
Figure 129 Manipulation passive expectation failure.....	178
Figure 130 Locomotion rotational tendency passive expectation failure .....	179
Figure 131 Locomotion linear tendency passive expectation failure .....	179
Figure 132 Object location prediction scheme.....	180
Figure 133 Manipulation active surprise inference system input dataset .....	181
Figure 134 Manipulation active expectation failure.....	181
Figure 135 Exponential law for straight line synergy .....	181
Figure 136 Manipulation active surprise inference surface .....	182

Figure 137 Locomotion active surprise inference system ZMP input dataset .....	183
Figure 138 Locomotion active surprise inference system LP input dataset.....	184
Figure 139 Locomotion active surprise inference system scheme .....	184
Figure 140 BoS on VHP for double support phase.....	185
Figure 141 Linear law for locomotion synergies .....	185
Figure 142 Locomotion surprise inference surfaces.....	186
Figure 143 I/O Scheme for manipulative reaction generation .....	188
Figure 144 Inference surface for manipulative decision parameters $KM_{RX}$ and $KM_{RY}$	189
Figure 145 Trials trajectory and decision parameter (X coordinate component) .....	189
Figure 146 I/O Scheme for locomotive reaction generation .....	190
Figure 147 Inference surface for locomotive decision parameters $KL_{RX}$ .....	191
Figure 148 Step surprise levels (left) and decision parameter (right) .....	192

## **LIST OF ABBREVIATIONS**

ANFIS – Adaptive Neuro Fuzzy Inference Systems

BN – Bayesian networks

CNS – Central Nervous System

CoM – Centre of Mass

CPU – Central Process Unit

CANBus – Controller Area Network bus

DoF – Degree of Freedom

EC – Evolutionary computation

EP – Evolutionary Programming

ER – Evolutionary Robotics

ES – Evolution Strategies

F/T – Force/Torque

FS – Fuzzy Systems

FIS – Fuzzy Inference Systems

FZMP – Fictitious Zero Moment Point

GA – Genetic Algorithms

Gbps – Gigabit per second

GCoM – Ground projection of the Centre of Mass

IMU – Inertial Measurement Unit

LL – Leak Lane

LP – Leak Point

NN – Neural networks

SDT – Signal Detection Theory

TEO – Task Environment Operator

VHP – Virtual Horizontal Plane

ZMP – Zero Moment Point



# CHAPTER 1

## Introduction

### 1.1 The Motivation and Origin of the Thesis

From the first Industrial Revolution, the automation of machines has dramatically grown up. One of the Automation branch has been the development of humanlike machines to replicate the human behaviour. The desire or necessity of performing tasks, in the same way that humans do, has motivated the research in mechatronic systems adapted to daily live environments. These kinds of machine are the humanoid robots. The word ‘robot’ was introduced by Karel Čapek (1890-1938) into his play R.U.R. (Rossum's Universal Robots) (Čapek, 1923). Several years after, the term ‘robotics’ was first used in Runaround, a short story published in 1942 (Asimov, 1942), by Isaac Asimov (1920-1992). In both cases, the robot was thought like an anthropomorphic machine. Nevertheless, the design of the first robotic devices is very different than the exposed by Čapek and Asimov.

The first successful robot was produced by Unimation in 1961. The UNIMATE was installed in General Motors factories for die casting handling and spot welding (Rosheim, 1994). The industrial robot was merely an object manipulator or tool positioner with 6DoF. Exploiting this concept, the industrial robot has had a great success improving industrial processes.

But this kind of robots was far from having the anthropomorphic design of the robots dreamt by Čapek and Asimov. The question is why researchers chase the dream of designing humanoid robots. The answer can be widely discussed but two main reasons support it, from machine design point of view.

First of all, the human body is one of the most complex ‘machines’ of the nature and replicate this complexity is a big challenge and only a few institutions are dedicated to the creation of humanoid robots. Humanoid robots program of the RoboticsLab started on 2001 by developing the 7DoF biped robot Leroy. Since 2002 several research projects has been carried out to develop the RH full size robot series. The main achievements of the program were the development of RH-0 and RH-1 platforms, from mechatronics point of view. In this sense, the RoboticsLab team has developed a new prototype, called TEO (Task Environment Operator), to implement the research advances regarding locomotion, perception and behaviour control during task execution.

The second reason to investigate in humanoid robotics is related with our living environment. Things in our world are designed to be used by humans, so the ‘universal robots’ would be those with anthropomorphic shape that can adapt itself to the real world and not in the opposite way. It means that the robot must have some kind of ‘intelligent behaviour’ to perform tasks in real-world domains where uncertainty cannot be effectively modelled. In this way, robots must have a means of reacting to an infinite number of possibilities. To know enough about an environment is only possible in restricted domains such as a chess game or virtual worlds where there are a limited number of possible states. For more complicated domains it is necessary to find an appropriate balance between reactive and deliberative control. Therefore, the difficulty of a full size humanoid robot design has motivated that research efforts had been divided in different fields. They can be sorted as follows: bipedal locomotion, dexterous manipulation, perception, learning and adaptive behaviour and human-robot interaction (Behnke, 2008). Taking in account this classification, the RoboticsLab research group has focus its activities to develop stable biped locomotion, exoceptive and proprioceptive perception and behaviour control architectures (Kaynov, 2008; Arbulú, 2009).

The work performed during these first years has established the foundations for humanoid robotics research in the RoboticsLab. But new problems must be addressed. Lessons learned from the previous RH platforms have been applied in the new prototype TEO (Figure 1).

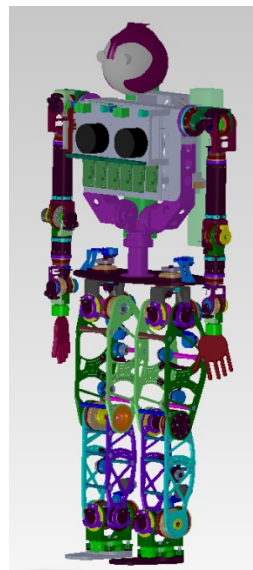


Figure 1 Robot TEO

Huge mechanical and electronic improvements have been achieved, incrementing operability and computation speed. The RH’s old electronics limited the software architecture and performance of the developed modules. Offline gait generation was achieved and applied to the robotic platforms and basic stability, based on simple inverted pendulum model, was implemented. New robotic platform TEO will enable the development of new software modules with a notorious modification: their ‘online’ approach. In this way, new visions of the robot behaviour can be adopted. Postural and high level tasks analysis will be developed and tested in robot TEO.

The origin and motivations of this Thesis are due to the new direction taken by the RoboticsLab in humanoid robotics research. This Thesis is focused on the development of new algorithms for postural analysis. Online task performance will be improved by means of the implementation of a new preview controller, using sensor information and comparing it with stored models.

## 1.2 Objectives of the Thesis

This PhD Thesis is focused on the improvement of the system control architecture of the humanoid robot and attempts to discuss problems and issues that should be considered when the control system of a humanoid robot is designed.

The central objectives are:

- Design of novel human inspired control architecture for effective and stable postural control. This Thesis is mainly focused on the predictive feedforward loop presented in the human control architecture case. The control architecture should predict the humanoid robot behaviour and anticipate the next execution step in case of postural correction needed.
- The operation of the control system is task oriented. The development is focused on the study of general manipulation and locomotion tasks. Other kinds of task are combinations of parameterized units of the basic tasks. The new task instance depends of the scenario conditions, goal of the task, etc. Because of this high number of possibilities, this Thesis has been oriented to the study of the most generic type of tasks.
- The modules composing the control architecture are inspired in the corresponding human systems and their operation:
  - Sensation systems
  - Human inspired perception composition
  - Evaluation and construction of reactions based on surprise generation concepts
  - Execution of reaction based on reflex and automatic motor responses based on synergies

To accomplish these three main objectives it is necessary to meet with the following intermediate goals:

- Development of human inspired sensorial perceptions. The information from sensorial sources will be processed to create perceptions. Following the principle of human inspiration, it will be performed applying neuro-fuzzy perception evaluators which will output useful parameter to take decisions, not for control. Two kinds of perception will be created: exoceptive and proprioceptive. Meanwhile sensations are a set of raw information independent of the task being performed, the output parameters from both perceptions are task related.

- Reactions driven by surprise. The parameters forming the proprioceptive and exoceptive perceptions are the basis for predictive postural control. This prediction will be driven by the generation of different levels of ‘surprise’. The output from the exoceptive and the proprioceptive perceptions is then evaluated depending of the task. The result from this evaluation will be a surprise level or event. It will indicate whether a reaction should be triggered, what reaction should be activated and in which manner.
- Online posture adaptation. Attending to the evaluation of perceptions and the ‘surprise events’ generated, the trajectories of the body joints should be modified to compensate the disturbances. The normal execution of the tasks could be interrupted or modified to keep postural control. This motor modification will be implemented mainly by means of the execution of predefined adjustable movement patterns called synergies.
- Experimentation of the human inspired control architecture. This objective will be firstly accomplished by means of simulations of the components and systems developed. After the simulation process, the operation of the modules developed will be tested in available mechanical systems, such as the robotic humanoid platform TEO.

## 1.3 Contributions of the Thesis

This thesis tries to propose a new human inspired and task oriented approach to the design of a control system for humanoid robots. All aspects of the design process as well as the detailed architecture and control algorithms were developed and implemented.

The main contributions of this thesis focus on the following:

- Development of novel human inspired perception systems. New methods of processing sensorial data needed for postural control has been proposed. The study of the evaluation of the sensorial data by humans is the inspiration to perform an alternative method to compose perceptions. The application the neuro-fuzzy technique enhances learning and processing of sensorial data without using models of the perceptual system. The output of the complex perceptual evaluation performed by the fuzzy system is then applied in decision making for improving postural control.
- Development of new decision making system for anticipating motor responses of the robot. The complex behaviour of the human Central Nervous System related with postural control has been explored. The principles extracted from this study have been extrapolated to the humanoid robot system. The concepts of reflex and automatic reactions have been implemented to speed postural control up. The system provides a decision based on perceptions and experience from previous tasks. As well, it is able to gain the robot control, stop the current task performance and trigger a reaction if it is needed.

- Development of the task oriented postural feedforward system for humanoid robots. The preview feedforward system developed allows anticipating reactions improving postural control and balance. This loop is added to the existing feedback balance control loop. Its main contribution is the evaluation of future consequences of the task performance. In this way, it could introduce corrective parameters into the pending execution steps of the task or it could take the entire control of this execution and start a new postural task.

Finally, it should be mentioned that the proposed Thesis is a complex study that considers the postural control system of humanoid robots as a whole. It stresses the human inspiration and the tasks orientation of the robot, covering all levels of postural control.

## 1.4 Guide to the Thesis

This PhD Thesis has been arranged into eight chapters, including this introductory chapter, as follows:

- Chapter 2: It describes the foundations of human postural control system, explaining briefly all higher levels involved and their operation. The conclusions extracted from this review are the high level principles applied in the humanoid postural control system exposed in this Thesis.
- Chapter 3: Based on the principles extracted in Chapter 2, the novel humanoid postural architecture is proposed. It is composed by the same high level components than the human control system. The description performed in this Chapter starts from the establishment of the basic structure of the architecture. In subsequent section, each module from this high level architecture is decomposed and described deeper in detail. The chapter concludes with the complete low level postural control system, integrating all components described before in the Chapter.
- Chapter 4: Once the humanoid robot architecture has been exposed, this Chapter exposes the foundations applied for the development of each module described in Chapter 3.
- Chapter 5: As the human case, the postural control system is integrated by different devices and system that support the perception, processing and actuation chain. In this Chapter, the human sensorial, processing and actuation systems are briefly reviewed. They are as well compared with the systems integrated in TEO humanoid robot from a functional point of view. That is, this Chapter compares the human physiology with the humanoid's one.
- Chapter 6: Taking in account the foundations exposed in Chapter 4 and the functionality of the devices exposed in Chapter 5, each module of the humanoid postural control system has been implemented. This Chapter exposes the development of the mentioned modules and their integration in the postural control architecture.

- Chapter 7: In this Chapter, the results of experimentations are exposed and analysed. These experiments consist of functional testing of each module and the whole system performance.
- Chapter 8: The last Chapter exposes the conclusions extracted from all work done and the future works proposed to continue with the development of the system established by this PhD Thesis.

## CHAPTER 2

# Human Postural Control

### 2.1 Introduction to Human Posture Control

The postural control correspond to a complex motor response that involves the integration of a variety of sensorial information, elaboration and execution of movement patterns (Horak & Macpherson, 1996). The human postural control system is developed from birth and it is critically influenced by sensor system maturation and the development of the Central Nervous System (CNS). During the growth process, humans learn to control posture by means of experience acquired in response to sensorial inputs. So, the human posture control system is basically composed by a sensor input system which collects information, an integration system which process this information, and an end-effector system which performs the movements to keep the right posture. Figure 2 shows the high level structure of the CNS physiology that will be described in this Chapter.

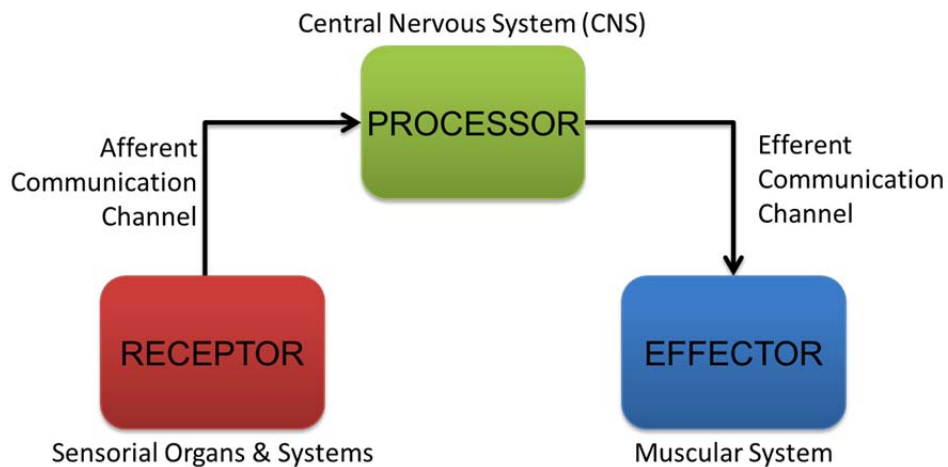


Figure 2 Basic human postural control system components

The postural control is performed continuously because it is the foundation of any kind of task. That is, one task can be considered as a sequence of controlled and learned postures. During the execution of each posture of the sequence, the sensorial inputs are evaluated to generate CNS stimuli that are transmitted to the neural processor centres. Depending on the result of the evaluation, different levels of postural control could be fired if it would be necessary. These reactions are classified in reflex, automatic or voluntary movements depending on the response velocity required.

Another factor influencing response velocity is the architecture of the human postural control system. There exist two basic modes of operation of the system when a disturbance is detected: reactive and predictive. The schemes that implement these operational modes in the postural control architecture are a reactive feedback loop and a predictive feedforward system. The aim of this Thesis is to study the operation of this predictive postural control mechanism, in which the sensorial inputs are used to predict the possible consequences from perturbations. According to the human system operation, the main function of this predictive system is preparing the effector system to apply a reaction. It is essential when higher level disturbances are detected or faster reactions are required than the feedback control loop can manage or trigger.

All these operational issues are related to the task performed and, due to this, it is necessary to establish a set of task parameters to be controlled. It is obvious that the selection of the parameters depends on the task complexity. To minimize this problem, this Thesis has been focused on postural control during two basic independent actions: locomotion and manipulation. With this selection, balance and equilibrium problems in locomotion can be isolated from postural control during a pure manipulation task. In this way, the solution to complex tasks postural control will be a combination of these basic sub-problems. Nevertheless, the basic principles for postural control, described in this Chapter, are shared by both task problems.

### 2.1.1 Manipulation Problem

The dexterous manipulation skill is, with upright locomotion, the most important feature that defines the human being. It is well known that the manipulation capacity has been a determinant factor in the human being evolution. Thanks to this skill, humans have been able to build objects and tools that have favoured the specie evolution. The manipulation capacity is also a differentiate element between human beings and animals. This importance, joined with the possibility of avoiding the balance problem during manipulation task performance, is the reason to consider this postural control problem independently. It is possible if the support base of the robot is fixed or intrinsically stable. In this case, the voluntary movement of throwing and catching a ball is considered as a sequence of upper limbs postures (Figure 3 (a)). Whether the ball trajectory suffers a deviation that is captured by the sensorial system, the hand location must be modified by the reaction produced (Figure 3 (b)).

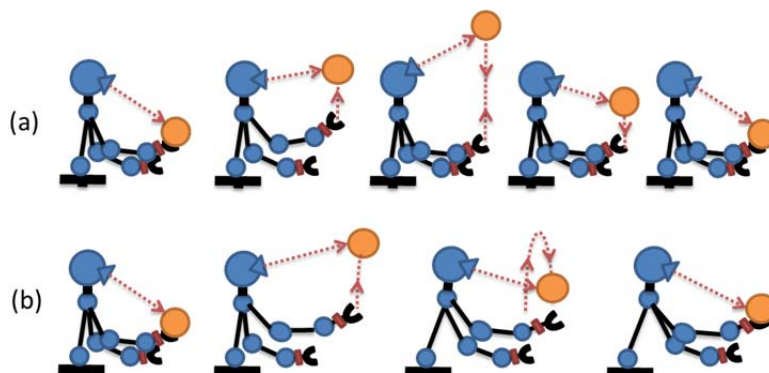


Figure 3 Manipulation task postural control: (a) Normal behaviour. (b) Task deviation corrected by postural control system

Human control system can estimate the deviation from expected trajectory and the approximate position where the ball should fall. Different control systems may be involved depending of the deviation level. In the case of low deviations, the manipulation feedback control system should be fast enough to modify the hand location. But in case of high disturbances and deviations, other strategies may be necessary and human anticipatory system may be involved.

If high deviation is detected, the target point to catch the ball will be further from the expected. In this case, feedback control may be not as fast as required and the human would miss the ball. In order to solve this issue, the human anticipatory feedforward system can trigger a reaction consisting in the arm movement towards the surroundings of the estimated target location. This kind of operation is driven by unexpected events and it is the fastest mechanism the human body has. But speed is opposite to precision. The goal of these movements is positioning the hand as near as possible of the estimated target location. Thus, the feedback control can take the control again and finish the task with success.

## 2.1.2 Locomotion Problem

Upright locomotion is one of the most important characteristics that define the human being. It enables humans to use the upper limbs only for manipulation tasks. Nevertheless, upright stance and stable locomotion require a complex postural and balance control system supported by the combination of different sensorial perceptions. It is also important to explain that balance is considered as the ability to maintain the body's position over its base of support (Berg, 1989; Spirduso, Francis, & Macrae, 1995). Taking in account that the human body is never absolutely stable, a control system is required to avoid the body from falling. Due to this, "postural control" and "balance control" have been used indistinctly to refer to the act of keeping the body close to the Equilibrium Point (Karlsson & Frykberg, 2000). In general, maintaining postural or balance control means to perform movements of the Centre of Mass (CoM) relative to stability limits in order to maintain equilibrium.

In this way, balance control can be divided into static and dynamic balance control problems, depending on whether the supporting base is stationary or moving:

- 1) Static balance control: It is used for keeping a stable position in the space during upright stance. Sway is limited to a minimum level in which the CoM is maintained inside the support base while upright standing.
- 2) Dynamic balance: It is related to the movement of the CoM during locomotion task performance. The dynamic balance involves keeping a proper posture while the CoM and the support base are moving. This kind of balance tries to maintain the CoM inside specific stability limits during movements that involve the dynamic modification of the supporting area.

Therefore, the strategies used to regain balance, during upright stance or locomotion, are influenced by these balance control problems. The postural control act will consist of keeping one of the mentioned balance states or switching from one to another to prevent falling.

External forces exerted over the body cause loss of balance during locomotion (Figure 4). In this case, the static balance control maintains posture until the level of external disturbance exceeds a pre-established limit. After that, the postural control system switch to other strategy and dynamic balance control acts to regain equilibrium.

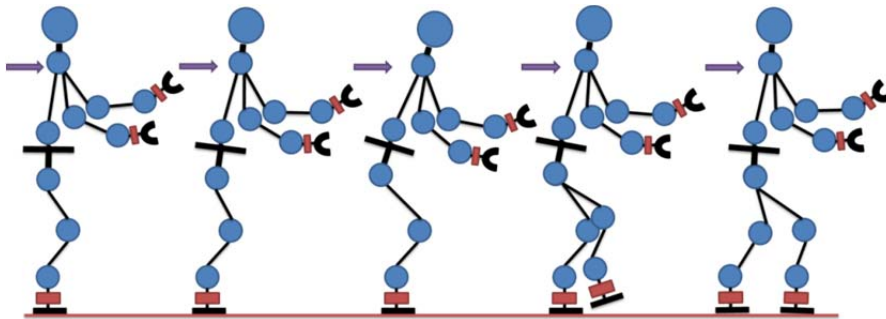


Figure 4 Locomotion task postural control

## 2.2 Physiology of the Postural Control System

To understand how humans control their posture, it is necessary to know the physiology of this control system. Attending to Figure 2, we can distinguish four main parts that compose the Central Nervous System:

- RECEPTOR (information input):
  - Exoceptive system
    - Vestibular system
    - Visual system
  - Proprioceptive system
    - Articular nervous endings
    - Muscular spindles
    - Cutaneous
- PROCESSOR (Integration centres)
  - Spinal cord
  - Cerebral trunk
  - Motor cortex
  - Associated areas: Cerebellum, Basal ganglia.
- EFFECTOR (action system)
  - Skeletal muscle system
- Communication channels
  - Afferent system
  - Efferent system

The sensorial information is captured by the corresponding receptors of the peripheral nervous system. This information is transmitted by means of the afferent sensitive neurons of the peripheral nervous system. Then the information arrives to the Central Nervous System where it is processed.

The level of the sensation captured and the velocity of the response needed determine where the information must be processed and which reaction must be triggered. Therefore, the reflex reactions are the fastest response and they are processed in the spinal cord. Following, the automatic medium latency reactions are generated in the cerebral trunk and, at last, the voluntary slowest movements are planned by the motor cortex.

After this information processing, the resulting actions are transmitted to the motion system by means of the efferent neurons to perform the movement. The hierarchical structure of the human postural control system is shown in Figure 5 and the functions and components of each system implied in postural control will be explained further in detail.

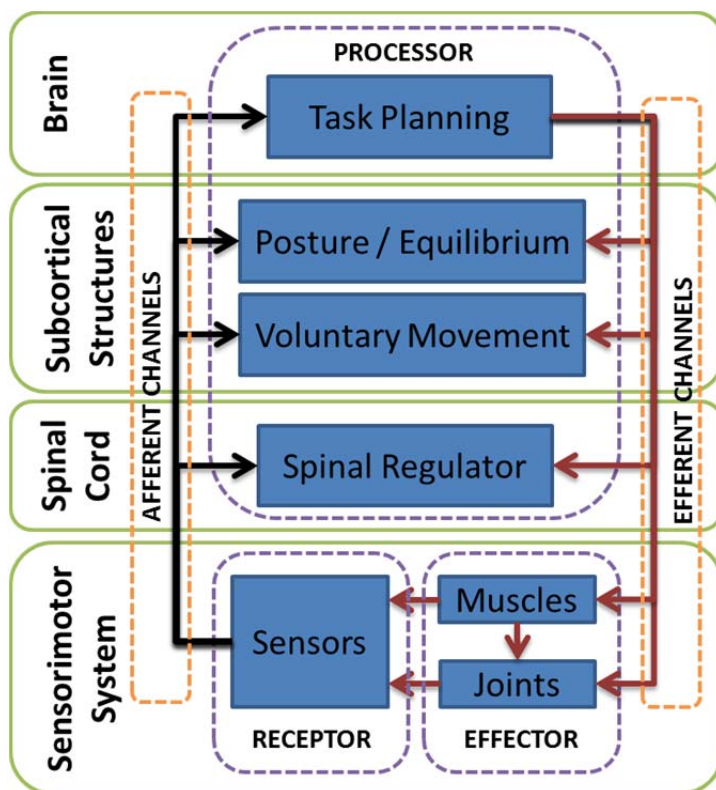


Figure 5 Motor neural control hierarchical structure

## 2.2.1 Sensorial System: Receptor

As stated before, the sensorial system is composed by two main parts depending of the origin of the stimulus. The exoceptive system captures external stimulus which has no direct physical interaction with the body (i.e. images). By the other hand, the proprioceptive system collects the information of the body itself (i.e. joint angles).

### 2.2.1.1 Exoceptive Sensation Systems

The exoceptive sensation is composed by the information about environmental circumstances or disturbances. The exoceptive perception will be then the result of the processing of the stimuli sensed. This information comes from the vestibular and visual sensorial systems.

### 2.2.1.1.1 Vestibular System

An essential aspect of the physiology of human postural control system is the operation of the vestibular apparatus for tracking the position of the head/body in space (Delaney, 1998) and the body inertial forces. The vestibular apparatus is composed by two separate entities: the semicircular canals and otolithic system (Baloh & Honrubia, 2001).

#### 1) The Semicircular Canals.

The semicircular canals are the angular sensing elements shown in Figure 6. There are six canals, three on either side of the head, and they are located in the inner ear. The semicircular canals consist of a horizontal canal, a superior and a posterior canal at right angles amongst themselves, so that they cover all three planes in space. In this way, the canals can respond to angular movement of the head/body about any of its axes. The canals themselves are filled with a fluid called endolymph. This fluid acts upon a structure called the cupula which resembles a water-tight door. This structure bend the hair cells sited on the crista to generate the sensorial output signal. The cupula is concerned with equilibrium control during motion and with angular acceleration (rotation of the head/body), but is unaffected by linear acceleration.

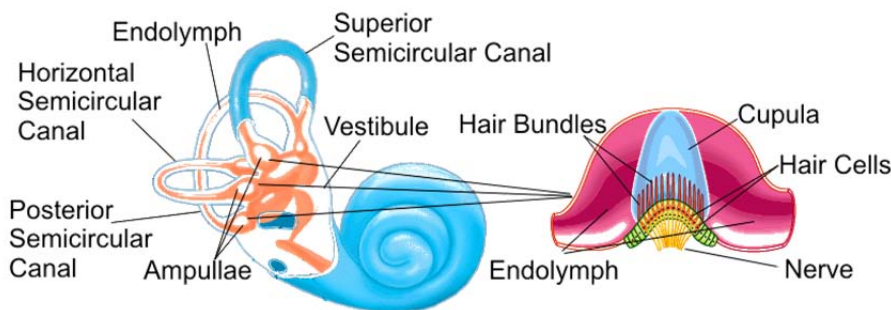


Figure 6 Semicircular Canals (adapted from Encyclopaedia Britannica, Inc.)

#### 2) The Otolithic System.

The vestibular otolithic system is composed by the saccule and utricle. The saccule is primarily located in a vertical plane meanwhile the utricle is primarily oriented horizontally. The sensory membrane of each organ is called the maculae. The maculae are covered by one membrane containing otoliths that are calcium carbonate crystals. The sensor operates by responding to a component of the movement of sensory hairs along a specific axis, the direction of which is determined by the position of a reference hair, the kinocilium, with respect to other hairs, the stereocilia (Figure 7).

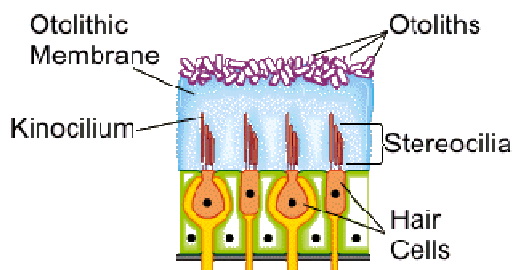


Figure 7 The maculae (adapted from Encyclopaedia Britannica, Inc.)

The otolithic system is sensitive to multiple directions of linear acceleration. For any pattern of acceleration and gravity the hairs respond with a specific pattern of stimulation. The brain then applies pattern recognition to the stimulation pattern and resolves the pattern into three orthogonal axes with respect to the head.

### 2.2.1.1.2 Visual System

This system detects, transmits and interprets visible light stimuli (wavelengths between 400 and 725nm). The eyes, which are the sensorial organs, can distinguish brightness and colour.

The photoreceptors inside the eyes are rods and cones located in a specialised epithelium called the retina. In each eye the retina contains about 6 million cones and 120 million rods. In the peripheral region of the retina both rods and cones converge on bipolar cells. The bipolar cells converge on ganglion cells giving rise to the one million nerve fibres in each optic nerve.

In addition to allowing us to detect hazards in the environment, vision plays a direct and important role in stabilizing balance and postural control by providing the nervous system with continually updated information regarding the position and movements of body segments in relation to each other and the environment. Visual system triggers the muscle activation required for postural corrections, but it can be compensated for by other information sources (Kejonen, 2002).

### 2.2.1.2 Proprioceptive Sensation Systems

The proprioceptive or somatosensory system receptors are located in muscles, joints and skin. They give information about the position of the limbs and the body, the distension of the respective muscles, vibrations, pressure, etc.

There are some essential inputs for postural control produced by proprioception. During locomotion or upright stance, the information from ankle joints should be recognized, as it is affected by the movement of the centre of gravity, resulting in torque changes around the ankle joint. As well, the importance of proprioception in postural control during manipulation when reaching and grasping objects (Gentilucci et al., 1994).

#### 2.2.1.2.1 Articular Nervous Endings

The majority of sensory innervation of the articulation is found in the joint capsule. The receptors in these capsules give information about the movements and positions of the body parts relative to each other (mechanoreceptors). There are four main types of receptors with different sensorial functions (see Figure 8):

- 1) Ruffini endings: located on the flexion side of the joint. They give information about static joint position, intra-articular pressure and, as well, range and rotation of the joint.
- 2) Pacini corpuscles: mechanoreceptors sensitive only to rapid variations of deformation, that is, they are joint acceleration sensors.

- 3) Golgi corpuscles: located in the posterior side of capsule. Monitors tension in ligaments, especially at the end of the range of motion.
- 4) Free nerve endings: widely distributed over all articular structures. They constitute the joint nociceptive system (pain stimuli).

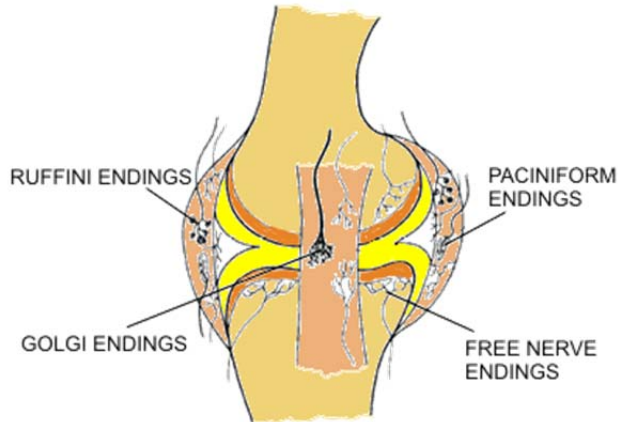


Figure 8 Articular sensor receptors

#### 2.2.1.2.2 Muscular spindles

The muscle spindles give information about the changes in muscle length and tension (dynamic stretch), and they can also be activated by passively stretching the entire muscle. Lots of them are dispersed inside the muscle and they are connected to multiple sensory endings (Figure 9).

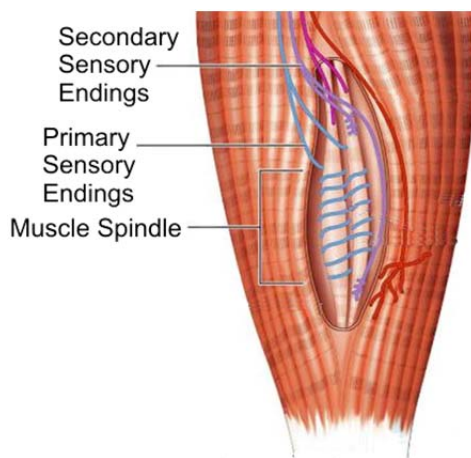


Figure 9 Muscle spindles

#### 2.2.1.2.3 Cutaneous

Some of the receptors described in section 3.2.1 are also located in the cutaneous system. Depending on the velocity of response, these receptors detect fast variations or static stimuli. The pressoreceptors (Ruffini Endings and Merkels discs) detect pressure and body sway, whereas the mechanoreceptors (Pacini and Meissner corpuscles) can determine both the site and velocity of an indentation of the skin, as well as acceleration and pressure changes (Vallbo & Johansson, 1984).

## 2.2.2 Integration centres: Processor

The main processor of the stimuli involved in posture balance control is Central Nervous System (CNS), shown in Figure 10. The mechanisms and the CNS parts involved in motor information processing depend on the voluntary nature of the reaction. The voluntary movements needed for balancing posture are planned within the brain; meanwhile, other involuntary balance actions are commanded by other CNS structures (i.e. the spinal cord).

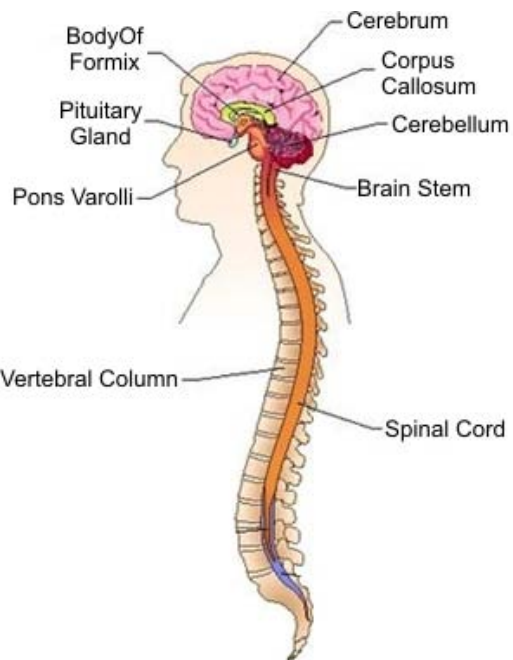


Figure 10 Central Nervous System (Adapted from Kopp Illustration, Inc.)

### 2.2.2.1 Spinal cord

Two important functions of the spinal cord are the communication of the information coming from the brain to the rest of the body and the initiation of reflexes in response of the body to the high level surprising stimuli. Although the speed at which the information travels from sensor system to the brain and back to muscles is very fast, sometimes it is necessary a greater signal communication speed. This is where the reflex action, triggered by the spinal cord, comes into play. As a defence mechanism, the body reacts faster than the normal time it usually takes.

### 2.2.2.2 Cerebral trunk

It is located under the brain base. The cerebral trunk connects the spinal cord with other cerebral structures. It controls the automatic functions of the human body. In this sense and related with balance control, the cerebral trunk maintain the stance posture of the body against gravity.

Parts of the Central Nervous System as pons, bulbus and spinal cord, are endowed with programs of posture and movement, which are used by the organism when necessary, without the necessity of the involvement of regions located in a higher level in the central nervous system (Brandão, 2004).

### 2.2.2.3 Cortical

Voluntary movements require the participation of the third and fourth levels of the hierarchy: the motor cortex and the association cortex. These areas of the cerebral cortex plan voluntary actions, coordinate sequences of movements, make decisions about proper behavioural strategies and choices, evaluate the appropriateness of a particular action given the current behavioural or environmental context, and relay commands to the appropriate sets of lower motor neurons to execute the desired actions.

The motor cortex comprises three different areas of the frontal lobe: the primary motor cortex (Brodmann's area 4), the premotor cortex, and the supplementary motor area (Figure 11). Thus, the pre-motor cortex and supplementary motor areas appear to be higher level areas that encode complex patterns of motor output and that select appropriate motor plans to achieve desired end results.

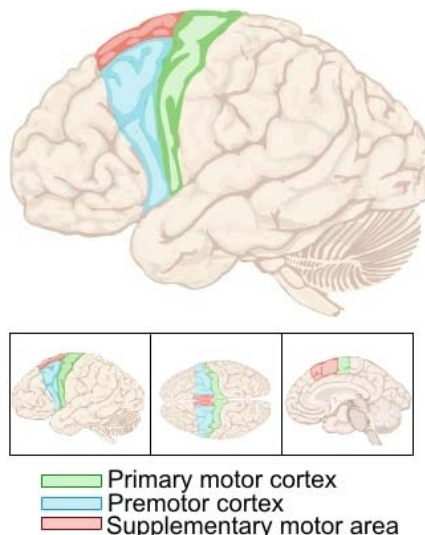


Figure 11 Motor Cortex Areas

Virtually all "voluntary" movements involve conscious activity in the cerebral cortex. However, this does not mean that each contraction of each muscle is willed by the cortex itself. Instead, most control used by the cortex involves the patterns of function in the lower brain areas (in the spinal cord, in the brain stem, in the basal ganglia, in the cerebellum) and these lower centres in turn send most of the specific activating signals to the muscles.

### 2.2.2.4 Associated areas: Cerebellum, Basal ganglia

The basal ganglia and cerebellum are large collections of nuclei that modify movement on a minute-to-minute basis. Motor cortex sends information to both, and both structures send information right back to cortex via the thalamus. (Remember, to get to cortex you must go through thalamus.) The output of the cerebellum is excitatory (positive), while the basal ganglia are inhibitory (negative). The balance between these two systems allows for smooth and coordinated movement (Figure 12).

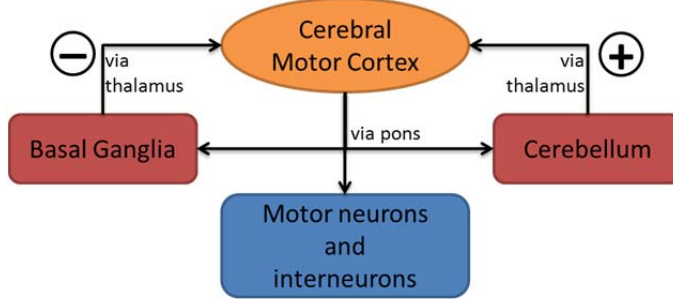


Figure 12 Cerebellum and Basal Ganglia functions

### 2.2.3 Action System: Effector

Skeletal muscles are composed by numerous muscle fibres, distributed along the entire length of the muscle. All fibres are roughly parallel in orientation. A single muscle fibre is in turn subdivided into several thousand parallel units called myofibrils. The mechanisms of contraction lie within these tiny myofibrils.

The total muscle output is the summation of tension developed by each of the motor units within the muscle. Simplified muscle models, considering the muscle as a single force generating unit, predict input-output characteristics. The variables affecting muscle output (tension) are the following:

- 1) Activation level (in the single component model this is the average activation level of all motor units in the muscle).
- 2) Instantaneous length of the muscle.
- 3) Shortening velocity of the muscle.

Coordinated control of the body segments is a complex aspect of human postural control, owing to the multiple Degrees of Freedom (DoF) of the controlled system (Bernstein, 1968). These DoFs build the posture up by the sum of several basic mechanisms (Massion, 1984) based on the muscular tone, which is usually defined as the resistance to passive movement (Bodensteiner, 2008). The muscle tone is regulated both by the brain and spinal cord and the brain is kept informed of the ever-changing status of this tone.

In addition, spinal reflexes transmitted to the muscles through the spinal cord are responsible, among other functions, for all of the skilled movements of the trunk and limbs and standing erect, walking, and running. Therefore, muscles have two main roles in postural control that define the following functional classification:

- 1) Rest or tonic muscles: this kind of muscles maintains the tensional state of the body to counteract gravity force, keeping a balanced position. The body remains in this case in static postures.
- 2) Phasic muscles: Their main function is producing movement. They provide a stable background for voluntary activity.

## 2.2.4 Communication channels

Motor signals are transmitted directly from the cortex to the spinal cord through the corticospinal tract and indirectly through multiple accessory pathways that involve the basal ganglia, the cerebellum and various nuclei of the brain stem.

### 2.2.4.1 Afferent system

The afferent information channel carries impulses from sensory organs to processor centres (CNS). It is composed by the afferent neurons, also called sensory or receptor neurons, connected directly to the sense organs and interneurons that connect each neuron with others.

### 2.2.4.2 Efferent system

Efferent neurons are also called as motor neurons. They mostly carry responses to the muscles or glands, bringing about the movement. The efferent neuron forms an electrochemical pathway towards the effector system.

The most important point of comparison between afferent vs. efferent neurons is that they perform an exactly opposite function and follow an opposite electrochemical pathway in the central nervous system loop (Figure 13).

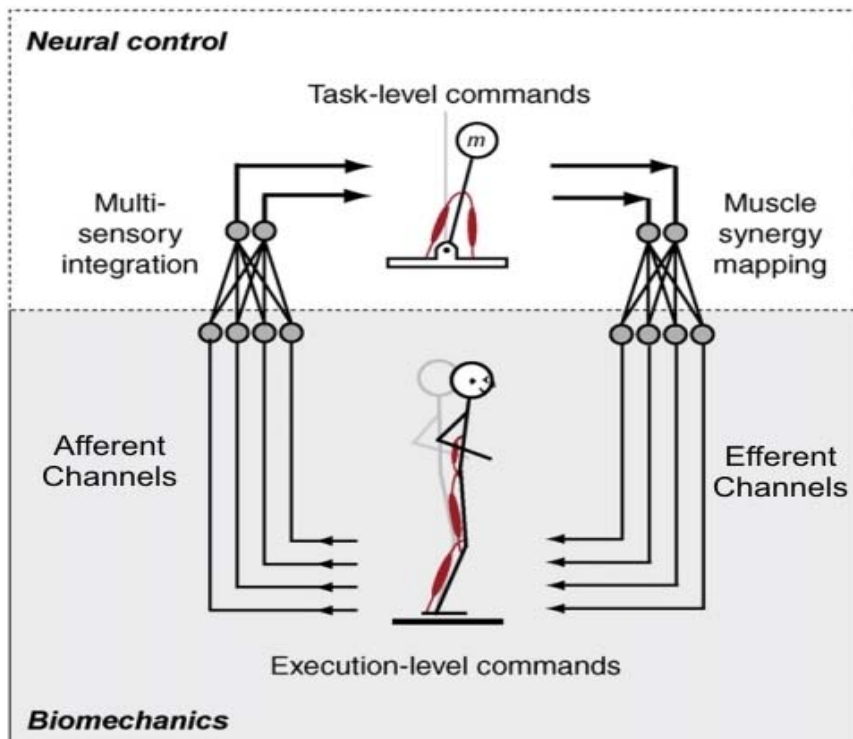


Figure 13 Multisensory integration systems(Ting & McKay, 2007)

## 2.3 Foundations of Postural Control

Different theories were developed in the past to explain how the human body controls its posture. The two major theories make the difference in the internal organization of the responses and the way they are triggered. In the reflex/hierarchical theory posture and balance are the result of hierarchically organized reflex responses triggered by sensory input (Granit & Burke, 1973). But nowadays, postural control has been oriented to a systemic point of view. Today researchers recognize that postural control is complex and context-dependent and that all levels of the nervous system must be examined to account for this complexity (Kandel, Schwartz, & Jessell, 2000). Although some controversy exists regarding the range of subsystems involved, there is general agreement that the neurological system, the musculoskeletal system, the sensory system, the environmental context, and the task demands are important contributors to postural control (Kamm, Thelen, & Jensen, 1990).

Besides relying on their feedback systems, humans also maintain balance using anticipatory motor action. During human movement, two control actions are performed continuously and in parallel: movement and postural control. Meanwhile movement control system commands body limbs position, the postural control performs actions to maintain balance taking in account the proprioceptive information. Figure 14 shows this basic idea, but this control system is defective in the sense that it only provides information about the feedforward and feedback postural adjustments produced by voluntary movements.

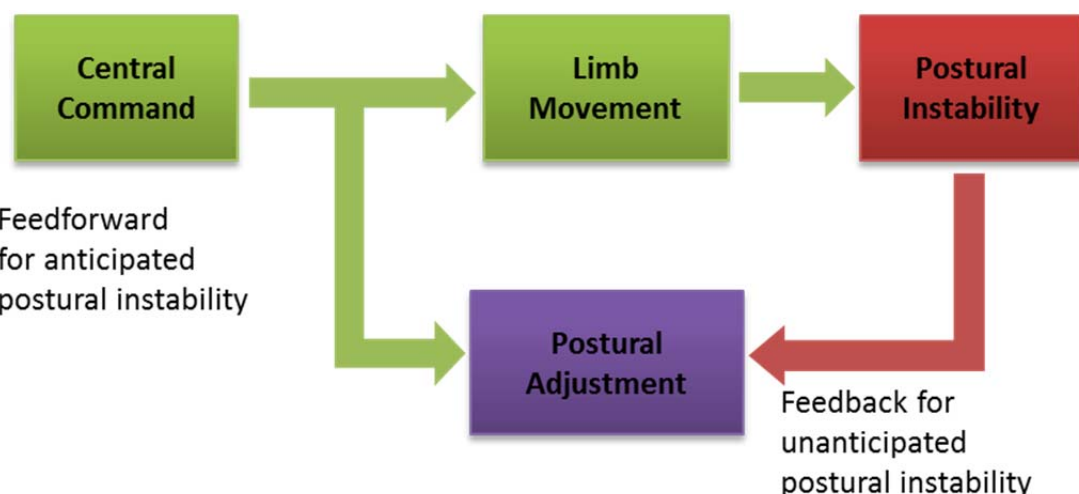


Figure 14 Feed-forward and feedback postural adjustment from (Kejonen, 2002)

It is important to state that posture and movement are close related but they are essentially different. From a biomechanical point of view, the movement can be described as the combination of motor gestures. Purposeful or voluntary motor acts are performed moving one or several body segments towards a goal (Agid, 1990); meanwhile other segments must be positioned in order to regain posture and equilibrium. It is ease to point out that voluntary movements are one source of postural perturbations.

Therefore, posture poses a static and dynamic dual nature. The former, static or postural fixation, is a local mechanism to maintain the body segments in stationary positions against internal (e.g. weight) or external forces (e.g. load ported) (Martin, 1967). The latter, dynamic posture component is the continuous looking for keeping the desired target according to the task performed.

### 2.3.1 Levels of Reaction of the Postural Control System

Three different reaction levels have been established depending of where the stimuli information is processed and the system producing it, as shown summarised in Table 1 (Diener & Dichens 1986, Schmidt 1991, Nashner 2001, Schmidt & Lee 1999). The motor response to external perturbations can be reflex, automatic or voluntary.

Table 1 Properties of the three motor systems in balance movement control

System property	Motor System		
	Reflex	Automatic	Voluntary
Processor	Spinal	Brainstem/subcortical	Cortical
Activation	External stimulus	External stimulus	External stimulus Self-generator
Response	Local to point of stimulus and stereotyped	Coordinated and stereotyped	Unlimited variety
Role in Postural Control	Muscle force regulation	Resist disturbances	Purposeful movements
Latency	Fixed 20-60ms	Fixed, 130-170ms	Variable >150ms

#### 1) Reflex reactions

This motor reaction to outside perturbation is processed in the spinal nervous system. The role of this reflex is to regain postural stability by a rapid muscle response (Rothwell & Lennon, 1994). Any kind of action threatening the posture of the body is detected by an afferent input via muscle and tendon proprioception, which initiates the first muscle movement by acting the appropriated muscles all over the body. The spinal response is very fast (20-60ms) after perturbation detection. The reflexes do not contribute directly to the recovery of balance (Nashner, 1993).

#### 2) Automatic reactions

The first response against perturbations is an automatic reaction that occurs as medium-latency muscle responses (130-170ms). These reactions are coordinated and transmitted through brain trunk and affect all muscles of the legs, torso and neck (Allum, Bloem et al., 1998). In addition to the medium-latency responses, long-latency responses have been found to co-occur with them in the antagonist muscles (Diener, Dichgans et al., 1984). Automatic responses can be considered as overlearned, "long-loop" reflexes that rapidly respond by resisting disturbances (Diener et al., 1984;

Nashner & McCollum, 1985). Automatic reactions are context-dependent and adaptable to the specific balance demands. The pre-programmed patterns of automatic reactions could be adapted to the environment conditions by experience and learning.

### 3) Voluntary movements

In contrast to reflex and automatic responses, voluntary movements are based on conscious information processing by the brain motor centres. Voluntary postural adjustments displace the position of the centre of gravity and, hence, the ground reference points associated. Postural adjustments and voluntary movements can be produced at the same time during continuous movements. The latency of this response occurs between 220 and 360 milliseconds after perturbation.

## 2.3.2 Psychophysics and Postural Control

According to the International Society of Psychophysics and different authors, it is a discipline within the psychology science focused in the investigation of the relationship between physical stimuli and the unleashed sensations and perceptions. This must be a quantitative and measurable relationship (Bruce, Green, & Georgeson, 2003; Gescheider, 1997).

The described sensory organs provide great amounts of quantitative information to the central nervous system. In the case of postural feedback, muscle sensors detect limbs position and, at the same time, visual perception provides the same information. It is obvious that exoceptive and proprioceptive sensations are complementary but a lot of information is redundant. The captured information must be processed, classified and integrated in order to command actions in the proper way. With this sensation processing the raw data coming from sensory organs is converted into perceptions. It has been suggested that such filtering and integration of redundant information is performed by minimum-variance estimations, ascribing weights to each modality according to its relative precision (vision and touch (Ernst & Banks, 2002), vision and audition (Ghahramani, 1995), and other combinations of sensory input (Jacobs, 1999; Van Beers, et al., 1999; Welch, et al., 1979)).

Psychophysics also refers to a general class of methods applied to the quantitative study the relations between physical stimulus magnitudes and the corresponding magnitudes of sensation. These methods try to solve four main problems related to stimuli process: detection, identification, discrimination and scaling. Detection relates to the interest of knowing whether one stimulus was received or not. If the knowledge of stimuli has been produced is not relevant but their characteristics, identification might be performed after detection. Both problems are solved quickly and almost simultaneously when they concern stimuli which are strong and clear enough. However, under conditions of weak and noisy signals, detection of something is performed but clear identification is not possible. In such a case, the discrimination of the received information is needed to filter out the consistent signal attributes. The last perception problem refers to the level of its magnitude and how this level must be interpreted (scaling).

The first kind of methods is related to the subjective perception of an observer. These classical psychophysical methods try to calculate thresholds of event occurrence (happen/not happen). The second type of methods tries to solve the subjective influence of the observer when the report of perception is given. The so called modern methods provide objective information from the trials such as occurrence time or perception location. These methods are (Ehrenstein & Ehrenstein, 1966):

### 1) Classical Psychophysical Methods

#### a. Method of Limits

In the method of limits, a single stimulus is changed in intensity in successive, discrete steps and the observer's response to each stimulus presentation is recorded. The experiments are usually performed in alternate ascending and descending series. The average of the intensity of the last "detected" and the first "not detected" stimulus is recorded as an estimate of the absolute threshold.

The comparison of a standard constant stimulus with other "weaker" or "stronger" allows calculating the difference threshold. Then, it is the difference of intensity between the stimuli of the first trial on which the response differs from the previous one.

#### b. Method of Constant Stimuli

In this method, a fixed set of stimuli is presented multiple times in a quasi-random order that ensures each will occur equally often. After each stimulus presentation, the observer reports whether or not the stimulus was detected (absolute threshold) or whether its intensity was stronger or weaker than that of a standard (difference threshold). After multiple experiments, the proportion of "detected" and "not detected" (or, "stronger" and "weaker") responses is calculated for each stimulus level. The data are then plotted with stimulus intensity along the abscissa and percentage of perceived stimuli along the ordinate. The resulting graph represents the so-called psychometric function.

#### c. Method of Adjustment

The simplest and quickest way to determine thresholds is to let a subject adjust the stimulus intensity. In the case of measurements of the absolute threshold, the experiments are performed until stimulus is just perceived or vice versa, depending on ascending or descending trials. For difference threshold calculus, the user must adjust the stimulus intensity until it will be notoriously different from, or to just match, some other standard stimulus.

### 2) Modern methods

#### a. Forced Choice Methods

One of the potential difficulties that arise with the traditional methods is that the participant might be deceiving the experimenter. The forced-choice method provides a more objective approach than methods exposed previously. In this method, the observer is required to make a positive response on every trial regardless of whether

detection of the stimulus was performed. On every trial, the subject either has to say when the stimulus occurred or where it occurred.

b. Signal Detection Theory (SDT)

SDT provides the basis for a set of methods used to measure both the sensitivity of the observer in performing the perceptual task and any response bias that the subject might have. According to SDT, the sensorial signal is characterized as a distribution of values on a continuum of sensory evidence rather than as a single value. Also, on any given trial there is some "noise" present in addition to the signal. Therefore, trials on which a signal is present are typically called signal plus noise trials.

In conclusion, these techniques provide quantitative information about a physical variable (e.g., movement direction, amplitude, velocity, acceleration, etc.) and the threshold at which such stimulus is noticed by a subject.

One key point of the human postural control system is the way the disturbances are sensed and how this perception commands body reactions. Using psychophysical principles, it is possible to model these disturbances as unexpected events or surprise events produced depending on the task context (Dey, 2001).

Since surprise depends on the 'unexpectedness' of the stimulus (Ortony & Partridge, 1987), at least the three following layers and each corresponding test must be distinguished in order to provide an exhaustive model of surprisingness generated by expectation failure (Lorini & Falcone, 2005).

- 1) Mismatch-based Surprise: based on sensory-motor expectations, it is generated by the mismatch between active knowledge and disturbance perception, exceeding some threshold value (Macedo, et al., 2004; Meyer, et al., 1997)(function of Unexpectedness). It is based on some form of 'statistical' learning (Baldi & Itti, 2010) and its intensity is function of the degree of certainty and the value of the goal.
- 2) Passive Prediction-based Surprise: surprise results from a conflict or inconsistency between the updated set of knowledge and the perceived sensation (Ortony & Partridge, 1987). Passive expectations are formed after the surprising event has occurred (Spitz, 2011).
- 3) Implausibility-based Surprise: This refers to those (quite numerous) situations in which the input proposition expresses information related to non-existent knowledge (function of Incredulity).

Summarizing, capture surprise events or feeling surprise seems to play several functions:

- 1) Redirecting attention on the mismatching facts, concentrating cognitive processing resources on them.
- 2) Activating resources for possible practical activity; physical arousal, bodily preparation for fast reaction.

- 3) There are also long term effects (and functions) of the perceived surprise for a bad prediction (e.g. increasing controls before and during the actions).

### 2.3.3 Sensorimotor Integration in Postural Control

To maintain postural control during both static and dynamic situations, individuals rely on their sensory (visual, vestibular and somatosensory) systems to provide information such as their limbs locations and movement with respect to the surrounding environment. The Central Nervous System then interprets the sensory information and commands the musculoskeletal systems to adjust the body parts position trying to keep a desired or stable posture. However, since human beings are constantly interacting with their surroundings, one must not ignore the environment when studying postural control. The influence of environmental factors such as light conditions, concurrent distracting factors, special surface characteristics, etc. are affecting the requirements to the postural control. Similarly, it is easily understood that the postural control demands during the task of walking and other locomotive activities are different from the demands when humans perform manipulation tasks (Figure 15).

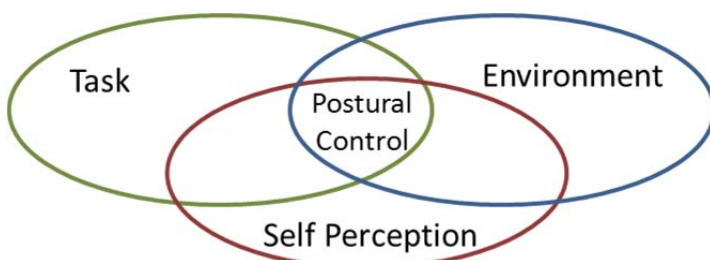


Figure 15 Postural control (PC) is influenced by factors related to the individual, the task, and the environment adapted from (Shumway-Cook et al., 1995)

Since postural control has been defined as the control of the body's position in space, it must be performed adjusting parameters such as centre of mass, base of support, joint momentum, etc. The adjustments are counterbalancing actions of the limbs, the head and the trunk influenced by the muscular strength, previous experience, etc.

#### 2.3.3.1 Motor Strategies to Control Balance

The particular case of postural control during locomotion has been extensively studied in order to try to understand the mechanisms that humans use to solve the balance problem during upright stance, walking, etc. One of the main conclusions is the existence of learned patterns that are automatically triggered in response to determined stimuli. These patterns are called motor strategies or 'synergies' (e.g. Bernstein, 1967; Sherrington, 1906). According to Sherrington, the control of the movement related to the synergies is composed by a reflex motor unit above the voluntary motor unit. Such reflex movements are organised more naturally into collective functional units defined over groups of muscles and joints (Kelso & Saltzman, 1982). By the other side, Bernstein suggests that a restricted number of programs may underlie most of our behaviour.

For any given perturbation, one or more muscle synergies may be activated so that their combined influences define the resulting muscle activation pattern (Ting, 2007). Extending the concept, complex synergies can be in general considered as programs for controlling some distinctive motor performance extended in space and time, built upon basic synergies of coordinated reflexes as substrate (Arbib, 1987).

Therefore, synergies can be classified according the direction of action of the perturbations. All of them can be decomposed in anteroposterior disturbances (sagittal plane) and mediolateral disturbances (frontal plane). Studies of quiet stance have suggested separate postural strategies for balance in both planes depending on the stance position (Day, et al. 1993; Winter, et al. 1996). There are three main mechanisms that can be applied to regain balance in such planes depending on the level of the disturbance.

The first is the ankle strategy. In this one, the body can be regarded as a stiff pendulum, and balance adjustments are mainly made in the ankle joint, with the person swaying like an inverted pendulum (Nashner, 1985). This postural adjustment is applied in the anteroposterior direction to compensate low intensity disturbances.

In the hip strategy, the resulting motion is primarily focused about the hip joints (Horak, et al. 1990). It can be applied independently or in combination of the ankle strategy. The hip joint movement is triggered when the external disturbance increases and the ankle strategy is not enough to keep balance. Figure 16 and Figure 17 show how the levels for strategy triggering changes depending of environmental conditions (flat surface stance vs. narrow beam). The hip strategy, same as ankle one, acts in the anteroposterior direction.



Figure 16 Strategy trigger modification influenced by environment conditions

When these postural corrections become insufficient, the base of support must be adjusted. (Carr, et al. 1987; Horak, et al. 1990) This action will be seen as protective stepping reactions. The modification of the support base leads new balance stability limits.

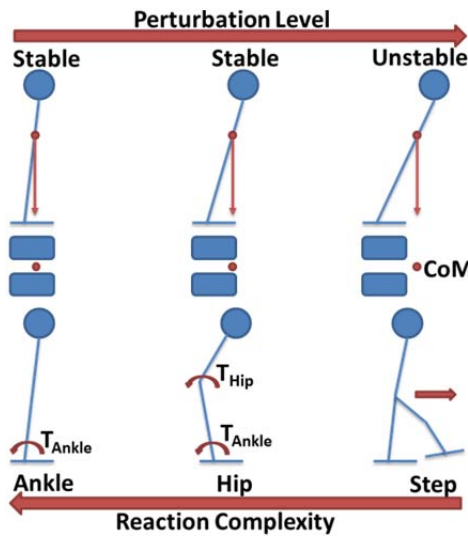


Figure 17 Balance strategies

In the mediolateral direction or frontal plane, the disturbances are compensated by the lateral movement of the hip joint in the case of upright stance. But if disturbances appear during walking, the compensation changes to the ankle strategy.

Other examples of synergies considered in different studies include a multi-link strategy and muscle amplitude synergies (Allum & Honegger, 1993), the ankle, knee, and hip eigen-movements (Alexandrov et al., 1998), axial synergies (Crenna et al., 1987), and reciprocal and co-contraction strategies (Sliper & Latash, 2000). All these examples are based on a common assumption that regularity in the behaviour of a set of elements is a sufficient sign to claim an existence of a synergy (Latash et al., 2005).

### 2.3.4 Basic Postural Control System Schemes

Postural control can be seen as a response to sensory information on a feedback basis, but when a balance threatening situation can be predicted, an anticipatory strategy can be used (Ghez & Krakauer, 2000). Postural control strategies may therefore be either “reactive” (compensatory), “predictive” (anticipatory), or a combination (Pollock, et al. 2000).

In a feedback system, sensed signals are compared to reference signals by means of comparators (Figure 18). The difference between a feedback signal and the reference is the error signal. Feedback control is usually used for slow movements and for maintaining posture. For instance, it is originated by the sensorial events associated to an unexpected balance lost (compensatory). They are the result of the interaction between the body and its environment. The body adapts itself to the external conditions thanks to the sensorial information (exoceptive and proprioceptive).

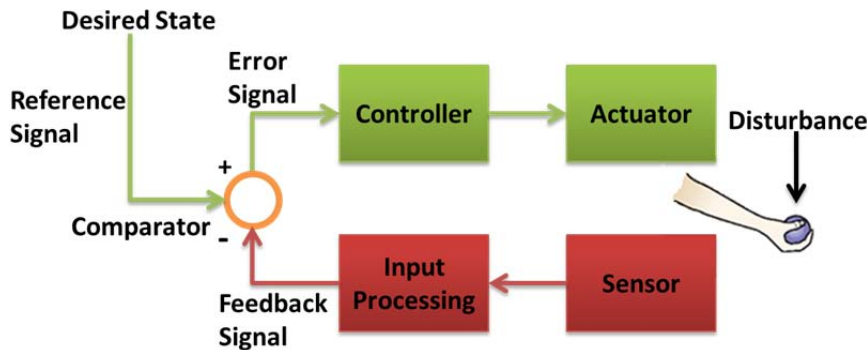


Figure 18 Feedback control scheme (Kandel et al., 2000)

In a feedforward control, state variables (e.g. joint angle) and advance information about disturbance are received by sensors and fed forward by the controller (Figure 19). Feedforward control is essential for rapid movements and relies on advance information to adjust controlled variables. When a disturbance repeats itself and, therefore, it can be predicted, its correction can be improved through an “in advance” system. This system predicts possible disturbances and generates an answer program whose goal is to maintain the stability. This answer allows carrying on some previous position adjustments before executing an intentional movement (previous experience). If the feedforward had not existed, the body would have been unstable and would have fallen down.

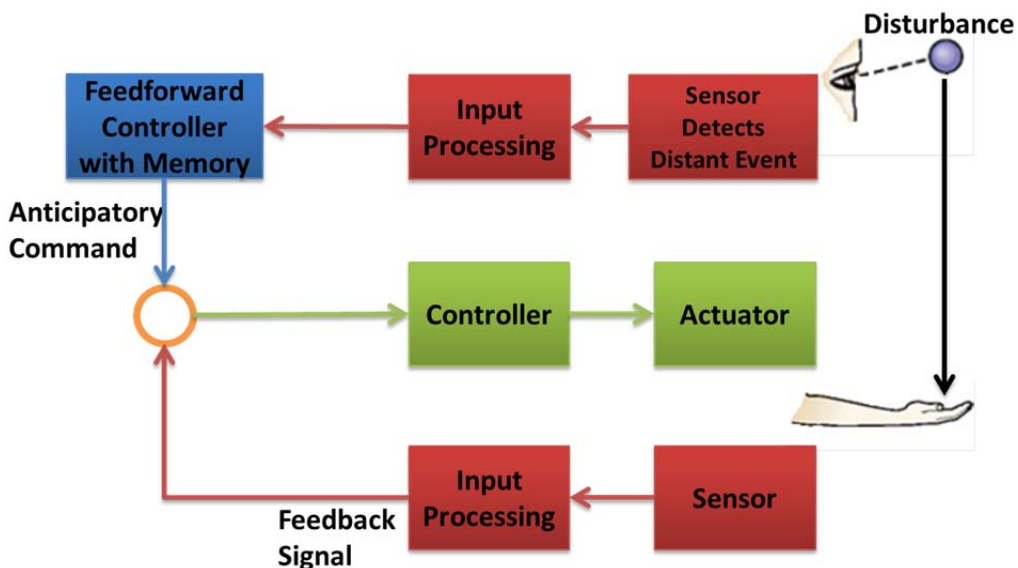


Figure 19 Feedforward control scheme (Kandel et al., 2000)

Closely related to the concepts of feedforward and feedback control we find open and closed loop control schemes, respectively. These concepts used by (Kandel et al., 2000) provide descriptions of two different ways in which the nervous system behaves in controlling movement. Feedback control is often referred to as closed loop control because the outgoing commands, the effectors (or actuators), the feedback signals and the control centre all form a loop. In this case, the element sensed is directly the actuator and, mainly, it is proprioceptive information (Figure 18). Feedforward control is often referred to as open loop control in order to emphasise that the sensory signals come from exoceptive stimuli (i.e. visual information). The feedforward control

complements the feedback control to increment the velocity of response against disturbances (Figure 19). In fact, the architecture for human postural control is based on the combination of feedback and feedforward schemes. A direct mapping of the task parameters into the appropriate muscle activation patterns could constitute a task specific feedforward controller adequately solving the control problem (D'Avella et al., 2008).

## 2.4 The Human Postural Control System

Taking into account the basic principles of human postural control, it is possible to develop a full control system scheme. The components involved in this system are interrelated by means of feedback and feedforward information flows. Many researchers have developed theories regarding the operation of the sensorimotor system that controls posture and balance (Nashner, 1985; Horak et al., 1990; Rothwell & Lennon, 1994; Winter, 1995; Kandel et al., 2000; Mahboobin, et al. 2002; Peterka et al., 2002). The resulting control scheme joins all the basic principles but some of them have little differences, depending how the operation of the whole system is considered. Figure 20 shows one holistic approach of the human being postural control system. In this scheme, there exist two position inputs: postural and movement.

Postural control (orientation and balance) is related to the proprioceptive perception meanwhile movement control corresponds to the voluntary actions. The proprioceptive information is merged with other sensorial sources to build the body schema which shows a representation of the body's configuration together with its relationships with the external world. All these components belong to the feedback control loop.

The movement control is, in fact, the desired position of the body. As the target position, the central neuron system commands each muscular group with its own local control loop. At the same time, this command position is feedforwarded and compared with the resulting information of balance to make the proper adjustments.

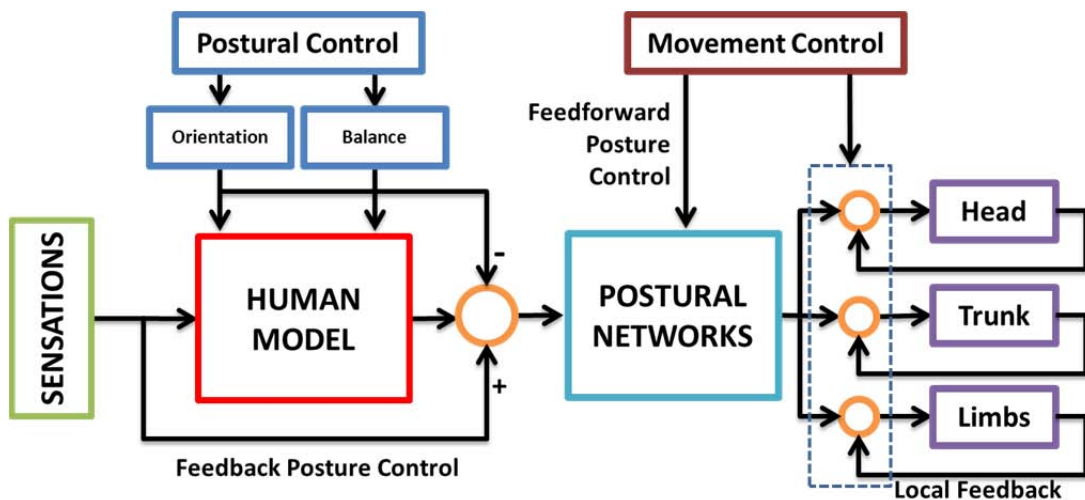


Figure 20 Human postural control architecture adapted from (Massion, 1998)

In the model of Figure 20, the human body is represented by a simplified model in which sensor and balance information's are the variables. The scheme shown in Figure

21 incorporates this model inside the 'processing & integration' module, avoiding the duplication of input information to the comparator produced in Figure 20 . In this case, the result of the comparison is a corrective command of the body orientation that is the center of the feedforward control loop.

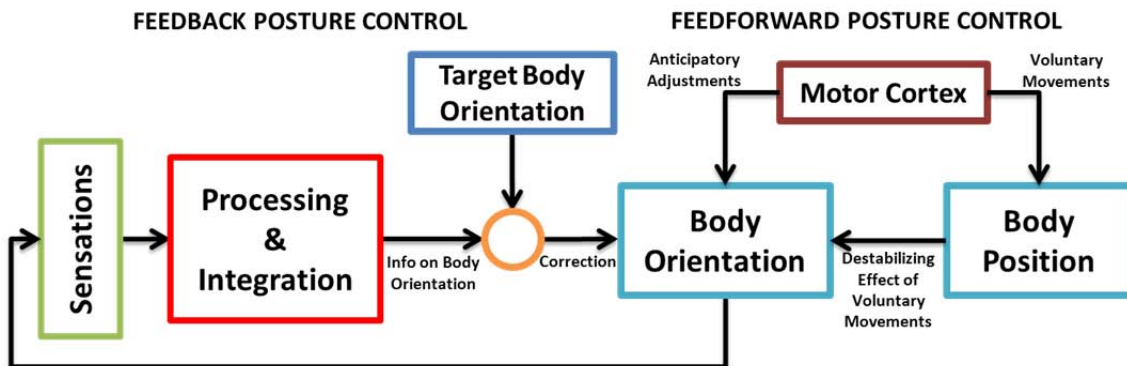


Figure 21 Human postural control scheme



## CHAPTER 3

# High Level TEO Humanoid Postural Control Architecture

### 3.1 Introduction to Humanoid Posture Control

The human postural control system, outlined in Chapter 2, is the result of millions of years of evolution. Its complex operation and physiology are still being researched and are far from being completely understood. Although technology evolution is much faster than biology evolution, the same problems must be addressed and they are continuously under development.

The case of humanoid robotics is very particular. This technology deals with the dream of designing an artificial human-like machine. Many reasons have been exposed to justify the design of humanoid robots. Some authors argue that these kinds of design are semi-optimal for the dexterous manipulation of objects and for other complex motions, but they also recommend not copying the human form without functional motivation (Ambrose & Ambrose, 2004). Another very practical reason to design humanoid robots is that they will be able to operate in the same environments that humans operate in today (Brooks et al., 2004). This is due to the world is adapted to the human body shape and it is easier to design machines adapted to our world than modify it. This allows the robot operation in a whole range of situations in which a non-humanoid robot would be quite ineffective. There are two main human characteristics to replicate in humanoids robots: appearance and behaviour.

Lots of human-like mechanical designs have been developed during last fifty years, from first prototype Wabot-1 (Kato, 1973) to cutting-edge humanoid robots ASIMO (Hirose, Haikawa, Takenaka, & Hirai, 2001), HUBO (Oh et al., 2006) and HRP-3 (Kaneko et al., 2008). From a mechanical point of view, the development of these robots has taken the advantage of leading technologies existing in their time but the concepts used were based on traditional mechanical solutions. For instance, joint designs have been mainly created with rotary motors joined to mechanical transmissions to increase velocity and torque at their output. But mechanical limitations and the desire of high human appearance favour the searching for new solutions for the humanoid robot design. In this sense, the field of bionics seeks to design technology by mimicking the salient features of biological structures (Vincent et al., 2006). Lessons learned from bionics state that success of natural inspired designs relies on effective embodiment: on clever morphology and use of material properties

(Eaton, 2008). Taking this in account, it is obvious that it is necessary to develop new human inspired technologies to enable this embodiment. In this way, full body humanoid robot development has been slowing down during last decade and the mechatronics research efforts have been redirected to solve more focused problems: artificial muscles, advanced materials, etc.

It has been demonstrated the feasibility of building full body humanoid robots. However, it has been recently paid attention to the second main issue involved in human being replication: the imitation of human behaviour. As described in Chapter 2, the main studies regarding physiology and human behaviour date back the turn of 20th Century. The advances achieved in the knowledge of the human organism during the last decades have made possible a better understanding of the underlying mechanisms that produce the different human behaviours. There is a variety of human behaviours and their classification is complex. In this work only physical behaviours related with movement will be considered. Attending to their nature, behaviours can be classified as innate or learned.

Innate or instinctive behaviours will be those, conscious or unconscious, that have a biological and genetic basis, are performed naturally, and are reinforced by practice. The human being has acquired this kind of innate behaviours thanks to thousands years of evolution, and they are “hard-wired” in the Central Nervous System. In general, instinctive behaviours are considered as “pre-programmed” responses triggered by external stimuli. They usually fit into one of the following categories (Meyer, 2006):

- 1) Reflex: it is the most basic innate behaviour. Correspond to the basic reflex arc involving only a few neurons.
- 2) Orientation behaviours: they are coordinated movements like walking, etc.
- 3) Kinesis: it is a change on the speed of movement or a change rate of turn which are directly proportional to the stimuli intensity.
- 4) Taxis: it is a movement directly toward (positive) or away from (negative) a stimulus.

Learned behaviours are skills acquired or modified by the experience resulting from a learning procedure. Taking this into account, it is obvious to conclude that innate and learned behaviours are close related by means of experience. The human being acquires new skills and knowledge through trial and error, observation of other individuals or memory of past events. In general, learned behaviours will always be (Meyer, 2006):

- 1) Non-heritable: behaviour acquired only through observation or experience.
- 2) Extrinsic: it is caused by social interaction.
- 3) Permutable: pattern or sequence may change over time.

- 4) Adaptable: it is capable of modification to suit changing conditions.
- 5) Progressive: subject to improvement or refinement through practice.

The better understand of the human postural control system operation has enabled the development of a large number of control schemes in cybernetic/robotic and biomechanical fields. In the former, theoretical and experimental situations as standing posture and free fall (Gorce, et al., 1995; Gorce & Vanel, 1997), walking (Fujimoto & Kawamura, 1995; Kajita & Tani, 1995; Kajita et al., 1992; Takanishi et al., 1990; Vukobratovic et al., 1970), run-to-walk and vice versa (Hodgins, 1991), (Hodgins, 1994; Raibert, 1986), have been studied considering static or dynamic 2D/3D problems. In the latter field, studies are focused on experimental postural analysis (Bouisset & Zattara, 1981), organization of the postural control (Nashner & McCollum, 1985) or biomechanical modelling to study postural control (McCollum & Leen, 1989), gait initiation (Brenière & Dietrich, 1992), musculoskeletal control (Van Der Helm & Rozendaal, 2000) or jumping (Levine et al., 1983).

These works are contributions for a better human behaviour understanding. They are studies about the dynamic equilibrium problem as part of more complex behaviours. These studies deal more generally with the selection of strategies to balance the external perturbation (force and moment) acting on the human structure. In these cases, the matter under control is the desirable posture during and after the performance of a voluntary movement. From the initial posture, the movement is the succession of instantaneous postures subjected to external perturbations. Then, the reactions against these perturbations are computed and deployed according to the response velocity required and the origin of the disturbance.

The postural state and the perturbations are captured by two sensorial systems or perceptions. The proprioceptive perception captures the internal state of the body, that is, the limbs position. The exoceptive perception senses the external perturbations from a variety of sources. All the perceptions are fed into the postural control system after a complex processing stage, performed by the own sensor organs and the brain processing centres. This complexity is solved by the postural control system in order to produce a properly response against perturbations.

It has been stated that human posture control is composed by the two main types of control loops. The first one, the closed or feedback loop maintains the posture and reacts to disturbances during slow movements. But this system is not enough to regain balance when fast reactions are needed. In this case, it exists a complementary open loop control system that helps to anticipate and to prepare the body against postural disturbances. This feedforward mechanism enables fast reflex and automatic reactions.

The development of humanlike machines has motivated a deeper research in human postural control systems. Early developments of humanoid prototypes were built to research the first postural problem humans must face up in the first year of their life: the equilibrium maintenance. The increase in computer processing power has enabled the fast development of these prototypes and the construction of full size humanoid platforms, which are able of performing complex postural tasks.

The step up in mechatronics and computing has favoured the development of high complexity control schemes and their transformation into ‘human inspired’ control systems. The final goal of these control schemes is to imitate the human behaviour as much as possible.

This human inspiration has caused a change in how the researcher considers the humanoid platform. The humanoid robot was only a mechatronic platform to test tasks and control schemes. Now, new robotic platforms have been developed to study the cognitive aspect of the human nature. In these platforms, the understanding of cognition and the analysis of how humans perceive the environment, how they interact within it and how the information is processed and applied, are the key point of control. This is one of the reasons why techniques, derived from the study of human behaviour, are taking more importance in postural control. Genetic algorithms, neuro-fuzzy controllers, etc. used in Artificial Intelligence are being applied in control, due to their similarity with real human processing.

During the last decade, the RoboticsLab research group has been introduced in the development of humanoid robots. The prototype RH-1 (Arbulu & Balaguer, 2010; Arbulu, Kaynov, Cabas, & Balaguer, 2009; Monje, Pierro, & Balaguer, 2009a, 2009b; Pierro, Monje, & Balaguer, 2008, 2009) was the first anthropomorphic mechatronics design carried out. It was useful to understand the challenging of the humanoid robot mechatronics and control design. With the new humanoid robot prototype TEO (Task Environment Operator), Roboticslab has applied lessons learned with RH-1. New improvements in mechatronics enable the change on the control philosophy from classical control techniques towards human behaviour inspired control.

This Thesis deals with this change and the development of human inspired control architecture for TEO humanoid robot. The first version of the control scheme deployed for TEO humanoid robot was a classic feedback control system to regain stability. It matches with the feedback loop in the human control schemes exposed in Section 2.3.4. The architecture proposed in this work adds the open feedforward loop to complete the human inspired postural control scheme.

## 3.2 Performing Humanoid Tasks

It has been exposed that human actions are a mixture of different kind of behaviours composed by simpler tasks. By means of the learning process, tasks become more complex and they enhance the human capabilities during growth. Thus, a task should not be considered simply as a succession of fixed motor patterns. It might be considered as a flexible, adaptable and configurable motor sequence that, as well, includes mechanisms for dealing with unexpected events.

In this way, TEO humanoid robot tasks are not mere sequences of joint angles, velocities and accelerations. There are complete sets of configurable modules established to enable the human inspired postural architecture. Figure 22 represents the structure of TEO tasks. One task frame is composed by a main movement, which can be configurated to perform different movements with the same shape. As well, the mechanisms to react against perturbations have been added by means of the

integration of motor patterns or synergies. Finally, it has been included a module which combines motion sequences, depending on the control requirements.

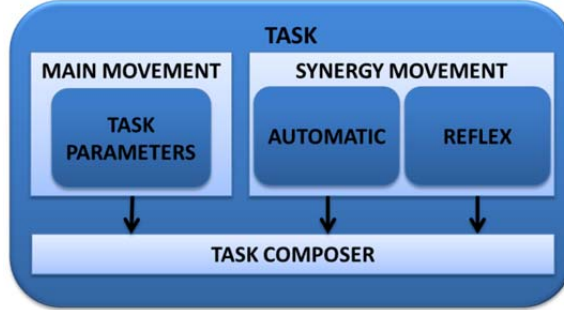


Figure 22 Humanoid task modules

Then, complex behaviours are those groups of tasks sharing one main characteristic that defines them. Thus, the study of postural control has been divided into manipulation and locomotion behaviours or groups of tasks. In Chapter 2 two specific task problems were introduced. These specific tasks have been selected from each one of those behaviours to illustrate and test the results obtained from development of this PhD Thesis.

### 3.3 Human Inspired Postural Control Architecture

The main objective of the Thesis is to propose and design novel human inspired and task oriented control architecture for humanoid robots. This development has been deployed for robot TEO which is the third generation of humanoid robots from RoboticsLab research group. The research in the field of humanoid robots started with the development of the platform RH-1. This mechatronic system integrates a postural control to maintain equilibrium during locomotion tasks. The high level control scheme is shown in Figure 23.

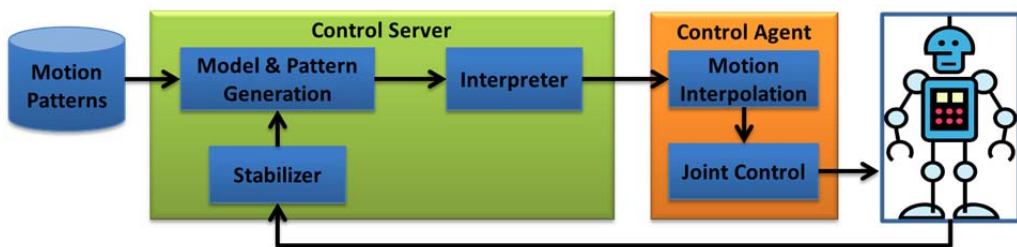


Figure 23 RH-1 Control architecture

In this scheme, a central pattern generator computes a statically stable locomotion task. It is composed by a sequence of joint positions or postures whose stability was ensured offline. These positions are transmitted to the joint controllers and executed. An internal joint control loop minimizes the posture position error. But this loop is not enough to regain balance if higher disturbances act over the robot. In this case, a second control loop for dynamic stability or 'stabilizer' maintains postural balance during locomotion by means of ZMP and CoM allocation control. The first loop

corresponds to the internal PID control of each individual joint. It is performed by the driver device that actuates every degree of freedom. Due to this nature, it is impossible to perform whole body postural corrections only with this loop. On the opposite, the ‘stabilizer’ considers the robot as a whole and it supervises the parameters influenced by the body dynamics. These parameters can be computed online thanks to the use of a simple inverted pendulum model that reduces significantly the processing time.

Another important aspect of this architecture is the availability of sensor data and its treatment. The only sensor devices integrated in the kinematic chain of the RH-1 robot are incremental encoders used to measure joint angles. This kind of sensors does not provide information about the dynamics of the robot. The use of the simplified model of the robot body helps to estimate the dynamics and its influence in balance.

The unfeasibility of obtaining direct sensor data regarding the body dynamics, such as limb accelerations, forces exerted on the body, etc., causes an increase of computing time. Due to this, the admissible level of perturbation is low and the time to reaction high.

Apart from the restrictions in control, RH-1 robot presented great limitations which did not allow a correct motion performance in terms of mechanical robustness (high joint looseness), stability, and energy consumption (necessity to be connected to the electrical net since battery could not supply the required energy for more than a while), not to mention the realization of high-level tasks such as manipulation, complex gait generation, or complex human-robot interaction (Monje et al., 2011).

TEO robot comes to substitute RH-1 humanoid robot to overcome its limitations. The design of the new platform turns the humanoid robot into a cognitive robot that enables the implementation of human inspired concepts. The novel postural control architecture proposed for TEO humanoid robot is compounded by two differentiated parts: the feedback and the feedforward control loops. It is shown in Figure 24.

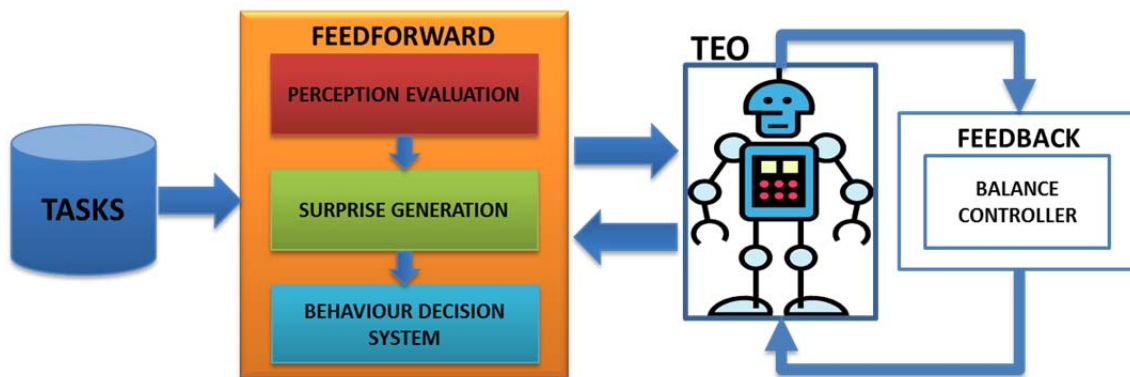


Figure 24 TEO Control architecture

This Thesis deals with the development of the feedforward control loop shown in Figure 24. It has been inspired in the architectures for human postural control system stated in Section 2.4. As commented before, human body has different levels of reaction depending of the required response velocity. Automatic and reflex acts are the fastest levels of reaction against disturbances. These reactions are activated by the inputs coming from the corresponding sensorial organs. The information from these organs is

transmitted to the processing centres in which the reaction is built. Once the response is composed it is sent to the muscles to perform the programmed action.

The novel TEO postural controller has been inspired in this operation and the mechatronic design of the robot supports it, as described in Chapter 5. In this way, the described ‘foundations of postural control’ are applied in TEO control architecture (Figure 24).

Apart from the levels of motor reaction, the basis of the postural control is the sensorimotor integration and the way of enabling it. As reviewed in Section 2.3.3, several theories have been developed to explain how the sensorial information is captured, processed and, executed through the corresponding action. Multiple systems are involved in postural control in a multilevel structure. Taking this into account, it has been established a sensorial evaluation module to compute the input information and to compose the named ‘perceptions’.

The exoceptive perception will capture the external perturbations (Table 2). This perception is composed by different sensor devices that accomplish the same function as one system of the human body (see Chapter 5):

Table 2 Human vs. humanoid exoceptive perception

<b>Exoceptive Humanoid System</b>	<b>Exoceptive Human System</b>
Inertial Measurement Unit (IMU)	Vestibular System
Force / Torque Sensors (F/T)	Muscles / Skin
Vision (3D cameras)	Vision

The proprioceptive perception measures the internal body status. The sensorial data is provided by joint position and velocity sensors (Table 3).

Table 3 Human vs. humanoid proprioceptive perception

<b>Proprioceptive Humanoid System</b>	<b>Proprioceptive Human System</b>
Relative Encoder	Joint Velocity
Absolute Encoder	Joint Position

Each perception is processed following psychophysics principles that relate physical stimuli with the corresponding sensation. The captured information must be processed, classified and integrated in order to command actions in the proper way. To evaluate the sensorial input using psychophysical principles, the perceptual process has been modelled considering perturbations as unexpected events or surprise events produced depending on the task context. This operation is performed by the module ‘surprise generation’ from Figure 24.

Another basic principle used in TEO postural control architecture is integrated in the module ‘Behaviour Decision System’. Based on the concepts of automatic and reflex reactions, this module modifies the actual task according to surprise events with the help of pre-programmed synergies. These strategies have been defined as quasi-static postural mechanisms learned by experience. The operation of this module is supported by the definition of task as complex behaviours stated in Section 3.2.

Based on these foundations, inspired in human postural control, the high level of the novel TEO postural control architecture has been developed and presented. Next sections study in depth every one of the modules outlined.

## 3.4 Perceptual Evaluation

TEO humanoid robot has been equipped with different sensing devices that provide the necessary information to compose the proprioceptive and exoceptive perceptions. The raw data coming from the sensors composes the robot sensations and it must be processed to be useful in postural control.

The result of the sensor data evaluation depends highly on the task being performed. It means that the resulting perception will not be the same if the task performed is, for instance, pure manipulation or pure locomotion. It is the task oriented perceptual system which filters the information and uses it in the proper way. Taking this into account, two premises can be established for TEO robot perceptual evaluation:

- 1) Same sensorial inputs will produce different perception depending on the task performed.
- 2) Exoceptive and proprioceptive perceptions will be composed by different sensorial sources depending on the task performed.

The first premise means, following psychophysical principles, that the processor centres filters the sensorial information to speed the result of the evaluation up and to produce an accurate response (detection, identification, discrimination and scaling). Second premise remarks the task dependant nature of the perception production as well. For instance, the use of data related with equilibrium is unnecessary in a manipulation task when the robot is seated.

Summarizing, not all information might be used in all cases and the information might not be applied in the same way in every task. Figure 25 shows the modules in charge of perceptive evaluation in TEO control architecture. Sensations composed by the information captured by sensory devices are evaluated forming the proprioceptive and exoceptive perceptions. Both sets of perceptual information is then available in the system to be used depending of the postural control necessities.

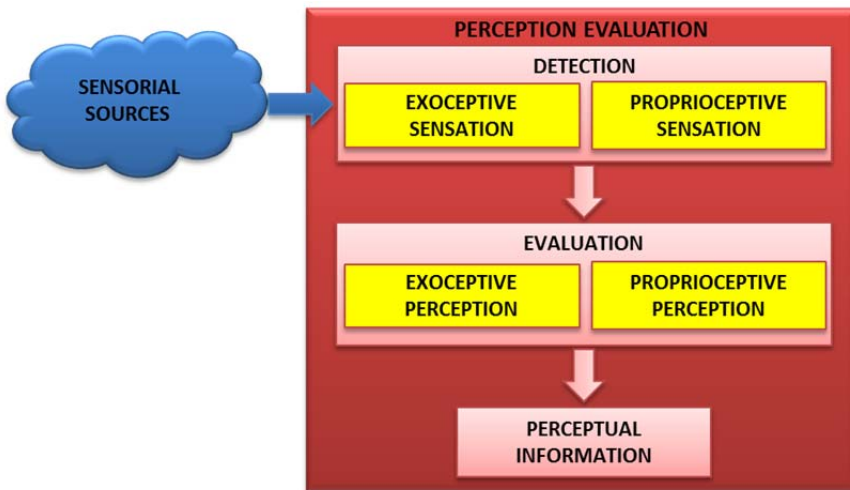


Figure 25 Perception evaluation

### 3.4.1 Sensation Detection

The first step to perform reactions against any perturbation is to perceive it. While sensation is related with the process through which the senses pick stimuli up and transmit them to the brain, the perception deals with the organization and interpretation of the sensed information.

The process to compose perceptions starts in the sensory receptors that detect and convert stimuli into electrical signals. The robot sensory system operates in the same way than the human's, following the same pathway. Complex sensing devices filter and discriminate stimuli for generating proper electrical signals. Then, such signals are transmitted to the processor centres where the information is turned into perceptions (Figure 26).

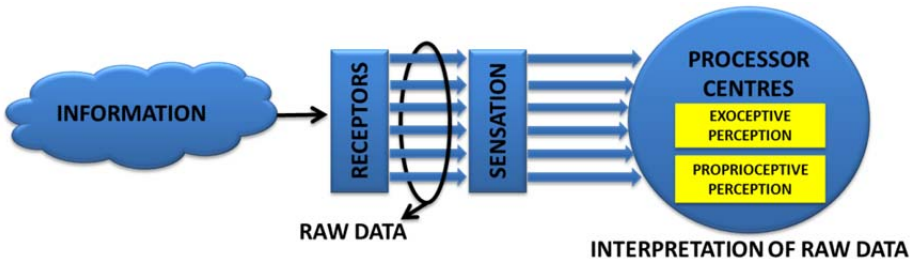


Figure 26 Sensations pathway

The production of sensations is performed by the electro-mechanic sensing devices. In most of the cases, the electronic devices have better performance capturing information and pre-processing it than the human sensory organs. But in the same way, it is necessary to establish some boundaries inside where the information to compose perceptions is relevant. It is performed using the psychophysics concept of sensory thresholds Figure 27.

Different levels of stimuli can be captured by sensory devices. The difference between the highest and lowest levels establishes the measurement range. But all this range is not always useful. It depends of the sensation to deploy. There exist threshold values that determine if a sensation must be produced or even if it is too high. In the first case, the lowest threshold establishes the minimum relevant perturbation level from which the corresponding perception would be obtained. On the opposite, the highest threshold indicates that stimuli above this level saturate the sensation and the subsequent perception.

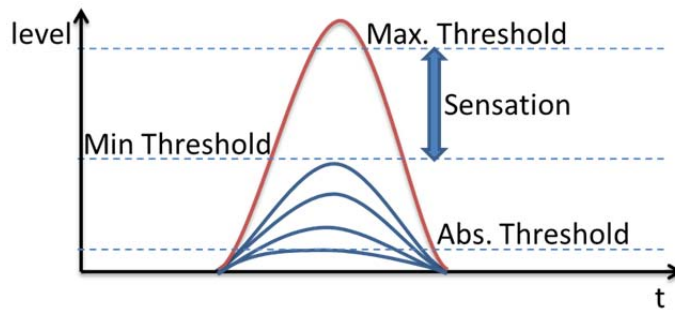


Figure 27 Sensation Thresholds

Related to the signal measurement, the absolute threshold corresponds with the smallest detectable level of stimulus which could not coincide with the minimum useful value. The last important concept is related to the difference threshold that indicates the minimum change between two stimuli to conclude they are not the same.

All these concepts are related to each sensory device performance and, more important, to the task the perception is composed for. The main advantage of this procedure is to rule out unnecessary sensations for the task under question. For instance, ankle forces used for ZMP evaluation are unnecessary while robot is seated. It reduces the data to be processed and increases its performance.

Once the sensation is composed by the raw sensor data, it must be classified, evaluated and converted into perceptions. This process is constraint by the nature of the scheme established, in which the perceptions are task dependant.

### 3.4.2 Perception Evaluation

The concept of sensation is related to each individual sensory device and the process of capturing information. Firstly, the electro-mechanic transducers convert stimuli into electrical signals. At this stage, the raw data is still inside the sensory device. Previously to be dispatched to the central processor system, this data is interpreted to compose computer understandable sensorial information.

This pre-processing constitutes one important difference with the human sensorial system, in which the sensor devices transmit only electrical impulses to the processor centres where the information is interpreted. The result of the sensation detection is a stream of information from the each sensory device transmitted using the proper format and protocol.

This stream of information from every device is at the processor centres disposal. But the sensorial information is not completely useful at this time. Every sensing device provides information about a particular kind of stimuli that can come from internal or external sources. Taking this into account, the first task of the processor centres is the classification of the sensorial information depending on its origin. The result of this reorganization is the composition of the proprioceptive and exoceptive perceptions. They are sets of interpreted sensorial information classified by the origin of the stimuli and they are available in the system for being used.

### 3.4.2.1 Proprioceptive Perception Evaluation

The proprioceptive perception is composed by sensations coming from ‘inside’ the body. This information is collected by absolute encoders, located in every DoF, that measure the relative angle between two adjoins links of the robot. These angles are measured taking into account the upright stance posture as the ‘home’ posture for the robot. The proprioceptive perception is divided in two groups due to the disposition of TEO robot hardware architecture: upper and lower body proprioception. They are used in the different task according to Figure 28.

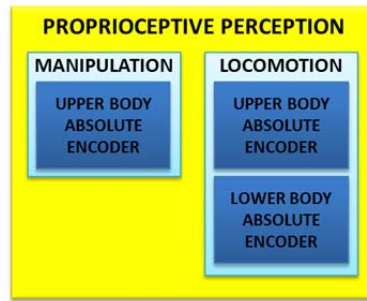


Figure 28 Components of the proprioceptive perception

The sensorial information is transmitted to two processor units to compute the upper and lower proprioception independently. It speeds the proprioceptive evaluation up and it simplifies the output of the sensorial evaluation, improving postural control performance. Then, this proprioception is obtained by means of two neuro-fuzzy evaluation systems. Each one computes one of the body groups in which the robot has been divided Figure 29.

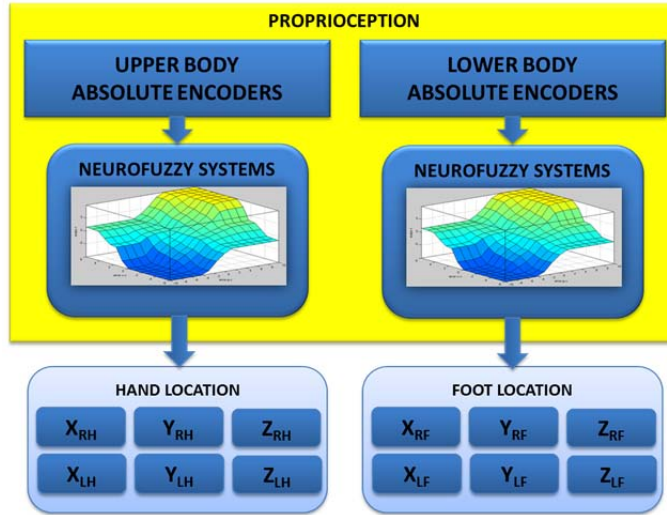


Figure 29 Body limbs location evaluation

The evaluation of the upper body absolute encoders outputs the hands location. Meanwhile, the feet location is obtained after the evaluation of the lower body absolute encoders' information. In this way, the proposed system evaluates the forward kinematics of each extremity using the human-like computing style of fuzzy systems.

### 3.4.2.2 Exoceptive Perception Evaluation

The exoceptive perception in TEO robot is composed by sensations coming from Force/Torque sensors, an Inertial Measurement Unit (IMU) and the vision sensor (Kinect™). These sensory devices will be described further in detail in Chapter 5. Following the task oriented system concept, the exoceptive perception is composed by different sets of information from the available sensorial sources. Figure 30 shows the basic tasks established and the sensors involved in composing the exoceptive perception in each case. This chart exposes, for instance, that vision system is applied in both manipulation and locomotion tasks. In this case, the sensorial device is the same but the set of information used in each task is different.

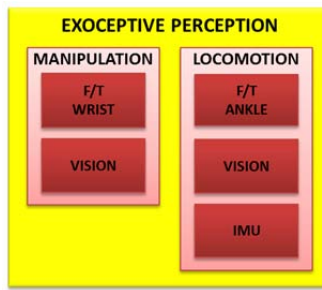


Figure 30 Components of the exoceptive perception

As well, same perceptual sets can be composed by different sensory devices. This is the case of the sensation about forces exerted on the robot. F/T sensors and the IMU device capture information about the same sensorial source and the information they provide is complementary. This issue enriches the resulting perception.

In this way, the Inertial Measurement Unit, allocated inside TEO robot torso, provides direct information about robot movement and, as well, it can be used to determine the

movement tendency. Figure 31 illustrates which the outcomes from IMU sensation evaluation are.

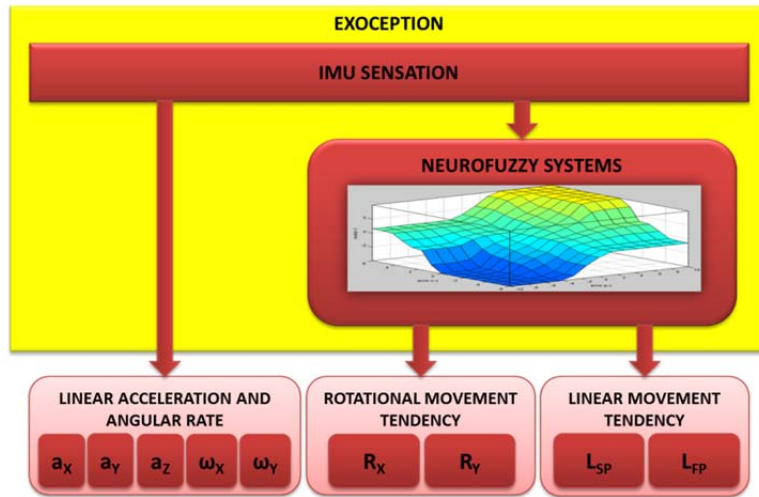


Figure 31 Inertial measurements evaluation

Rotational and linear movement tendencies must be computed from angular rate and linear acceleration respectively. Both movement tendencies are affected by inclination and gravity of the sensor device. Therefore, these parameters must be corrected to eliminate these errors. The results are the movement tendencies in the sagittal and frontal planes directions. These outcomes are evaluated, following the human inspiration concept, by neuro-fuzzy systems. The other devices that measures forces exerted on the robot are the F/T sensors. These sensory devices measure reaction forces and torques in the ankles and the wrists. That is, this kind of sensors measures the interaction between bodies.

In the case of wrists, the sensors capture the information related with the contact between the robot hands and the manipulated object (Figure 32). Furthermore, this data could be used to estimate the characteristics of objects, such as weight, or the interaction impact over the manipulation task and the robot arms (payload limit, etc.)

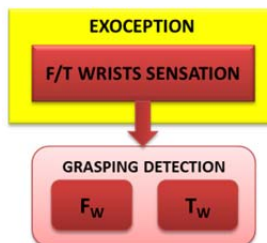


Figure 32 Wrists forces and torque measurements evaluation

The ankle F/T sensors are only applied in locomotion tasks because they measure the ground reactions. Three main outputs are obtained from these sensors (Figure 33). One of them is obtained directly and it indicates the support phase during locomotion. The other two outputs are processed by the corresponding neuro-fuzzy system. The processed outputs compute the ZMP actual location and the feet angles on the ground. The reaction forces and torques measured by these sensors are useful to compute the ZMP location that denotes the actual balance state of the robot. Taking into account

the possible ZMP movement, which is the result from the IMU data interpretation, the future robot balance status can be previewed and reactions can be anticipated.

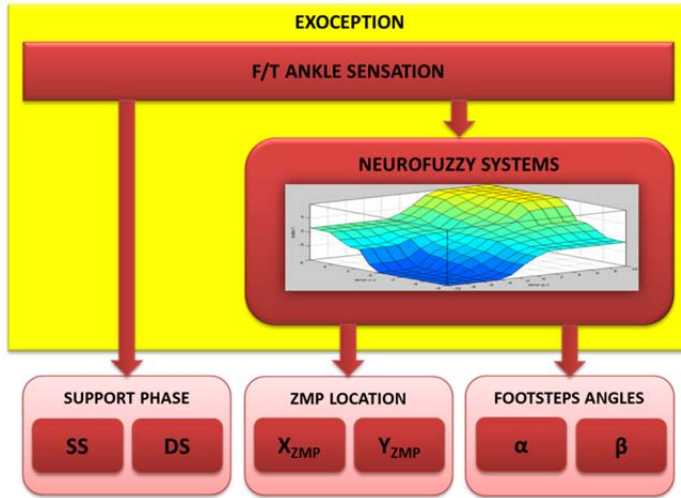


Figure 33 Ankles forces and torque measurements evaluation

The last exoceptive perception evaluation is related with the vision system. This is the only system capable of extracting some information from distant objects and the environment without contact. The goal of this evaluation is to obtain the location of the corresponding work object and, whether it is in movement, to determinate its trajectory. The high level scheme for evaluating this information source is shown in Figure 34.

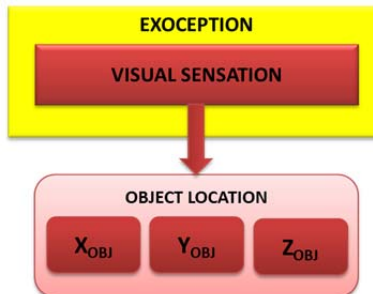


Figure 34 Objects movement evaluation

## 3.5 Surprise Generation

It has been described how sensory devices generate raw data called sensation and, after pre-processing, the information is organized into perceptions. In this stage, only perceptions are available. Now, the problem is how to apply all this information in postural control.

The mechanism established in the feedforward loop to trigger reactions is based on the evaluation of surprising events. Perturbations can be considered as unexpected events and, the output of its processing, the activation of a surprise (Ortony & Partridge, 1987). Then, the information from perceptions is the base for this evaluation. The

system selects and combines information from the available sets, depending on the necessities of pre-established output surprises.

Nevertheless, the concept of surprise is a high level envelope that explains the process of any kind of unexpectedness. Taking this into account, surprisingness is generated by lower level mechanisms called expectations. The failure of a determined expectation elicits a surprise event. The expectation failure can be classified in:

- 1) Active expectation failure or prediction failure. It is produced when a prediction about an outcome has not been produced by an input proposition.
- 2) Passive expectation failure or assumption failure. It is caused when an outcome, originated by a determined input proposition, is not predicted but some assumptions about it can be established. If this output doesn't fit into these assumptions, the surprise should be elicited.
- 3) Unanticipated incongruity. It is related to unexpected events never experimented before.

To clarify these concepts the manipulation case will be used as example. When the robot performs the task of 'throwing a ball and catch it' the normal behaviour is considered when the ball goes straight up and falls straight down to any point very close to the initial position (Figure 35).

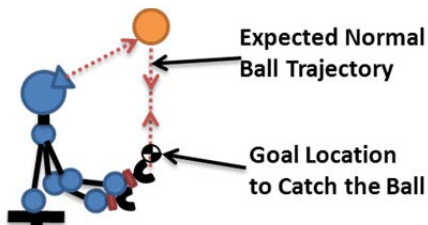


Figure 35 Normal 'throwing a ball and catch it' task

Nevertheless, unexpected deviations can occur during the fly of the ball. This unexpected situation causes surprise or an expectation failure. Taking into account the normal task behaviour established, the expected ball's trajectory can be predicted at any time ( $t_{k+T}$ ), as exposed in Figure 36. In this case, in order to anticipate the hand movement, the prediction failure event should be elicited when the evaluated distance between two consecutive predictions exceeds an established threshold. Then, high deviations can be detected with anticipation and an automatic complex synergy could be triggered in order to solve this issue.

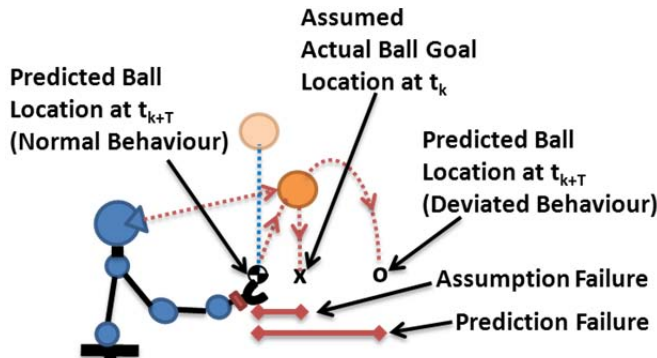


Figure 36 Deviated ‘throwing a ball and catch it’ task

At the same time, the system is able to measure the ball’s location and, as well, the hand’s location in a determined time period ( $t_k$ ). Whether we consider valid the assumption of straight line fall trajectory at any time, it is possible to compute the distance between hand and the assumed ball falling location (Figure 36). Then, the assumption failure will drive a reflex reaction with the aim of correcting the hand location as fast as possible.

Therefore, the reaction movements performed to solve both situations to catch the ball properly are considered reactions driven by surprise events.

Passive and active expectations require a certain degree of previous knowledge about the matter that can cause surprise. These two forms of expectation failures have been considered to be applied for surprise generation in TEO robot (Figure 37). Unanticipated incongruity implies the integration of other kind of intelligent module that will be able to classify the event and to learn about it.

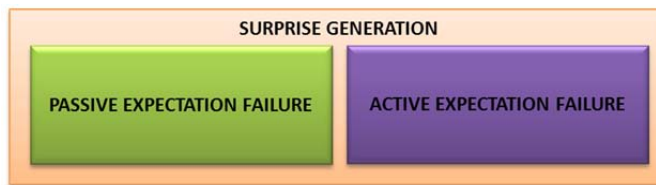


Figure 37 Surprise generation modules

In this way, passive expectation failure module will produce surprise events when some predefined thresholds will be exceeded by the input proposition. In the case of active expectation, predictions about critical issues related with tasks performance are continuously verified. Then, the surprise event is triggered if these predictions fail, always taking into account the task context.

### 3.5.1 Passive Expectation Failure

The passive expectation failure or passive assumption is produced when it is not possible to form previous expectations about an input proposition. It is the case in which sensorial inputs are compared with assumed operating thresholds. These expected levels are not defined by predictions but by the context of the robot (task, environment, etc.).

Surprise occurs when a task does not follow a perceptual parameter that has been identified. Each perceptual parameter has associated different thresholds to compare the level of unexpectedness. Figure 38 shows the surprise events established for manipulation and locomotion tasks.

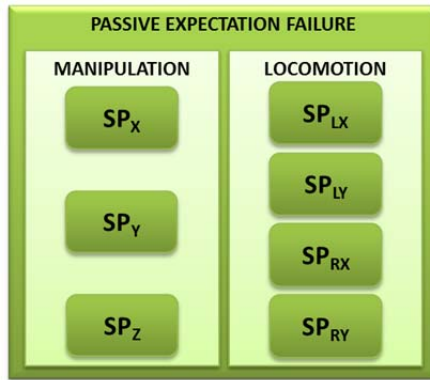


Figure 38 Passive expectation failure

In the case of manipulation tasks, the surprise is related with the location of the working object and it is driven by the visual perception. The location of the object is estimated by the vision system and its distance to the hand is evaluated. The surprise ( $SP_x$ ,  $SP_y$ ,  $SP_z$ ) is then produced whether any of the coordinates of the object differs from the final location when a straight down trajectory is assumed. In this case, the evaluation of the height of the ball can also be used to decide if the manipulation task can be achieved or should be stopped because the object is under the minimum admissible height.

For the locomotive tasks, the passive expectation failure is related with the movement tendency of the robot. The surprise events are elicited when linear ( $SP_{lx}$ ,  $SP_{ly}$ ) or rotational ( $SP_{rx}$ ,  $SP_{ry}$ ) movement exceed the established thresholds to keep robot balance.

In summary, this kind of surprise events is generated by a comparative process between the perceptual inputs and established limitations related with the operating context.

### 3.5.2 Active Expectation Failure

The active expectation failure or prediction failure is produced by the mismatch between the input proposition and the predicted one. In this case, perceptual inputs may be computed to obtain an anticipatory prediction of the possible robot future state that might be compared with the actual state. The grade of the surprise event will depend on the level of disparity between the input proposition and the predicted one, from the basis of no surprise until a 'panic' level.

In this case, the complexity of the perceptual inputs, the composition of the prediction and the comparison between both increase the surprise generation latency. The surprise events for manipulation and locomotion are shown in Figure 39.

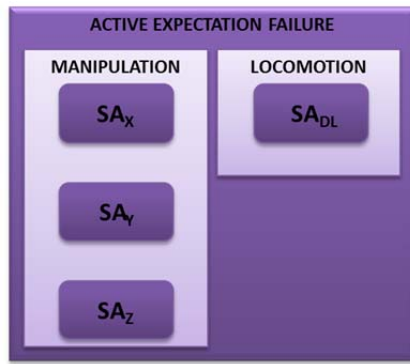


Figure 39 Active expectation failure

The prediction for manipulation task is related with the final location of the object. The comparison of the actual perceived hand location and the predicted goal position will elicit a graded surprise event. The aim of this surprise generation is to anticipate the arm movement towards the goal location in order to catch properly the object. For the locomotion task, the prediction is related with the future location of the ZMP and, therefore, the evolution of the stability. This surprise information will be applied in the pre-selection of possible future strategies to keep balance.

### 3.6 Behaviour Decision System

At this stage, there has been described how perturbations are perceived by the sensorial system. After that, it has been introduced the system which transforms sensations into ‘understandable’ information (perceptions). At last, perceptual information is interpreted and converted into surprise events that will be used by the control system to act against perturbations.

But, before of performing the high level description of the behaviour decision system, it is important to define what is understood by ‘reactive behaviour’ or reaction. The postural control system developed in this Thesis adds an anticipative component to the classical feedback control loop. Meanwhile, feedback loops are clearly reactive systems this nature is not obvious in the case of the predictive system. Besides, the term ‘reaction’ is usually understood like an action opposed to a perturbation performed for correcting a deviation from an expected behaviour.

The decision system should anticipate a behaviour that will help the system to achieve the goal of a task. Therefore, it cannot be considered strictly a reactive system because it doesn’t act against something that has just happened. Then, taking into account all these considerations, the use of the term ‘reaction’ should not be used for the output of this decision system.

However, the anticipated actions deployed by the decision system can be defined as reactions against future consequences evoked by sensorial stimuli. That is, given a determinate task, it is possible to know so the correct behaviour as the deviation caused by determined perturbations. It means that the perceptual knowledge will drive the decision because the consequence of the perturbation is previously known. Then, it is possible to say that the anticipative postural control system reacts against the future task state.

Therefore, inside the behaviour decision module, the surprise events are processed to decide:

- 1) If any kind of future action or reaction is needed.
- 2) The kind of reaction that would be the most appropriate.
- 3) How the selected reaction should be performed.

By means of evaluating the information from active and passive expectations (surprise events), it can be determined if a reaction might be selected and executed. The reaction is selected among all available motor synergies related with the corresponding task. These synergies are motion patterns that are filled in using the results from the expectations evaluation (surprise task parameters). The outcome of this module will be a parameterized synergy that could be executed to enhance postural control. The high level operation of this behaviour decision module is shown in Figure 40.

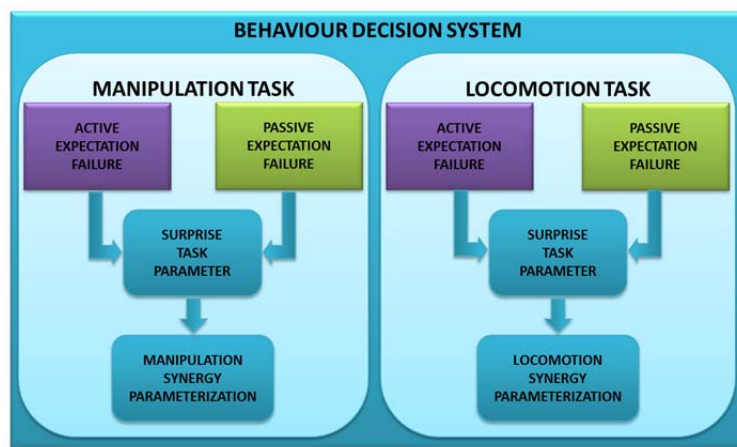


Figure 40 Behaviour decision module

The three kinds of decision subjects the system must perform and the basic operation described are close related with the kind of task, as it is shown in Figure 40. Thus, it is important to describe how this system performs the decision process in each kind of task.

In the case of manipulation tasks proposed, the decision of the anticipative system is not related to the reaction against any perturbation but to the correct finalisation of the task. The proposed task consists of throwing a ball up and catching it before it falls to the ground. This kind of task has two phases. The first one is the programmed or voluntary movement. This is the conscious movement of throwing upwards the ball. The second phase corresponds to an unconscious movement driven by the evaluation of visual stimulus. The visual sensation, captured by the visual sensors (the eyes in the human case), is transformed into a visual perception about the approximate measure of the location of the object during its flight. At the same time, the location of the hand with which the task is being performed is measured by internal sensors. Both kinds of perceptual information are merged and evaluated. A surprise event is elicited whether there exists any kind of difference between hand and object location. Then, this event will be used to select a predefined reaction and the level of the parameters (i.e. joints

velocity) to carry out a corrective arm movement. Thus, this reactive behaviour is driven by surprise.

The locomotion postural control is related to upright stance and normal walking tasks because, even though they are basically different, they are close related. These two kinds of locomotion problems face the reaction against disturbances in two different ways. Both control problems use the same sensorial sources and their derived perceptions. Nevertheless, the main difference arises when the decision process about reactions must be performed. It is caused by the high difference on the dynamics conditions of each situation. While upright stance is a completely static posture, locomotion is dominated by dynamics. These conditions will influence the evaluation of the inputs during decision process and the recommended reaction. It means same levels of surprise evaluated will not produce the same decision results and the reactions derived from these decisions will be, as well, completely different. Thus, the set of synergies or predefined movement patterns composing reactions is related with the dynamical constraints of the task and it will be different in each case. The upright stance and the postural sway control is an intensively studied problem in the biomechanics field. Different strategies have been demonstrated to be involved during sway balance control, such as the ankle or the step synergies. On the other hand, postural control on dynamic walking is related to the movement of the Centre of Masses and the reactions will be focused on the modification of its movement characteristics. Thus, two behaviours can be established for the locomotive reactions, which are not surprise driven but surprise based. The reactions can be substitutive, when the current action is stopped and replaced by the reaction execution, or additive, when the reaction is a movement added to the action being performed.

Further on, the decision system will be developed more in detail based on the task behaviour described.



## CHAPTER 4

# Foundations for Postural Control

## 4.1 Basic Principles of Humanoid Postural Control

The humanoid robot control problem can become extremely complex depending on the specified desired behaviour and the structure of the system. This control problem has been usually divided into two main sub-problems: biped locomotion and dexterous manipulation. This division is caused by the complexity of both problems and the necessity of study each one avoiding mutual interferences.

As described in the introductory chapters, the humanoid robots performance can be compared with humans in a variety of aspects. The main factors to be compared are the sensorial caption, the information processing and the execution of actions. Regarding sensorial information caption, artificial sensor devices have even better features than human sensors but a precise and huge amount of information available is not always needed. The main advantage of the human system compared with the robot's one is the vast capacity of the first one to process information in parallel. The last factor, the actuator system, may have the same performance regarding speed but the number of degrees of freedom is far from the human being's. Taking this into account, the way to increase the humanoid robot performance must be achieved by the information processing improvement. This can be achieved applying the following improvements:

- 1) Sensorial information processing improvement: fast mechanisms to evaluate information from sensor devices must be studied.
- 2) Task dependant filtering: the redundant and unnecessary sensorial information can be discarded. This reduces the amount of information to process and increases its speed.
- 3) Prediction of reaction: the outcome of the system may be a prediction of the reaction that can be executed if a trigger level is exceeded.

The biped locomotion question corresponds not only to the study of dynamic posture (walking, running, etc.) but to static posture during standing with or without small voluntary lean movements. Humans are capable of maintaining postural stability over a wide range of complex scenarios and body configurations, correcting the body posture through a process of rejecting (and sometimes accommodating) external disturbances

and self-induced perturbations. This is mainly achieved by activating the appropriate strategy to overcome the perturbation.

The study of manipulation problem usually is performed with the help of static or wheeled platforms to avoid the necessity of maintain balance. But a whole anthropomorphic machine is necessarily composed of both locomotion and manipulation systems (legs and arms). During manipulation tasks, the interaction with objects or with the environment generates reaction forces applied to the robot body. In this way, the manipulation subsystem, that is, the upper body of the humanoid robot is as well source of postural perturbations.

This Chapter deals with the underpinning principles of humanoid postural control. These basic principles are already applied in most of the existing humanoid platforms, but usually from an engineering point of view.

As outlined in previous chapters, humanoid postural control system can have a human inspired design, incorporating the core principles of human postural control to the humanoid robot. This human inspired principle has been considered to evaluate all issues involved in TEO robot control. In following sections, topics such as reference points (CoM, ZMP, etc.) or simplified robot models, such as the simple inverted pendulum used in postural control, are briefly revisited.

Additionally, the foundations on computing that enable the processing of information to perform postural control will be briefly exposed. The computation techniques exposed are inspired in human behaviours and processing procedures, which are important premises for this Thesis.

## 4.2 Human Dynamics Foundations

Postural control principles in humanoid robots have been improved during last decades thanks to a deeper knowledge about human behaviour. Modern techniques have enabled complex investigations, simulations and analysis of results. This section presents some of these foundations that were applied in the development of this PhD Thesis.

### 4.2.1 Human Dynamics Simplified Models

Because of the humanoid robot is a complex machine, the study of its behaviour requires a lot of computation capacity. Favoured by this limitation, different simplified models of the mechanics and its behaviour has been developed. Many investigations have demonstrated that human postural control system acts with the same principles from these simplified models (Gage, et al., 2004; Kuo, 2007; Kuo, Donelan & Ruina, 2005).

The use of robot body simplified models enables a faster system development and it reduces the analysis complexity. Two different simplified models have been applied during the development of the novel human inspired architecture proposed in this PhD Thesis: the 2D simple and 2D double inverted pendulums.

It was decided to use 2D models instead 3D models because the bio-inspired technique applied in the system development favoured the decomposition of robot movement into frontal (X) and sagittal (Y) planes. Moreover, the computing of the reference points exposed in Section 4.2.2 gains the advantage of using these models.

Next, both models and the equations for obtaining the required information about their movement are briefly presented.

#### 4.2.1.1 The Simple Inverted Pendulum

The simple inverted pendulum is the most basic model but it has multiple uses in humanoid robotics. It is applied from biomechanical analysis of movement to postural or balance control in humans and biped robots. As can be seen in Figure 41, it consists of a mass (M) linked to a pivot point (o) by means of a massless bar of longitude (L).

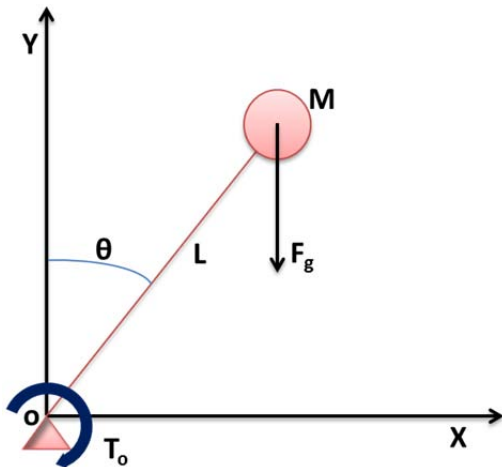


Figure 41 2D simple inverted pendulum

The punctual mass M is the total mass of the modelled system concentrated in the Centre of Mass (CoM) of such system and the longitude L is the distance from the pivot to the CoM. If gravitational force ( $F_g$ ) is considered the only force acting in the system, the movement of the inverted pendulum will be:

$$\sum T_o = I \cdot \ddot{\theta} = M \cdot L^2 \cdot \ddot{\theta} \quad (4.1)$$

$$T_o = F_g \cdot L \cdot \sin \theta = M \cdot g \cdot L \cdot \sin \theta \quad (4.2)$$

Combining (4.1) and (4.2):

$$M \cdot g \cdot L \cdot \sin \theta = M \cdot L^2 \cdot \ddot{\theta} \quad (4.3)$$

$$\ddot{\theta} = \frac{g}{L} \cdot \sin \theta \quad (4.4)$$

This dynamics equations correspond to the two dimensional case. It can be extended to the three dimensional case (Kajita, et al. 2001). The high simplicity of this model implies loss of information from the real system. To solve this issue, more complex models based on simple inverted pendulum has been developed, such as the double inverted pendulum from Figure 42, the Reaction Mass Pendulum (S. H. Lee & Goswami, 2009) or the Variable Impedance inverted pendulum (Sugihara & Nakamura, 2003).

#### 4.2.1.2 The Double Inverted Pendulum

The double inverted pendulum increases the complexity of the simple inverted pendulum. It is composed by two punctual masses ( $M_1$ ) and ( $M_2$ ) joint by massless links ( $L_1$ ) and ( $L_2$ ). The upper mass ( $M_2$ ) models the upper body with all mass concentrated in the CoM of this substructure and, the lower mass ( $M_1$ ) models the lower body in the same way. Thus, the double inverted pendulum has 2DoF that usually correspond to ankles (o) and hips (1) joints. Figure 42 shows the 2D double inverted pendulum structure.

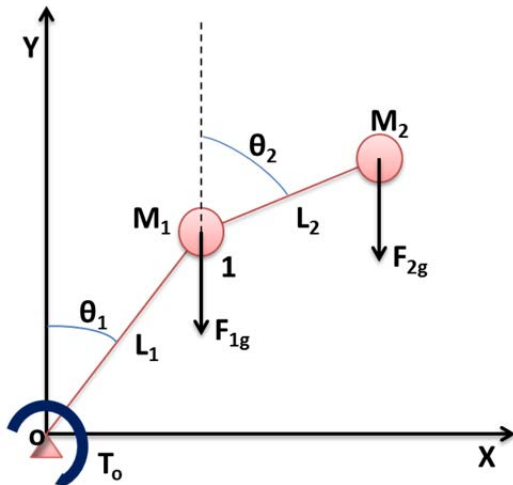


Figure 42 2D double inverted pendulum

Considering only gravitational force action on the system, the equations of its movement are:

$$\vartheta = \theta_1 - \theta_2 \quad (4.5)$$

$$M_2 L_2^2 \ddot{\theta}_2 + M_2 L_1 L_2 \dot{\theta}_1 \cos(\vartheta) - M_2 L_1 L_2 \dot{\theta}_1^2 \sin(\vartheta) - M_2 L_2 g \sin(\theta_2) = T_0 \quad (4.6)$$

It is clear that the dynamics of both parts of the pendulum are coupled, which increase the complexity of its control. By the other hand, this model represents more accurately the humanoid robot structure, considering the manipulative and locomotive parts separately. The double inverted pendulum is more appropriate when the control strategies require more information about dynamics (Bardy, et al., 2002; Kaynov, et al., 2009; Stephens, 2007) or it is necessary to model the manipulative part of the robot as well as the locomotive one.

## 4.2.2 Reference Points

The way humans cope with disturbances is clearly a learned set of behaviours. The operation of the human postural control is still under study and it is not completely unravelled. One of these topics under study is how human postural control uses the sensorial information to maintain balance.

The study of body kinematical and dynamical properties has established the existence of different particular reference points which characterize the consequences of movement in balance control. In fact, inside the humanoid robotics field, it is necessary to represent, compute and measure sensorial information to quantify this kind of parameters involved in the postural control law.

The development of this novel human inspired and task based postural control architecture is related to the study of two specific reference points (Figure 43). The first one is the Centre of Masses (CoM) that simplifies the body structure. The second one is the Zero Moment Point (ZMP) which is one of the most used indicators of postural stability. The study and use of these reference points has been boosted by the challenge of developing walking robots and the necessity of balance control during its locomotion. As they characterize the evolution of posture, their application in this Thesis is fundamental for anticipating the consequences of postural disturbances.

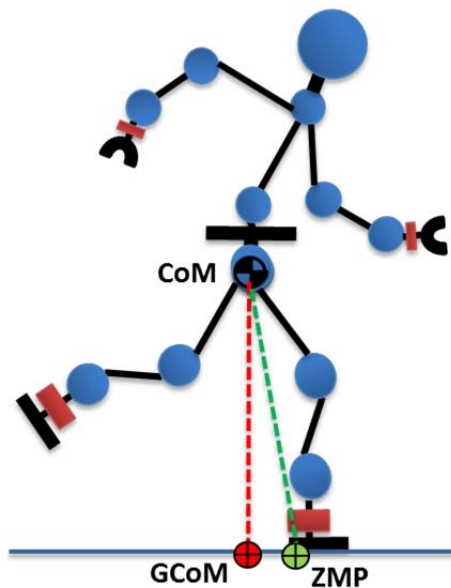


Figure 43 Reference Points

### 4.2.2.1 The Centre of Mass (CoM)

The centre of mass (CM or CoM) is the average position of a multi body system's mass at every instant in time (Ruina & Pratap, 2010). From the dynamical point of view, it is the point in which the resulting external forces and torques can be considered to be applied on. At the CoM, the net external force on the robot is non-zero, but the net torque on the robot will be exactly zero. The location of the CoM for an n-link robot can be calculated by equations from (4.7).

$$x_{CoM} = \frac{\sum_{i=1}^n m_i x_i}{\sum_{i=1}^n m_i}; y_{CoM} = \frac{\sum_{i=1}^n m_i y_i}{\sum_{i=1}^n m_i}; z_{CoM} = \frac{\sum_{i=1}^n m_i z_i}{\sum_{i=1}^n m_i} \quad (4.7)$$

Where  $m_i$  is the mass of the  $i$ -link and  $P_i = (X_i, Y_i, Z_i)$  is the position vector of the centre of mass of the  $i$ -link.

Taking the  $X_{CoM}$  and  $Y_{CoM}$  component and setting the  $Z_{CoM}$  component to zero, the projection of the CoM on the floor (GCoM) can be described with:

$$GCoM = \frac{\sum_{i=1}^n m_i p_i}{\sum_{i=1}^n m_i} \quad (4.8)$$

$$\sum_{i=1}^n (GCoM - p_i) \times m_i g = 0 \quad (4.9)$$

In quasi-static the case, if the GCoM remains within the support polygon the humanoid robot will not tip over or fall. However, when the motions become faster, the dynamic forces increase their importance and this criterion is not sufficient anymore to ensure postural stability (Dekker, 2009).

#### 4.2.2.2 The Zero Moment Point (ZMP)

Zero Moment Point is one of the basic reference points in postural balance. It is under continuous study and improvement because the understanding of its behaviour constitutes one important foundation for postural control. Thus, there exist multiple definitions accepted for describing the Zero Moment Point but they all have in common that the ZMP is the unique point for which the resulting moment is zero:

$$\sum T_x = 0 \quad (4.10)$$

$$\sum T_y = 0 \quad (4.11)$$

Where  $M_{x,y}$  are the moments about X and Y axis generated by the ground reactions caused by forces and torques acting on the body (Vukobratović et al., 2008). Alternatively, the ZMP can be thought to be that point inside the support area where the net moment, produced by any kind of force or moment acting on the robot, has no component along the horizontal axes. The ZMP as a function of the CoM position, net CoM force and net moment about the CoM can be expressed as:

$$x_{ZMP} = x_{CoM} - \frac{F_x}{F_z + Mg} z_{CoM} - \frac{T_y(\vec{r}_{CoM})}{F_z + Mg} \quad (4.12)$$

$$y_{ZMP} = y_{CoM} - \frac{F_y}{F_z + Mg} z_{CoM} - \frac{T_x(\vec{r}_{CoM})}{F_z + Mg} \quad (4.13)$$

Where  $M$  is body mass,  $T_x/T_y$  are the components of the moment about the CoM and  $g$  is the gravity acceleration. Equations (4.12) and (4.13) define the ZMP location on the ground within the support area in either the single or double support phase during locomotion. The computation of these equations implies the knowledge of the CoM location and actions exerted on the body. The first issue is usually solved by means of using one of the simplified models exposed before. The second issue is related to the measurement of the forces and torques acting against the body. This is solved thanks to the use of sensors. Inertial sensors provide information about characteristics of motion caused by voluntary postural changes or external forces. Then, modelling the

body like a simple inverted pendulum, the ZMP can be expressed as function of the acceleration of the CoM as:

$$x_{ZMP} = x_{CoM} - \frac{z_{CoM}}{g} \ddot{x}_{CoM} \quad (4.14)$$

$$y_{ZMP} = y_{CoM} - \frac{z_{CoM}}{g} \ddot{y}_{CoM} \quad (4.15)$$

Taking into account the previous definition of ZMP, it is also possible to compute it measuring the reactions on the support base. It can be achieved by means of force and torque sensors. Specifically, the use of this kind of sensors in the robot ankle structure enables this ZMP computation (Figure 44).

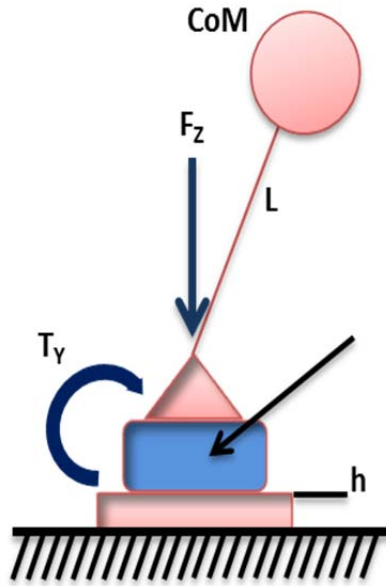


Figure 44 Model for ZMP computation using F/T sensor measurements

Then, based on the model from the previous figure, the ZMP can be obtained applying the equations (4.16) and (4.17).

$$x_{ZMP} = \frac{T_{pitch}}{F_z} + \frac{h \cdot F_x}{F_z} \quad (4.16)$$

$$y_{ZMP} = \frac{T_{roll}}{F_z} + \frac{h \cdot F_y}{F_z} \quad (4.17)$$

These equations are only valid for one sensor and, hence, they can be only applied to compute ZMP in single support phase. In the case of the double support phase, it is necessary to calculate the weighted average of the sensor measurements from both legs. The resulting equations for ZMP are (4.18) and (4.19)

$$x_{ZMP} = \frac{T_{pitch}^R \cdot X^R + T_{pitch}^L \cdot X^L}{F_z^R + F_z^L} \quad (4.18)$$

$$y_{ZMP} = \frac{T_{roll}^R \cdot Y^R + T_{roll}^L \cdot Y^L}{F_z^R + F_z^L} \quad (4.19)$$

One condition to ensure postural stability is the location of the ZMP inside the support area. But this condition is not always necessary to ensure stability. ZMP location changes with the body motion and it can be sometimes located outside the convex hull of the support area. Then, it is renamed as Fictitious ZMP (FZMP) because, in reality, the ZMP can only exist within the support polygon (Dekker, 2009) and, considering strictly the ZMP definition, whether the ZMP reaches the supporting are edge, the humanoid robot could turn over.

## 4.3 Human Inspired Soft Computing

Classical methodologies for systems control are based on the knowledge of the system behaviour from which analytical and mathematical models can be established. These methodologies are based on the development of mathematical theories that dealt with over-idealized approximations of the control problems bearing little relation to theory (Zadeh, 1962). But this approach is not feasible when the system complexity is high or when the methods should cope with imprecision, uncertainties and partial truth. Modern relativism remarks the human ability to understand distortions and make rational decisions in an environment of uncertainty and imprecision (Zilouchian & Jamshidi, 2001). This is the basis for defining an intelligent control methodology.

Taking this into account, “soft computing” can be defined as a set of methodologies that deals with uncertainty, approximation and partial truth in order to get feasibility, robustness and low solution cost (Zadeh, 1994). In traditional hard computing, the main computation goals are precision and certainty. However, in soft computing, the precision and certainty carry a cost that must be traded off. It has been stated that humans take advantage of their huge and parallel process capacity to perform postural control. This could be almost emulated by supercomputing systems but not by embedded systems for humanoid control. Then, whether imprecision in control is tolerated, it enables a reduction in computational load which improves computation speeds and control robustness.

As well, the biological and human inspiration of soft computing techniques is one of the most important reasons why one of them has been applied in this PhD Thesis. Each one of these techniques, which will be briefly presented in this section, is inspired in different biological behaviours. They can be applied to solve non biological problems which behaviour can be correlated with the biological case. However, the power to emulate biological behaviours, which is the case of the system developed in this PhD Thesis, favours the application of these methodologies.

Some of the principal methodologies are the following:

- Evolutionary computation (EC)
- Bayesian networks (BN)
- Neural networks (NN)
- Fuzzy systems (FS)

Furthermore, these methodologies are complementary rather than competitive. Then, it is possible to combine some of these techniques resulting in hybrid systems, such as neuro-fuzzy systems, in which each technique contributes with its strengths to the whole system.

Thus, this section provides an overview of the mentioned techniques used for intelligent control, the main human inspired characteristics they have, and their possible application in humanoid robots' postural control. This brief description also provides a perspective of soft computing in humanoid postural control. However, more detailed description of the hybrid neuro-fuzzy system will be presented due to its application in different modules of the developed human inspired postural control system.

### 4.3.1 Evolutionary Computation

Evolutionary computation is based on the application of Darwinian principles to solve engineering problems. This kind of computation is the joining of several techniques based on this idea in which, given a population of individuals and due to environmental conditions, a natural selection is naturally performed, surviving the fittest. Thus, the fitness ones among the population are growing.

It is easy to see such a process as optimization that works as follows. Given an objective function to be optimized, it can be randomly created a set of candidate solutions. The objective function is used as an abstract fitness measure (the better). Based on this fitness, some of the best candidates are chosen to seed the next generation by applying operators such as recombination and/or mutation. Recombination is applied to two selected candidates, the so-called parents, and it produces one or two new candidates, the children. Mutation is applied to one candidate and results in one new candidate. Applying recombination and mutation leads to a set of new candidates, the offsprings. Based on their fitness, these offsprings compete with the old candidates for a place in the next generation. This process can be iterated until a solution is found or a previously set time limit is reached (Eiben & Schoenauer, 2002).

Based on this operation, the first one of these techniques is the Evolutionary Programming (EP) (Jong, Fogel & Schwefel, 1997). It is a stochastic optimization strategy that stress in the behavioural union between parents and evolved individuals. Similar to EP, the Genetic Algorithms (GA) evolves a population evaluating their solutions (Holland, 1992). Nevertheless, GA differs from EP in the problem encoding, the exponential number of offspring required and the genetic operators used to produce mutations by GA.

The next set of techniques is the so called Evolution Strategies (ES). As in the previous techniques, its goal is the optimization of a quality function with respect to a set of decision variables or control parameters. ES operate on populations of individuals in which each individual comprise a set of endogenous strategy parameters that enables evolution. These endogenous strategies are used to control certain statistical properties of the genetic operators, especially those of the mutation operator. During each evolutionary strategy iteration, offspring individuals are generated from the set of

parent individuals. The strategy-specific parameters are called “exogenous strategy parameters” which are kept constant during the evolutionary loop (Beyer & Schwefel, 2002).

The last technique briefly commented is the Differential Evolution. It is a method used to optimize real-valued functions by means of improving a candidate solution related to a given measure of quality. During the optimization process, a population of candidate solutions is maintained and new candidate solution is generated by combining the existing ones. Then, the candidate solution that has the best score or fitness is kept. One difference with the previous methods is that DE doesn’t make assumptions about the problem to optimize and it can search very large spaces of candidate solutions. However, DE do not guarantee an optimal solution is ever found (Price, Storn, & Lampinen, 2005).

Related with robotics applications, Evolutionary Computation has turned on the so called Evolutionary Robotics (ER). It is a methodology that uses EC algorithms to develop controllers for autonomous robots. In this case, the populations are controllers which are repeatedly modified according to a fitness function (Harvey, Husbands, & Cliff, 1992). These controllers can be generated from a variety of methods including neural networks, fuzzy logic controllers and simple look-up and parameter tables that relate sensor inputs to motor outputs (Augustsson & Wolff, 2002). As well, this technique has been used to shape behaviours and evolve them to obtain new behaviours. They are related to trajectory planning on mobile robots (Dozier, 2001) or footstep planning in legged locomotion (Hong, Kim, & Kim, 2009). And, of course, ER is one of the methods applied in the vast field of robot learning (Ra, Park, Kim, & You, 2008).

### 4.3.2 Bayesian Networks

Bayesian networks (BN) are, as well, known as belief networks or Bayes nets. They are probabilistic graphical models used to represent knowledge about an uncertain domain. In this graphical model, each node represents a random variable; meanwhile the edges between the nodes represent probabilistic dependencies among the corresponding random variables (Figure 45). These conditional dependencies in the graph are estimated by using statistical and computational methods, combining different methodologies (Mihajlovic & Petkovic, 2001).

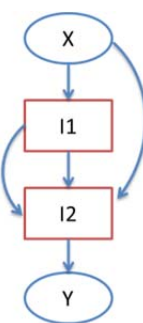


Figure 45 Bayesian Network example

BN have application in a wide variety of fields such as statistics, the machine learning or the artificial intelligence societies because these kinds of network are both mathematically rigorous and intuitively understandable. Bayesian Networks are used mainly in three different tasks:

- 1) Unobservable variables inference

BN is a complete model for variables and their relationships that can be used to solve queries about their behaviour. For instance, the evaluation of observable variables can be used to find out updated knowledge about hidden variables. The process of computing the posterior values for a subset of variables given the actual knowledge is called probabilistic inference.

There exist exact and approximate inference methods. The exact methods find out a solution with minimal error but with a high computational cost. Example of this type of methods are the variable elimination or AND/OR search (Echegoyen, et al. 2007). The use of approximate methods increases the computation velocity but, as well, increasing the goal error. Some of the most common approximate inference algorithms are importance sampling, stochastic MCMC simulation, mini-bucket elimination (Marin, et al. 2011).

- 2) Learning

Bayesian Networks can be used in machine learning to obtain parameters of the network or its own structure. Parameter learning is a classification problem in which a learner attempts to construct a classifier from a given set of training instances with class labels (Su, Zhang, Ling, & Matwin, 2008). In this case, the network is known meanwhile only a representative set of its parameters are available. It is possible to have the opposed case in which the parameters and representative data are known but the model that relates them is unknown. Then, Bayesian Networks can be used to produce actionable models where the structure of the model accurately captures the causal relationships in the data (D. Eaton & Murphy, 2007).

The application of Bayesian Networks on robotics is clearly focused in behaviour and task learning. These methods are applied in task learning by demonstration (Chatzis, Korkinof, & Demiris, 2012), in which the task parameters are learned from the data obtained from different trials. The other important application of BN is the analysis of visual information and pattern recognition in images (Chen, Pau, & Wang, 2005).

### 4.3.3 Neural Networks

Neural Networks (NN) are composed by interconnected artificial units called neurons that mimic the properties of biological neurons. Artificial Neural Networks are used to understand biological systems behaviour or for solving artificial intelligence problems. Neural Networks constitute an attempt to abstract the complexity of biological systems. The human brain consists of over ten million of interconnected neurons. The connexion between two neurons is weighted and adjusted adaptively according to the task under execution in order to improve the overall system performance.

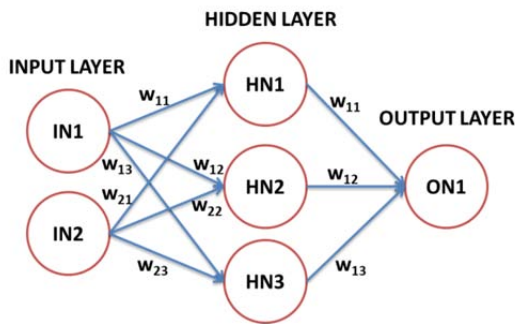


Figure 46 Multilayer Neural Network

An artificial Neural Network is composed by a number of layers formed by individual neurons (Figure 46). This structure is called a multilayer NN where there is an input layer, one or several hidden layers and an output layer. Neurons from adjoint layers are connected by a weighted link. As well, each neuron has an equation governing their dynamic operation.

The NN weights must be adjusted by means of a recursive learning or training process which is accomplished by the minimization of a certain objective function. The optimal values of the weights are stored as the strengths of the neurons' interconnections (Tzafestas, 1995). There exist two main NN architectures from which other NNs types are derived. The basic net structures are (Rojas, 1996):

- 1) Feedforward networks.

In feedforward NNs, signals travel one way only from input to output. There is no feedback loops from the output to any neuron in any layer. Thus, output doesn't affect the evaluation process. Feedforward NNs tend to be straight forward networks that weight inputs to elicit outputs. This type of organisation is also referred to as bottom-up or top-down.

- 2) Feedback networks.

Feedback networks can have signals travelling in both directions by introducing loops in the network. Feedback networks change their state continuously until they reach an equilibrium point, remaining in this point until the input set changes. Feedback architectures are also referred to as interactive or recurrent.

The NN computation is suitable for problems where conventional computation approaches are not effective. This is produced by the classical methodologies dependent from accurate problem mathematical modelling. Typical examples applied in robotics are speech and pattern recognition or robot kinematical control. The incorporation of NNs in robotic vision enables the object identification by pattern recognition. The training process consist of presenting to the system a set visual properties of the object that it must identify (Makhoul, 1991). Close related with the pattern recognition problem is the speech recognition one (Lippmann, 1989). It as well consists of identifying speech features corresponding to sound patterns previously learned.

Neural Networks are applied in kinematic control of robots. The network is trained with accurate data that characterize the robot kinematics. Then, NN provides a fast method to compute the necessary joint angles for reaching to a desired end point (Jasin, Charney, & White, 1988).

#### 4.3.4 Fuzzy Systems

Fuzzy Systems (FS) are those based on the Fuzzy Sets Theory introduced mainly by Lotfi A. Zadeh (Zadeh, 1965) in 1965. The main characteristic of fuzzy sets is that their elements have certain degree of membership to them, expanding the classical binary classification membership (yes/no – [0,1]). Then fuzzy set theory permits the gradual assessment of the membership of elements in a set. This idea is presented in the Figure 47 in which the human feature of height is classified applying different membership functions.

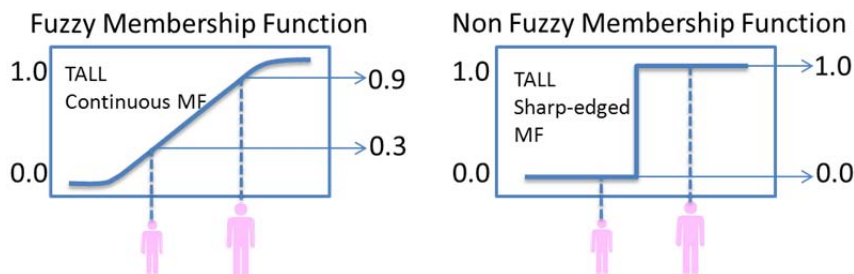


Figure 47 Fuzzy vs. non-fuzzy membership functions

One feature of FSs is the ability to realize a complex nonlinear inference between an input set and the output. This inference process synthesizes multiple simple input/output relations. This inference process is similar to that applied in Neural Networks. The rule describes the simple input/output relation and it defines a ‘fuzzy’ area. Then, successive combinations of rule areas change the shape of the output area. This is the essential idea of FSs and the origin of the term ‘fuzzy’ (H. Takagi, 1997). Fuzzy logic systems can handle problems with imprecise or incomplete data and, as well, it can model nonlinear functions of arbitrary complexity.

Fuzzy Inference Systems (FIS) development starts with the establishment of a set of rules provided by the designer. They are formulated using human language conditional ‘if-then’ statements. The fuzzy systems convert these rules to their mathematical equivalents. The rules usually must be provided by a designer that understands the system, who can describe the system accurately. This will minimize the inference error in the resulting representation of the system’s behaviour. Once the rules have been defined, the system is ready to perform the inference process.

Briefly, the first step of the inference process is to take a set of crisp inputs and determine the degree to which these inputs belong to each of the appropriate fuzzy sets (‘fuzzification’). Then, the rules are evaluated by inference using fuzzy set operations. After the inference step, the overall result is a fuzzy value. This result should be ‘defuzzified’ to obtain final crisp output (Mendel, 1995). This description is represented graphically in Figure 48. This system corresponds to a Mamdani type FIS

in which the output is ‘deffuzified’ using an output membership function (Mamdani & Assilian, 1975).

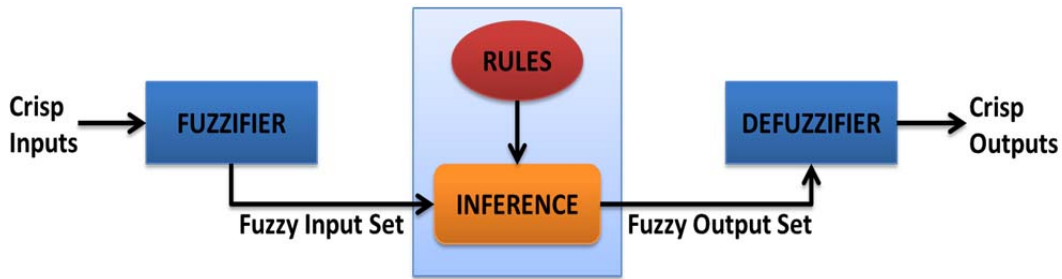


Figure 48 Mamdani fuzzy inference system

The second type of fuzzy inference system is the so called Sugeno FIS (Takagi & Sugeno, 1985). The main difference with Mamdani FIS is that the deffuzification stage is not necessary because the output is already numeric. It is usually obtained by weighted average of the result from the inference evaluation (Figure 49).

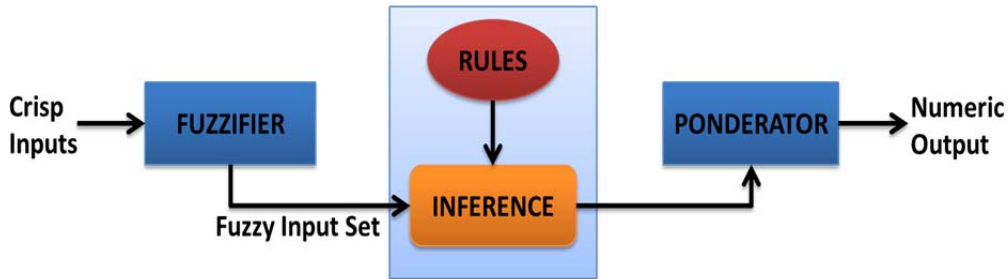


Figure 49 Sugeno fuzzy inference system

Then, the fuzzy set theory can be used in a wide range of domains in which information is incomplete or imprecise. The main application related to robotics is the control of mobile autonomous robots. The navigation applications gains the advantage of the FIS ability for processing inaccurate information captured from the robot environment (Carinena et al., 2004). As well, FIS can be applied in the control of mobile robot evaluating different behavioural units driven by sensorial information sets (Safiotti, 1997).

The use of classic FIS systems is constraint by the increasing complexity of the system to model. Thus, the main solution to overcome this problem is the combination of methods exposed until now. The result of this combination is a Hybrid System.

### 4.3.5 Hybrid Systems

The nature of the problem under study favours the application of one specific intelligent technique among others, because of its particular computational properties. For instance, neural networks are good at recognizing patterns but they are unable to explain the motivation of the decision. Fuzzy logic systems, which can reason with imprecise information, are good at explaining their decisions but they cannot acquire the rules to perform decisions automatically (Fuller, 1999).

The answer to overcome these limitations is the creation of intelligent hybrid systems where two or more techniques are combined. Thus, in a hybrid system, each individual technique contributes with at least one feature unable to be performed by the others.

The use of intelligent hybrid systems is growing rapidly and the neuro-fuzzy inference system is one of these alternatives. In this PhD Thesis, Neural Networks are used to tune membership functions of fuzzy systems that are employed for sensorial evaluation or decision making, mimicking the human internal processes involved in postural control.

Although fuzzy logic can encode expert knowledge directly using rules with linguistic labels, its definition and tuning, based on the expertise of the designer, usually takes a lot of time. Because of this, neuro-fuzzy hybrid system gains the advantage from neural networks learning techniques to automate the tuning process, reducing development time while improving performance.

Hybrid Systems set is composed by a wide number of combined methodologies. Here, two of the main Hybrid System will be briefly exposed.

#### **4.3.5.1 Fuzzy-Neuro Systems**

In theory, Neural Networks and Fuzzy Systems are equivalent regarding the methods to obtain results, inferring the outputs from the inputs. In practice, each technique has its own advantages and disadvantages. For neural networks, the knowledge is automatically acquired by, for instance, the backpropagation algorithm, but the learning process is relatively slow and analysis of the trained network is difficult because NNs are like black boxes. Due to this, it is impossible to extract structural knowledge (rules) from the trained neural network. Furthermore, the learning procedure cannot be simplified adding any special information about the problem into the neural network (Fuller, 1995). Meanwhile, fuzzy logic provides an inference mechanism to enable a system to deal with cognitive uncertainties in a human way .

The computational process proposed for the development of fuzzy-neural systems starts with the design of a "fuzzy neuron". This structure is based on the understanding of biological neuronal morphologies and learning mechanisms. This leads to the following three steps in a fuzzy neural computational process (Fuller, 1995):

- 1) Establishment of fuzzy neural models inspired by biological neurons.
- 2) Modelling of connections (synapses), which integrates fuzziness into neural network.
- 3) Application of learning algorithms to adjust the connection's weights.

Combining these computation steps it is possible to obtain two possible models for the fuzzy neural systems. The first model is composed by a fuzzy interface module which transforms the linguistic statements into an input vector for the neural network. The training of this network will depend on the desired outputs or decisions (Figure 50).

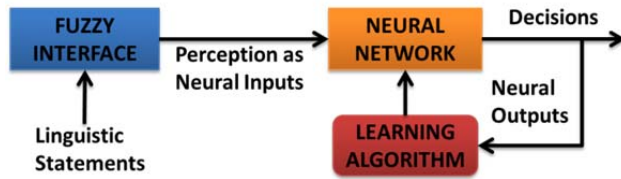


Figure 50 Model of fuzzy-neural system (adapted from (Fuller, 1995))

The second model consists of a multi-layered neural network that drives the fuzzy inference mechanism (Figure 51).

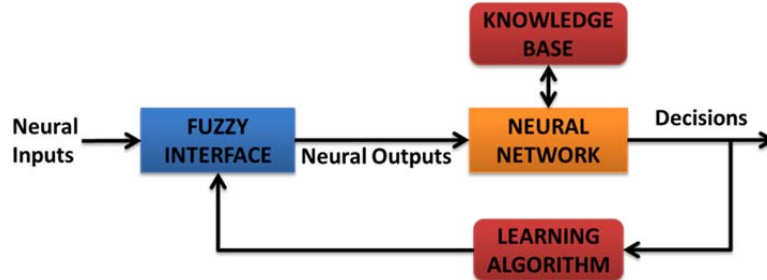


Figure 51 Fuzzy driven neural network system (adapted from (Fuller, 1995))

Fuzzy neural systems are applied in applications in which it is useful the learning capacities of this kind of methodologies. Specifically, this capacity enables the possibility of evolving the fuzzy neural system by means of the application of evolutionary algorithms. Then, the fuzzy system is adapted and improved online with new datasets captured during its operation. In robotics, this methodology is used in adaptive controllers such as the joint controller based on force measurements developed by Kiguchi. This system improve the controller learning from the data acquired in unknown operational conditions (Kiguchi, Watanabe, & Izumi, 2000). In the case of mobile robots navigation, the use of this kind of hybrid systems enables the adaptive robot navigation. The sensor data captured during robot movement is used to improve the trajectory planning and obstacle avoidance systems (Song & Sheen, 2000).

#### 4.3.5.2 Neuro-Fuzzy Systems

The neuro-fuzzy hybrid system is, as well, the result of the combination of FIS systems with NNs, such as the previous case. But, in this case, the fuzzy system gains the advantage of the learning capacities from the neural network.

One of the main problems in the development of classic fuzzy systems is representation of the system under study. The designer needs an accurate knowledge of the process to be controlled. To overcome the problem of knowledge acquisition, neural networks are extended to automatically extract fuzzy rules from numerical data obtained from the system.

There are two major formulations of neuro-fuzzy systems. The first one group those systems based on Mamdani rules, such as POP-Yager (Quek, Wahab, & Aarit, 2000) or eFSM (Tung & Quek, 2010). The second formulation group those systems based on Sugeno type rules, such as Denfis (Kasabov & Song, 2002) and Anfis (Jang, 1993).

The main difference between these methods is related with the possibility of interpretation of the resulting system. The Mamdani based systems allow posterior interpretation because they obtain a structured knowledge of the underlying system. This issue is not possible in Sugeno type systems but, on the other hand, this type has higher levels of computational efficiency and robustness.

The neuro-fuzzy system interested in this Thesis is the Adaptive Neuro-fuzzy System (Anfis) established by Jang. The features exposed for the FIS systems, joint with the powerful available tools for Anfis system development, have favoured the selection of this method to develop the postural control architecture proposed in this PhD Thesis. Furthermore, the human style fuzzy reasoning of Anfis system matches the human inspiration requirement of this Thesis.

Anfis systems are based on a five layer structure (Figure 52). These layers are:

- 1) Layer 1: it generates the fuzzy membership values for each input variable.
- 2) Layer 2: it multiplies the incoming signals from the previous layer and it calculates the firing strength of the rule.
- 3) Layer 3: it is in charge of computing the normalized firing strength.
- 4) Layer 4: the nodes of this layer calculate the contribution of the each model rule in the output.
- 5) Layer 5: It calculate the weighted average for the global output of the system.

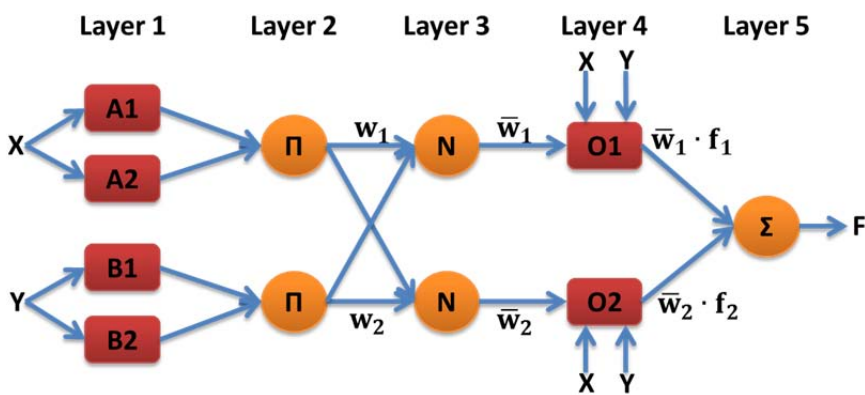


Figure 52 Anfis Model Structure (adapted from (Jang, 1993))

Two main missions have been assigned to Anfis developed modules of the postural control architecture. The first one is the sensorial evaluation. The development of robot perceptual evaluation system has profit from the available dataset from acquired measurements. In this case, the evaluation of sensorial raw data accomplishes, at the same time, the filtering and interpretation processes to produce directly an applicable output. The second mission of the developed Anfis modules is the evaluation of the sensorial evaluation outputs to take postural control decisions. In summary, the Anfis tool is very useful for system modelling, evaluation of information and decision making processes for human inspired artificial systems.



## CHAPTER 5

# Human Versus Humanoid

## 5.1 Physiology of Humanoid Control System

Chapter 2 established the foundations about human postural control. Following a bottom up process, the description explains the human postural control architecture from perceptions to motor responses, presenting each one of the architecture components, their function and their interactions. But Chapter 2 was more focused on the high level functions and the overall operation of the postural control system. Therefore, this chapter describes the physiological components that support the behaviour of the human postural control system.

The physiological components review performed in this chapter has been organized taking into account the postural control process flow and the organs involved in each stage. This control process starts when the sensorial information is captured by the corresponding receptors of the peripheral nervous system. Then, the sensorial information is transmitted by means of the afferent sensitive neurons of the peripheral nervous system, arriving to Central Nervous System where it is processed. The processing centres evaluate all information and decide about the most appropriate action to take. The resulting action is transmitted to the motion system by means of the efferent neurons to perform the movement.

Thus, the review starts with the description of the sensorial organs and how they capture the sensations. It continues with the description of the integration centres in which the sensorial information is converted in perceptions, which are more adequate inputs for complex postural control. Besides, these processing centres decide about the postural control action, if required. The last part of the review is related to the description of the motion actuators, which execute the postural reactions, and to the communication channels among systems.

In the same way than Chapter 2 described the human postural control foundations, Chapter 3 and Chapter 4 presented the foundations for humanoid postural control. The systems described in these chapters were inspired by the knowledge acquired during the study of the human case. The humanoid postural control architecture established has two main characteristics: human inspiration and task orientation.

The exposition of the humanoid postural control system has followed the same guidelines followed by description of the human case. Because of that reason, this

chapter presents in parallel the components involved in humanoid postural control. Thus, in each section, the human organ is presented and then the humanoid device that tries to accomplish the same function. In this way, it is possible to compare the performance of both cases.

In summary, this chapter compares basic systems from the human physiology with the mechatronic systems integrated in the humanoid robot TEO.

## 5.2 Sensorial System

In Chapter 4, the control foundations for postural control of humanoid robots were described. But control theories and architectures are based on ‘perceptions’ or information provided by sensing devices.

As stated before, the sensorial system is composed by two main perception types depending of the origin of the sensed stimulus. The exoceptive perception is composed by the information about environmental circumstances or external stimuli. This perception is the result of the combination of the information coming from the vestibular and visual sensorial systems. Nevertheless, the proprioceptive system collects the information of the body state itself (i.e. joint angles).

### 5.2.1 Exoceptive Perception

As described in Chapter 2, exoceptive human perception is composed by the vestibular system and the visual system. Both of them provide complementary information to keep the body balance. The vestibular apparatus is the non-auditory portion of the inner ear. It serves three primary purposes in human (Hain & Helminski, 2000; Mann, 1997):

- 1) It plays the dominant role in the subjective sensation of motion and spatial orientation of the head, acting on the musculature of the neck (VestibuloCollic Reflex or VCR).
- 2) It adjusts muscular activity and body position to maintain posture (VestibuloSpinal Reflex or VSR).
- 3) It stabilizes in space the fixation point of the eyes when the head moves, providing a stable image upon the retina (Vestibulo-Ocular Reflex or VOR).

The sensors located at the vestibular system are composed mainly by two structures. The former, the hair cells of the maculae (otolith system) that signal head position and linear acceleration in two directions (Benson et al., 1986; Fernández & Goldberg, 1976a, 1976b; Guedry, 1974). The later, the cupula located inside the semicircular canals sense angular rotation (velocity and acceleration).

For the study of the vestibular system implications in postural control, it is important to consider the response and thresholds of the vestibular organs as individual inertial sensors. The postural and movement perception are the result of the integration of the information of each sensor in the Central Nervous System.

Another important consideration is the subjectivity of the presented data, that is, not all humans have identical perception values: they depend of physical limitations, environment, test conditions, etc. The vestibular response information is the result of statistical studies of data obtained from different experiments.

Regarding to the response to rotational movement perception, it has been found that the minimum threshold of perception is established by the Mulder's Law (DeHart & Davis, 2002), which describes the level below which accelerations are not sensed by this system (called Mulder's Constant). This value is calculated as the product of the intensity or magnitude of acceleration ( $^{\circ}/s^2$ ) and time(s).

To perceive an angular acceleration during a movement in any direction, the mentioned product must reach the Mulder's Constant as a threshold value. For instance, a large acceleration of  $20^{\circ}/s^2$  during 0.1s, assuming a Mulder's Constant of  $2.5^{\circ}/s$ , will not be felt. The same acceleration will be perceived for durations higher than 0.125s. The most commonly accepted minimum threshold values of the:

- Stapleford (Stapleford, 1968):  $3.2^{\circ}/s$  for roll;  $2.6^{\circ}/s$  for pitch; and,  $1.1^{\circ}/s$  for yaw.
- Oman (Oman & Young, 1969):  $1.5^{\circ}/s$  for all three axes.
- Mulder (Guedry, 1974):  $2.5^{\circ}/s$  for all three axes.

Recent studies have documented the range of detection for angular velocities and acceleration from  $0.5^{\circ}/s$  to  $500^{\circ}/s$  (maximum threshold). These perceptions were sensed in a range of frequencies from 0.1Hz to 10Hz (Aw et al., 1996; Ciaravella et al., 2006). Table 4 summarizes the limitations of the semicircular canals to detect movement (see Figure 53).

Table 4 Rate of turn and angular acceleration thresholds from vestibular system

	Rate of Turn	Angular Acceleration
Dimensions	Roll / Pitch / Yaw	
Min. Threshold	$0.5^{\circ}/s$	$0.03^{\circ}/s^2$
Max. Threshold	$500^{\circ}/s$	$0.065^{\circ}/s^2$
Bandwidth	10Hz	10Hz

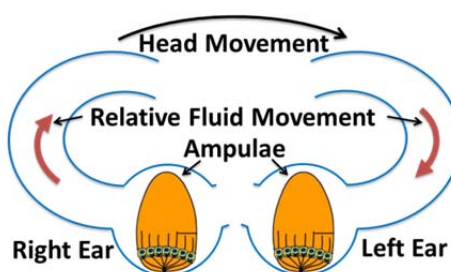


Figure 53 Semicircular canals detection scheme

The linear acceleration perception senses the initiation and variation of movement as well as the gravity. The minimum variation of movement that can be detected depends of the principal axis of perception. In the Z (vertical axis) the threshold is  $0.15\text{m/s}^2$ ; for both X (roll) and Y (pitch) axes the threshold is  $0.06\text{m/s}^2$  (Jones & Young, 1976; Previc & Ercoline, 2004).

The maximum threshold for linear acceleration detection is about  $4g$  (Patane et al., 2004). Due to the inertial characteristics of the otolith organ, the bandwidth of the system is about  $2\text{Hz}$  (Benson, 1990; Benson et al., 1986; Hoeman & Van Der Vaart, 1978). Table 5 shows the limitations of the otolith sensing operation shown in Figure 54.

Table 5 Linear acceleration thresholds of the vestibular system

	Linear Acceleration		
Dimensions	X	Y	Z
Min. Threshold	$0.06\text{m/s}^2$	$0.06\text{m/s}^2$	$0.15\text{m/s}^2$
Max. Threshold	$40\text{m/s}^2$ ( $4g$ )	$40\text{m/s}^2$ ( $4g$ )	$40\text{m/s}^2$ ( $4g$ )
Bandwidth	2Hz	2Hz	2Hz

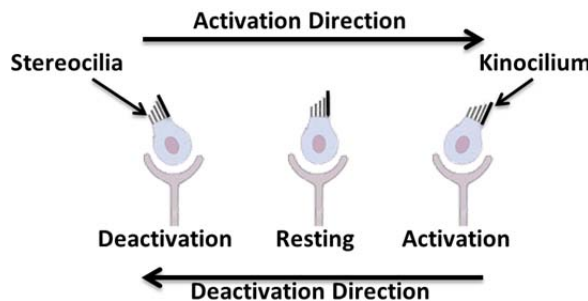


Figure 54 Otolith organ detection scheme

All these perception characteristics correspond to each sensing organ but the information they provide must be integrated by the Central Nervous System. This sensor fusion is shown in Figure 55. The inputs of the model are the resulting data from the otolith and canals systems: rate of turn ( $\omega$ ), linear velocity and acceleration ( $a_{Gi}, \dot{a}_{Gi}$ ). After different processing steps, the result of canal–otolith fusion are the estimated of rate of turn ( $\hat{\omega}$ ), the estimate of head attitude ( $\hat{g}$ ) and the estimate translational acceleration ( $\hat{a}_i$ ) (Mergner & Glasauer, 1999).

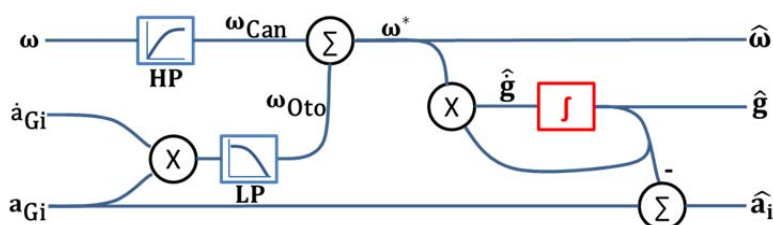


Figure 55 Human sensor fusion scheme (from (Mergner & Glasauer, 1999))

Sometimes the information processed has a mismatch with the inputs from the environment. This produces the so called vestibular illusions. There are two types. The first one, the somatogyral illusions are produced when the semicircular canals receive wrong data. It includes the Leans, the Graveyard Spin & Spiral and the Coriolis illusions (Gillingham & Previc, 1993; Sipes & Lessard, 1999). The second type, the somatogravic illusions produced by wrong linear acceleration perception, includes the Inversion, Head-Up and Head-Down illusions (Gillingham & Previc, 1993; Tokumaru et al., 1998).

Another aspect influencing vestibular perceptions is the inability to distinguish translational motion from changes in orientation relative to gravity (tilt/translation ambiguity) (Angelaki et al., 1999; Angelaki & Yakusheva, 2009; Merfeld et al., 1999). The mentioned ambiguity is resolved in the brain merging all signals of the vestibular perception (Angelaki & Cullen, 2008).

Because the vestibular apparatus provides this information only with respect to the head, it cannot accomplish postural adjustments on its own or encode sustained constant velocity motion (Bütnér & Waespe, 1981; Fernández & Goldberg, 1976a; Fetsch et al., 2010; Si et al., 1997). Sensors in the neck, visual perception and perhaps other postural muscles (somatosensation and proprioception) are extremely important in signalling to the central nervous system body changes like active movements (Mittelstaedt & Mittelstaedt, 2001; Sun et al., 2004), which comprise most natural self-motion.

These two systems operate in conjunction with the visual one to form an outstanding control system that maintains us in a wide variety of stable and unstable postures. Numerous studies have shown the implication of the visual stimulation in postural control. (Van Asten et al., 1988; Berthoz et al., 1979; Dijkstra et al., 1994; Lee & Lishman, 1975). In a well-lit environment with a firm base of support, healthy persons rely on somatosensory (70%), vision (10%) and vestibular (20%) information for upright postural control (Fay B Horak, 2006; Peterka et al., 2002).

Light is electromagnetic radiation to which eyes respond. In light of a single wavelength, or spectrally pure light, the extreme range is from 380nm to 740nm. The sensitivity of the eye falls off at the ends of this range, so that 400nm to 700nm is a good approximation. The retina is the light-sensitive part of the eye composed by a dual organ, a rod network and a cone network. The rods are sensitive to weak light, inoperative in strong light, have maximum sensitivity at about 507nm and are very sensitive to motion, but give no colour discrimination. The cones are sensitive to strong light, insensitive to weak light, have a maximum sensitivity at 555nm and are responsible of the acute and colour vision.

Regarding focusing, the eyes can resolve two sources separated by about 6' of arc in everyday life and it can be exceptionally resolved down to about 4' or 3' of arc, depending on the object viewed. The absolute limit of visual acuity, under laboratory conditions with fine gratings, seems to be between 1' and 2' of arc.

The refractive index of the eye medium varies with wavelength similarly to water, so that n=1,3318 at 656nm (red) and n=1,3435 at 405nm (blue). This gives the eye a

difference in power of about 1.5D over the visual spectrum, where D is the focal distance. The effect is to focus blue light at a shorter distance than red light.

Fechner found that the minimum difference of brightness that can be sensed is a ratio of physical intensity of about 1-2% (Fechner, 1858). At very low or very high levels of illumination, this property fails

The visual system is tolerant of errors in the retinal image, correcting them when it is possible. The eye has considerable spherical and chromatic aberration, so the image produced on the retina is quite poor. The mental image is much sharper, refined by the visual system. Other relevant visual features are:

- Accommodation: It is the capacity of the eye to obtain a clear image from an object at a specific distance. It is produced by the variation in the curvature of crystalline lens. It depends of luminance, the reflection of light, the age, etc. (Bruce et al., 1996)
- Visual acuity: It is the spatial resolving capacity of the visual system. This may be thought of as the ability of the eye to see fine detail. Visual acuity is limited by diffraction, aberrations and photoreceptor density in the eye (Smith & Atchison, 1997).
- Adaptation: It is the response of the eye against different luminance levels. Its adjustment is produced by the opening and closing of the pupil. The velocity of adaptation is faster if there is a change from low to high luminance than the change from high to low luminance level.
- Contrast: Object perception depends of the difference of luminance and colour between the observed object and the background. Contrast is an important parameter in assessing vision. In reality, objects and their surroundings are of varying contrast. Therefore, the relationship between visual acuity and contrast allows a more detailed understanding of our visual perception (Capó-Aponte et al., 2009).
- Motion detection: It is related with the Dynamic Visual Acuity (DVA). It is the capacity of the eye to discern fine detail in a moving object (Aznar-Casanova et al., 2005). Belonging to a more general class of visual perception, it can be differentiated the real motion (Goldstein, 2009), the apparent motion (Anstis & Mackay, 1980), induced motion or motion contrast (Nawrot & Sekuler, 1990) and motion aftereffects (MSEs) (Anstis et al., 1998). The additional classes of motion perceptions are demonstrations that continuous motion is not necessary for the experience of visual motion. Humans can render changes in reality at roughly 13-15 frames per second (fps, or Hz)(Kent, 2010). Any event which happens faster than 1/60th of a second (16.6ms) falls between perceptual frames and is considered to be subliminal or imperceptible to human consciousness (Marcel, 1983).

- Visual Field: It is the extension of view captured by the retina. Some calculations establish the maximum field of view varied horizontally from -59° to +110°, and vertically from -70° to +56° (Grigsby & Tsou, 1994).

Similarly to vestibular system, the visual perception is conditioned by some illusions caused by the environment. Some of these visual illusions are (Gibb, 2007; Oman & Young, 1969; Whiteside et al., 1965):

- Linear perspective illusions
- Upsloping terrain or narrow or long runway
- Downsloping terrain or wide runway
- Black-hole illusion
- Autokinetic illusion
- False visual reference illusions
- Vection illusion

In that way, the experimental results in (Fukuoka et al., 1999) suggest that the visual feedback system contains a large time delay and, consequently, it only complements the vestibular system to maintain postural control. Numerous analyses of the relationship between visual stimuli and postural responses have been carried out (Dichgans et al., 1976; Diener et al., 1982). These analyses reveal that the visual feedback system primarily utilizes information in a relatively low frequency range (up to 0.4Hz). However, the role of the visual system in postural control is still under study (Nagata et al., 2001).

Once the main features of the exoceptive perception systems of the human body involved in postural control have been outlined, the corresponding systems that capture the same information in humanoid robotics will be exposed. The vestibular system behaviour is reproduced by the so called inertial system. This system is in charge of angular position, velocities and accelerations sensing. Complementing the information for postural control, the modern visual systems based on stereo cameras provide image sequence that must be post-processed to obtain useful data for such control. In following sections the devices integrated in TEO robot for vestibular and visual perceptions are described.

### **5.2.1.1 Inertial System**

The human vestibular system can be correlated with an inertial measurement system in a humanoid robot. As described before, the vestibular system is located in the head and senses its position, linear acceleration and angular rotation (velocity and acceleration). Meanwhile, in humanoid robotics, the inertial sensor position can vary among different robot developments but mainly are located in the torso (Buschmann et al., 2009; Gienger et al., 2005; Kajita et al., 2003; Kim et al., 2005; Xia et al., 2007). Its

position is related to simplified robot models and different body reference points like the Centre of Mass or the Zero Moment Point (Popovic et al., 2005). In this way, the inertial sensor provides information to enable the computation of these models and reference points inside the control loop.

The inertial system used in TEO robot is the Inertial Measurement Unit (IMU) MTi™ from the company Xsens™ (Xsens, 2009). It is important to remark that an IMU is not just a sensor. These kinds of unit comprise 3D accelerometers, 3D gyroscopes, commonly abbreviated to gyros, and 3D magnetometers (compass), as sensor devices. They also integrate electronics to process and communicate the sensed information in a proper format.

An accelerometer measures specific force applied to a body that produces its movement and, consequently, it senses the body acceleration. The transducer usually acts following an axis of detection. These transducer can be classified according to the nature of the sensor element in (Sensr, 2011):

- Capacitive accelerometers: The accelerometer senses the electrical capacitance change between a static condition and the dynamic state.
- Piezoelectric accelerometers: They use materials such as crystals, which generate electric potential from an applied stress (acceleration).
- Piezoresistive accelerometers: (strain gauge accelerometers) work through measuring the electrical resistance of a material when acceleration is applied.
- Hall Effect accelerometers: They measure voltage variations stemming from a change in the magnetic field around the accelerometer.
- Magnetoresistive accelerometers: They work through measuring changes in resistance due to a magnetic field. The structure and function is similar to a Hall Effect accelerometer except that instead of measuring voltage, the magnetoresistive accelerometer measures resistance.
- Heat transfer accelerometers: They measure internal changes in heat transfer due to acceleration.
- MEMS-Based Accelerometers: MEMS (Micro-Electro Mechanical System) technology is based on a number of tools and methodologies, which are used to form small structures with dimensions in the micrometre scale.

The gyroscope measures angular rate or orientation, both without an external reference. The main classes of gyroscopes are (Groves, 2008):

- Spinning-mass gyros: They operate on the principle of conservation of angular momentum. Part of Newton's second law of dynamics, this states that the angular momentum of a body with respect to inertial space will remain unchanged unless acted upon by a torque (force x distance). Therefore, if a spinning mass is mounted in an instrument case such that it is free to rotate

about both of the axes perpendicular to its spin axis, it will remain aligned with respect to inertial space as the case is rotated. Such a device is known as a gyrocompass.

- Optical gyros: They are based on the principle that, in a given medium, light travels at a constant speed in an inertial frame. They work measuring the change of the path length of a light beam.
- Vibratory gyros: A vibratory gyroscope comprises an element that is driven to undergo simple harmonic motion. The vibrating element may be a string, beam, pair of beams, tuning fork, ring, cylinder, or hemisphere. All operate on the same principle, which is to detect the Coriolis acceleration of the vibrating element when the gyro is rotated.

A magnetometer is used to measure the strength and/or direction of a magnetic field, usually the Earth magnetosphere. Common types include:

- Fluxgate magnetometers: The fluxgate magnetometer is based on what is referred to as the magnetic saturation circuit. Two parallel bars of a ferromagnetic material are placed closely together. The susceptibility of the two bars is large enough so that even the Earth's relatively weak magnetic field can produce magnetic saturation in the bars (Primdahl, 2002).
- Resonance magnetometers: make use of the resonant response of an atomic (or molecular) system subjected to the static magnetic field to be measured, generally in the presence of an auxiliary oscillating field (Hartmann, 1972).
- SQUIDS (Superconducting Quantum Interference Devices): It is a magnetic field sensor converting the magnetic flux threading the SQUID loop into a voltage across the device (Drung et al., 2007).

Independently of the technology used in the transducers of the unit, the IMU is capable of calculating roll, pitch and yaw in real time, as well as outputting calibrated 3D linear acceleration, rate of turn (gyro) and (Earth) magnetic field data.

Table 6 IMU sensing thresholds

	<b>Rate of Turn</b>	<b>Linear Acceleration</b>	<b>Magnetic Field</b>
<b>Dimensions</b>	<b>Roll/Pitch/Yaw</b>	<b>X/Y/Z</b>	---
<b>Min Threshold</b>	0.05%/s	0.015m/s <sup>2</sup>	0.1mGauss
<b>Max Threshold</b>	300%/s	50m/s <sup>2</sup> (5g)	750mGauss
<b>Bandwidth</b>	40Hz	30Hz	10Hz

This IMU implements a sensor fusion algorithm where the measurement of gravity (by the 3D accelerometers) and Earth magnetic north (by the 3D magnetometers)

compensate drift errors from the integration of rate of turn data (angular velocity from the rate gyros). This system is often called an Attitude and Heading Reference System (AHRS).

This inertial measurement enables movement assessment at a single point without the requirement of a reference but the output quantities are represented in one signal. (Veltink et al., 2001)

### 5.2.1.2 Force/Torque Sensor System

Another complementary system used in humanoid robotics to sense external forces and torques are the F/T sensors. Although they could be considered as part of the proprioceptive system, they measure external forces (i.e. gravity effects). The main difference with the vestibular system and the inertial devices are that an F/T sensor has the capacity of static forces and torques perception.

In the case of the upper limbs, F/T sensors usually are located in the wrists. These devices measure the forces and torques produced when manipulating objects or when in contact with the environment (Zhang et al., 2005). In the lower limbs, the sensors commonly are located in the ankle joints. They sense the reaction forces of the ground (Nishiwaki et al., 2002) and the forces exerted in the ankle joint by the body movement itself. Due to this, this kind of devices is not clearly mapped with any human sensorial organ.

In postural control, F/T sensors are used to determine the margin of stability of the humanoid robot. According to the Vukobratovic theory of stability, ensuring the stability of the movement consist basically of keeping the ZMP reference point inside the effective area of support (Vukobratovic & Borovac, 2004):

$$PZ = \frac{n \times M_P^{gi}}{F_{gi} \cdot n} \quad (5.1)$$

Where P is the normal projection of the ankle on the ground.

The mechanical structure of TEO robot integrates two F/T sensors in the wrists and another two in the ankles. These sensors from the company JR3, Inc. has the main features shown in Table 7.

Table 7 JR3 Force/Torque sensors characteristics

	<b>Model</b>	<b>Fx, Fy</b>	<b>Fz</b>	<b>Tx, Ty, Tz</b>
<b>Wrists</b>	50M31A	100N	200N	5Nm
<b>Ankles</b>	85M35A	250N	500N	212Nm

The JR3 F/T sensors are monolithic titanium device containing analogue and digital electronics systems. Foil strain gages sense the loads imposed on the sensor. The strain gage signals are amplified and combined to become analogue representations of the force loads on the three axes (Fx, Fy, Fz) and the moments or torques about the

three axes (Tx, Ty, Tz). These sensors provide a serial RS-485 data stream at 2Mb/s which contains complete 6 axis data. The axes on standard JR3 sensors are oriented with the X and Y axes in the plane of the sensor body, and the Z axis perpendicular to the X and Y axes. The reference point for all loading data is the geometric centre of the sensor. When viewed from the Robot Side of the sensor the forces and moments are related by the Right Hand Rule (JR3, 2011).

### 5.2.1.3 Visual System

Vision is important for postural control and many studies have demonstrated its relevance performing experiments with open or closed eyes (Edwards, 1946; Travis, 1945). The influence of vision in postural control depends of its efficiency regarding monocular or binocular vision (Isotalo et al., 2004), visual acuity (Paulus et al., 1984), visual contrast (Leibowitz et al., 1979), object distances and room illumination (Brandt et al., 1986).

Vision seems to influence balance by reacting to motion and it also triggers the muscle activation required for postural corrections (Brandt et al., 1986). Originally, peripheral areas of the retina have been considered involved in self-motion perception meanwhile central areas have been related to external motion perception. Moreover, recent studies have confirmed that the central retina contributes to balance control as well, particularly for lateral sway reduction (Bardy et al., 1999; Paulus et al., 1984). The best performance in postural balance is achieved in distances less than 2m (Brandt et al., 1986) and the fast integration of visual information cues enables muscular reactions within 100ms from perturbation (Nashner, 1978).

Vision systems in humanoid robotics try to replicate the functions of the human vision. Performance on an artificial system will depend of its components, whether they are hardware or software. A computer vision system could be classified into two categories:

- Task oriented: In this kind of systems the environment conditions are well known and the system components are selected to accomplish a specific function (object detection, inspection, classification, etc.)
- General purpose: The main difference of these systems is the variability of the environment conditions. Due to this, the hardware system is composed by general purpose components and the software processing increases its complexity.

In this case, the goal is to imitate the human vision in order to integrate visual perception in the postural control system. Due to this, the vision system selected must accomplish the following conditions:

- Binocular vision (3D perception)
- Colour perception
- Frame rate above 15Hz

- Ranges of vision as much closer to human as possible
- Fully programmable for motion detection, object classification, etc.

Taking into account these desirable characteristics the vision system selected for TEO robot is the Microsoft Kinect™. This low cost device, combined with an external image processing, provides TEO robot with the capacity to detect moving objects, optical flows, self-motion, etc. and apply the resulting information to improve postural control.

This device is composed by two different vision sensor systems:

- An infrared laser projector combined with a monochrome CMOS sensor, which captures video data in 3D under any ambient light conditions.
- 2D colour 640 x 480 pixels VGA camera

The operation of the 3D sensor consist of the projection of an infrared structured light that is captured by the monochrome camera and therefore, through software processing, reconstruct a 3D scene. Thanks to the open source application programming interfaces (API) available, such as OpenKinect (OpenKinect, 2012) or (Manctl, 2012), it is possible to make gesture recognition, movement analysis, etc. Table 8 shows the summary of the Kinect™ main features compared with the human ones.

Table 8 Comparison between human and artificial vision systems

	Kinect™	Human
<b>Frame Rate</b>	30Hz	13-15Hz
<b>Colour Resolution</b>	8-bit VGA (640x480 pixels)	576Mpixels
<b>Mono. Resolution</b>	11-bit VGA (640x480 pixels)	
<b>Nominal Range</b>	1.2m – 3.5m	0.25m – ∞
<b>Extended Range</b>	0.7m – 6m	
<b>Field of View</b>	±57° horizontally ±43° vertically	-59° to +110°, horiz. -70° to +56° vert.
<b>Movement Range</b>	±27° vertical 0° horizontal	±30° vertical ±35° horizontal

## 5.2.2 Proprioceptive Perception

As described in Chapter 2, in humans the proprioceptors organs are located in muscles, joints and skin. They give information about the position of the limbs and the body, the distension of the respective muscles, vibrations, pressure, etc. Table 9 summarizes the main characteristics of the proprioceptors located in the skin and the

second, Table 10 summarizes some properties of the sensor organs involved in the perception of muscle and joint movement.

Table 9 Human skin proprioceptors

Type	Sensor	Sensation	Signals	Adaptation
<b>Mechano receptors</b>	Meissner corpuscle	Flutter & Stroke	Frequency/Velocity & Direction	Rapid
	Pacinian corpuscle	Vibration	Freq.: 50-700Hz	Rapid
	Ruffini ending	Skin Stretch	Direction & Force	Slow
	Merkel receptor	Steady pressure, texture	Location & Magnitude	Slow
	Free nerve ending	Touch, Pressure	Location & Magnitude	Slow
<b>Thermo receptors</b>	Free nerve ending	Temperature	Temperature change	Rapid
<b>Nocio receptors</b>	Free nerve ending	Temperature	Tissue damage	Rapid
		Mechanical	Contact	Slow
		Polymodal	Tissue damage	Slow

Table 10 Human articular proprioceptors

Type	Sensor	Sensation	Signals	Adaptation
<b>Mechano receptors</b>	Free nerve ending	Muscle stretch	Muscle length & velocity	Rapid initial transient and slow sustained
	Golgi Tendon Organ	Muscle tension	Muscle contraction	Slow
	Pacini corpuscles	Joint Movement	Direction & velocity	Rapid
	Ruffini endings	Joint pressure	Pressure & Angle	Slow
	Golgi corpuscles	Joint torque	Twisting force	Slow

There are some essential inputs for postural control produced by proprioception. Regarding the cutaneous proprioception, it has been explored the role of skin mechanoreceptors to detect body sway during standing. Cutaneous perception information contributes to reflex regulation of balance encoding the direction of the ankle movement (Kavounoudias et al., 2001; Roll et al., 2002). It also contributes to awareness of our body in space and specify the support on which the feet are resting (Maurer et al., 2001). Various studies have shown the stabilizing influence of tactile information from any body part on human stance. For instance, posture equilibrium is improved by only a light active touch of a finger on an external support (Jeka & Lackner, 1994) or even when the leg or shoulder is passively touched (Rogers et al., 2001).

The proprioceptors located in joint capsules give information about the movements and positions of the body parts regarding to each other. This information is integrated in the postural control but their role has not been fully defined yet (Kejonen, 2002). Any change in muscle length and tension is measured by the muscle spindles, independently if the change is caused by internal or external forces (passive or active movement). Recent findings suggest that the perception from the trunk and the hip may be more important in triggering human balance corrections than ankle proprioception. The perceptive input from the lower legs mainly helps with the final shaping and inter-muscular coordination of postural and gait movements (Allum et al., 1998).

Summing up, tactile and proprioceptive feedbacks from skin and muscles would operate complementarily for maintaining postural control: low level perception would be assigned predominantly to tactile inputs whereas larger amplitude body perturbations, needing muscle contractions to restore balance, would involve predominantly muscle proprioception.

### 5.2.2.1 Joint/Muscles

The proprioceptive perception in humanoid robotics deals, as in the human case, with the perception of the kinematic chain position and how it is moving. The human body movements are originated by a combination of linear motors (muscles) and rotational or spherical joints. There are two main differences between humans and TEO humanoid robot regarding the components that produce the movement. The first one is the use of rotary motors instead of linear ones to produce the movement and, the second one, is the use of only rotary joints. Another difference regarding limb positions is the location of the sensors. In the human case, sensors are located in actuators (muscles) and joints meanwhile, in TEO humanoid robot, the position sensors are only located in joints.

The position of the human body links is sensed by means of both proprioceptive and exoceptive perceptions even though, with only proprioceptive perception, positions could be measured. The information of muscle spindles are populated to obtain the actual position of the limbs in every moment (Ribot-Ciscar et al., 2003). Taking this in consideration, the information of each joint sensor of the mechanical chain in TEO robot must be processed to obtain the extremities' position. This is performed by means of solving the direct and inverse kinematic problems.

The movement of each mechanical part of the humanoid robot is sensed by means of absolute and incremental (relative) encoders located in the joints. The incremental encoder is located at the joint input (motor/actuator) and it measures motor position and velocity. The absolute encoder, located at the joint output, senses its angle (limb position).

The incremental rotary encoder provides cyclical outputs (only) when the encoder is rotated. The device used in TEO robot is the low profile RENCO RCML15 optical encoder. It has 1024 line count resolution with A/B output format in phase quadrature. Its operating frequency is 500KHz. The encoder provides 1024 pulses each motor turn.

The relative position of every link is sensed by the AVAGO 7500 AEAS single-turn absolute optical encoder. This device generates a unique code for each position. When powered up, the absolute encoder does not require a home cycle even if the shaft was rotated while the power was switched-off. It has 11 digital tracks plus 2 sine/cosine tracks to generate a precise 16 bit Gray code. The information is provided by means of a serial output at 16MHz.

### **5.2.2.2 Cutaneous**

The cutaneous perception in TEO robot is circumscribed to the robot feet sole. It has been designed a flexible sole with embedded hall sensors and magnets to sensed rough terrains (Balaguer et al., 2011).

The irregularities of the ground are perceived by a matrix of this kind of sensor in each footstep. The result is a digital map of the ground stepped. It can be used to complement the information of the ground reaction captured by the ankle force/torque sensors. The system performing this perception is under development but it could be integrated into the postural control systems as soon as it will be ready.

## **5.3 Integration Centres**

As stated in Section 2.2.2, the information provided by body sensors are processed by different parts of the Central Nervous System. The place where the information is processed depends of the nature of the response. The responses can be classified according to the reaction time or latency from reflex reactions to voluntary movements, passing through automatic behaviours. The fastest response is the reflex reaction but it is close related to the automatic behaviours because both of them are processed in the spinal cord. The reflex actions can be classified according to four aspects (Dubuc, 2011; Purves et al., 2008):

- 1) How the reflex was developed:
  - a. Innate reflex: genetically determined.
  - b. Learned reflex: acquired through experience.
  
- 2) The nature of the resulting motor response:
  - a. Somatic: control skeletal muscles
    - i. Superficial reflexes (skin and mucous membranes)
    - ii. Stretch reflexes (deep tendon reflexes)

- b. Autonomic reflexes: control visceral muscles
- 3) The complexity of the neural circuit involved:
- a. Monosynaptic: sensory neuron synapses directly onto motor neuron
  - b. Polysynaptic: include one or more interneurons between the communication pathways.
- 4) The site of information processing:
- a. Spinal reflexes: not requiring input from the brain
  - b. Cranial reflexes: integrated within the brain

The interesting reflex acts for postural control are those somatic, monosynaptic or polysynaptic, processed in the spinal cord. The information produced by a stimulus follows a neural pathway called reflex arc. The reflex arc typically consists of five components:

- 1) The receptor at the end of a sensory neuron that reacts to a stimulus.
- 2) The sensory neuron conducts nerve impulses along an afferent pathway towards the Central Nervous System.
- 3) The integration centre consists of one or more synapses in the Central Nervous System (monosynaptic/polysynaptic).
- 4) A motor neuron conducts a nerve impulse along an efferent pathway from the integration centre to an effector.
- 5) An effector responds to the efferent impulses by contracting.

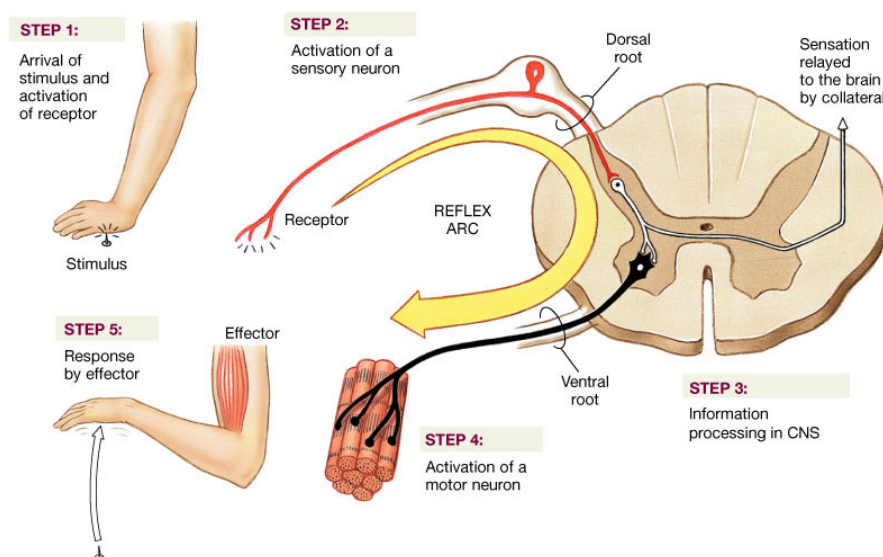


Figure 56 Human reflex arc

The spinal cord integrates spinal reflexes and contains central pattern generators. These are fast responses with a latency of 20-60ms. The brainstem and cerebellum control postural reflexes with a medium reaction time about 130-170ms.

The slowest response against a stimulus is the voluntary movement. Voluntary movements require a high level processing of the brain and associated areas (cerebellum and basal ganglia). The basic function of the brain cortex areas is to produce behaviours, which in postural control are, first and foremost, movements. The role of the basal ganglia is to select and trigger well-coordinated voluntary movements. Finally, the cerebellum regulates the sequence and duration of the elementary movements that compounds the posture control behaviour. On average, humans have a reaction time of 250ms to a visual stimulus, 170ms for an audio stimulus and 150ms for a touch stimulus.

TEO robot architecture divides posture control processing between the Central Process Unit (CPU) and one intelligent servo-drive that control each joint. Both systems are interconnected by means of a CANBus, described in Section 5.5.1.

### 5.3.1 CPU's

The mainboard integrated in TEO robot has an Intel<sup>TM</sup> Core 2 Duo E6400 (2 x 2.13GHz) processor. It is the 'brain' of the robot in which posture reactions and movement control is calculated. Table 11 shows the comparison between CPU and brain capacities (Intel, 2008; Merkle, 1988, 1989):

Table 11 Comparison between human brain and CPU processing capacities

	CPU	Brain
<b>Transistors</b>	291 Millions	100 Billions (neurons)
<b>L1 Cache</b>	Code and Data. 32KBx2	7 chunks $\pm 2^1$
<b>L2 Cache</b>	2MB shared cache	
<b>Memory</b>	2GB at 1066MTransfers/s	1015 synapses at about 10 impulses/s
<b>Power Cons.</b>	45 watts avg.	25 watts avg.

The most determinant difference between human brain and artificial CPU's is the huge capacity of the brain to perform multitude of parallel processes. Different approaches has been performed or are still running to replicate human brain (Pearn, 1999) but they doesn't reach the human brain cognitive capacity and, as well, they are not market available. Nevertheless, the gap between human brain and artificial processing systems can be reduced by the use of simplified kinematic models that reduce the number of computations (see Section 4.2).

---

<sup>1</sup> Chunk: fragment of information

### 5.3.2 ISCM8005 Intelligent Drives

In the described reflex arc, the fastest responses involve the minimum amount of neurons and the integration of the information at the spinal cord level. These reactions are ‘pre-programmed’ patterns transmitted to joints, performing a low level control of position, velocity, etc. The use of intelligent servo-drives tries to emulate this low level reflex arc. This kind of drivers has a built-in Digital Signal Processor (DSP) that enables control with the minimum CPU involvement. In this case, the driver can maintain the desired joint angle against external disturbances (see Figure 57). This behaviour corresponds to the fastest reflex arc in which only one motoneuron is involved and the reaction is processed in the spinal cord.

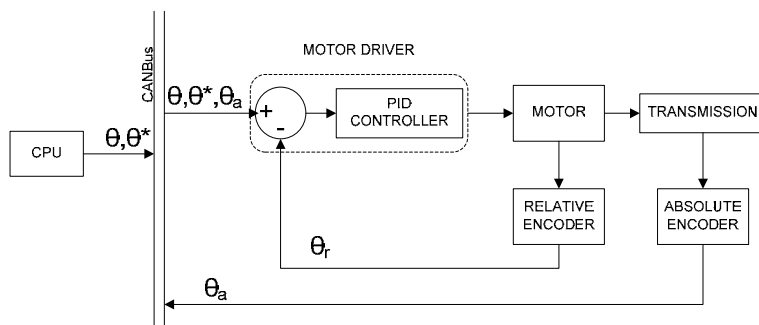


Figure 57 TEO robot reflex arc

Taking into account the transmission rate and the amount of information, the artificial reflex arc established has  $128\mu\text{s}$  of latency per joint. The total transmission delay per limb is not linear and it will depend on the task performed.

## 5.4 Action System

Postural muscles act predominantly to sustain posture against gravity. Control of posture is a prerequisite for efficient motion performance. Posture control depends of muscles capable of supporting continuous contractions, meanwhile voluntary movements often require fast and forceful muscle actions.

Due to this double nature of the muscle activity, muscles contain fibres that meet these different tasks. Muscles with strong postural functions mainly consist of slow response muscle fibres with a great resistance against fatigue. Nevertheless flexor muscles, responsible of voluntary motion (i.e. legs), are mainly composed of fast response fibres producing relatively large forces and rapid fatigue.

Basic mechanics of movement explain how the muscles in combination with the skeleton generate motion. The musculoskeletal system follows the mechanical principle of the lever to move or lift a load against another force. The component parts that are used in a lever are as follows:

- Lever: the bone
- Fulcrum (F):pivot point of the lever, which is usually the joint

- Muscle Force (M): force that draws the opposite ends of the muscles together
- Resistive Force (R): force generated by a factor external to the body (e.g. gravity, friction etc.) that acts against muscle force
- Torque: the degree to which a force tends to rotate an object about a specified fulcrum

There are different types of levers dependent upon the position of fulcrum, effort and resistive force (Figure 58).

- First Class lever (a): Muscle force and resistive force is on different sides of the fulcrum (i.e. the head resting on the vertebral column).
- Second Class lever (b): Muscle force and resistive force act on the same side of the fulcrum, with the muscle force acting through the level longer than that through which the resistive force acts (i.e. raising the body up onto the toes).
- Third Class lever (c): Muscle force and resistive force act on the same side of the fulcrum, with the muscle force acting through the lever shorter than that through which the resistive force acts (i.e. flexion of the forearm).

Most of the limbs of the human body are articulated by third class levers.

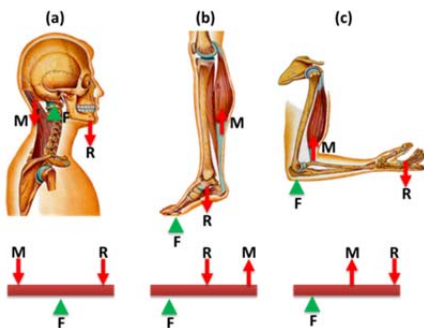


Figure 58 Human joints lever: (a) Class I, (b) Class II and (c) Class III

Muscles play four roles in producing joint movements: agonist (prime mover), antagonist, synergist, and fixator. A given muscle can play any of these roles, often moving from one to the next in a series during an action. Agonists and antagonists are opposing muscles. This means that when an agonist creates tension, the antagonist produces an opposing tension, thereby contributing to control at the joint. Synergists aid the motion of an agonist.

Although every musculotendinous unit (muscle belly and tendons attaching it to the bone) has a specific name, it is common to group muscles according to the motion they create. Flexors create motion that would bring the distal segment closer to the torso, while abductors cause a limb to move laterally, away from the body.

This movement scheme can be replicated using linear actuators but, in TEO robot extremities, it has been applied a classical robotic joint design. Each joint has been designed with a rotary motor with a transmission to reduce velocity and increase

torque. In this way, measurements related to joint movement cannot be directly mapped with human joint parameters.

### 5.4.1 Motor and Transmission

The joint design is different in the lower limbs than in the upper limbs. The bigger demand of torque of the leg joints forces the use of an elevated transmission rate design. For this reason, the lower extremities joints use a transmission composed by a Harmonic Drive™ and a pulley/belt train (Figure 59 (a)). The upper limbs use only Harmonic Drive™ with fixed reduction rate to increase the output torque (Figure 59 (b)).

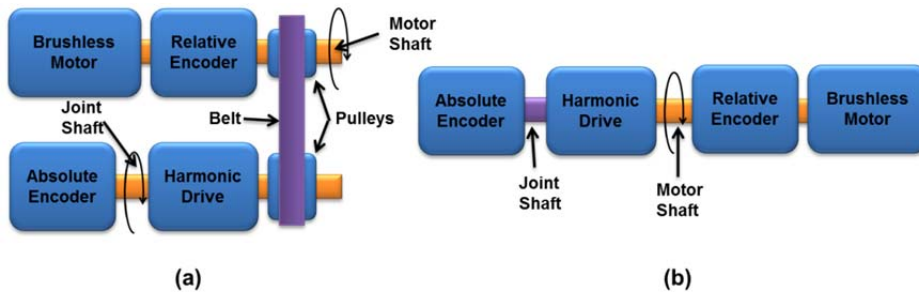


Figure 59 Lower limbs joint (a) and upper limbs joints (a) design

The articular joints were designed considering an estimated TEO body weight about 65Kg and a step velocity of 0.75m/s. The resulting features of each joint are shown in Table 12.

Table 12 TEO robot joints features

Joint	Reduction	Max. Torque	Max. Velocity	Joint Angle Limits
<b>Ankle Sagittal</b>	235.2	19,83 Nm	28 rpm	-20° / +20°
<b>Ankle Frontal</b>	270.4	25,50 Nm	12 rpm	-85° / +85°
<b>Knee</b>	235.2	19,83 Nm	28 rpm	0° / +150°
<b>Hip Sagittal</b>	523.2	49,34 Nm	6 rpm	-120° / +45°
<b>Hip Frontal</b>	192	16,19 Nm	34 rpm	-40° / +30°
<b>Hip Axial</b>	400	37,72 Nm	8 rpm	-30° / +24°
<b>Waist Frontal</b>	480	45,26 Nm	7 rpm	-15° / +60°
<b>Waist Axial</b>	160	15,09 Nm	21 rpm	-180° / +180°
<b>Shoulder Frontal</b>	160	15,09 Nm	21 rpm	-180° / +180°
<b>Shoulder Sagittal</b>	160	15,09 Nm	21 rpm	-45° / +120°
<b>Arm</b>	160	13,49 Nm	41 rpm	-60° / +60°
<b>Elbow</b>	160	13,49 Nm	41 rpm	-100° / +100°
<b>Forearm</b>	160	11,30 Nm	29 rpm	-40° / +55°
<b>Wrist</b>	160	11,30 Nm	29 rpm	-105° / +105°

## 5.5 Communication Channels

The information sensed by the proprioceptive and exoceptive systems must be transmitted to the described processor centres. This communication is performed by the afferent and efferent channels.

Sensory or afferent neurons carry the captured information towards the central nervous system. They transmit sensations experienced on or within the body, such as, pressure, pain and temperature amongst other sensations.

Motor or efferent neurons take signals from the central nervous system to the muscles and glands. Most Motor neurons are stimulated by interneurons, although some are stimulated directly by sensory neurons. These interneurons are found exclusively within the spinal cord and the brain.

In this way, there is a closed loop in the nervous system of sensation, decision and reactions. The elapsed time from perception to action is called the response time and it is composed by:

$$\text{Response Time} = \text{Reaction Time (RT)} + \text{Movement Time (MT)}$$

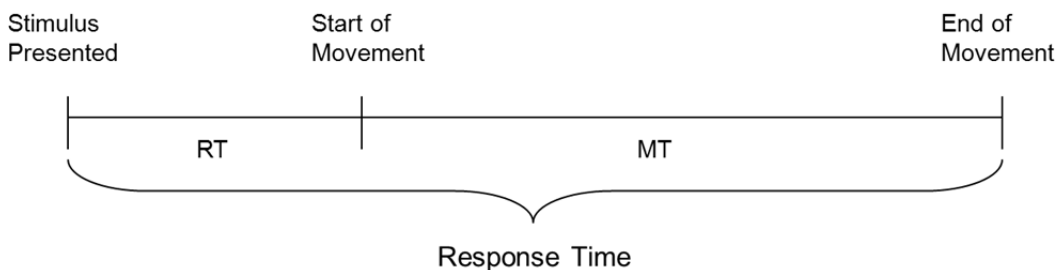


Figure 60 Human reaction time

The Reaction Time is the elapsed period between the presentation of a stimulus (premotor time) and the initial movement response (motor time).

The Movement Time begins with the start of physical movement to completion of movement. This time is modelled using Fitts' Law (Fitts, 1954), which value is highly task dependant:

$$MT = a + b \cdot \log_2 \left( \frac{2D}{W} \right) \quad (5.2)$$

Where:

- a represents the start/stop time of the device (intercept)
- b stands for the inherent speed of the device (slope).
- $\log_2 \left( \frac{2D}{W} \right)$  is the Index of Difficulty of the movement.
- D is the distance from the starting point to the centre of the target.

- W is the width of the target measured along the axis of motion.

The nerves of the skeletal muscles and large sensory nerves (temperature, touch, pressure, joint position) have a transmission rate between 12m/s and 120m/s. These velocities depend of the morphology of the neurons of the communication channel and the distance. The longer distance to transmit a stimulus, the faster the transmission velocity is. Considering a maximum pathway of 1m, the maximum delay time is about 8ms per transmission channel in the case of the reflex arc in the lower limbs. The total delay time due to neuronal channel communication is 16ms both direction (perception/reaction).

One important aspect to take in account is the existence of multiple communication channels in the human body. In this way, the communication and processing of the information in human body is performed in parallel in different areas of the Central Nervous System, improving exponentially the reaction performance.

The perception information in TEO robot has been divided depending of the importance of the perceptual information for postural control. High velocity CANBus networks are used to transmit the main proprioceptive information from all joints. The exoceptive perceptions (visual and inertial) are transmitted using USB 2.0 interfaces, meanwhile F/T information is transsmited by RS-485 interface. The communication between the two mainboards (the brain) of the robot is implemented by means of a high-speed Ethernet connection. The whole communication architecture is shown in Figure 61.

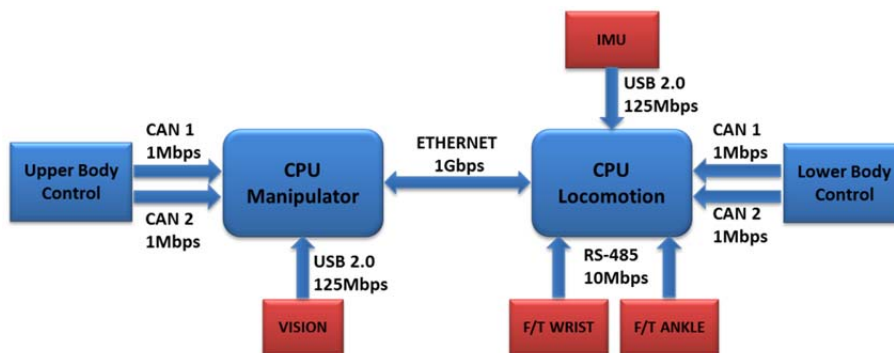


Figure 61 TEO robot communication architecture

### 5.5.1 CANBus

Controller Area Network (CAN or CANBus) is a field bus standard designed to allow devices to communicate with each other without a host computer. It is a message-based protocol, multi-master broadcast serial bus (Pazul, 1999).

The CAN Bus interface uses an asynchronous transmission scheme controlled by start and stop bits at the beginning and the end of each message. The information is passed from transmitters to receivers in a data frame composed by an Arbitration field, Control field, the Data field, a field for error control (CRC), the confirmation of read message (ACK field). The frame begins with a 'Start Of Frame' (SOF), and ends with an 'End Of Frame' (EOF) space. The data field may be from 0 to 8 bytes (see Figure 62).

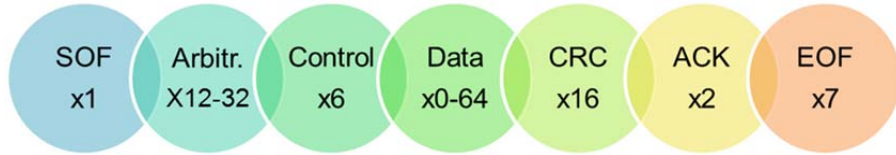


Figure 62 CAN Message Frame

The transmission data rate selected for TEO robot communication is 1Mbps, being this velocity the top end. In this case, the transmission time of complete frame (128 bits) is 128 microseconds. Each lower limb has six devices attached to one CANBus communication channel and the upper limbs have seven CAN devices attached to two buses. Taken this into account, the time to communicate 8 bytes to one whole lower limb in the worst case would be about 768 microseconds. This time doesn't consider possible communication delays neither the responses from the CAN devices to the CPU controller.

It can be compared the reaction time of the human reflex arc with TEO reflex arc (Figure 57). In the case of the robot, the communication of the position perceived only travels in one direction and, after processing ( $t_p$ ), the motor is directly commanded because it is directly connected to the driver. Delays appear when more than one joint is connected to the CANBus and the hardware controls the message priority of the different transmitters.

Table 13 Comparison of the reflex arc latency

	<b>Human Reflex Arc</b>	<b>TEO Reflex Arc</b>
<b>Time (one joint)</b>	16ms max.	$128\mu s + t_p$

### 5.5.2 Ethernet

Ethernet is a family of computer networking technologies for local area networks (LANs) commercially introduced in 1980. Systems communicating over Ethernet divide a stream of data into individual packets called frames. Each frame contains source and destination addresses and error-checking data so that damaged data can be detected and re-transmitted (Seifert, 2001).

This kind of communication channel is used to inter-communicate the CPU controller of upper body with the controller of the lower body. The connexion has a transmission rate of 1Gbps.

### 5.5.3 USB serial bus

Secondary devices with information such as visual perception or inertial measurements communicate with postural controllers by means of USB (Universal Serial Bus) with a maximum transmission data rate of 125Mbps (Intel et al. , 2000).



## CHAPTER 6

# Low Level TEO Robot Architecture

## 6.1 Low Level Postural Control Architecture

Section 3.3 exposed the human inspired and task oriented novel postural control architecture developed for the humanoid robot TEO. It presents three main modules. The first one is the task database with all the abilities that TEO robot can perform. The second one is the feedback control module, which supervises the normal operation of the robot and its equilibrium when walking on even terrains. The last module corresponds to the key point of this PhD Thesis: the feedforward postural control loop.

The study of the human postural control system reveals the existence of the two kinds of control loop mentioned. Previous postural control systems developed for humanoid robots in the RoboticsLab research group were based only on one of them for different reasons. The development of the new TEO robotic platform has brought the opportunity of improving the previous works.

Chapter 3 exposed the feedforward module architecture and its operation from a high level. Taking this into account, the aim of Chapter 6 is the study in depth of each part presented in Chapter 3. Here, each feedforward module component and its low level operation are explained more in detail. The expanded module architecture is presented in Figure 63. That chart shows the perception evaluation module in its left side. This module is in charge of capturing sensations and, as well, transforming them into usable information by the control system called perceptions.

In the middle position, the surprise generation module is in charge of processing the perceptual information. The sensorial information is converted in two kinds of surprise events: active and passive. The active events are related with predictions about the future status of a determined variable. The passive surprise is related, by the other hand, with the actual state of the variable under study.

The last module, at the right side, is the behaviour decision system. It must deal with all surprise produced and decide whether a reaction should be elicited. This module is close related with the task structure defined in Figure 22, because of its main outcome is the parameterization of reactions and the modification of the task execution flow when it is needed.

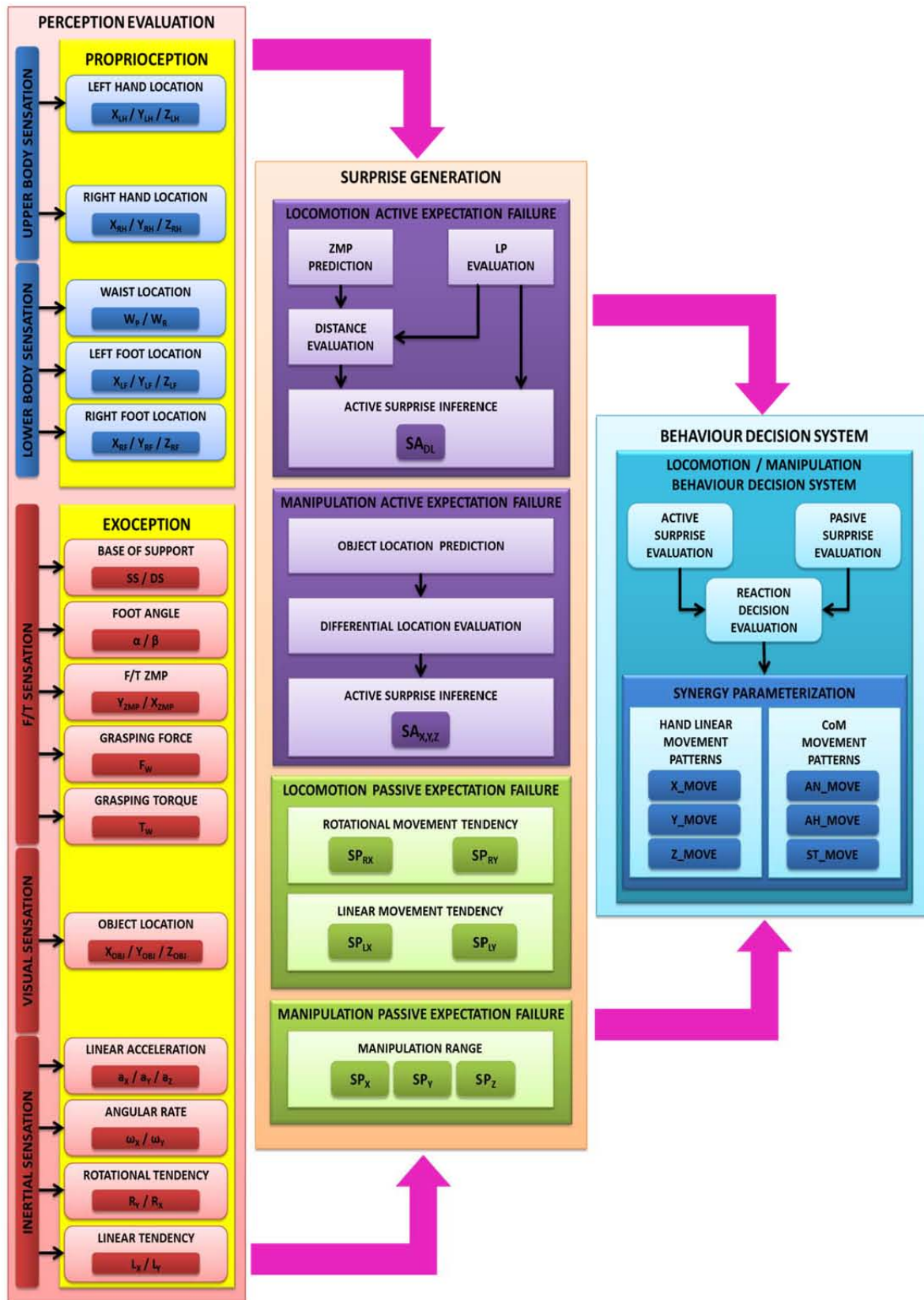


Figure 63 Feedforward module low level architecture

Next sections will describe all these modules: their inputs, how the system processes them and their outcomes.



## 6.2 Sensorial Evaluation

Sensations can be divided in two main groups attending to the location of the source. If stimuli come from an external source the sensation is called exoceptive. Otherwise, the sensation relative to internal body parts, their conditions, etc. is called proprioceptive. The sensation capturing system is composed by highly specialized sensory organs that are an extension of the Central Nervous System. The result of the brain's interpretations of the sensations is called perception and, attending to the classification made before, there exist two main perceptions: exoception and proprioception.

These perceptions explain to the body how to respond to the stimuli. In the same way, the humanoid robot processing system must evaluate the information coming from the mentioned sensorial sources. The human inspiration of this PhD Thesis favours the searching of methods and systems that made robot behaviour more natural and human-like. Another important factor to select a sensorial evaluation system is the fuzzy nature of the sensations. Due to these reasons, the evaluation of complex perceptions for the robot TEO has been based in the implementation of neuro-fuzzy sensation inference systems. This method combines the human-like reasoning style of fuzzy systems with the learning and connectionist structure of the neural network.

Other reasons to use this technique are the non-dependence from the human experience to generate the inference system and its ability to generate the resulting system from a training process, knowing only system input and output data, as described in Chapter 4. Therefore, it is possible to construct a sensorial evaluation system having a set of sensorial input data and the perceptual output it causes. Following, the proprioceptive and exoceptive perceptions developed for humanoid robot TEO are explained in detail.

### 6.2.1 Proprioceptive perception

For robots to become effectively used in a wide range of application, they may gain the ability to work in unpredictable and changing environments. The locomotion and manipulation problems presented before cover the most of this range. In both problems, proprioceptive perception resulting from absolute encoder information evaluation will help to reach this aim.

Proprioceptive perception in TEO humanoid robot is composed by the knowledge about the relative angle between adjoin links. Limb location is related to the solution of the forward kinematic problem, where a rigid body location is calculated using the joint angles of the kinematic chain connected to it. These devices measure the absolute angle ( $q_k$ ) of the joint when moving in relation to the pre-established zero position. The upright posture has been used to establish the initial condition of the absolute encoder. That is, it corresponds with a zero angle measurement in each joint. This posture is the basis for modelling the system by means of the application of Denavit-Hartenberg algorithm. The kinematic model for TEO humanoid robot is presented in Figure 64.

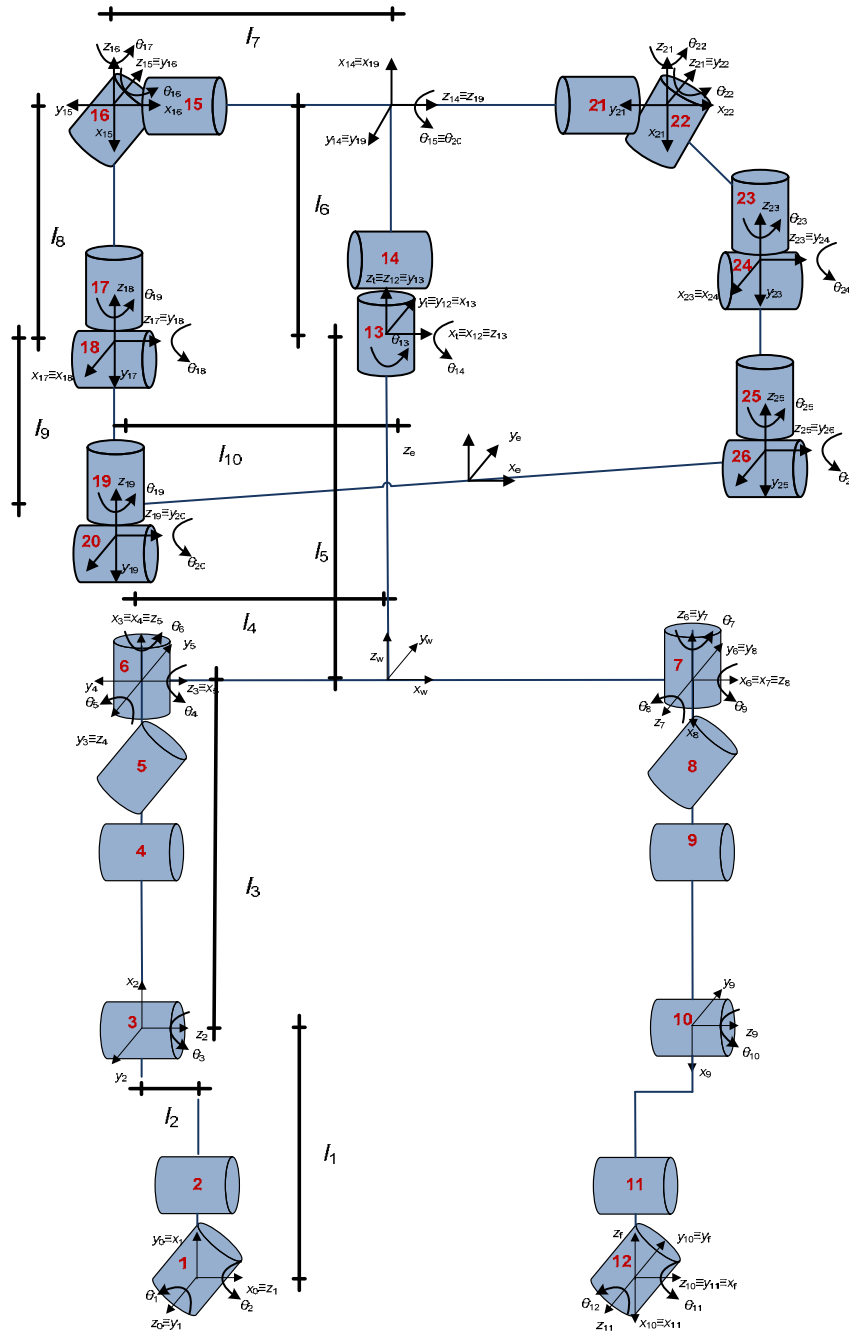


Figure 64 TEO robot kinematic chain

The Denavit-Hartenberg algorithm is the most used method to solve forward kinematics problem. Unfortunately, forward kinematics do not stay so simple. The kinematics of serial chains of manipulators become increasingly difficult due to the number of links added. Because of this, the computation kinematics is divided into sub-problems easier and faster to solve. Table 14 shows this sub-problem division and the desired outputs that are calculated by means of homogeneous transformations. It is important to note that the origin reference frame has been located at the waist of the robot. It is also aligned with the cross point of the hip rotation axes. But this approach does not meet the bio-inspired conception of the perception system due to the nature of the algorithm and the methods needed to calculate the desired output.

Table 14 Sub-problem division

	<b>Output Location</b>	<b>Homogeneous Transformations</b>
<b>Upper Body (16 DOF)</b>	Torso	${}^0T_{14} = {}^0T_{13} {}^{13}T_{14}$
	Right Hand	${}^0T_{20} = {}^0T_{14} {}^0T_{15} {}^{15}T_{16} {}^{16}T_{17} {}^{17}T_{18} {}^{18}T_{19} {}^{19}T_{20}$
	Left Hand	${}^0T_{26} = {}^0T_{14} {}^0T_{21} {}^{21}T_{22} {}^{22}T_{23} {}^{23}T_{24} {}^{24}T_{25} {}^{25}T_{26}$
	Head	${}^0T_{28} = {}^0T_{14} {}^0T_{27} {}^{27}T_{28}$
<b>Lower Body (14 DOF)</b>	Right Foot	${}^0T_6 = {}^0T_1 {}^1T_2 {}^2T_3 {}^3T_4 {}^4T_5 {}^5T_6$
	Left Foot	${}^0T_{12} = {}^0T_7 {}^7T_8 {}^8T_9 {}^9T_{10} {}^{10}T_{11} {}^{11}T_{12}$

The corresponding Denavit-Hartenberg parameters of TEO humanoid robot and the homogeneous transformation matrix have been detailed in Annex I.

Sensation is captured by means of absolute encoders integrated in every joint and its processing must be as fast as possible due to the high number of joints. Proprioception evaluation in humans is a fast parallel process due to the multiple communication channels and processor centres in charge of this task.

The first bottleneck in TEO robot proprioceptive perception evaluation is the communication architecture. Proprioceptive sensors are connected to four CANBus communication nets. At least, six sensor devices and other motion devices are connected to each net. The other aspect of perception evaluation is related to processing issues. TEO robot processing system is composed by two CPUs in charge of sensation process, balance control, etc. Due to this, the proprioceptive perception evaluation has been divided into upper body (manipulator) and lower body (locomotive) sub-problems. It reduces the number of degrees of freedom for processing and it is also conditioned by the double processor system architecture.

Then, the required time to evaluate the proprioceptive perception will depend on the communications delay, and the processing time will depend on the variable CPU processing time ( $t_{CPU}$ ) and the communication latency ( $t_{com}$ ). It has been proved that the communication loop for controlling 6DoF per limb cannot be less than 7ms. Thus, the minimum processing time will be at least equal to this value. It is expressed by equation (6.1). The main objective of the novel proprioceptive evaluation module will be the minimization of the processing time ( $t_{CPU}$ ).

$$t_{eval} = t_{com} + t_{CPU} = 2 \times 0.007 + t_{CPU} = 0.014\text{ms} + t_{CPU} \quad (6.1)$$

Due to the communications bottleneck imposed, the way to improve system performance can be achieved by the implementation of a bio-inspired parallel sensation processing system. The application of neuro-fuzzy evaluation of perceptive information can help to achieve this goal. According to the sub-problem division

commented before and the process to build a neuro-fuzzy inference system, the upper body and lower body TEO proprioception's have been created.

### 6.2.1.1 Lower body proprioception modelling

The aim of the lower body proprioceptive perception evaluation is to determine the location of both feet ( $f$ ) in relation with the reference frame ( $o$ ) of the humanoid robot. This reference point was selected as origin to obtain the Denavit-Hartenberg parameters of the robot. It is located in the same level of the hip frontal joint, in the middle of both legs ( $l_{WL1}$ ) and under the waist link ( $l_{WL2}$ ). The scheme for waist and feet location evaluation is shown in Figure 65 and it is described in detail in Annex I.

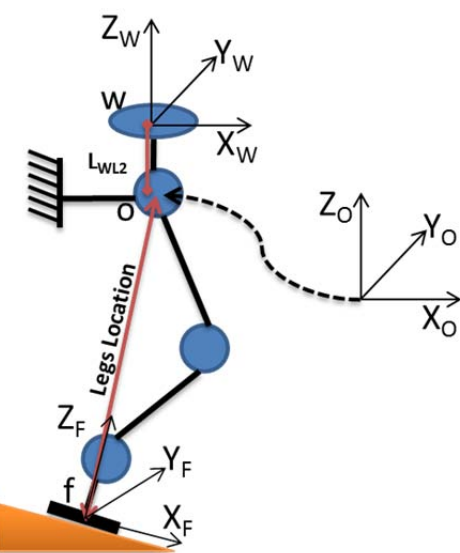


Figure 65 Feet location ( $X_F, Y_F, Z_F$ ) and waist location ( $X_W, Y_W, Z_W$ )

Every foot location is calculated solving the forward kinematic problem of each leg from the reference *o-frame*, located at the every leg hip joint. The legs can be considered as two 'manipulators' with six DoF and their end effector location is defined by vector ( $\vec{L}_F$ ) from equation (6.2). As well, the selected location of the reference *o-frame* simplifies the waist location computation, which can be obtained only considering the movement of hip joints. Nevertheless, waist location is very constrained by mechanical and operational conditions. During even upright locomotion task, for instance, waist orientation must have the same Z component direction ( $Z_W$ ) than gravity acceleration.

$$\vec{L}_F = \vec{o}f \quad (6.2)$$

Therefore, the constraint of the vertical orientation of the waist causes the necessity of evaluating waist roll and pitch. Roll deviations are caused by turning on sagittal plane joints (Figure 66 (a)) and pitch deviations by turning on frontal plane joints (Figure 66 (b)). The influence of each leg or joint will also depend on the phase of the locomotion task. The three possible cases that can occur:

- 1) During single support phase, only turns on sagittal plane joints of the supporting leg roll the waist.

- 2) During double support phase, the movement of any sagittal plane joint can cause the elevation of the one of the legs. Then, this case is converted in the single support one.
- 3) Joints in the frontal plane can pitch the waist. The movement of this kind of joint must be coordinated to avoid waist pitch unless it was a requirement of a specific task.

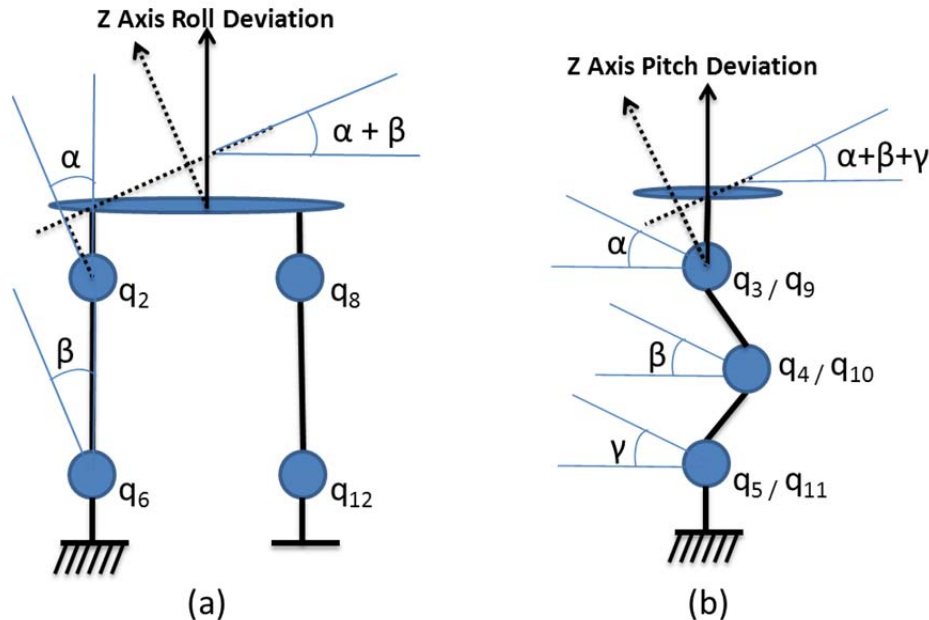


Figure 66 Roll (a) and pitch (b) Z axis possible deviations

Once the system model is known, the starting point for the development of the neuro-fuzzy proprioceptive evaluation is to obtain the input and output datasets that models the system behaviour. The input dataset is firstly constrained by the locomotion task conditions. They impose the commented waist orientation. As well, joint turn angle constraints were considered with the aim of reducing the range of each input for the neuro-fuzzy system and improving the training process Table 15.

Table 15 Lower body joint angle limits

	JOINT	JOINT NUMBER	ANGLE LIMITS
LEGS	Hip Axial	1 / 7	-30° to +24°
	Hip Sagittal	2 / 8	-120° to +45°
	Hip Frontal	3 / 9	-40° to +30°
	Knee	4 / 10	0° to +150°
	Ankle Frontal	5 / 11	-20° to +20°
	Ankle Sagittal	6 / 12	-85° to +85°

Taking into account the constraints mentioned before, it is necessary to build one dataset to train the neuro-fuzzy network and, another one to check it. Both datasets are composed by the combination of a serial of inputs and outputs previously calculated. The input data is composed by random values of the joint angles, within their movement range. The output data is obtained solving the forward kinematic problem of the TEO lower body for each set of the random inputs. Both datasets are shown in Table 16.

Table 16 Lower body datasets

	Input Dataset	Output Dataset
<b>Right Leg</b>	$q_1 q_2 q_3$ $q_4 q_5 q_6$	$X_{RF}$ $Y_{RF}$ $Z_{RF}$
<b>Left Leg</b>	$q_7 q_8 q_9$ $q_{10} q_{11} q_{12}$	$X_{LF}$ $Y_{LF}$ $Z_{LF}$
<b>Waist</b>	$q_1 q_2 q_3$ $q_4 q_5 q_6$ $q_7 q_8 q_9$ $q_{10} q_{11} q_{12}$	$W_P$ $W_R$

The result of the training is eight neuro-fuzzy systems for lower body proprioception evaluation. Figure 67 scheme summarizes this proprioception evaluation.

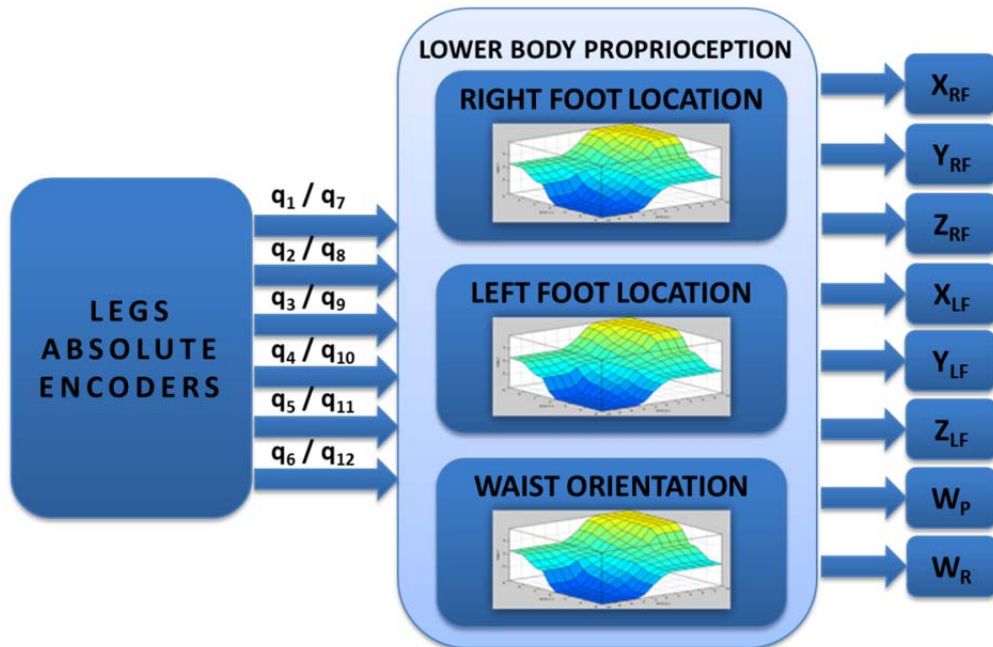


Figure 67 Lower body proprioceptive perception evaluation scheme

### 6.2.1.2 Upper body proprioception modelling

In the upper body case, the aim of the proprioceptive perception evaluation is to determine the location and orientation of hands (h) and torso (s) regarding the bottom waist (o) of the system. Every coordinate of each hand is composed by the sum of the torso location and the corresponding arm joint configuration Figure 68.

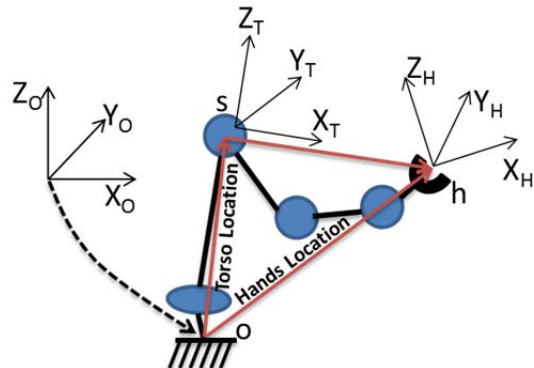


Figure 68 Torso location ( $X_T, Y_T, Z_T$ ) and hand location ( $X_H, Y_H, Z_H$ )

It is important to remark that it is only valid for manipulation tasks without locomotion. Including locomotion, it would be necessary the addition of the waist position and the orientation related to the Base of Support. Thus, in this case, the vector for torso location ( $\vec{L}_T$ ) is expressed by equation (6.3) and the vector for hands location ( $\vec{L}_H$ ) by equation (6.4).

$$\vec{L}_T = \vec{o}s \quad (6.3)$$

$$\vec{L}_H = \vec{o}s + \vec{s}h \quad (6.4)$$

As commented before, the first step is to calculate the input and output datasets that models the system behaviour. They are obtained from the offline solution of the upper body kinematic equations, taking into account the premise of no lower body movement. Furthermore, other constraints applied in calculating these datasets are the joint mechanical turn limitations from Table 17.

Table 17 Upper body joint angle limits

	<b>Joint</b>	<b>Joint number</b>	<b>Angle limits</b>
<b>Body</b>	Waist Axial	13	-45° to 45°
	Waist Frontal	14	-15° to 15°
<b>Arms</b>	Shoulder Frontal	15 / 21	-180° to +180°
	Shoulder Sagittal	16 / 22	-45° to +120°
	Arm	17 / 23	-60° to +60°
	Elbow	18 / 24	-100° to +100°
	Forearm	19 / 25	-40° to +55°
	Wrist	20 / 26	-105° to +105°

As in the case of the lower body, the input dataset was obtained generating joint angles within the constraints, and the output data were calculated solving the forward kinematic problem for the previously computed inputs. This output dataset is composed by the X, Y and Z coordinates of each hand (Table 18).

Table 18 Upper body datasets

	Input Dataset	Output Dataset
<b>Torso</b>	$q_{13} q_{14}$	
<b>Right Hand</b>	$q_{15} q_{16} q_{17} q_{18} q_{19} q_{20}$	$X_{RH}$ $Y_{RH}$ $Z_{RH}$
<b>Torso</b>	$q_{13} q_{14}$	
<b>Left Hand</b>	$q_{21} q_{22} q_{23} q_{24} q_{25} q_{26}$	$X_{LH}$ $Y_{LH}$ $Z_{LH}$

Figure 69 summarizes the seven neuro-fuzzy evaluation systems for right/left hands. The estimation of limb location by means of processing the absolute encoder information through these neuro-fuzzy networks produces the upper-body proprioception.

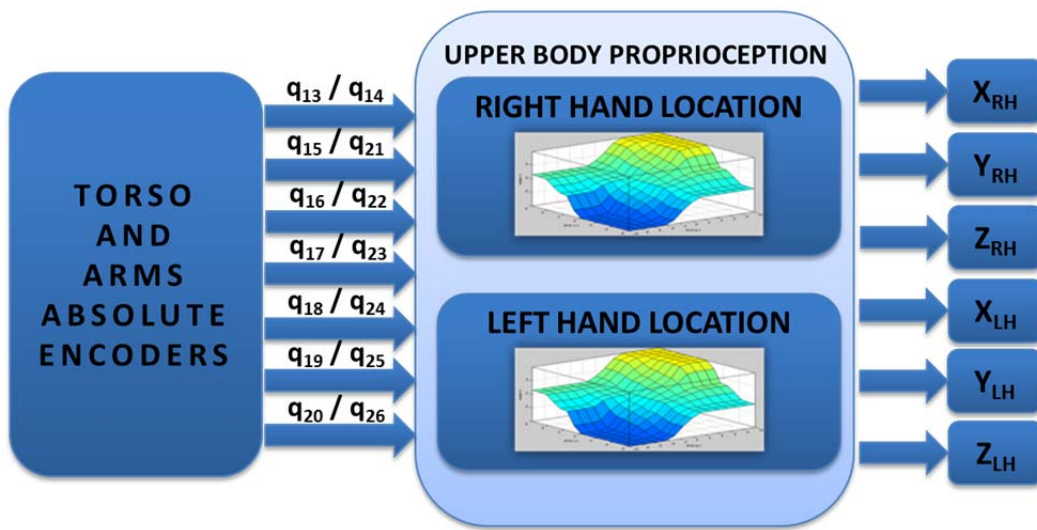


Figure 69 Upper body proprioceptive perception evaluation scheme

In conclusion, this proprioception evaluation permits to know limb location. This knowledge can be used directly or applied in the parameterization of the humanoid robot simplified models exposed in Chapter 4.

### 6.2.2 Exoceptive perception

Studies exposed in Chapter 2 reveal how humans employ exoceptive sensorial information. Sensorial processor centres generate appropriate exoceptive perception parameters according to the body posture and the task performed. Later, neural

reaction centres apply this information to evaluate different parameters that are extracted from ‘simplified models of the human body’. The result of this evaluation would be any kind of postural adjustment if it were necessary. These adjustments are usually performed by means of parameterizing and executing postural strategies.

In the same way, exoceptive sensorial information in TEO humanoid robot must be processed. Appropriate use of exoceptive sensorial information can help to improve task performance. To achieve this, it is important to recall that this perceptive information evaluation must be human inspired and task oriented.

Thus, neuro-fuzzy inference system was the method selected to evaluate exoceptive sensorial information, as well applied in proprioceptive perception generation. As it was seen before, neural networks and fuzzy inference systems are two human-inspired techniques used to evaluate information from TEO robot sensorial sources.

Three exoceptive sensorial systems have been integrated in TEO humanoid robot. The first one is the inertial measurement system composed by an Inertial Measurement Unit (IMU). This sensorial system is in charge of detecting changes in velocity and acceleration of the body like the human vestibular system does. The second sensorial system is composed by the ankle and wrist joints torque/force sensors. In humans, this function appears to involve sensors inside the muscle tendons. They measure forces exerted directly to the humanoid body because of close interaction (manipulation, ground reaction force, etc.) The vision system is the last sensorial system integrated in TEO humanoid robot. Human vision has many roles in tasks performance. For instance, it is used to measure object distance and relative movement or, as well, it plays a significant role in human balance control. These functions, among others, have been integrated in TEO humanoid robot.

Human perception processing is performed in different neural centres depending on the stimulus. This process is also performed in different areas of these neural centres depending on the task. As well, the exoception processing in TEO robot is task oriented because its information sources are highly influenced by the task performed. The division into manipulative and locomotive tasks helps the system to classify, to process and to apply the information in the proper way. Therefore, the neuro-fuzzy evaluation results of sensations have been established depending of this task oriented nature.

Another important issue to take into account about processing the exoceptive perceptions are the constraints of TEO electromechanical system. As reviewed in Chapter 5, exoceptive sensorial devices have, in many of their characteristics, better performance than human organs with the same function. Because of this, sensor devices do not constitute a constraint by themselves. Dynamics of the humanoid robot body are determined by the movement of its parts. The knowledge of electromechanical limitations and their interaction with exoceptive perception evaluation is determinant.

Opposite to proprioceptive case, the communication of sensed information to process centres is not a bottleneck due to each exoceptive source transmits its information through independent communication pathways.

In conclusion, the main constraint in exoceptive perception evaluation is the capacity of the processing centres and how the resulting information is employed. Next topics related with the exoceptive systems will expose more in detail the constraints that determine the information processing and its output.

### 6.2.2.1 Force/Torque system

Forces and torques are perceived by the human body by means of multiple sensitive organs. Those have in common that sensation is generated when several physical components interact. That is, these sensor organs need physical contact with the source of the captured magnitude. For instance, sensors allocated in muscle tendons measure the force exerted directly by the muscles attached to them or pressoreceptors from skin measures contact when handling. It would be possible to think that the vestibular system acts in the same way but it has a little difference. Vestibular system measures fictitious or inertial forces with or without direct contact.

TEO humanoid robot possesses as well this kind of perception's capability but only in ankles and wrists. Sensors incorporated to the ankle subassembly measure reaction forces and torques with the ground. By other hand, sensors in the wrist substructure measure direct contact when manipulating. These devices capture information in three dimensions in the indicated joints (Figure 70 (a) and (b)).

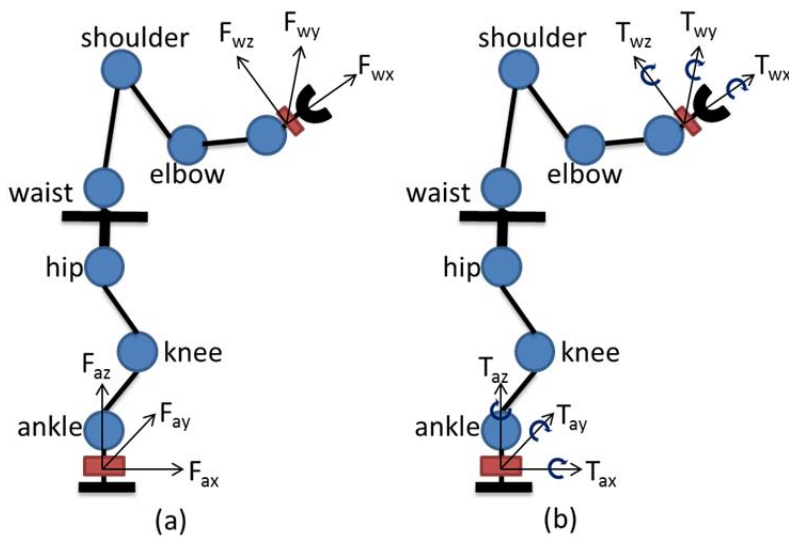


Figure 70 Force frames (a) and torque frames (b) of the F/T sensors

#### 6.2.2.1.1 Ankle sensors

The F/T sensors allocated in the ankles capture the information produced when feet contact ground. They measure the reaction forces and torques produced during the locomotive movement of the robot or stance. Taking this into account, the use of this information will be restricted to locomotion tasks.

The information from these sensors can be interpreted and applied in different ways. The first one is the determination of the locomotion stage. During locomotion two main phases are considered: double and single support phases. The direction of the vertical

reaction force in each foot, which is defined by the sign of the force, reveals whether the corresponding foot is on the ground or in the air (see Table 19).

Table 19 Robot support phase obtained from force evaluation

	<b>Right Foot</b>	<b>Left Foot</b>	<b>Phase</b>
<b>F<sub>z</sub> Direction</b>	+	-	Right Foot Single Support (SSR)
	-	+	Left Foot Single Support (SSL)
	+	+	Double Support (DS)

The second way of using F/T sensors information is the evaluation of each foot orientation related to the vertical direction. It could be a correction factor to evaluate the stability margin of the robot. The results of this evaluation are  $\alpha$  (pitch) and  $\beta$  (roll) angles of the ground reaction force vector (Figure 71). Assuming the complete surface contact between ground and foot, it will determine the angle of the ground under each foot independently.

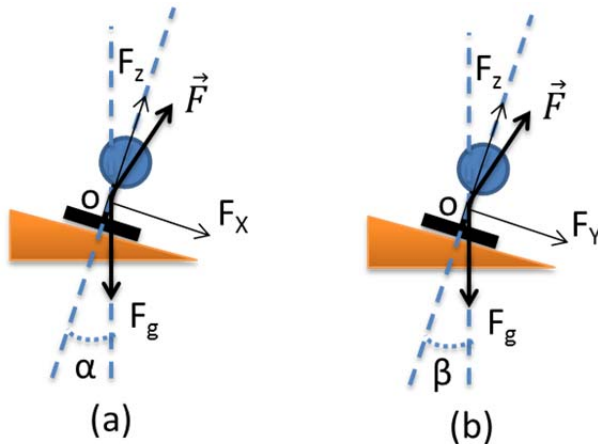


Figure 71 Ankle pitch ( $\alpha$ ) and roll ( $\beta$ )

$$\alpha = \cos^{-1} \frac{F_z}{\sqrt{F_x^2 + F_z^2}} \quad (6.5)$$

$$\beta = \cos^{-1} \frac{F_z}{\sqrt{F_y^2 + F_z^2}} \quad (6.6)$$

The third way of evaluation of the F/T sensor sensation is the stability margin based on ZMP computation. As described in Chapter 4, ZMP is one indicator of the robot balance. When the foot is placed on the ground, the reaction force vector can be used to determine the local ZMP. In this case, local ZMP indicator is not a reference of the robot's global stability. The ZMP related with the whole body is the result of the position weighted average from both feet local ZMP. The prediction of the evolution of ZMP position in relation with the support convex hull can be used to preview the evolution of

the robot balance. Taking into account that each foot could be placed in uneven terrain, the computation of the support area envelope and the ZMP turns into complex task.

Because of that, the use of a Virtual Horizontal Plane (VHP) makes these computations easier (Figure 72). The VHP is located at a  $H_{VHP}$  distance from the waist to the lowest foot on the ground. The foot projection has been assumed to have circular shape with constant radius ( $r_F$ ). Then, considering the waist projection ( $gw_o$ ) as the origin of the projected coordinates, the convex hull of the supporting area can be determined using the proprioceptive information about foot location.

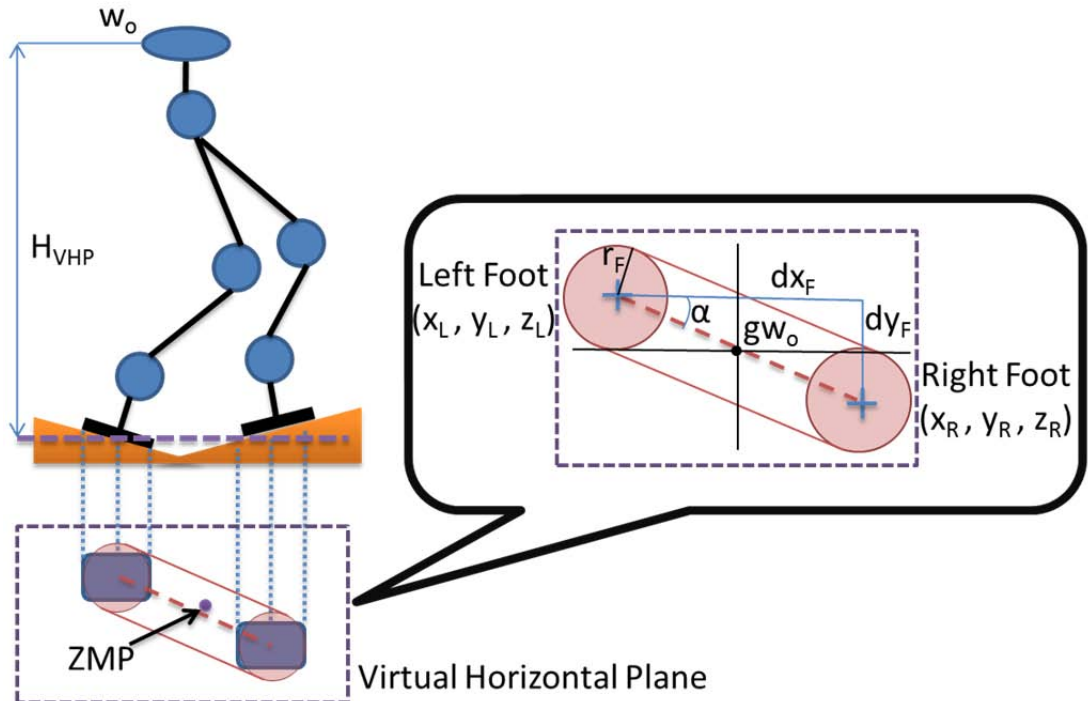


Figure 72 Virtual Horizontal Plane: projected support convex hull and ZMP

Therefore, taking into account the inputs from the F/T sensors, the mechanical capacities and the local ZMP coordinates, this exoceptive perception can be evaluated in the way shown in Figure 73.

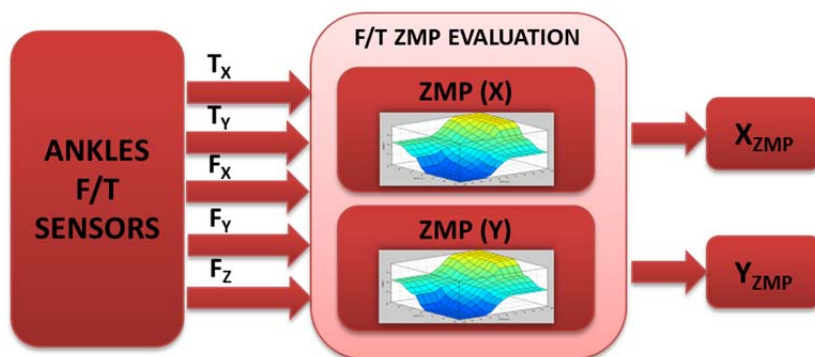


Figure 73 ZMP F/T sensors exoception scheme

The computation of the ZMP location using force and torque values is performed by two neuro-fuzzy inference systems. The input and output datasets necessary to train and obtain the inference system are presented in Table 20.

Table 20 ZMP F/T exoception input/output datasets

Input Dataset			Output Dataset
	Force	Torque	
<b>Right Foot</b>	$F_x$	$F_z$	$X_{ZMP}$
<b>Left Foot</b>	$F_x$	$F_z$	
<b>Right Foot</b>	$F_y$	$F_z$	$Y_{ZMP}$
<b>Left Foot</b>	$F_y$	$F_z$	

### 6.2.2.1.2 Wrists sensors

On the other hand, the information coming from wrists F/T sensors is only used for manipulation tasks. This exoception is related to object handling and the forces and torques caused by this interaction Figure 74.

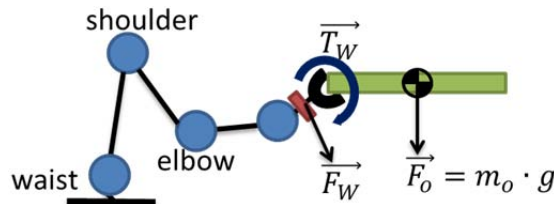


Figure 74 Wrist F/T sensors

The information about manipulation can be applied in different ways but it is only used for robot safety during handling. This mission is achieved evaluating the modulus of force and torque vectors from interaction (equations (6.7) and (6.8)).

$$|F| = \sqrt{F_x^2 + F_y^2 + F_z^2} \quad (6.7)$$

$$|T| = \sqrt{T_x^2 + T_y^2 + T_z^2} \quad (6.8)$$

Then, the human inspired force and torque exoceptive sensation evaluation scheme is represented in Figure 75.

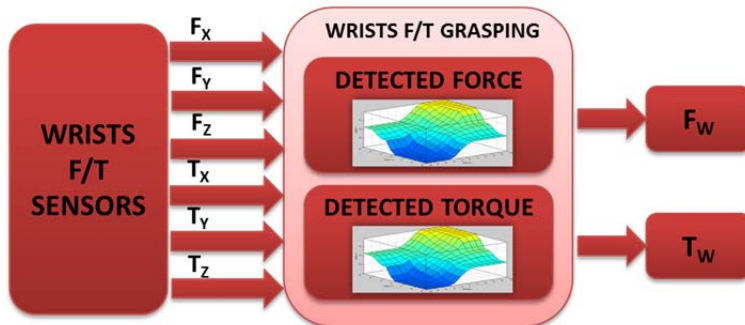


Figure 75 Wrists F/T sensors exoception scheme

From previous scheme, the input and output datasets that compose the base for neuro-fuzzy training are exposed in Table 21.

Table 21 Wrists F/T exoception input/output datasets

	Input Dataset				Output Dataset
<b>Right Wrist</b>	Force	$F_x$	$F_y$	$F_z$	$F_w$
<b>Left Wrist</b>	Force	$F_x$	$F_y$	$F_z$	
<b>Right Wrist</b>	Torque	$T_x$	$T_y$	$T_z$	$T_w$
<b>Left Wrist</b>	Torque	$T_x$	$T_y$	$T_z$	

### 6.2.2.2 Inertial system

The Inertial Measurement Unit (IMU) is a device with a similar role than the human vestibular system but also with very important functional differences. The inertial sensor device integrated in TEO robot mechanics is a complex system that performs by itself more than the vestibular apparatus' functions. The main feature that favours the use of this kind of devices is their processing capabilities. In the human case, all evaluation of the input information is performed by the Central Nervous System but the IMU has some processing capacity. In addition to more complex outputs, the IMU provide raw data regarding angular rate and linear accelerations (Figure 76). The combination of all output data is exclusively applied in locomotion tasks to keep robot balance.

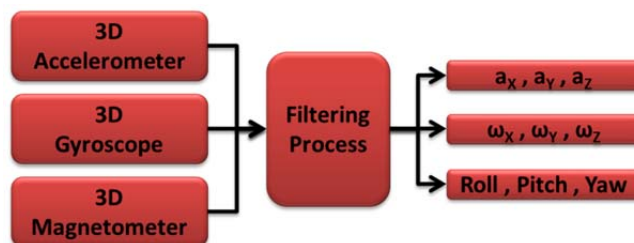


Figure 76 Inertial exoceptive output

Three main outputs from this exoception evaluation have been established combining the IMU information. The first one is related with the rotational robot movement tendency. This perceptual outcome is obtained from computation of the period for one rotation ( $T_R$ ) with the determined angular rate ( $\omega_x, \omega_y$ ). This measured rotation angle (Roll and Pitch) relates the angular velocity with the angular position of the robot body (equations (6.9) and (6.10)).

$$T_R = \frac{\omega_{x,y}}{2\pi} \quad (6.9)$$

$$R_{X,Y} = T_R \cdot \theta_{Y,X} \quad (6.10)$$

The evaluation of the rotational tendency of the robot during locomotion ( $R_x$  and  $R_y$ ) is performed by neuro-fuzzy networks in both of the directions under study (see Figure 77).

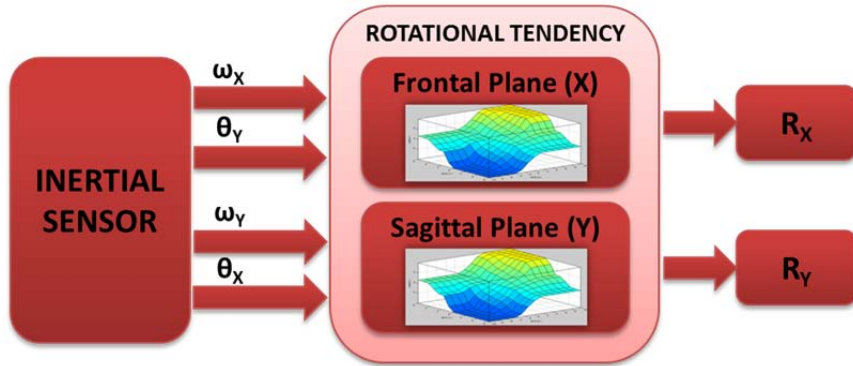


Figure 77 Robot body rotational tendency

The neuro-fuzzy networks must be trained using as input dataset the inertial information. The output dataset will be composed by the required rotational tendency value caused by a determined input. Both datasets are established in Table 22.

Table 22 IMU rotational tendency evaluation input/output datasets

	Input Dataset		Output Dataset
INERTIAL MEASUREMENT UNIT	Angular Rate	$\omega_x$	$R_x$
	Orientation	$\theta_y$	
	Angular Rate	$\omega_y$	$R_y$
	Orientation	$\theta_x$	

The second exoceptive outcome from the inertial measurements is the linear movement tendency of the robot. The linear acceleration vector measured by the IMU ( $a_x$ ,  $a_y$ ,  $a_z$ ) must be rotated, using the inverted rotation matrix ( $R_{RPY}$ ), to obtain the linear movement tendency in the principal axes ( $L_x$ ,  $L_y$ ,  $L_z$ ). This operation is expressed by equation (6.11).

$$\begin{pmatrix} L_x \\ L_y \\ L_z \end{pmatrix} = R_{RPY}^{-1} \begin{pmatrix} a_x \\ a_y \\ a_z \end{pmatrix} \quad (6.11)$$

The complexity of the inversion of the rotation matrix is avoided applying once again a trained neuro-fuzzy system for this computation. The result of this evaluation is the robot linear movement tendency in the frontal plane ( $L_x$ ) and the sagittal plane ( $L_y$ ), shown in Figure 78.

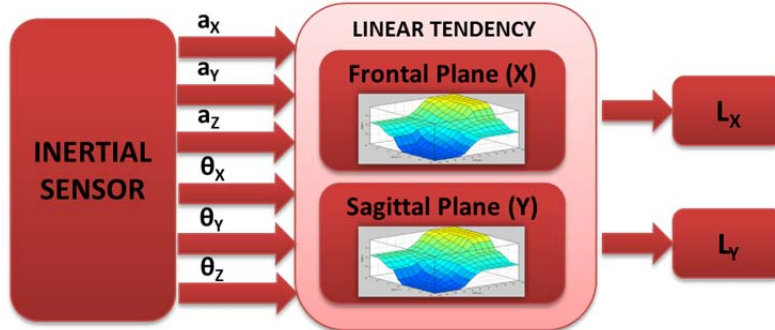


Figure 78 Robot body linear movement tendency

In the same way than the rotational tendency case, the neuro-fuzzy networks for linear motion must be trained using as input dataset the inertial information. The output dataset will be composed by the required linear movement tendency obtained from equation (6.11). The set of information used for the training process is shown in Table 23.

Table 23 IMU linear movement tendency evaluation input/output datasets

	Input Dataset	Output Dataset
INERTIAL MEASUREMENT UNIT	Linear Acceleration Vector	$a_x$ $a_y$ $a_z$
	Orientation Vector	$\theta_x$ $\theta_y$ $\theta_z$
	Linear Acceleration Vector	$a_x$ $a_y$ $a_z$
	Orientation Vector	$\theta_x$ $\theta_y$ $\theta_z$

The third and last exoceptive inertial evaluation is related to the prediction of body balance. Classical feedback balance control methods use vestibular information to prevent falling after the cause has been detected. But human postural control system also uses the vestibular exoceptive perception to preview postural balance lost, preparing the motor system to react. The feedforward mechanism enables faster reactions and, if it was necessary, it triggers higher level reaction systems (i.e. complex balance strategies).

Therefore, the aim of the robot inertial sensation evaluation is to enhance the postural control providing information, related with body balance, for reaction prediction. The output information from the IMU device is robot movement consequence, which can be caused by voluntary actions or external forces exerted on it. The study of the robot

balance can be simplified to the study of the movement of its CoM and, by extension, with the localization of the ZMP. Thus, this perception will be used for predicting the future ZMP position taking into account the sensation of the dynamics captured by the sensor.

The study of the ZMP location has been decoupled in the two principal coordinates and it is also profited from the simple inverted pendulum simplification for the locomotion. Based on this simplification, the movement of the CoM can be assumed circular and with constant acceleration during the period of time established to perform predictions (equation (6.12)). This will be explained more in detail further on. Then, equation (6.13) shows the evolution of one ZMP component depending on time.

$$\Delta\omega = \frac{\dot{x}_{CoM}}{z_{VHP}} \cdot t \quad (6.12)$$

$$\Delta x^{ZMP} = \omega_{CoM}^y \cdot t - \frac{1-z_{VHP} \cdot (t)^2}{(g+\ddot{z}_{CoM}) \cdot z_{VHP}} \ddot{x}_{CoM} \quad (6.13)$$

Therefore, it can be used information directly from the IMU device and it can be applied in the subsequent ZMP prediction module. Figure 79 shows the five datasets used to ZMP prediction.

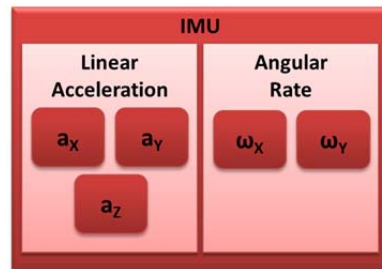


Figure 79 IMU outputs for ZMP prediction

### 6.2.2.3 Vision system

The information captured by the vision sensors is used to extract distant objects movement characteristics. The output comes from the vision sensor Kinect™ installed in the robot TEO head. This device enables a fast object detection making easier the feature extraction process by means of the integration of third party software tools. Figure 80 shows the robot kinematic scheme to perform perceptual composition.

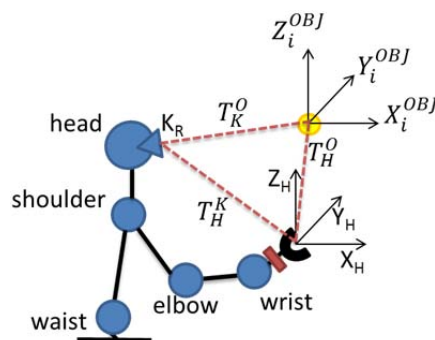


Figure 80 Model for visual perception

The vision sensor is used to extract the object location ( $X_{OBJ}$ ,  $Y_{OBJ}$ ,  $Z_{OBJ}$ ) with respect to its reference system ( $K_R$ ). But this information is not useful for a manipulative task. This location must be related to the manipulation tools, that is, to the hands. This will be performed afterwards by means of kinematic transformations (equation (6.14)).

$${}^0T_H = {}^0T_K {}^K T_H \quad (6.14)$$

In summary, the outcome from visual perception is the object location in a determinate time instant (Figure 81). The relation of the object location with the hand location will be a previous step in the surprise generation process.

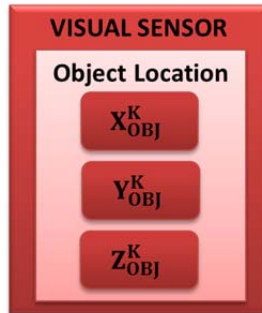


Figure 81 Objects movement evaluation

## 6.3 Surprise Generation

After sensation analysis was performed and the corresponding perceptions were generated, it is necessary to take decisions about postural control supported by this perceptual income. This decision process is based on the concept of surprise events driven by perceptual evaluation under determined context constraints.

Following the psychophysical principles exposed in Chapter 2, the surprise events are elicited by means of the comparison between the knowledge about the action and perceptions during its performance. When the comparison produce an unexpected result or exceeds any kind of threshold, a surprise event could be generated. That is, the result of the comparison process is produced by an expectation failure.

Two types of expectation failure could be produced. The passive expectation failure is produced when the actual perception exceeds any established threshold. This kind of limitations represents values affecting the proper action performance. The second type of failure is the active expectation failure. It is produced when some prediction about the future status of an action is established and it is not accomplished at any time.

Therefore, after the sensorial evaluation performed by the humanoid robot, the next step is the generation of surprise events, which will support the decision making system for the selection of the proper mechanism to react. As well, due to the task context dependence, this generation has been classified following the manipulative and locomotive task division.

### 6.3.1 Passive Expectation Failure

According to the Signal Detection Theory (SDT), the act of sensorial signal evaluation consists of providing quantitative information about a continuous physical variable. This information is compared with a threshold at which such stimulus is noticed by a subject. As well, this evaluation depends of a lot of factors than only the nature of the stimuli such as the subject's conditions, the task context, etc.

Different thresholds have been established for manipulation and locomotion tasks taking into account the goals for each one.

#### 6.3.1.1 Manipulation Tasks

The passive expectation failure for manipulation tasks is related to the assumption about the behaviour of the ball when it is thrown upwards. It has been assumed that the normal execution of this task implies a straight ball trajectory when it goes up and falls down.

At any execution time period, this assumption is considered and the possible location to catch the ball can be computed. The difference between hand location and the assumed ball location will be used to evaluate the passive expectation failure. The surprise event should be elicited when this distance exceeds a pre-established threshold and its intensity will depend on the module of the distance.

The object location characteristics are generated by the analysis of the visual perception. It provides information about object location by means of the geometrical analysis of the captured frame. This information relates the object location regarding to the camera reference frame.

Thus, it is necessary to transform the coordinate frame to relate the object location to the hand position, based on relations from Figure 80. This transformation is performed by the module from Figure 82 in which three neuro-fuzzy networks obtain the transformed coordinates by inference.

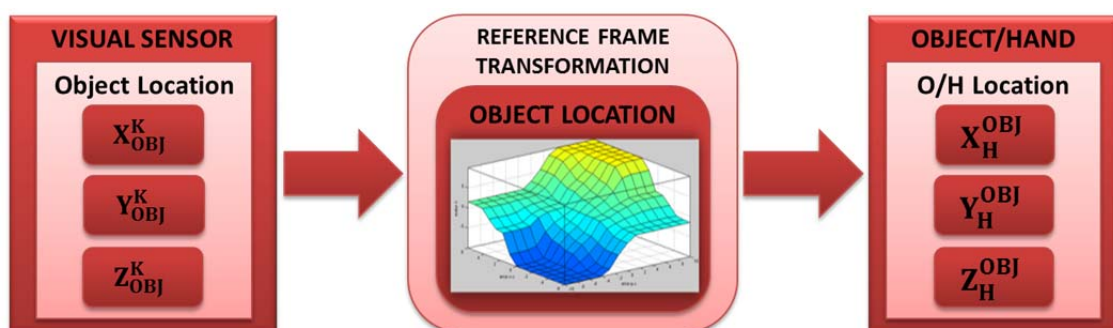


Figure 82 Object location reference frame transformation

After the working object has been properly related to the working hand reference frame, it is possible to evaluate the distance between hand and object. If any of the object coordinates ( $X_H^{\text{OBJ}}$ ,  $Y_H^{\text{OBJ}}$ ,  $Z_H^{\text{OBJ}}$ ) exceed the minimum distance threshold the surprise event would be elicited ( $S_x$ ,  $S_y$ ,  $S_z$ ). Figure 83 illustrates the module established to generate the corresponding surprise event related with object location.

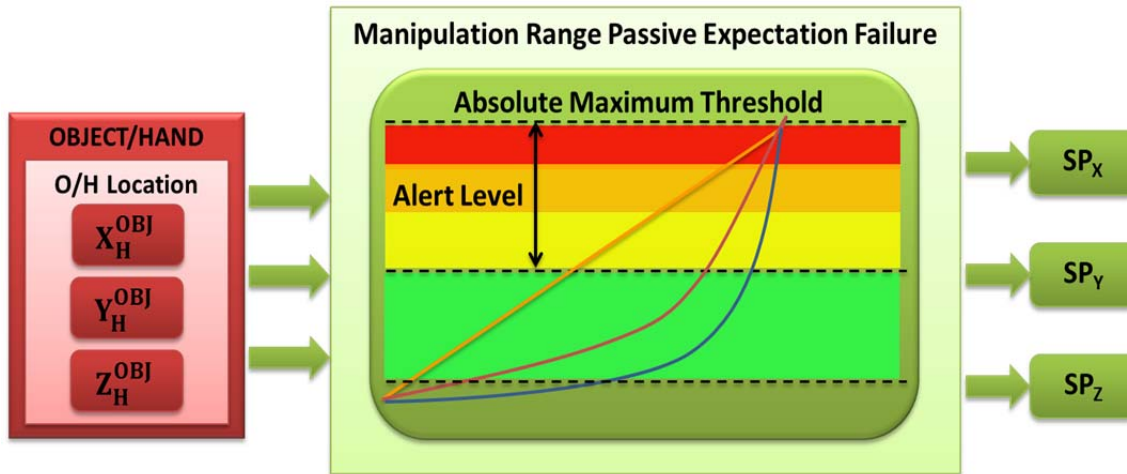


Figure 83 Manipulation passive expectation failure

### 6.3.1.2 Locomotion Tasks

During a locomotion task, inertial stimuli perceived are related to the change of the motion tendency of the body, from upright stance until running. Commonly the motion study is simplified to the investigation of the behaviour of the body CoM. Then, every motion condition is characterized by the dynamics of this point and its relation with its environment.

These conditions are measured by means of the IMU, which captures CoM motion behaviour. Then, the CoM movement evolution can be related with its rotational and linear motion tendency.

The rotational tendency of the robot can be determined comparing the information about rotational movement in the same way than human's, applying concepts like the Mulder's Law (DeHart & Davis, 2002). As described in Chapter 5, it determines the sensation of rotational movement taking into account angular acceleration and time. Its minimum threshold fixes the value at which rotation starts to be perceived by human vestibular system (Mulder's Constant=2,5°/s).

There is no immediate translation of this method to the humanoid robot system due to the characteristics of the IMU device. Therefore, the surprise evaluation gains the advantage from the use of the simple inverted pendulum model.

Taking it into account, the surprise evaluation is performed attending to equation (6.10) and resulting in equation (6.15). In this equation, the rotational tendency from perception evaluation ( $R_{X,Y}$ ) is considered constant during the evaluation period ( $T_{eval}$ ).

$$SP_R = T_{eval} \cdot R_{X,Y} = K_T \cdot R_{X,Y} = K_T \cdot T_R \cdot \theta_{Y,X} \quad (6.15)$$

Then, the result of this operation must be compared with the pre-established thresholds to generate a graded surprise event ( $SP_{RX}$ ,  $SP_{RY}$ ). The basic scheme of this module is shown in Figure 84.

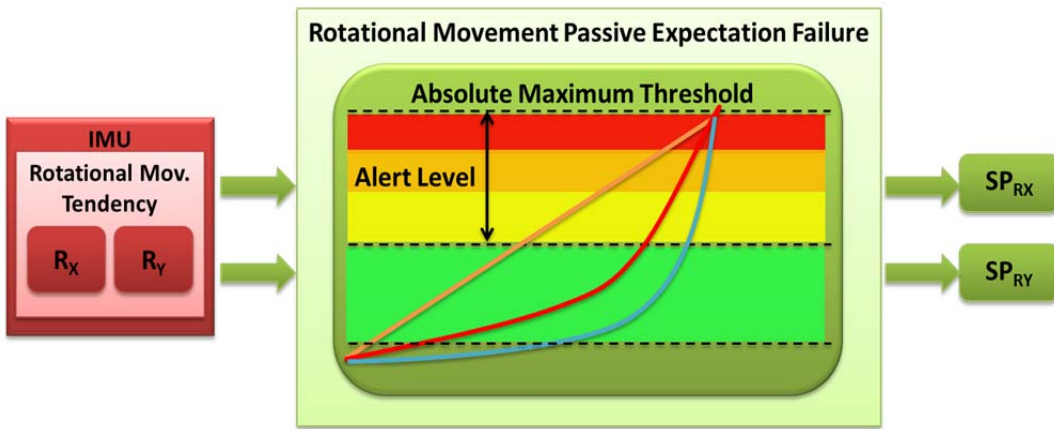


Figure 84 Rotational surprise evaluations

The method used to identify all thresholds levels has been based on the study of TEO robot simplified to a simple inverted pendulum for locomotion tasks. This simplification is useful to characterize the mean angular velocity by means of the relation from equations (6.7) and (6.14), which is task dependant. This angular velocity relates the simple pendulum with one of the main features for defining a locomotion task: the step time. Then, the ‘Rotational Motion Constant’, that is given in equation (6.15), will depend on the linear velocity imposed by the task step time. As a design constraint, TEO humanoid robot has been designed for a maximum step time of 0,75m/s, which is the value shown in Table 24.

$$\hat{\omega}_T = V_T / R_{SP} \quad (6.16)$$

$$T_R = \frac{V_T / R_{SP}}{2\pi} \quad (6.17)$$

Another parameter related with the task is the named ‘Task Constant’. In this case, it corresponds to the angular feature of the task ( $\theta_{Y,X}$ ) introduced in equation (6.10). It has been established as the maximum angles (pitch and roll) considered as normal during the current task performance. In the case of upright locomotion, these angles should be within  $0^\circ$  to  $5^\circ$  range. Values above these thresholds should cause certain degree of surprise. Therefore, the upright locomotion ‘Task Constant’ is fixed in  $5^\circ$  in Table 24.

The last constant defined is imposed by sensory device limitation. It is related to the sensation capture and its transmission to the processor centre. The ‘IMU’s Constant’ is the latency time ( $K_T$ ) needed to have the sensed information available (5ms).

Then, the minimum rotational sensation that can be detected by TEO system is related to the minimum sensor performance. This value is the ‘absolute minimum threshold’. Next, the minimum threshold from which any grade of surprise should be elicited is the ‘minimum threshold’.

As well, the maximum level of surprise should be produced when the ‘maximum threshold’ is reached. All kind of values exceeding this last threshold can cause instantaneous robot falling. Table 24 shows the constants for a maximum speed locomotion tasks and the thresholds obtained from this tasks conditions and IMU sensor limitations.

Table 24 Rotational tendency

<b>IMU's Constant</b>	0,005s
<b>Rotational Motion Constant</b>	1,57s <sup>-1</sup>
<b>Task Constant</b>	5deg
<b>Abs. Min. Threshold</b>	0,12
<b>Min. Threshold</b>	0,4
<b>Max. Threshold</b>	40

Regarding linear movement tendency, the perception of the CoM acceleration senses the initiation and variation of movement. The IMU device is able to sense these accelerations but its measurements are also affected by gravity and rotation. The evaluation perception eliminates these deviations from linear acceleration sensation.

Then, the surprise evaluation (Figure 85) will be performed taking into account this corrected acceleration values ( $L_x$ ,  $L_y$ ). The resulting surprise ( $SP_{LX}$ ,  $SP_{LY}$ ) is graded taking into account as the same concepts explained for rotational movement tendency.

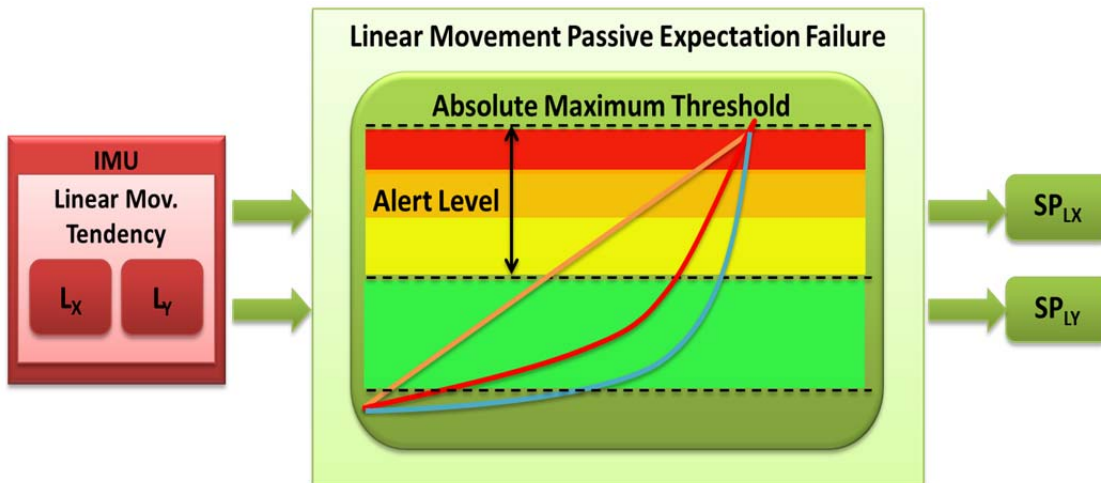


Figure 85 Linear surprise evaluations

In this specific case, equation (6.18) exposes how the linear surprise thresholds have been obtained. The linear movement perception and the 'IMU's Constant' are multiplied by the 'Tasks Constant' ( $K_T$ ). Moreover, equation (6.19) relates this established constant with the 'Linear Motion Constant' that, in this case, is the locomotion velocity ( $V_T$ ).

$$SP_L = \frac{T_{eval} \cdot L_{X,Y}}{V_T / D_T} = K_T \cdot K_D \cdot L_{X,Y} \quad (6.18)$$

$$K_D = D_T / V_T \quad (6.19)$$

In this way, Table 25 shows thresholds values and the task dependant constants for the locomotion task with linear velocity of 0,75m/s.

Table 25 Linear tendency

<b>IMU's Constant</b>	0,005s
<b>Linear Motion Constant</b>	0,75m/s
<b>Task Constant</b>	0,087s
<b>Abs. Min. Threshold</b>	0,33
<b>Min. Threshold</b>	32,7
<b>Max. Threshold</b>	163,6

## 6.3.2 Active Expectation Failure

The active expectation failure is based on predictions about task performance. In such case, predictions are related with task main goals. For instance, the main goal of the manipulation task established is to catch a ball and the prediction may be related with the proper hand position to accomplish the goal.

For the locomotion task, one important goal is to keep balance to be able to perform stable motion. The predictions regarding balance evolution will help the system to improve equilibrium and anticipate reactions against higher level perturbations.

### 6.3.2.1 Manipulation Tasks

It was stated in Chapter 5 that there are different classes of motion tracking perceptions. As well, it was established through the review of different works that a continuous motion tracking is not necessary for the experience of visual motion. Human can capture images at about 15fps and the perception is lost when changes occur faster than 16.6ms. These thresholds are related only with the visual sensation, that is, with the capturing of raw data. The power of the human visual system lies in the brain process of each frame.

In the case of TEO robot, continuous visual perception analysis is not possible. The process capacity of microcomputer systems limits highly the visual analysis performance. Therefore, the aim of the active expectation evaluation of the visual perception is to predict the conditions to carry out properly the manipulation task.

In the manipulation task proposed, the main goal is to catch a moving object that is falling down. In order to achieve this task, the grasping location may be predicted to compare it with the actual location of the hand. The bigger is the difference of locations, the higher active surprise should be elicited. This operation corresponds with Figure 86.

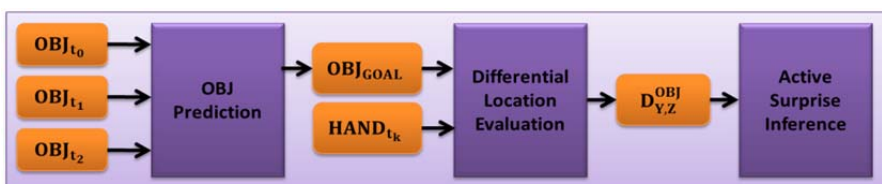


Figure 86 Manipulation active expectation failure inference system

In Figure 86 chart, the visual perception ( $OBJ_{t_k}$ ) is used to predict the landing location ( $OBJ_{GOAL}$ ). It is performed making the assumption of considering the equations of movement of a vertical shot to predict the goal location. This predictive operation is performed by module from Figure 87.



Figure 87 Object landing location prediction module

Once the grasping location has been predicted, the distance from hand location ( $HAND_{t_k}$ ) to the predicted location is computed ( $D_{Y,Z}^{OBJ}$ ) in all coordinates (Figure 88).

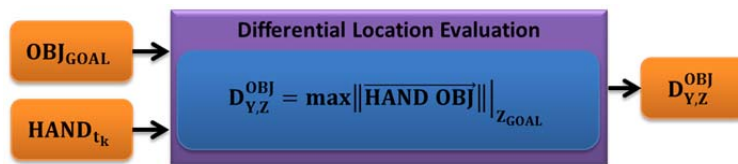


Figure 88 Distance from hand to grasping location

The last step to generate the manipulation active surprise is to compare it with a reference value. In this case, the surprise is proportional to the computed distances (Figure 89). The modulus of the surprise value indicates its level and the sign could be used to indicate the reaction movement direction.

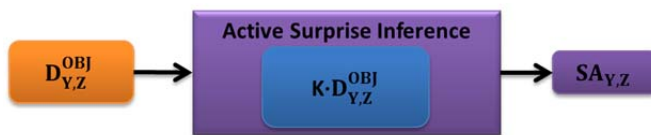


Figure 89 Manipulation active surprise inference module

### 6.3.2.2 Locomotion Tasks

Keeping balance and fall avoidance is one of the most studied problems about humanoid robot locomotion. Classical balance control techniques are based on feedback loops in which a reaction is triggered after balance perturbation occurred. This reactive nature of the system limits the reaction time, the level of permissible perturbations, etc. It is important to recall that the human control system possesses this kind of reactive loops but, as well, it is able to predict future consequences of perturbations, anticipating reactions or preparing the body to act.

In the case of TEO postural control system, the active expectation failure inference system integrated in the feedforward loop has the capacity of predicting the ZMP evolution (Figure 90). The inference system uses the information from perceptions regarding ZMP and the interaction of the robot with the base of support. The actual ZMP ( $ZMP_{t_k}$ ) and the inertial information help the system to predict possible future ZMP locations after different time periods ( $ZMP_{t_k+T}$ ). Then, the distance from each predicted

ZMP location to the Leak Point ( $D_{t_k+T}^{LP}$ ) is used to take a decision about the balance status in a specific time period ( $t_k + T$ ), enabling an anticipatory reaction when necessary.

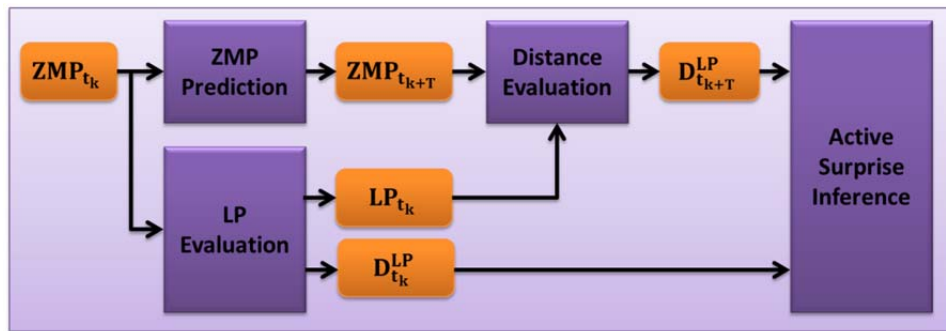


Figure 90 Locomotion active expectation failure inference system

This surprise inference system is composed by four main modules:

- 1) ZMP prediction
- 2) Leak Point evaluation
- 3) Predicted ZMP-LP distance evaluation
- 4) The active surprise inference module.

The ZMP prediction module (Figure 91) is in charge of the computation of the future ZMP locations in different temporal horizons ( $T_i$ ).

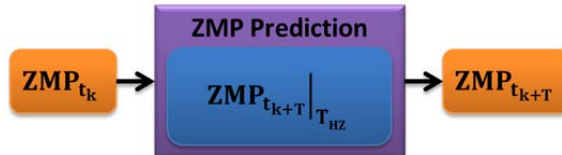


Figure 91 ZMP prediction module

This evaluation is based on the assumption of the robot operating like a simple inverted pendulum. The computation of ZMP, based on this simplification, is given by equations (4.14) and (4.15) which enable the prediction of future ZMP location. This prediction is constraint by the following assumptions:

- 1) The predictions are based on the establishment of several prediction horizons.
- 2) The acceleration is constant during the time period under study.
- 3) Predictions are only a tool for taking postural control decisions.

Thus, the equation for ZMP prediction is given by (6.20) in which  $H=t_k+T$  is the prediction horizon and  $Z_{VHP}$  is the distance of the waist to the Virtual Horizontal Plane that will be explained later on.

$$ZMP_H = ZMP_{t_k} + \omega_{t_k}^{CoM} \cdot H - \frac{1-Z_{VHP} \cdot (H)^2}{(g+\ddot{z}_{CoM}) \cdot Z_{VHP}} \cdot a_{t_k}^{CoM} \quad (6.20)$$

Hence, it is necessary the establishment of these prediction horizons. They may be determined by different parameters such as the architecture of the system, the delay time to process all sensorial information or, due to the human inspiration of this Thesis, the latency time for the different kinds of reaction (see Table 1). The materialization of these horizons is supported by the establishment of the concept of ‘Reaction Boundaries’. Taking the ZMP position as reference for body balance, two concentric circumferences could be established around it. The circumferences correspond to future ZMP positions, moving with constant acceleration ( $\vec{a}$ ), after a specific temporal horizon ( $T_i$ ) for each boundary. The acceleration vector defines a Leak Line (LL) that crosses the Base of Support (BoS) through the Leak Point (LP). Figure 92 illustrates the concept for two boundaries based on two types of human reactions.

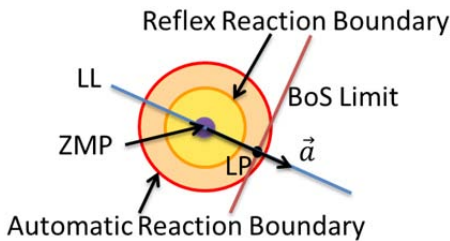


Figure 92 Reaction Boundaries

Reflex reactions are those triggered when a stimulus causes a high level of surprise and a rapid movement is required. These reactions are fast, simple and their latency is very short (see Table 13). As well, this kind of reaction is used as the starting point for others more complex movements. Then, the time to decide that a reflex reaction is needed is very restrictive. It was decided to establish the time for generating a surprise event for a reflex reaction in  $H=40ms$ , which is a mean value inside the human latency range.

The area between the inner reflex response boundary and the outer boundary has been assigned for the generation of surprise events related with automatic reactions. These types of reaction are medium latency responses against high level perturbations that cannot be counteracted by reflex movements. Then, the time to trigger an automatic reaction surprise event is  $H=120ms$ . The automatic responses may be selected among a set of strategies, such as the ankle or the step synergies, based on the parameterization of movement patterns.

It is important to recall that these surprise events do not trigger reactions by themselves. They are mere indicators of the possible evolution of the ZMP and, hereafter, they must be used by the system in conjunction with other information to take a postural control decision.

Parallel to the ZMP prediction, it must be computed the Leak Point as the intersection between the Leak Line and the Base of Support. This point will be the place of the support polygon through which the ZMP could leave the BoS convex hull, turning the posture of the robot into potentially unstable. As will be shown hereafter, the LL can intersect the BoS in different points. The selected LP will be the most distant

intersection point to the ZMP in the same direction of the acceleration vector (Figure 92). Then, the module in charge of the Leak Point evaluation, shown in Figure 93, computes the location of LP point and, as well, its distance to the ZMP.



Figure 93 Leak Point evaluation

All these evaluations are supported by the definition of a Virtual Horizontal Plane (VHP) that simplifies computations, such as the ZMP, when the robot walks on uneven terrains. In (Sugihara, Nakamura, & Inoue, 2002) this concept was exposed but here the application is slightly different, due to inherent problems related with Sugihara definition such as:

- 1) The VHP is located under the robot foot and its depth depends on the precise knowledge of feet location.
- 2) It is necessary the knowledge of the CoM location and the feet dimensions to compute the support polygon.

The VHP defined in this Thesis is related to the robot lower ankle position and the origin of the F/T sensor measurements. Thus, no extra knowledge about external conditions is necessary. The definition of the support polygon is based on the assumption of circular foot shapes. This footprint pattern is more related with the F/T sensor measurement area around its origin. It also facilitates the computing of the Base of Support envelope depending on the step phase. Figure 94 and Figure 95 show the double and simple support phases respectively.

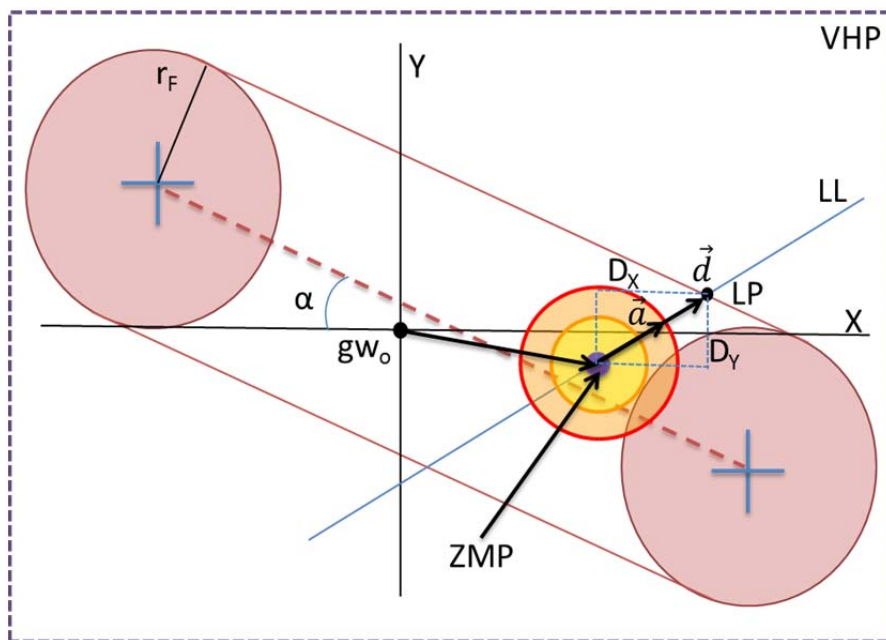


Figure 94 Double support phase

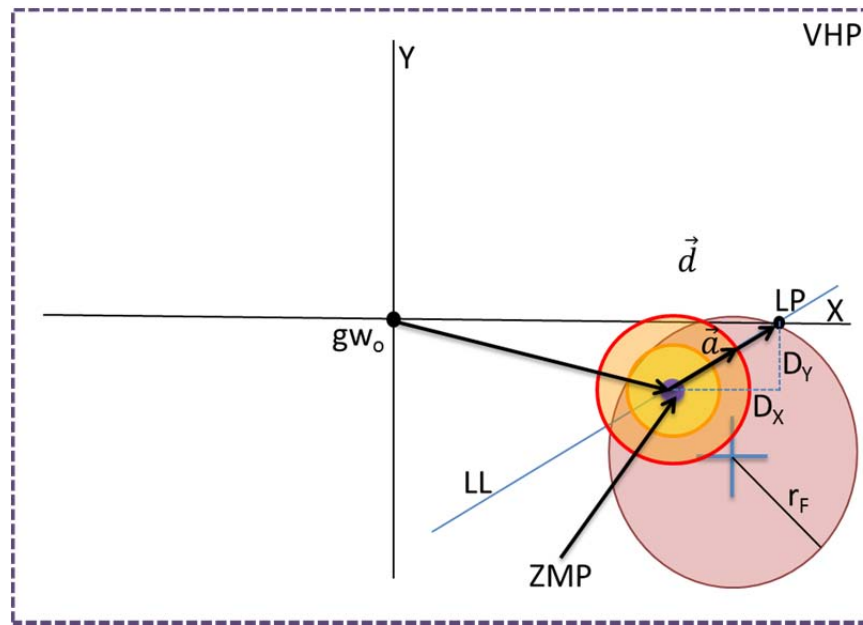


Figure 95 Single support phase

The next step on this generation process of surprise events is the evaluation of the distance from each boundary to the LP (Figure 96). The comparison of each one of these distances and the corresponding from ZMP to LP determines if LP is inside one of the established boundaries or not.

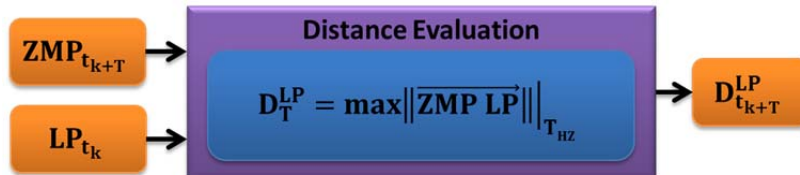


Figure 96 LP to boundaries distance evaluation

The last stage for active surprise event generation is performed by the inference module (Figure 97). It is in charge of comparing all the distances computed before and it outputs are a surprise vector for postural behaviour decision.

Based on the concept of reaction boundaries, meanwhile the distance from ZMP to LP is higher than the distance from the LP to any boundary, the robot will remain in a stable posture at least until another prediction was performed.

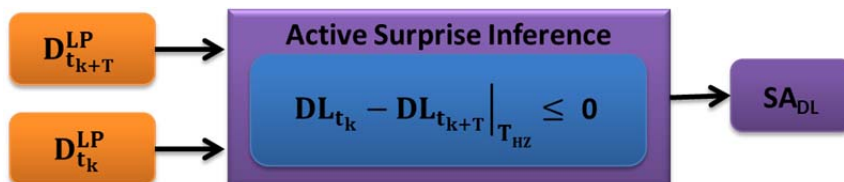


Figure 97 Active surprise inference module

## 6.4 Behaviour Decision System

The high level operation of the behaviour decision module, described in Chapter 3, exposed how surprise can be used to carry out motor reactions. This section describe more deeply the process flow involved in the evaluation of surprise event during task performance. This description follows the task classification established and it links the decision with the corresponding reaction to carry out.

As general guideline, the process to evaluate surprises should start with those that indicate the worst possible consequences when any kind of event is elicited. Usually, it occurs when predictive/active expectation fails and, hence, the process might start with the evaluation of active surprise. The predictive expectation failure is based on the establishment of some future situation that has to be accomplished. Nevertheless, the assumption expectation is more related to the actual state of the task. Then, time horizon gives more priority to predictions than to assumptions during the surprise evaluation process.

Other issue influencing the surprise evaluation process is the nature of the task. It has been mentioned before that manipulation task achievement is surprise driven meanwhile, during locomotion task, the surprise events are responses to perturbations perceived that can disturb the normal task performance. In the first case, the process of evaluation is performed sequentially. Prediction is usually performed once at the beginning of the task. The performance of more predictive actions will depend on the duration of the task. After prediction has been evaluated, surprise generated by goal assumption failure starts to drive the reaction. In the locomotion case, the sequence of surprise evaluation can output a reaction or not, depending on surprise levels. Following, the mechanism and process flow involved in the evaluation of surprises is developed for each specific case.

### 6.4.1 Manipulation Tasks

Recalling the behaviour during a manipulative task (Figure 36), its performance has been split in a voluntary movement phase and a surprise driven movement phase. After voluntary movement has concluded, the trajectory of the shoot object begins to be tracked and object location information is provided by visual perception. This location information joint with the proprioceptive perception of the hand location is the base to formulate a prediction. The object trajectory will follow a straight vertical trajectory or a parabolic trajectory depending on its angle of departure. Taking this into account, the system can predict an approximate location to catch the object using only two points of the trajectory.

The first one is assumed to be coincident with the last hand location during the shooting action and the second one is measured by the visual perception. Then, applying physics of movement, one possible goal location can be computed. Whether a difference between hand and possible goal location is detected, the active surprise event is elicited and an appropriate movement synergy will be triggered. The success

on the achievement of catching the object only evaluating the active expectation is related to the error committed in the prediction.

Although the arm movement after active surprise evaluation was enough to complete the task, passive surprise evaluation is as well performed. This case is supported by the assumption of a vertical descendent trajectory of the object. Meanwhile prediction is performed at the beginning of the object flight, passive expectation failure system is continuously evaluating perceptual incomes and eliciting new surprise events. It seeks two main objectives. The first goal is the minimization of the error committed by prediction and, the second one, is driving the arm movement when low or medium active surprise levels were elicited. If no one of these cases is presented the passive surprise event will not take effect over the robot system. Figure 98 presents the graphical representation for the decision module operation explained.

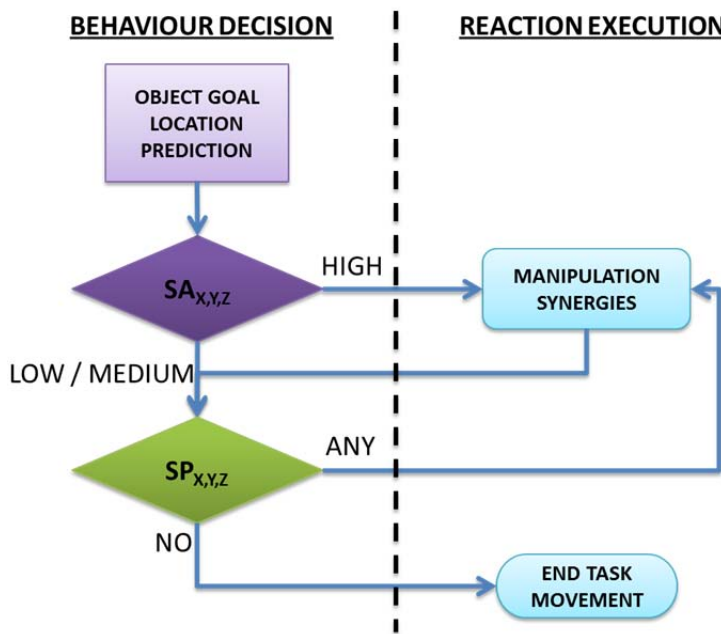


Figure 98 Manipulation behaviour decision process

The decision system is supported, besides the surprise generation system, by the establishment of the different movement patterns or synergies to perform reactions. Taking in account the kind of reactions described in previous chapters and the operation described before, the reactive movements caused after active surprise evaluation could be considered as reflexes. The longer latency reactions activated after passive surprise evaluation could be classified as automatic reactions. But in the manipulation case, this classification is only possible attending to the latency of the reaction because the established synergies could be triggered by both passive and active surprise events. It seems obvious that the more complex is the synergy the more time to set it up will be needed. Then, because of the manipulation task proposed has short execution time, the reaction movements should be set up and executed as fast as possible. This behaviour fits better with the reflex reaction type.

Figure 99 shows the movement patterns established to perform reactions based on surprise evaluation. These synergies are:

- 1) X\_MOVE: movement along X axis hand coordinate.
- 2) Y\_MOVE: movement along Y axis hand coordinate.
- 3) Z\_MOVE: movement along Z axis hand coordinate.

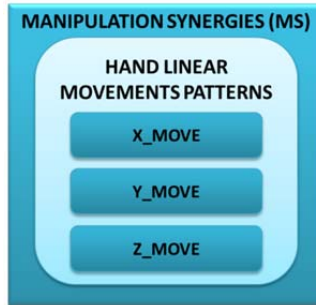


Figure 99 Manipulation synergies

Each synergy definition, which is out of the scope of this work, has been made attending to the underlying philosophy of this kind of movement. They involve the least number of joints to speed up the synergy setting up process. Such process is based on the application of a linear parameter to the command sequence of each involved arm joint. The result is a movement with a modulated amplitude or movement range.

### 6.4.2 Locomotion Tasks

The decision making system for locomotive tasks is highly influenced by their dynamics, as it was exposed previously. Nevertheless, their foundations appear to be the same for anticipative reactions. Thus, the static upright posture and dynamic walking tasks have been included in the same group named 'locomotion tasks'.

These tasks are composed by sequences of successive postures. Each one of these postures can be considered as quasi-static whether the environmental conditions remain constant during a considered period of time. Therefore, perturbations are actions that modify the dynamical characteristics of the quasi-static posture.

In this case, the foundations of the active and passive surprises generation are the tracking of those dynamical features of the task. The decision procedure follows the same philosophy than the manipulation decision system. The first type of surprise evaluated is the active expectation failure. It is based on the prediction of the possible future location of the Zero Moment Point, considering those quasi-static conditions and different prediction horizons. Another difference with the manipulative case is that this evaluation does not generate any kind of reaction. Instead of performing a reaction, the value of the surprise event is combined with the passive surprise events that indicate the movement tendency of the robot in each considered direction. The operation of this decision module is represented in Figure 100. In this scheme, it also can be observed that the decision and surprise evaluations are performed continuously and this evaluation only finishes when the task has been indicated as complete. This decision process flow is performed for the sagittal and frontal plane directions because the locomotion passive surprise has been divided in these components. Furthermore, the

passive surprise value is determined by the maximum level of surprise between  $SP_L$  and  $SP_R$ , having more priority linear movement tendency if equal.

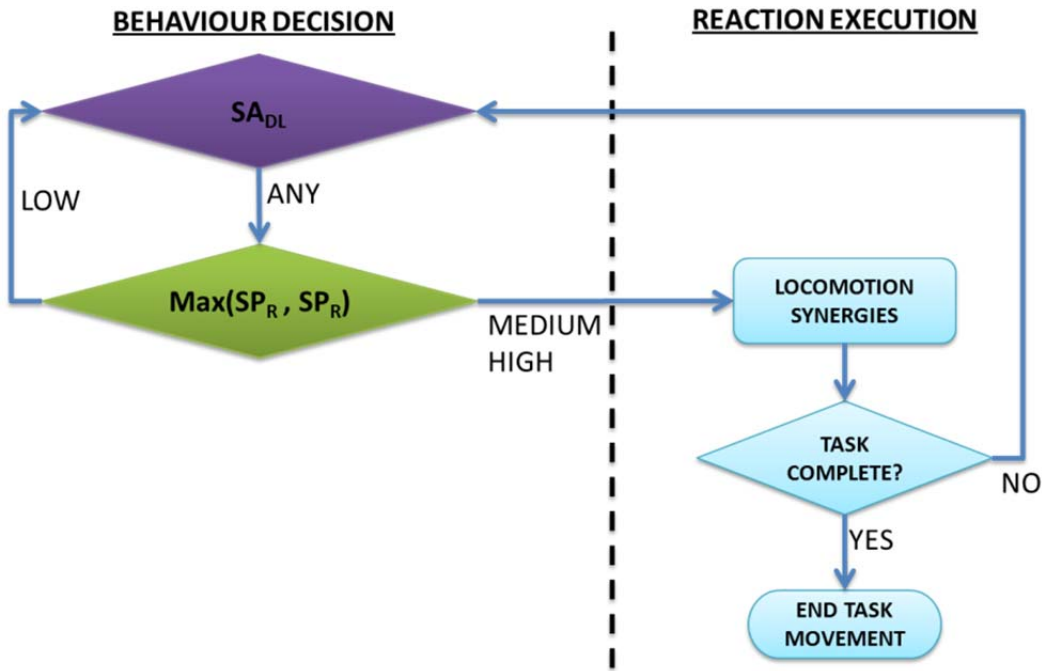


Figure 100 Locomotion behaviour decision process

Then, the decision system will trigger a graded reaction based on both kind of surprises and the decision chart from Table 26.

Table 26 Locomotive reaction decision chart

		ACTIVE SURPRISE		
		LOW	MEDIUM	HIGH
PASSIVE SURPRISE	LOW	NR	NR	R
	MEDIUM	NR	R+	R+
	HIGH	R	R+	R++

In this chart, NR corresponds with no reaction; R and R+ with a reaction based on the fastest and simplest synergies available and, the last type, R++ will be performed by means of complex synergies activation such as the step strategy.

Figure 101 presents three synergies available for perturbation compensation during locomotion tasks:

- 1) AN\_MOVE: it performs the ankle synergy based on the behaviour of the simple inverted pendulum model (R).
  - 2) AH\_MOVE: this synergy is the combination of the ankle and hip movement, acting like a double inverted pendulum (R+).

- 3) ST\_MOVE: it consist of the performance of a step and it is the most complex strategy available (R++).

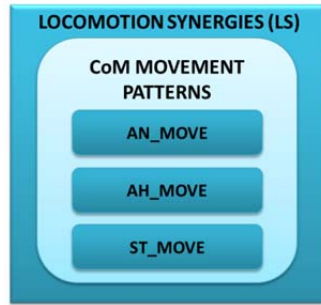


Figure 101 Locomotion synergies

The synergies established for locomotion tasks are, as well, close related with dynamics. They have been established taking into account the simplified robot models, such as the simple inverted pendulum, to perform a matching process between the captured robot behaviour and the CoM movement of the simplified model.



## CHAPTER 7

# Implementation of the Human Inspired Postural Control System

## 7.1 Task Frame Overview

In previous chapters, the novel human inspired TEO humanoid robot postural architecture has been exposed. Chapter 3 presented the high level architecture scheme, each one of its modules and their behaviour. After that, the theoretical and hardware foundations for supporting those modules development were presented in Chapter 4 and 5. Then, each component and system unit were explained more in detail in Chapter 6.

Once TEO feedforward postural control loop has been designed, it must be developed and tested. The procedure followed to accomplish the experimental stage has been based on the task orientation of the control architecture.

Thus, experiments and developments have been performed following the two main premises maintained during all the Thesis description:

- 1) Human inspiration: the behaviour of each part of the feedforward loop has been established to replicate the corresponding one found in the human case. Thus, the expected result of each experiment must be considered in terms of correct behaviour and not in terms of high accuracy, minimum error, maximum performance, etc. That is, postural control performance is inherent to each individual. The final result will depend of the individual dexterity, experience or training, which is related with learning skills. In the same way, the proposed postural architecture will have a minimum level of correctness from which, applying machine learning techniques, it could be improved.
- 2) Task orientation: the human being acquires new abilities by means of experience during the growth process. The result is a database of skills or tasks an individual is able to carry out, with better or worse performance. Taking this into consideration, it seems adequate to relate postural control and tasks. Thus, experiments have been focused on the most general tasks: manipulation and locomotion. Within this task oriented frame, the postural control architecture has been developed and tested to carry out two tasks cases correctly.

Next, the task frame established is revisited focusing its description on the experimental development. The initial hypotheses and constraints will be established

for each task case, as well as its expected behaviour related with each one of the modules composing the postural control architecture.

### 7.1.1 Locomotion Framework

Bipedal upright locomotion is considered one of the most important factors for the development of the human being. This quality allowed the use of the free limbs for manipulative tasks. During the growth process, new locomotive skills are added by experience.

As well, humans learn to keep in balance during locomotion or upright stance in response to sensorial inputs. All mechanisms learned during this process are stored and, afterwards, converted to unconscious actions or synergies. In this way, when humans face similar situations, the postural control system anticipates and triggers actions automatically without the help of complex cognitive processes, improving balance control.

This anticipative behaviour is performed by means of a feedforward control loop that evaluates sensorial inputs to predict future task evolution. It allows the selection of the most appropriate strategy to maintain postural control in advance. This predictive process has been extensively studied and it has been used in this work to inspire the operation of TEO humanoid robot postural control.

In the humanoid robot case, the locomotive task problem is usually faced on even flat ground. Classic reactive feedback control systems are designed and calibrated to keep balance only in this case. Then, when different kind of disturbance happens than those pre-studied, the feedback control loop fails.

In addition, delays during the perturbation identification and reaction decision process limit the reaction performance triggered by this control loop. These two problems of the feedback control loop, joint with the fact that classical humanoid control architectures lack of human inspiration, favour the development and integration of this novel feedforward postural control loop.

Therefore, the even flat locomotion task has been considered as the basic experimental scenario to develop all experimental jobs. The inputs to the control system are composed by sensorial signals classified depending on their origin.

The voluntary movements from the locomotion task, captured by internal robot sensors, are one of the main sources of instability (Figure 102 (a)). Another input for the postural control system is originated by external forces exerted on the robot body (Figure 102 (b)). The last input considered is caused by the reaction forces when walking on rough terrains or slopes (Figure 102 (c)).

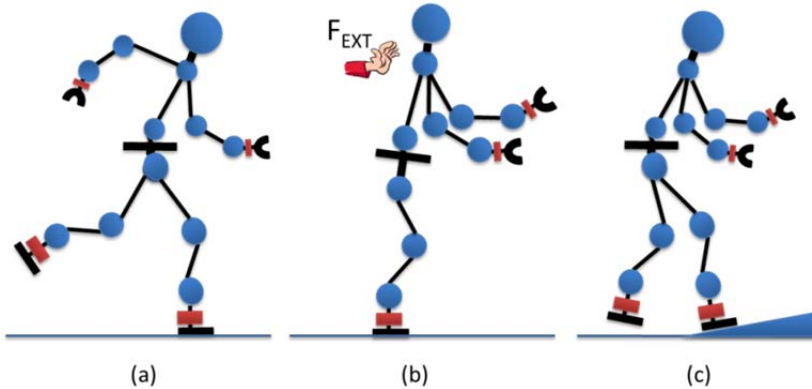


Figure 102 Locomotion perturbation sources

With these sensorial inputs, the postural control system must anticipate any kind of balance lost. The outputs of the feedforward postural control loop will be a parameterized movement pattern and the decision of executing it or not.

The development and operation of the postural control system is constrained and, at the same time, simplified by some assumptions which were explained in Chapter 4. These assumptions are:

- 1) It has been considered pure locomotion. That is, any kind of manipulation task must not be performed during locomotion.
- 2) The body dynamics have been modelled using a simple inverted pendulum simplification of the robot mechanical structure.
- 3) The predictive system behaviour is based on the study of the evolution of some balance margin indicators, such as the ZMP.

In summary, this locomotion framework is the basis for any simulation or experiment about balance loss prediction during locomotion tasks.

### 7.1.2 Manipulation Framework

The dexterous manipulation skill is, with upright locomotion, one fundamental characteristic that defines the human being. It is well known that the manipulation capacity has been a determinant factor for the human being evolution. Thanks to their manipulation ability human beings are able to build tools, modify their environment and improve their quality of life.

In the same way than locomotive skills, the manipulation dexterity is a process of learning and training carried out continuously since birth day. The main difference is the sensorial sources that the human control system uses to look out for manipulation activities. Besides, the treatment of these inputs and its consequences rely on similar processes.

All movement tasks are based on two kinds of action. The nature of the movement can be voluntary or driven by sensorial events. In the case of the locomotion task, the voluntary action corresponds to the whole task (every step) and the action driven by

the result from a sensorial event evaluation is considered a reaction. The voluntary movement and the reaction can be mixed and considered as a task adaptation. But the manipulation case is a bit different. The whole manipulation task can be a sequence of a voluntary movement plus an action driven by some kind of unexpected event. This case can be easily illustrated by the explanation of the scenario established for the manipulative postural control experiments.

The framework scenario established for the development of the postural control during manipulation is based on the action of throwing an object (ball) and then catching it before it falls down the ground. In this case, the voluntary movement ends when the hand reaches its final pre-programmed location where the ball starts going up. Then, the action of modify the hand location moving the arm is driven by the stimulus generated by the visual system. With this sensorial information, the system is able of estimate an approximate location to catch the ball. The movement action is a reaction driven by a sensorial input. The whole task will be composed then by a voluntary movement plus a reaction (Figure 103).

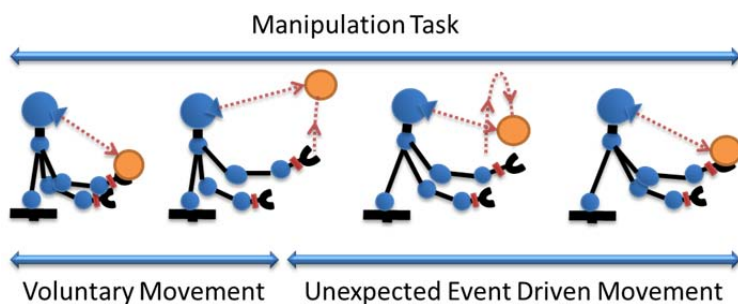


Figure 103 Manipulation task phases

Meanwhile the locomotion task involves feedback and feedforward loops for postural control, this kind of manipulation tasks favours mainly the control action produced by the feedforward loop. The demanding time requirements for the postural control system performance favour the use of predictive mechanisms to anticipate movements. Therefore, in the human inspired postural control architecture, the anticipation is performed with the help of the feedforward loop proposed in this PhD Thesis.

In this task scenario, the input of the postural control system comes from the visual system and the body location sensation. The visual sensation provides an estimation of the ball location. Comparing the humanoid and human visual systems, the electronic device selected has better performance in distance measurement than the biologic visual system because its image processing capacity. This advantage is reduced when other levels of visual process and task planning must be carried out. Then, the visual information is merged with the perception of the hand location to drive the arm movement.

Then, the main outcome from the system, after sensorial input evaluation, is the hand positioning. The motion of the arm is based on pre-programmed patterns that must be fulfilled with the error distance between hand and object. These synergies correspond with the reactions that complete the manipulation task.

The achievement of this kind of task has been constrained to improve its performance and its study. The main assumptions established in this process are:

- 1) The manipulation task must be performed in a static robot location. That is, the development is related only with manipulation and any kind of locomotion should be allowed.
- 2) The nature of the task implies that only upper body systems will be used. This will improve the computing time.
- 3) Movements for hand location correction are based on established synergies which will be activated depending on the perceptual evaluation results.
- 4) In case task could not be achieved because ball will be out of the arm range, task might be stopped.

The manipulation framework completes the main set of skills a humanoid robot should have. It complements locomotion and could be combined with it in order transport objects, to perform collaborative works, etc.

## 7.2 The Human Inspired Postural Control System

Previous Chapters described the framework of the postural control system developed in this PhD Thesis, from the high level architecture to the detailed description of each one of its modules. Besides, the postural control architecture has been developed following a bottom up procedure. Figure 104 illustrates the development pathway followed. The basis architecture of the architecture is the perceptual evaluation composed by the proprioceptive and exoceptive module. Following, the outcome from perceptions is the input of the surprise evaluation composed by the active and passive surprise modules. The last part is the decision system in which surprise events are evaluated and reactions are composed using predefined movement patterns or synergies.

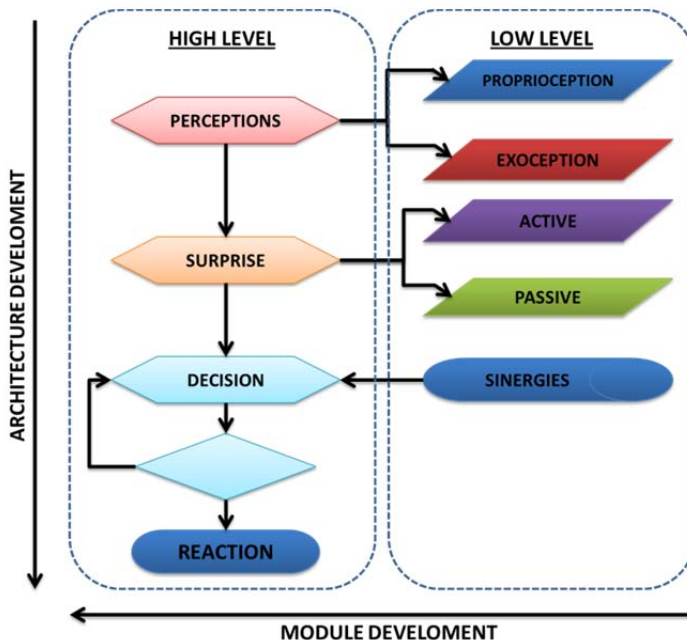


Figure 104 Development of the postural control architecture

This architecture has been developed applying human inspired techniques. The development of the low level modules has been based on the neuro-fuzzy hybrid method that imitates the inference reasoning performed by human brain. Next section will describe the development of this kind of systems following all the steps of the process and illustrating it by means of an example from the proprioceptive perception module.

### 7.2.1 Neuro-Fuzzy Modules Development Procedure

It has been intensively remarked during the exposition of this PhD Thesis the imperative premise of human inspiration of the system. In Chapter 4, different techniques inspired in human behaviours or reasoning were presented. Due to its versatility and power, the neuro-fuzzy methodology has been considered the most appropriate one to develop each module of the system.

Thus, this section illustrates the development of an inference system supported by the study of the right hand 'X' coordinate for proprioceptive perception. The following workflow, represented in Figure 105, can be extrapolated to all other modules. The method exposed is supported by the ANFIS tool from the Matlab<sup>TM</sup> Fuzzy Logic toolbox.

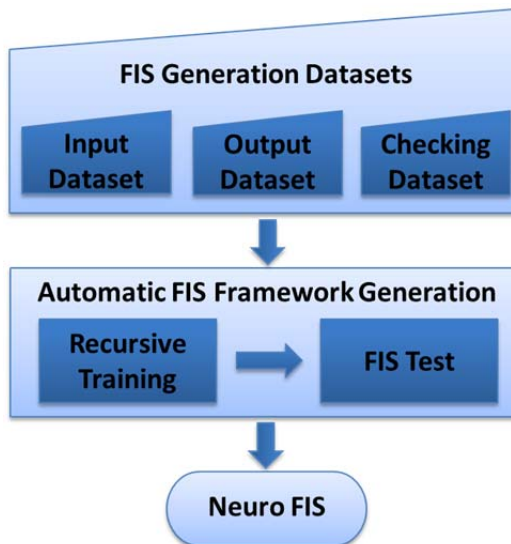


Figure 105 FIS development workflow

The neuro-fuzzy system produces an inferred output depending of its inputs. Due to that only one input can be inferred, it will be necessary to build as much fuzzy inference systems (FIS) as outputs has each module.

The starting point for the FIS development is the capturing of the robot behaviour to be modelled by the inference system. In the case of the proprioceptive perception used as example, the offline kinematic equations are used to obtain the datasets needed in the training process (see Figure 105) related to the forward kinematics of the robot.

These datasets are composed by the inputs joint angles, the output coordinate corresponding with each input set and a checking dataset to validate the resulting

system. Table 27 presents an example extracted from the training and checking datasets for the right hand 'X' coordinate.

Table 27 Datasets for right hand 'X' coordinate neuro-fuzzy network development

	Right Arm Joint Angles (INPUT)						Coordinate (OUTPUT)
	$q_{15}$	$q_{16}$	$q_{17}$	$q_{18}$	$q_{19}$	$q_{20}$	
<b>Training Dataset</b>	-0,21°	-1,26°	0,02°	-1,24°	0,66°	-1,27°	0,22 m
<b>Checking Dataset</b>	0°	-1,57°	0°	-1,57°	0°	0°	0,21 m

The following phase is the neuro-fuzzy system development itself. It comprises three main steps using the ANFIS toolbox:

- 1) Automatic FIS framework generation ('genfis1' Matlab™ function)
- 2) Neuro-fuzzy network training ('anfis' Matlab™ function)
- 3) Evaluation of the resulting fuzzy inference system ('evalfis' Matlab™ function).

'GENFIS1' was selected to build the basic FIS structure from training dataset using grid partitioning of the input work space. It creates all necessary elements that compose the FIS inference system:

- Input/output membership functions.
- IF-THEN rules.
- Initial ANFIS structure with parameters prepared for training (Figure 46).

Regarding membership functions (MF), this tool allows different combinations of input and output MF's. Each input/output value is mapped to a parameter (degree of membership) that is generated by one specific correlation function. For instance, 'gaussmf' input correlation function performs this mapping using Gaussian distributions. ANFIS tool needs a minimum of two MFs for each input to enable the later training process. In the case of the output, only constant or linear correlation functions are allowed.

The IF-THEN rules are generated by enumerating all possible combinations of membership functions of all inputs. Rules increase its number exponentially ( $2^n$ ) with the number of inputs ( $n$ ). Large number of inputs is not practical for any learning method using grid partitioning. It is possible to use this method due to the low number of inputs established in each TEO module. Table 28 presents the parameters available

to construct by combination the 64 rules for the inference system of this example. Each rule follows this pattern:

IF (q15 is in1mf1) ... AND (q20 is in6mf1) THEN (X is out1mf1)

Table 28 Rule parameters for combination

	<b>Input</b>	<b>Input Member Functions</b>	<b>Output</b>	<b>Output Member Function</b>
IF	q <sub>15</sub> is	in1mf1	T H E N	X is out1mf1
		in1mf2		
	q <sub>16</sub> is	in2mf1		
		in2mf2		
	q <sub>17</sub> is	in3mf1		
		in3mf2		
	q <sub>18</sub> is	in4mf1		
		in4mf2		
	q <sub>19</sub> is	in5mf1		
		in5mf2		
	q <sub>20</sub> is	in6mf1		
		in6mf2		

Table 29 summarizes the input parameters for 'genfis1' function and some features of the resulting FIS structure in the case of right hand 'X' coordinate evaluation.

Table 29 Example of right hand parameters genfis1

<b>Inputs</b>	n=6 (q <sub>15</sub> q <sub>16</sub> q <sub>17</sub> q <sub>18</sub> q <sub>19</sub> q <sub>20</sub> )
<b>Type of input MFs</b>	'gaussmf'
<b>Output</b>	1 (X coordinate)
<b>Type of output MFs</b>	'linear'
<b>Number of Input MFs</b>	12 (2 per input)
<b>Number of Output MFs</b>	64 (2 <sup>n</sup> )
<b>Number of Rules</b>	64 (2 <sup>n</sup> )

At this stage the training process could start. Such process consists of updating the node parameters of an adaptive multilayer feedforward network, according to given training data and a gradient-based learning procedure. This training task is performed by the 'anfis' function from the Matlab™ Fuzzy Logic toolbox. The 'anfis' function

applies a recursive method for tuning the parameters of the initial FIS according to the training and checking datasets. It is important that the number of training data points be several times larger than the number parameters being estimated. Table 30 shows the parameters used for training with 200 epochs and an error goal of 0,001.

Table 30 Training parameters of right hand X coordinate FIS

<b>Training method</b>	Hybrid (default)
<b>Training epoch number</b>	200
<b>Training error goal</b>	0,001
<b>Initial step size</b>	0,01 (default)
<b>Step size decrease rate</b>	0,9 (default)
<b>Step size increase rate</b>	1,1 (default)

The training process ends after a number of learning loops (epochs) is reached or, as well, if the pre-established maximum output error level is achieved. The statistics from one of these training loops are presented in Table 31. It can be observed that some default parameters were used during the training process which stopped at epoch 22 after error below 0.001.

Table 31 Example training error evolution

<b>Epoch</b>	<b>Output Error (m)</b>
1	0,00336826
5	0,00291183
10	0,00233490
15	0,00173527
20	0,00115504
22	0,000950358

Finally, the output of the command ‘anfis’ is the ‘X’ right hand coordinate FIS structure with the minimum checking error. At this stage, customized member function may be added if it was necessary. The last step would be the use of the FIS structure to perform fuzzy inference by means of a compatible inference engine or embedding it into an application.

## 7.2.2 Perceptions Development Results

The development of perceptual evaluation systems is the basis for the feedforward human inspired system development. The modules and systems developed follow the same structure from Chapters 3 and 6. Moreover, this development and the description presented in subsequent sections are supported by several assumptions and simplifications:

- 1) The development is simplified taking in account the robot symmetries.
- 2) Possible mechanical errors or misalignments have been disregarded. Virtual model and real robot have been considered identical. Posterior calibration process could be necessary depending on the task performance
- 3) The results presented in following sections are extracted from one of the perceptual components developed. It is possible because the perceptual evaluation is based on the same technique and the development process differs only in the input and output data sets.

In this way, the description of the results from proprioception evaluation is based on the right hand, for the upper body proprioception related to manipulation task, and on the right foot, for lower body proprioception related to locomotive tasks. The case of exoceptive perception development profits from the same premises. Thus, the force and torque sensorial system evaluation are based on the study of the same limbs than exposed in the proprioceptive evaluation. The inertial and vision sensations depend only on one device respectively but previous assumptions are as well valid for them. Next, results obtained from all human inspired perceptual systems developed, following the workflow described on Section 7.3.1, are presented.

### 7.2.2.1 Proprioceptive Perception Results

The fuzzy inference system is a human inspired mechanism highly appropriate for MISO (Multiple Inputs Single Output) or MIMO (Multiple Inputs Multiple Outputs) systems, that is, when multiple input data in parallel is presented to the evaluation system. The case of the neuro-fuzzy inference system corresponds with a MISO evaluation system. Figure 106 represents the structure of the proprioceptive system on a tree form. The bottom side correspond to the outputs of the system. It can be easily observed that it has twelve outputs. Attending to the MISO nature of the system and the characteristics of the neuro-fuzzy system (see Chapter 4), it is necessary to develop twelve neuro-fuzzy systems. In this section only the results from right foot and right hand are presented.

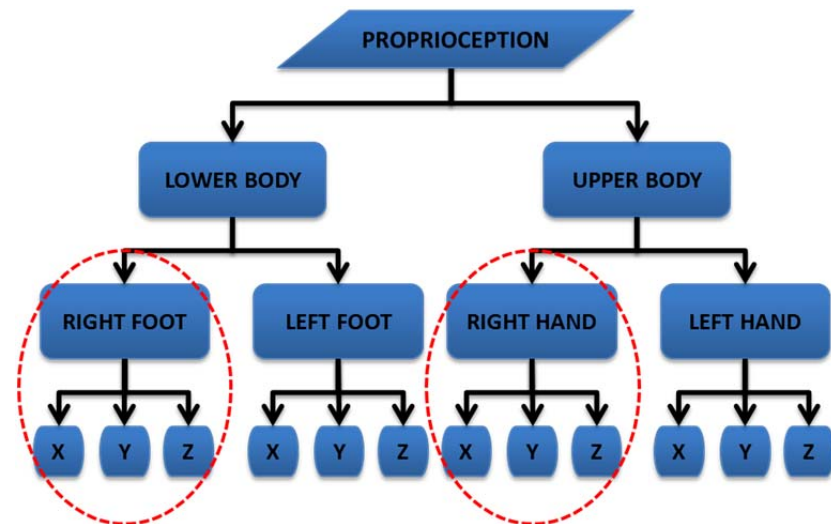


Figure 106 Proprioceptive system structure

The aims of the proprioceptive tasks experiments are:

- 1) Measuring the absolute angle of each under study limb joints during the task and obtaining the hand locations by means of:
  - a. Classical forward kinematics calculation.
  - b. FIS evaluation.
- 2) With the datasets obtained, a comparison process may be performed to determine the under study extremity location in the following cases:
  - a. Comparison of commanded positions against the kinematical evaluation of the angular data measured in each limb under study.
  - b. Comparison of extremity location commanded against the fuzzy inferred location obtained after the evaluation of the angles measured.

#### 7.2.2.1.1 Manipulation Tasks

The proprioceptive information used in manipulative tasks is regarded to hands location. The experiment carried out to evaluate the FIS developed consisted of the generation of three trajectories of throwing a ball with the right hand in three different arm configurations. Each task or experiment uses the initial and final arm configuration exposed in Table 32.

Table 32 Initial and final commanded configurations of the right arm

	Task	Right Arm Joint Angles (rad)					
		J15	J16	J17	J18	J19	J20
Initial Configuration	1	0,087	-0,174	0	0	0	0
	2	0,087	0	0	0	0	0
	3	0,087	0,174	0	0	0	0
Goal Configuration	1	-0,511	-0,517	0	-1,283	0	-0,513
	2	-0,511	0	0	-1,283	0	-0,513

	3	-0,511	0,174	0	-1,283	0	-0,513
--	---	--------	-------	---	--------	---	--------

Figure 107 represents a sequence of frames obtained from the simulation of the experiment number three. This task is carried out in 1s, starting from the arm configuration on the left to the final goal position on the right of the figure.

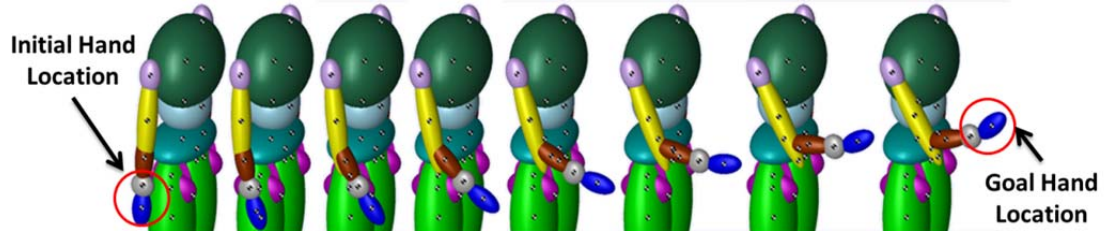


Figure 107 Manipulation task sequence

Table 33 summarizes the humanoid robot right arm initial and final configurations measured by the absolute encoders from each joint. Comparing the values from Table 32 and Table 33, it is easy to note the deviations caused by measurement tolerances of the sensors.

Table 33 Initial and final measured configurations of the right arm

Task	Measured Right Arm Joint Angles (rad)						
	J15	J16	J17	J18	J19	J20	
Initial Configuration	1	0,088	-0,174	0	0,0005	0	0
	2	0,087	0	0	0,0005	0	0,0005
	3	0,087	0,174	0	0,0005	0	0
Goal Configuration	1	-0,511	-0,516	0	-1,289	0	-0,513
	2	-0,511	0	0	-1,289	0	-0,513
	3	-0,511	0,174	0	-1,282	0	-0,513

The proprioceptive evaluation for lower body is the computing of the foot location that can be performed through forward kinematics computations or applying the human-inspired FIS modules developed.

The inference systems, developed by means of neuro-fuzzy techniques, have the mission of inferring X-Y-Z location components from each hand. Figure 108 exposes an example representation from the resulting inference surfaces for each foot location coordinate.

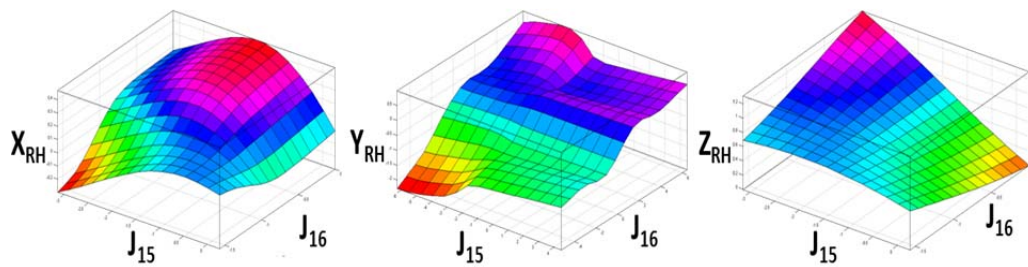


Figure 108 Right hand location inference surfaces

Applying both the kinematic and the inference methods, it is possible to evaluate the precision of approximate computing of the hand location achieved by the FIS perceptive modules, which is the main objective of the proprioceptive evaluation for the upper body.

Therefore, this comparison allows, as well, the assessment of results coming from human inspired and non-human inspired methods. In this way, the results of both robot hand position evaluations are shown in Table 34.

Table 34 Final evaluated right hand location

Task	Goal Position Kinematic Evaluation (m)			Goal Position FIS Evaluation (m)		
	X	Y	Z	X	Y	Z
1	0,3444	-0,5359	0,3900	0,3443	-0,5360	0,3896
2	0,3697	-0,3400	0,3449	0,3697	-0,3400	0,3446
3	0,3668	-0,2711	0,3502	0,3667	-0,2711	0,3499

The results exposed in Table 34 determine a mean error around 0,15mm in the approximate inferred right hand goal location. This error level is very low and demonstrates that this technique is adequate to compose this proprioceptive system.

The error committed during the complete task performance has been as well tracked. Figure 109 presents the error in the case of the kinematical evaluation of the sensed data. These charts show the high accuracy of this method.

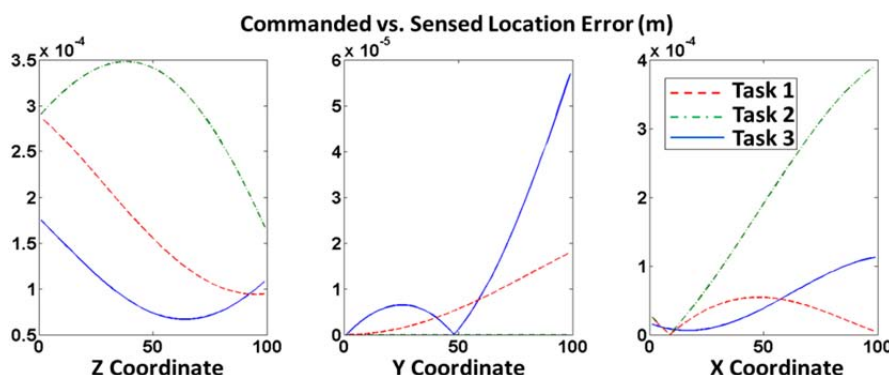


Figure 109 Right hand position kinematic evaluation error

The approximate right hand location is obtained by means of inference. Figure 110 exposes the error committed using this method in the three spatial coordinates. It is important to say that the highest errors are produced in the Task 3, which is physically unachievable. This task has a collision trajectory with the trunk of the robot and the high error is caused by out of range inputs to the FIS. Then, this kind of error produced can be used to predict collisions as well.

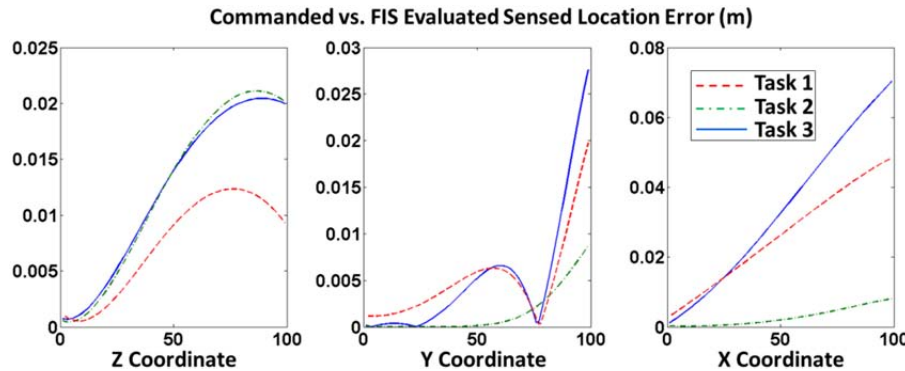


Figure 110 Right hand position fuzzy inference error

#### 7.2.2.1.2 Locomotion Tasks

Proprioception involved in locomotion tasks is related with feet location. The development of the fuzzy inference system in charge of this evaluation has been tested using the same method than the proprioception of the upper body. Considering a set of pre-planned locomotion tasks, it has been obtained feet location using classical methods and, then, by means of the inference system. This methodology enables a comparison process between classical kinematics computations and the fuzzy inference systems. In this way, it is possible to determine the error produced by the approximate FIS evaluation.

The aims of the locomotion experiments are the same one exposed before for manipulative perception evaluation. The angles for legs joints have been extracted from three different pre-planned locomotion tasks. Figure 111 represents the full sequence of frames obtained from one of the locomotion tasks. The locomotion sequence starts from the double support posture (DS) at the right of the figure. The beginning of the steps is produced keeping the left foot on the ground on single support phase (SS Left Foot) and advancing the right foot. Following another double support phase, the right foot stands on the ground (SS Right Foot) and the left foot moves ahead.

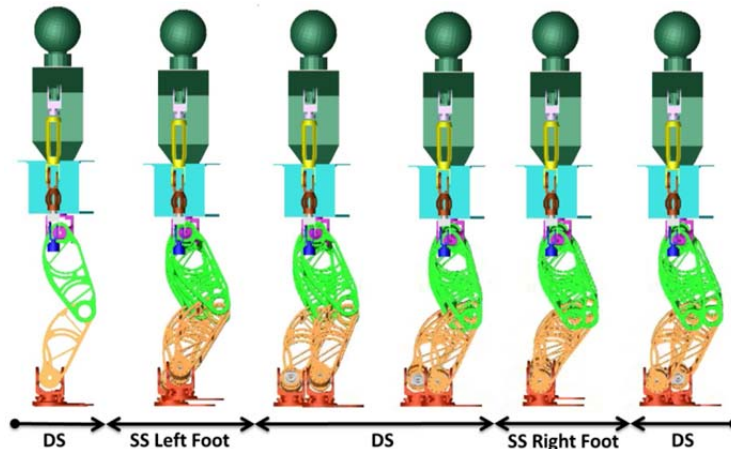


Figure 111 Locomotion task sequence

This task is performed in 6s but, taking into account the purpose of testing the proprioceptive system, it has been only considered the sequence DS-SS Left Foot-DS. In this part of the sequence the most interesting proprioceptive perception corresponds to the flying leg (right) that will be the matter of testing. The initial and final right leg configurations are shown in Table 35 for the three different locomotion tasks.

Table 35 Initial and final commanded configurations of the flying leg

	Task	Flying Leg Joints (rad)					
		J1	J2	J3	J4	J5	J6
<b>Initial Configuration</b>	1 / 2 / 3	0	0,003	0,308	-0,796	0,485	0,028
<b>Goal Configuration</b>	1	0	0,233	0,159	-0,655	0,496	-0,233
	2	0	0,259	0,295	-1,055	0,760	-0,259
	3	0	0,259	0,230	-1,014	0,784	-0,259

Then the joint angles measured by each joint's absolute encoder are summarized in Table 36, in which some measurement deviations can be observed due to sensor characteristics and mounting tolerances.

Table 36 Initial and final measured configurations of the right leg

	Task	Measured Right Leg Joint Angles (rad)					
		J1	J2	J3	J4	J5	J6
<b>Initial Configuration</b>	1	0,0005	0,004	0,308	-0,796	0,485	0,027
	2	0,0005	0,003	0,309	-0,796	0,484	0,028
	3	0,0005	0,003	0,309	-0,797	0,485	0,028
<b>Goal Configuration</b>	1	0,0005	0,234	0,159	-0,655	0,496	-0,234
	2	0,0005	0,259	0,296	-1,054	0,758	-0,259
	3	0,0005	0,259	0,232	-1,015	0,783	-0,259

It is important to recall that the goal of the proprioceptive evaluation for lower body is the computing of the foot location. It is achieved using the measurements of the joint angles and performing the forward kinematics computation with them. Applying the human inspiration basis of this PhD Thesis, this computing task is performed by an inference system. It has been developed three FIS modules using neuro-fuzzy development technique to obtain X-Y-Z location components from each foot. Figure 112 shows some representation of the resulting inference surfaces for each foot location coordinate.

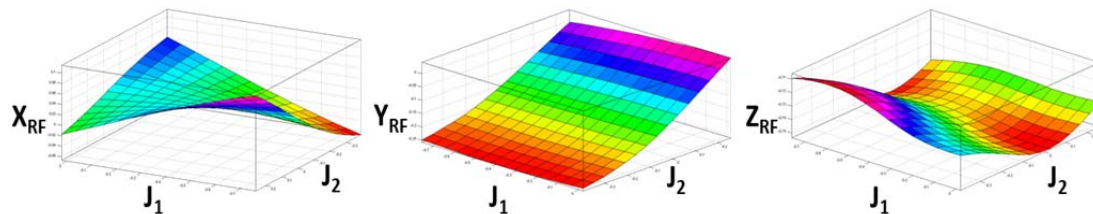


Figure 112 Right foot location inference surfaces

The computing of right foot location applying classical kinematic method compared with the results from the fuzzy inference system developed is the first aim of the study. The datasets obtained from both kinds of evaluation are shown in Table 37.

Table 37 Final computed vs. inferred right leg location

Task	Goal Position Kinematic Evaluation (m)			Goal Position FIS Evaluation (m)		
	X	Y	Z	X	Y	Z
1	0,0904	0,0230	-0,6899	0,0889	0,0226	-0,6893
2	0,1098	0,0229	-0,6311	0,1096	0,0226	-0,6318
3	0,1356	0,0231	-0,6314	0,1350	0,0224	-0,6321

By means of the analysis of the results exposed in Table 37, it is possible to determinate a mean error around 0,6mm in the approximate inferred leg goal location. This error is lower enough to achieve any kind of locomotion task.

As well, it is possible to track the error committed during all task performance. The following charts present the error between commanded positions and the evaluation of the measured data. Figure 113 shows this error in the case of the kinematical evaluation of the sensed data. This method is very precise and the error is mainly caused by measurement devices.

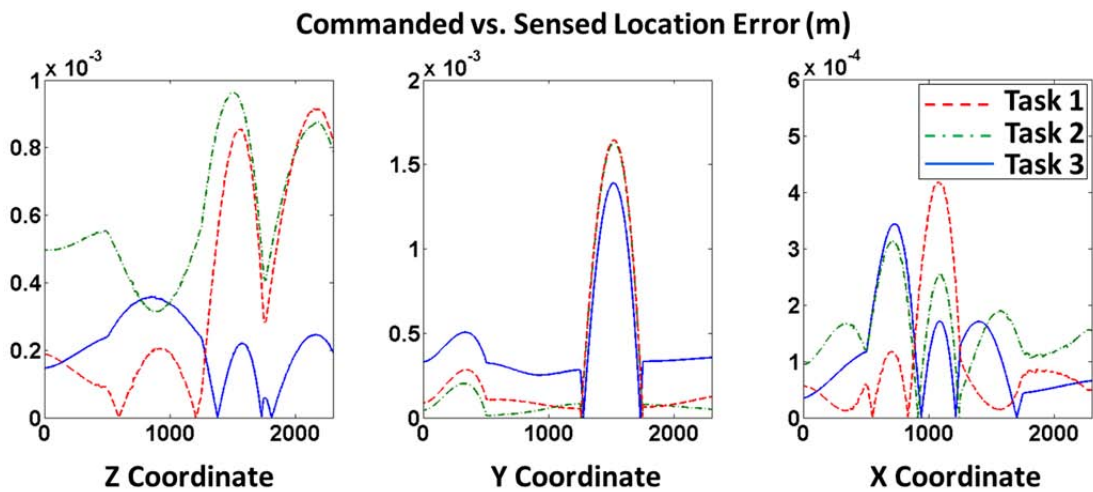


Figure 113 Right foot position kinematic evaluation error

Evaluating the sensed data by means of the developed FIS modules, it is possible to obtain the approximate foot location. Figure 114 shows the error committed using this method. The mean level is one order of magnitude higher than the kinematic evaluation, but it still remains enough precise for the purpose of perceptual generation. The situations in which the error is higher are produced near the zero configuration pose of the robot.

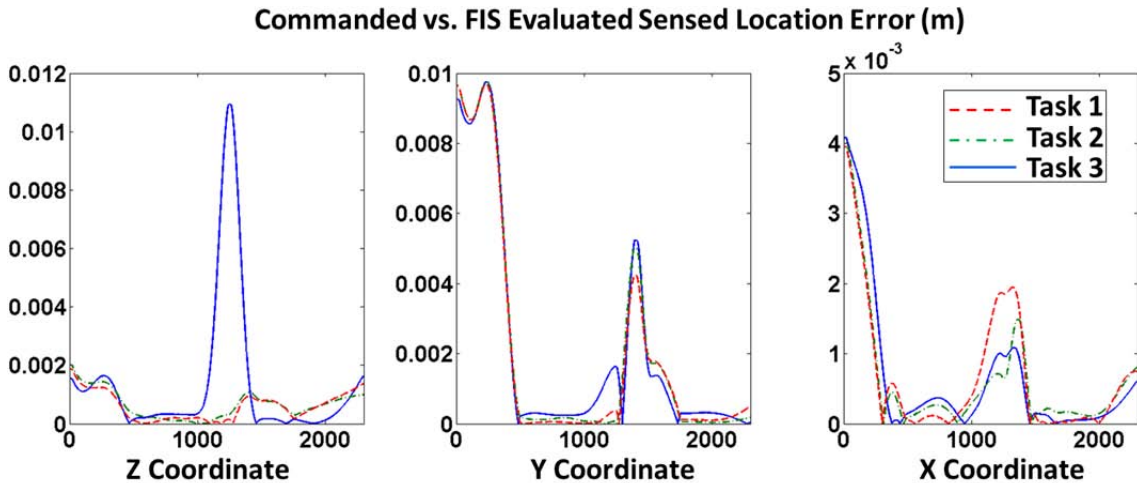


Figure 114 Right foot position fuzzy inference error

### 7.2.2.2 Exoceptive Perception Results

TEO humanoid robot has set of sensorial devices to capture exoceptive sensations as described in previous chapters. The information provided by each one of these devices is applied in different ways depending on the kind of task. Thus, the exoceptive perception evaluation is highly influenced by the task in which the information is used.

Then, this description of the exoception development has been organized by task. Depending on the task type, its exoceptive perception will be composed by different

sensorial sources evaluated. In summary, Table 38 presents the outcomes established for each exoceptive evaluation depending on the task.

Table 38 Exoceptive outcomes summary

Task	Sensorial source	Exoceptive Outcome
<b>Manipulation</b>	Visual Sensation	Object location relative to hands
	F/T Sensation	Manipulation Limitations
<b>Locomotion</b>	Inertial Sensation	Rotational Robot Tendency
		Linear Robot Tendency
	F/T Sensation	Foot Angle
		Foot on Ground
		ZMP

#### 7.2.2.2.1 Visual Perception for Manipulation Tasks

The aim of the exoceptive visual information is to extract information about distant objects. In the case of the proposed manipulation task, the main goal is the estimation of the ball location during its flying trajectory.

The humanoid perceptual system process every image provided by the visual sensor to extract the features related to the task. The results from image analysis are referred to the Kinect camera focus ( $\vec{KO}$ ) but they are not related to the manipulation tool ( $\vec{WH}$ ), being useless. Figure 115 (a) shows the relation of the visualized object with the robot origin of reference  $\vec{WO}$  as the sum of vectors  $\vec{WK}$  (waist-Kinect) and  $\vec{KO}$  (Kinect-object). In the same way (Figure 115 (b)), this relation  $\vec{WO}$  can be expressed as the sum of hand location vector  $\vec{WH}$  with the required reference between hand and object  $\vec{HO}$ .

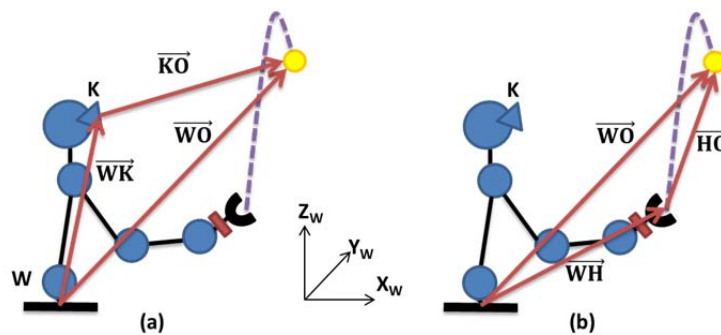


Figure 115 Waist-Kinect-object system (a) and waist-hand-object system (b)

Therefore, the visual perception evaluation is in charge of computing the object-hand vector components ( $\vec{HO}$ ). The considered output from the visual sensor enables the use of the object coordinates and tracking its movement.

Due to TEO upper body robot is under development, it has been established a series of trials to prove the FIS performance. These experiments consist of performing the task proposed, in which one ball must be thrown up, and capture the visual information ( $\vec{KO}$ )

with the Kinect sensor considering a static robot pose. Figure 116 presents four frames captured with the Kinect sensor during one of these trials. The duration of the task is about 1,15s and the system is able to process the object location every 35ms. The object location obtained for each frame and the right hand positions are shown in Table 39.

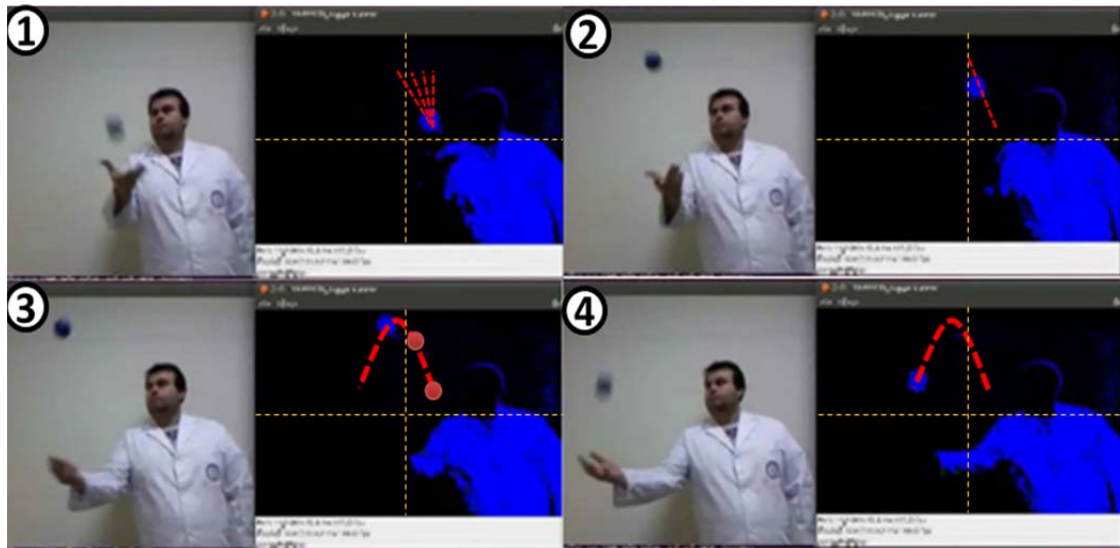


Figure 116 Object location and movement tracking

Table 39 Object locations to Kinect reference frame

Frame	$\overrightarrow{KO}$			$\overrightarrow{WH}$		
	X (m)	Y (m)	Z (m)	X (m)	Y (m)	Z (m)
1	1,02	-0,213	0,187	0,210	-0,340	0,234
2	1,012	-0,046	0,682	0,210	-0,340	0,234
3	1,005	0,061	0,715	0,210	-0,340	0,234
4	1,001	0,300	0,204	0,210	-0,340	0,234

The developed fuzzy inference system computes only the horizontal and vertical distances of the hand due to established constraints. Then, the resulting FIS is represented by the inference surfaces shown in Figure 117. They relate the Y and Z coordinates, corresponding to TEO robot reference frame, of right hand and the object to obtain the distance between them.

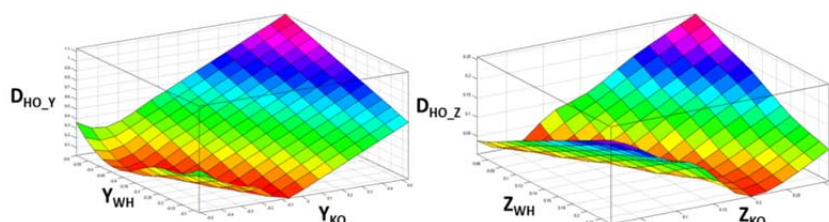


Figure 117 Hand-object distance inference surfaces

The inputs for the inference systems are the corresponding components from vectors  $\vec{KO}$  and  $\vec{WH}$ . The output of each system is the value of the corresponding  $\vec{HO}$  vector components. Table 40 summarizes the evaluation of the data obtained from the experimental example presented. The performance of the Y component inference is very accurate, with a mean error around 5mm. Error in the Z component is higher than the other component, resulting a mean value about 38mm for this component perception.

Table 40 Results from evaluation of the hand-object relative position

<b>Frame</b>	<b><math>\vec{WO}</math></b>		<b>Real Distance</b>		<b>Distance FIS</b>	
	Y (m)	Z (m)	dY (m)	dZ (m)	dY (m)	dZ (m)
<b>1</b>	-0,213	0,717	0,127	0,483	0,1226	0,542
<b>2</b>	-0,046	1,212	0,294	0,978	0,2941	1,0
<b>3</b>	0,061	1,245	0,401	1,011	0,401	1,056
<b>4</b>	0,300	0,734	0,640	0,500	0,6396	0,526

### 7.2.2.2.2 Force/Torque Perception for Manipulation Tasks

Force/Torque sensor placed at the robot wrists provide information about the interaction with handled objects. The FIS module developed determines the modulus of the force and torque sensed by the device from each hand. It is useful to evaluate critical parameters during manipulation such as payload limitations, etc. The development of the inference system is based on equations (6.7) and (6.8) and the measurement limitations of the sensors.

The resulting FIS module for force evaluation has three inputs ( $F_x$ ,  $F_y$ ,  $F_z$ ) and its output is the force module ( $F_T$ ). The mapping between input and outputs is represented in Figure 118. The system uses eight rules to evaluate the resulting force with a target error of less than 1N.

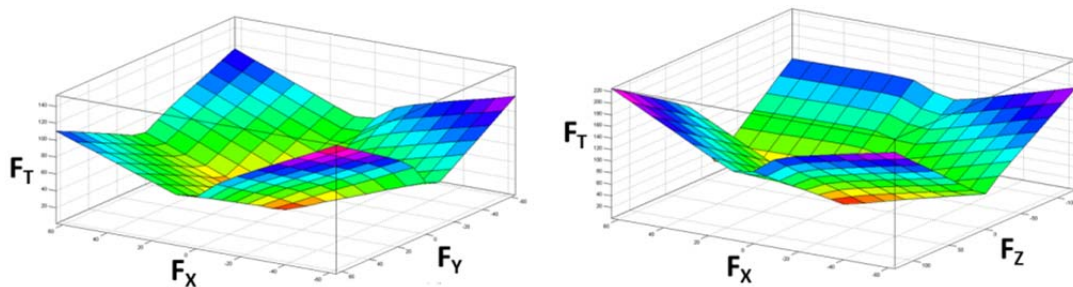


Figure 118 Wrists Force FIS inference surfaces

Parallel to the force inference system developed, the FIS module for torque evaluation has three inputs ( $T_x$ ,  $T_y$ ,  $T_z$ ) and its output is the torque module ( $T_T$ ). Two surfaces

representing the FIS inputs and output is shown in Figure 119. The system uses eight rules to evaluate the resulting torque with a target error of less than 0,1Nm.

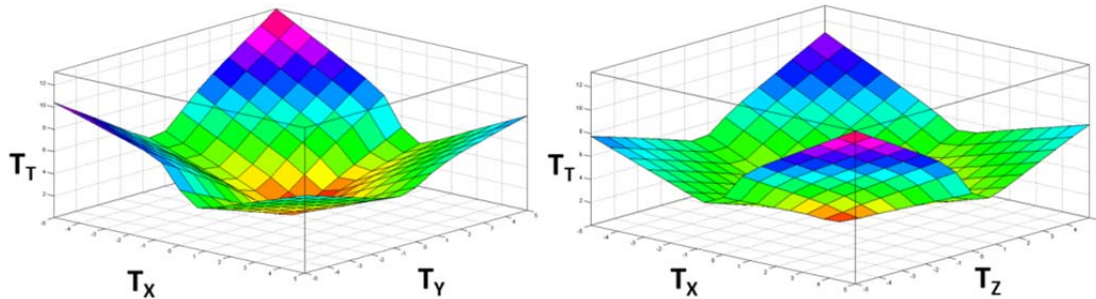


Figure 119 Wrists Torque FIS inference surfaces

After the FIS development process, the physical system from Figure 120 has been used to perform different measurement with the aim of validating the fuzzy inference module. This system allows performing measurements in each principal axis independently, that is, it is possible to measure only the force or torque exerted in one axis, maintaining the measurement in other axis equal to zero. The case of the Z axis torque corresponds to the torsional torque exerted on it and, due to that, it produces measurements in other axis, has been excluded from the evaluation.

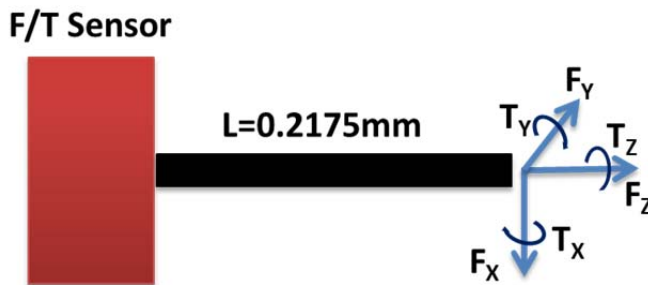


Figure 120 F/T Sensor validation system

Then, the results of the measurements performed, using a calibrated set of weights, are shown in Table 41. These measurements compose the validation dataset from which the performance of the inference system can be evaluated.

Table 41 Wrist F/T sensors measurements

Mass (Kg)	F/T Wrist Sensor				
	F <sub>X</sub> (N)	F <sub>Y</sub> (N)	F <sub>Z</sub> (N)	T <sub>X</sub> (Nm)	T <sub>Y</sub> (Nm)
0,5	5,11	5,32	5,04	1,11	1,16
1	10,3	10,26	10,09	2,24	2,23
1,5	15,06	15,07	15,2	3,28	3,28
2	20,02	20,04	20,1	4,35	4,36

The values from Table 41 are the inputs for the FIS module. Each force or torque value, the output is estimated independently in the same way than the measurement

was performed. It implies, for instance, an input vector with only one non-zero component (i.e.  $[F_x, 0, 0]$  for force in X axis). The outputs resulting from force evaluated are detailed in Table 42. Considering the evaluation performance, the mean error of the system is about 0,53N, which it is acceptable for this kind of perception.

Table 42 Force FIS evaluation results

Mass (Kg)	F/T Wrist Sensor					
	$F_{x\_T}$ (N)	Mean Error	$F_{y\_T}$ (N)	Mean Error	$F_{z\_T}$ (N)	Mean Error
0,5	4,3	0,80	4,22	1,10	3,83	1,21
1	10,3	0	9,85	0,41	9,48	0,61
1,5	15,4	0,34	15,3	0,23	15,4	0,20
2	20,5	0,48	20,5	0,46	20,6	0,50

Besides, the results from the evaluation of torque values are presented in Table 43. The mean error of the torque evaluation is 0,03Nm. This level of error is better than the required for manipulation torque perception.

Table 43 Torque FIS evaluation results

Mass (Kg)	F/T Wrist Sensor			
	$T_{x\_T}$ (Nm)	Mean Error	$T_{y\_T}$ (Nm)	Mean Error
0,5	1,12	0,01	1,03	0,13
1	2,27	0,03	2,21	0,02
1,5	3,29	0,01	3,29	0,01
2	4,34	0,01	4,38	0,02

#### 7.2.2.2.3 Inertial Perception for Locomotion Tasks

The Inertial Measurement Unit (IMU) is a complex device with sensor data processing capabilities that enables the direct use of the output information about the magnitudes measured. Nevertheless, comparing its operation with the human vestibular system, it is necessary to evaluate its output information to enrich the perceptual system.

Therefore, the inertial perception will be the result of the evaluation of the information related to kinetics provided by the IMU sensor. Two kinds of perception were established regarding motion tendency.

The first one computes the tendency of the robot to increase, maintain or decrease its motion velocity in a global reference frame. It denotes the variation of the translational momentum. As well, it can be used to determine the stability evolution and to predict the most appropriate reaction.

The inference system development related to linear motion tendency has been carried out according to equation (6.18). The training and checking datasets has been composed using motion information extracted from the IMU device. Then, two evaluation modules have been developed to determine the linear movement tendency in the sagittal ( $L_x$ ) and frontal ( $L_y$ ) planes. The resulting FIS modules for evaluating this perception have four inputs corresponding to the acceleration vector ( $a_x, a_y$ ) and its rotation ( $\theta_x, \theta_y$ ).

The performance of the FIS modules are verified by means of the evaluation of several test data sets (Table 44) using equation (6.18) and comparing its results with those coming from the FIS evaluation.

Table 44 Linear motion tendency test datasets

Test Dataset Number	$a_x$ (m/s <sup>2</sup> )	$a_y$ (m/s <sup>2</sup> )	$\theta_x$ (deg)	$\theta_y$ (deg)
1	-1,03	0,31	1,05	5,57
2	-6,16	1,21	1,15	34,50
3	-2,42	1,84	3,28	8,20
4	-2,07	-3,03	-10,52	5,18
5	4,5	9,80	60,8	-1,35
6	-0,33	-8,17	-54,52	1,66

In summary, the each ‘sugeno’ fuzzy inference system obtained has two inputs, one output and sixteen rules, which mapping surfaces are shown in Figure 121.

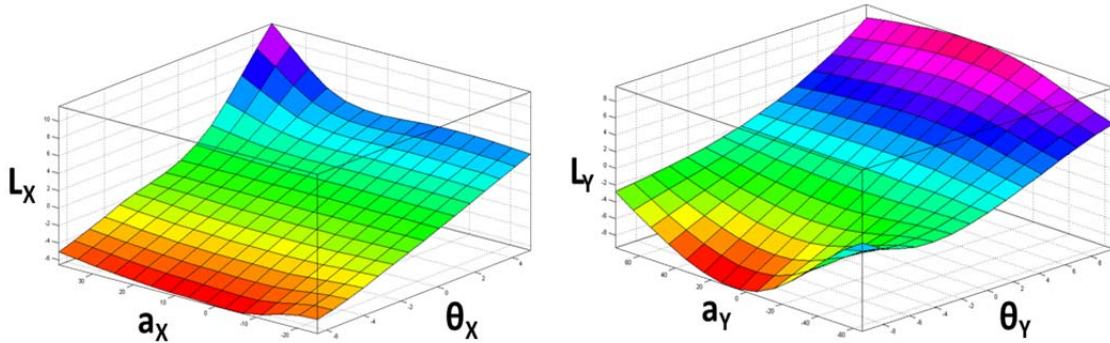


Figure 121 Evaluation surfaces from linear motion tendency FIS

Then, the comparison between both methods using the previous dataset is presented in Table 45. Relative to the linear motion tendency in the sagittal plane direction ( $L_x$ ), the mean error of the measurements is about 0,02m/s<sup>2</sup>. In the case of the frontal plane direction ( $L_y$ ), the mean error of the measurements is about 0,08m/s<sup>2</sup> and it is higher than the sagittal plane direction. It can be tolerated because the stability margin in this direction is higher than sagittal direction.

Nevertheless, the aim of this perception is to capture the linear component of the robot motion and its approximate level. Thus, no high precision is required, being the error levels obtained better than expected.

Table 45 Linear tendency results comparison (values in m/s<sup>2</sup>)

<b>Dataset Number</b>	<b>L<sub>X_EQ</sub></b>	<b>L<sub>X_FIS</sub></b>	<b>L<sub>X_ERR</sub></b>	<b>L<sub>Y_EQ</sub></b>	<b>L<sub>Y_FIS</sub></b>	<b>L<sub>Y_ERR</sub></b>
<b>1</b>	-1,0251	-1,03	0,0049	0,3099	0,31	0,0001
<b>2</b>	-5,0166	-5,08	0,0634	1,2097	1,21	0,0003
<b>3</b>	-2,3953	-2,40	0,0047	1,8370	1,84	0,003
<b>4</b>	-2,0615	-2,06	0,0015	-2,9791	-2,92	0,0591
<b>5</b>	4,4988	4,44	0,0588	4,7810	4,71	0,071
<b>6</b>	-0,3299	-0,33	0,0001	-4,7420	-4,40	0,342

The second inference system developed evaluates the rotational motion tendency of the robot. Based on equations (6.9) and (6.10), the rotational tendency constitutes a turn over indicator in the principal directions according to the sagittal ( $R_X$ ) and frontal ( $R_Y$ ) planes of the robot. The development of the FIS modules for both directions has been performed using the same data than the linear case. The main difference of this development process is the reduction of inputs. Only two inputs by module are used (Table 46), corresponding to the angular rate ( $\omega_X$ ,  $\omega_Y$ ) and the angle measured by the IMU ( $\theta_Y$ ,  $\theta_X$ ), respectively.

Table 46 Rotational motion tendency test datasets

<b>Dataset Number</b>	<b><math>\omega_X</math> (rad/s)</b>	<b><math>\omega_Y</math> (rad/s)</b>	<b><math>\theta_X</math> (deg)</b>	<b><math>\theta_Y</math> (deg)</b>
<b>1</b>	0,03	0,016	1,05	5,57
<b>2</b>	-0,79	1,06	1,15	34,50
<b>3</b>	-1,14	-2,00	3,28	8,20
<b>4</b>	0,50	2,59	-10,52	5,18
<b>5</b>	-0,02	0,14	60,8	-1,35
<b>6</b>	-1,45	0,47	-54,52	1,66

As in the linear motion FIS case, the each ‘sugeno’ fuzzy inference system obtained has two inputs, one output but it only has nine rules. Figure 122 presents the surfaces that map the inputs to infer the output.

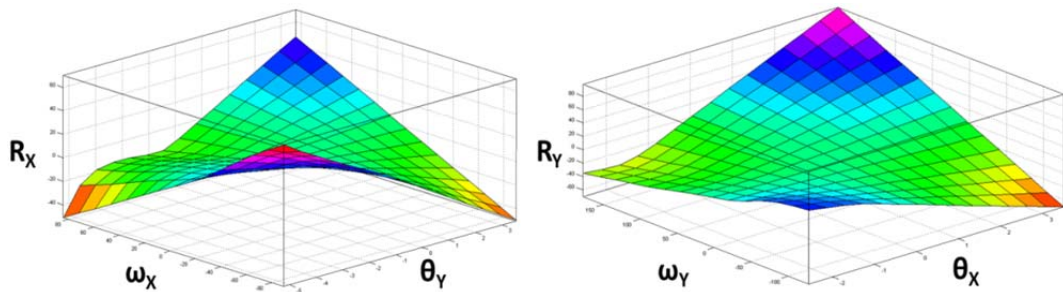


Figure 122 Evaluation surfaces from rotational motion tendency FIS

The results of the comparison between both methods, using the test dataset, are presented in Table 47. The rotational motion tendency FIS mean error in the sagittal plane direction ( $R_x$ ) is about 0,07rad/s and, in the case of the frontal plane direction ( $R_y$ ), it is approximately 0,1rad/s. In the same way, the result expected from this perception evaluation is merely an indicator of the rotational component of the motion. Because of that, high precision for the perceptual values are not required.

Table 47 Rotational tendency results comparison

Dataset Number	$R_{x\_EQ}$	$R_{x\_FIS}$	$R_{x\_ERR}$	$R_{y\_EQ}$	$R_{y\_FIS}$	$R_{y\_ERR}$
1	0,0266	0,0266	0	0,0027	0,0026	0,0001
2	-4,3378	-4,28	0,0578	0,1940	0,193	0,001
3	-1,4878	-1,23	0,2578	-1,0441	-1,66	0,6159
4	0,4122	0,412	0,0002	-4,3365	-4,32	0,0165
5	0,0043	0,0043	0	1,3547	1,35	0,0047
6	-0,3831	-0,294	0,0891	-4,0782	-4,08	0,0018

#### 7.2.2.2.4 Force/Torque Perception for Locomotion Tasks

Force/Torque sensory devices used in robotics provide information related to actions exerted over the robot that can have different origin. During locomotion tasks, the perception evaluation will be performed regarding to:

- 1) Sensorial information about ‘internal forces’ (i.e. the robot weight).
- 2) Sensorial information about reactions caused by external forces exerted over the robot with direct contact.

The complexity of the perception will always depend on the output provided by sensorial device. From the sensation evaluation outputs exposed on Table 38, the simplest perceptive information that can be obtained is relative to the foot-ground interaction detection. Taking into account only the sign of vertical force measured by the sensor ( $F_z$ ) it is possible to determine whether the foot is on the ground or not. It is equivalent to consider that the sensor measures a compressive force due to the robot weight. If the foot is on the air the force sensed is caused by the foot weight, which is

much lesser and expansive. This information will be applied further on to determine the Base of Support and the walking phase (simple or double support).

But more complex perceptions can be obtained from these sensorial devices. The first one is the foot angles. For each foot, taking into account the vector of reactions measured by the sensor, it is possible to determine the angle of the foot in both sagittal and frontal planes. The consideration of the forces measured as reactions indicates that the angles are evaluated only when foot is on the ground. As well, considering that the foot is perfectly parallel to the ground and completely placed on it, the angle evaluated denotes the soil inclination under the foot. The last issue considered in the development of the system that evaluates this perception is related to the number of necessary systems, due to the constructive symmetry of the sensor device. Therefore, the same neuro-fuzzy evaluation system can be used to compute the four angles, two by foot (Table 48 and Figure 123).

Table 48 Evaluated feet angles

<b>Right Foot</b>		<b>Left Foot</b>	
$\alpha_{\text{Sagittal}}$	$\alpha_{\text{Frontal}}$	$\beta_{\text{Sagittal}}$	$\beta_{\text{Frontal}}$

Then this evaluation is based on the development of only one neuro-fuzzy network to perform the evaluation by inference from equations (6.5) and (6.6).

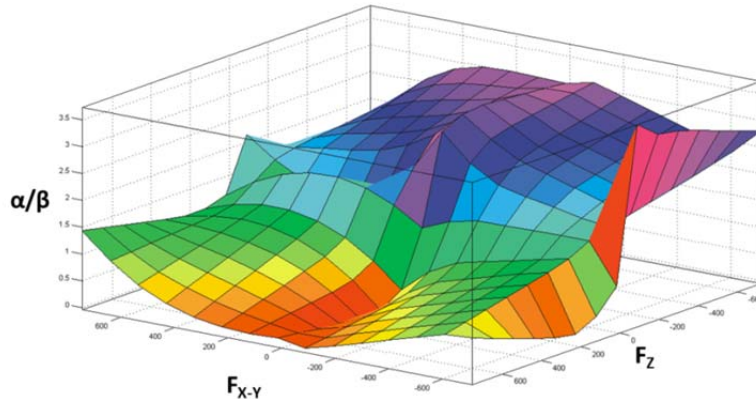


Figure 123 Foot angles  $F_{X-Y}$  vs.  $F_z$  inference surface

The second complex perception to evaluate is regarding ZMP computation. This indicator of the stability margins can be related to the reaction forces caused in any support surface. Specifically, during locomotion tasks, the reaction forces measured when feet contact the ground are used to compute ZMP. Then, the module developed to evaluate those sensed forces has the mission of providing an approximate value of the actual balance status of the robot.

The development of the neuro-fuzzy ZMP evaluation system is based on the data collected from three sources:

- 1) The real mechanics mock-up of the robot ankle and leg acting like the simple inverted pendulum (Figure 124 (a)).

- 2) The simple inverted pendulum virtual model that provides information of reaction forces considering this simplification for robot locomotion (Figure 124 (b)). The information extracted from this virtual model is used to validate the operation of the simple pendulum mock-up.
- 3) TEO robot platform for collecting data in double support phase (Figure 124 (c)). The consideration of robot walking like an inverted pendulum is more suitable to the single support locomotion phase. The addition of data collected from the sensors in double support phase movements enrich the training dataset of the neuro-fuzzy system and it improves the inference results.

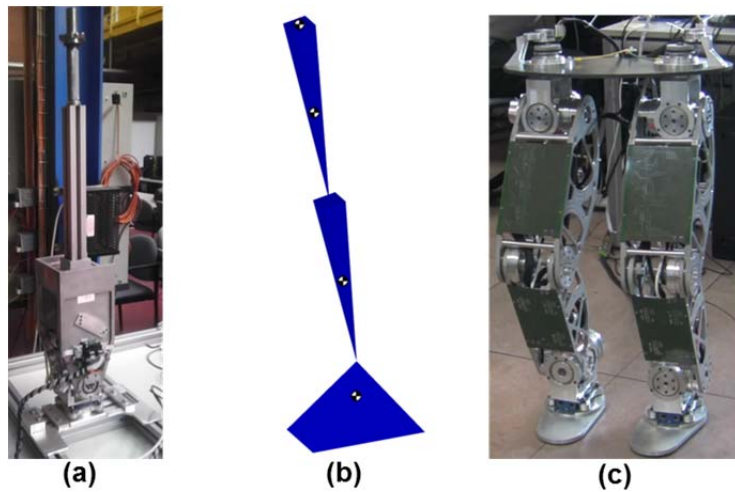


Figure 124 Simple inverted pendulum mock-up (a), simple inverted pendulum virtual model (b) and TEO lower-body (c)

Then, two FIS modules were trained to evaluate each component of the ZMP reference point. The  $X_{ZMP}$  component moves along the sagittal plane direction meanwhile the  $Y_{ZMP}$  component does it along the frontal plane direction. Figure 125 (a) and (b) presents two examples of the resulting evaluation surfaces that relates two FIS inputs with its output.

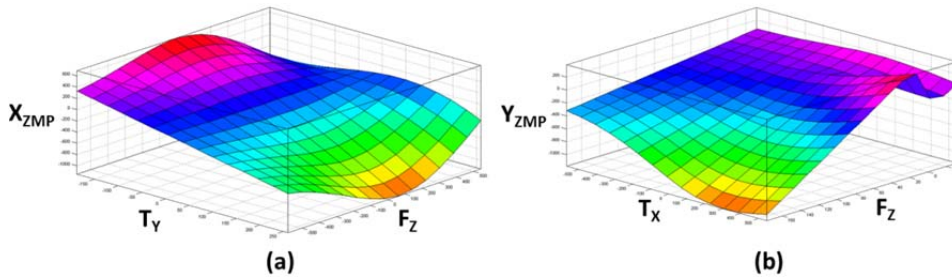


Figure 125  $T_Y$  vs.  $F_Z$  inference surface for  $X_{ZMP}$  (a) and  $T_X$  vs.  $F_Z$  inference surface for  $Y_{ZMP}$  (b)

By means of a simple movement test, the performance of the developed system has been proved. Figure 126 illustrates the pendulum movement in the sagittal plane to the left and maintaining double support.

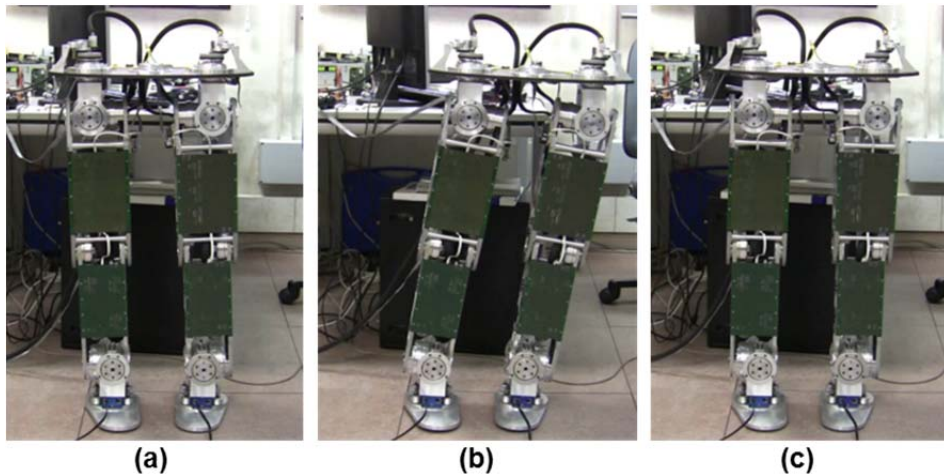


Figure 126 Pendulum movement task: (a) Initial position, (b) left movement and (c) final position

The data captured by the force/torque sensor system has been evaluated by means of classical ZMP computation and the fuzzy inference system developed. For  $X_{ZMP}$  component, Table 49 presents a brief set of input values and the ZMP values obtained. In this case, the mean error for this component is about 0,025m for the entire task values.

Table 49 Data comparison for  $X_{ZMP}$

$T_Y$ (Nm)	$F_x$ (N)	$F_z$ (N)	Computed $X_{ZMP}$ (m)	Inferred $X_{ZMP}$ (m)
0	-1,5	-125,8	0,0167	0,0310
0	-42,25	-56,25	0,107	0,07
-18,5	-57,75	-88,7	0,289	0,496
-1,5	-53,25	-125,37	0,0798	0,0817

In the case of the  $Y_{ZMP}$  component, the example extracted from the data captured by sensors is shown in Table 50. In the same way, the mean error for this component is about 0,05m after the completion of the movement.

Table 50 Data comparison for  $Y_{ZMP}$

$T_x$ (Nm)	$F_y$ (N)	$F_z$ (N)	Computed $Y_{ZMP}$ (m)	Inferred $Y_{ZMP}$ (m)
-0,5	-3	-125,8	0,0034	-0,0290
-21	-12,75	-56,25	0,217	0,232
-16	10,25	-88,7	0,1636	0,0444
3,5	0,75	-125,37	-0,0323	-0,1027

The evolution of the each ZMP component is represented in Figure 127 (a) and (b). The computed result (Comp.) and the inferred results (FIS) are represented in the same chart for each component. There exist sensor offset errors in both chart but it can

be better observed in the sagittal movement. This is one reason why the obtained mean error in this component is bigger. As well, the FIS systems have worst performance when high variation of measurements is presented in their inputs.

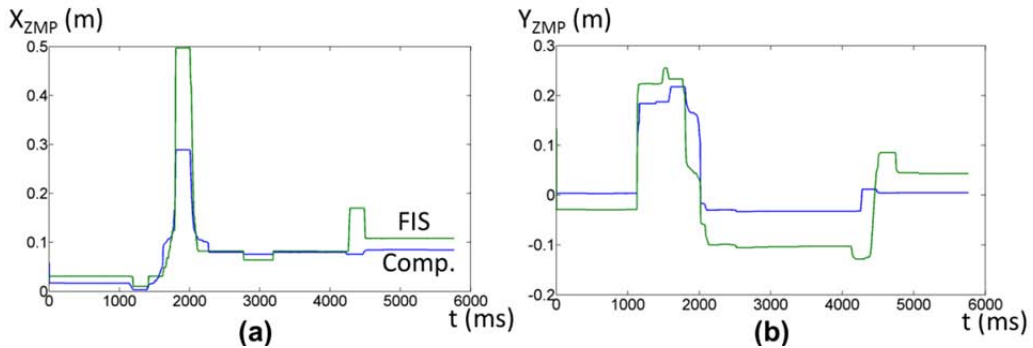


Figure 127 X<sub>ZMP</sub> (a) and Y<sub>ZMP</sub> (b) evolution during the pendulum movement

The error obtained seems to be high but the aim of this perceptual evaluation is the determination of an approximate ZMP location. It will be applied in prediction of balance evolution and, due to this, it is more important to know the ZMP evolution than obtaining an accurate value.

### 7.2.3 Surprise Development

The perceptual inputs provide information about the humanoid robot status, the environment conditions and the task the robot is carrying out. Because of the information related to the robot motion depends on the task, it can be established that the evaluation process of the huge amount of perceptual information is task driven.

The perceptual evaluation process followed is based on the human inspired concept of surprise. Then, the perceptual information evaluation has been achieved applying two basic concepts of the surprisingness theory: the passive and active expectation failures.

Following, the development of these classes of surprise applied in manipulative and locomotive tasks is exposed.

#### 7.2.3.1 Passive Surprise

Passive surprise is based on the failure of the some assumption about the task performance. For instance, it can be assumed when an object is thrown up that it will fall down following a linear vertical trajectory. Whether the evaluation of perceptions demonstrates that this assumption has failed, then a passive surprise even could be elicited.

Due to the surprise evaluation is task driven, the assumptions has been established considering each task proposed.

##### 7.2.3.1.1 Manipulation Tasks

The assumption made in manipulation tasks is the outlined in the example presented in the introduction of this section. The act of catching a ball when it is falling down has

been assumed in every time period as linear and vertical. Then, the passive surprise event is related to the absolute distance from hand to the object. Taking into account the vector from the hand to the object, the surprise will depend on the module of each vectorial component like in Figure 128 (a) and (b).

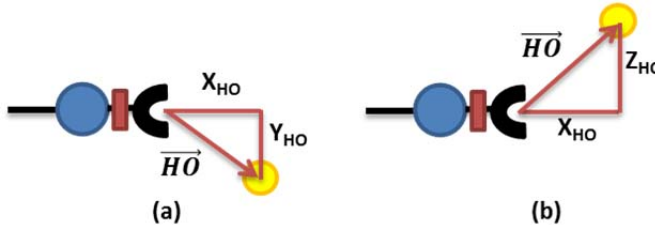


Figure 128 Horizontal plane (a) and vertical plane (b) hand-object components

Assuming that the proposed task is always performed with the right hand, the surprise will consist of the evaluation of the difference between hand and object in each coordinate component (Figure 83). The result is the surprise corresponding to the component in which the comparison had the highest surprise level ( $SP_x$  or  $SP_y$  or  $SP_z$ )

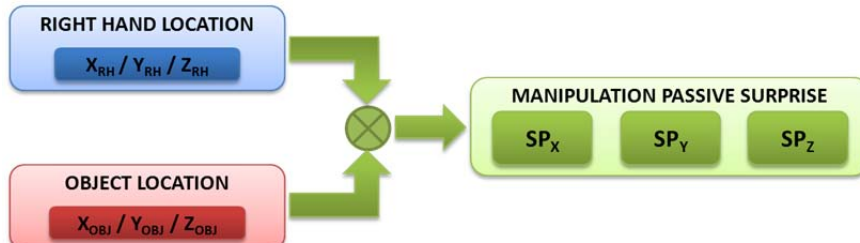


Figure 129 Manipulation passive expectation failure

This computed difference is compared with pre-established thresholds and the output ‘intensity’ of surprise is fixed. These thresholds have been established attending to the dynamical characteristics of the robot arm movement for each synergy proposed. Taking in account these two factors, the computed output surprise levels or ‘intensities’ are exposed in Table 51.

Table 51 Manipulation passive expectation surprise levels

Passive Surprise Level	$SP_x$	$SP_y$	$SP_z$
Low	0,235	0,235	---
Medium	0,47	0,47	---
High	1,175	1,175	0

These thresholds were obtained evaluating the performance of the reaction synergies or pre-programmed movement patterns that can be parameterized to carry out the tasks. The surprise level is related to the distance the hand should be moved toward and the velocity of the movement. But, there exist kinematical and dynamical limitations that constraint the reaction. Therefore, the passive surprise thresholds were established considering these constraints.

In the case of  $S_Z$ , the surprise level considered is produced when the object location is in the same or under the hand Z component level. Then, the surprise event is used to stop the task execution.

### 7.2.3.1.2 Locomotion Tasks

In the case of locomotion tasks, the assumption was made attending to the dynamical characteristics of the straight line walking task. Thus, two main features of locomotion were considered related to the orientation of the humanoid robot body during walking: the linear and rotational robot movement tendencies. Hence, it was assumed that both movement tendencies must be within different limits to maintain robot balance in locomotion.

The passive surprise thresholds, in the case of rotational tendency, were established in Section 6.3.3.2. The surprise level depends on the perception of body rotation and the duration of the same level of perception (Figure 130). The determination of thresholds to establish surprise levels were based on the study of the simple inverted pendulum that models the robot body during locomotion. Another constraint considered is related to the time period for surprise evaluation, which was considered constant.



Figure 130 Locomotion rotational tendency passive expectation failure

Hence, Table 52 presents the surprise levels computed for rotational movement tendency of the humanoid robot.

Table 52 Locomotion rotational passive expectation surprise levels

Passive Surprise Level	$SP_{RX}$	$SP_{RY}$
Low	0,98	0,30
Medium	3,92	1,21
High	9,81	3,03

The same concepts to compute rotational tendency are applicable in the linear motion tendency case (Figure 131). The simplifications of the operation like an inverted pendulum and the consideration of constant evaluation time make easier the surprise level establishment.



Figure 131 Locomotion linear tendency passive expectation failure

Table 53 exposes the surprise levels computed taking in account the linear thresholds from Table 25.

Table 53 Locomotion linear passive expectation surprise levels

Passive Surprise Level	$SP_{LX}$	$SP_{LY}$
Low	0,88	1,05
Medium	2,54	2,91
High	4,38	5,25

### 7.2.3.2 Active Surprise

Active surprise, in the opposite, is based on the failure of the predictions about the future evolution of any parameter related to the task. Using the same example described in the introduction of the passive surprise, whether past information related with the visual perception of the ball trajectory are analysed, it is possible to predict the location where the robot could catch the ball. Then different predictions can be made during object flying trajectory and they can be updated time by time. When two consecutive predictions differ, an expectation failure is produced.

Therefore, different predictive systems have been developed depending on the tasks proposed.

#### 7.2.3.2.1 Manipulation Tasks

The prediction in the manipulation task proposed is based on the kinematical equations of an object's vertical shot. The flying trajectory will depend on the initial velocity and the angle of the shot. Then, the trajectory could be vertical in straight line or parabolic. Considering the scheme from Figure 132, the object flight trajectory can be predicted knowing its origin and other near point from the flight trajectory.

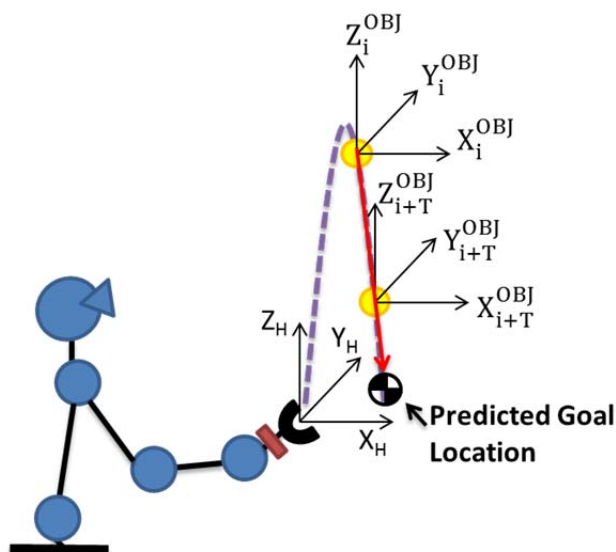


Figure 132 Object location prediction scheme

The origin is the last hand position obtained from the proprioceptive perception and the waypoints on the object flight trajectory are processed by visual perception (Figure 133). In this case, the use of more than one waypoint will enrich the prediction about goal location.

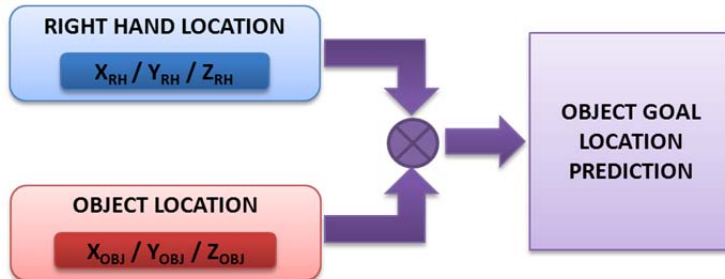


Figure 133 Manipulation active surprise inference system input dataset

The active surprise module computes the distance between the predicted object final location and the hand position and the module elicits a graded surprise event depending on this distance (Figure 134).

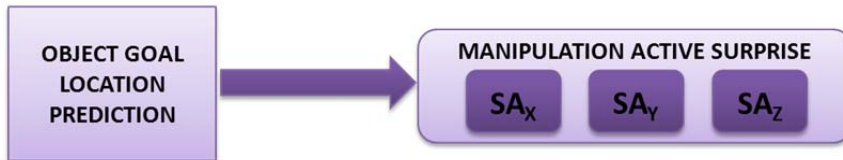


Figure 134 Manipulation active expectation failure

The surprise event has been graded taking in account mechanical limitations of the robot and the required synergic movement to achieve the task. Then, the surprise events scale follows an exponential law depending on the maximum distance to cover ( $d$ ) and the mechanical constant of the synergy ( $\tau_s$ ). Equation (7.1) and Figure 135 shows this exponential relation. As well, Table 54 exposes the graded values for a basic synergic movement of that moves on straight line following the X coordinate of the robot frame.

$$SA_{x,y,z} = e^{d/\tau_s} \quad (7.1)$$

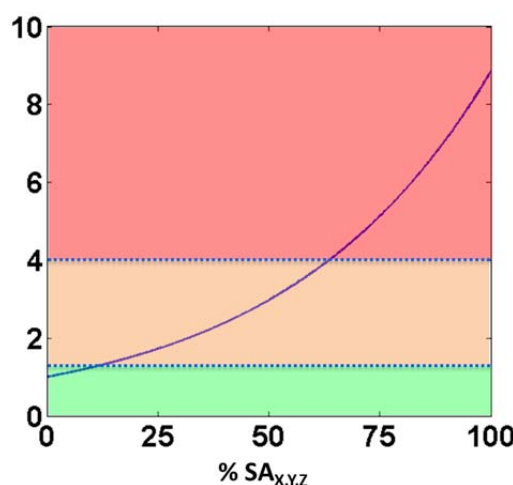


Figure 135 Exponential law for straight line synergy

Table 54 Manipulation active surprise levels

<b>Manipulation Active Surprise Level</b>	
<b>Low</b>	0 - 1,7
<b>Medium</b>	1,7 - 4
<b>High</b>	> 4

The generation of the surprise event has been implemented thanks to a FIS module that comprises the scheme from Figure 132. When the object is launched, the prediction about the components of the vector  $\vec{HO}_{GOAL}$  is formed thanks to visual exoception and arm proprioception. These components correspond to the orthogonal distance between hand and object. Thus, in the same way than passive surprise, the active surprise event will depend on the value of the distance. The prediction remains valid during task performance unless the object trajectory will be disturbed. In this case, the prediction could be updated or inhibited.

Then, the surprise event, based on predicted goal position where the thrown object should be caught, is generated by inference. Based on the synergy available, the FIS module has been trained to generate surprise by means of inferring the output from the evaluation of several trajectory waypoints. The more waypoints can be used the best the prediction will be but, for simplicity, it has been selected only two waypoints: the starting point, obtained by proprioception, and one flight waypoint, measured by exoception. Figure 136 represents some of the resulting inference surfaces in which the input dataset ( $X_{RH}$ ,  $X_{WP}$ ,  $Y_{WP}$ ) are evaluated.

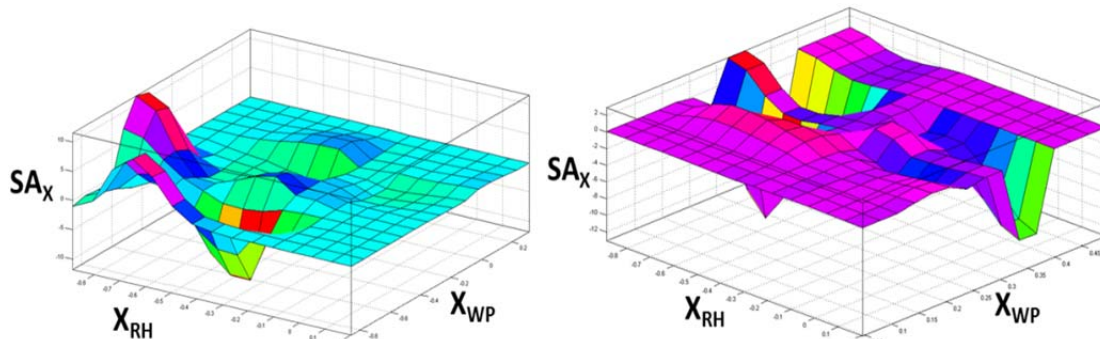


Figure 136 Manipulation active surprise inference surface

The evaluation of the FIS module developed to elicit manipulation active surprise has been performed by means of acquiring the input dataset from different ball thrown trials. The results of this inference process are shown in Table 55. It can be observed that the bigger is the coordinate increment, the higher is the surprise. It means that the object will follow a longer flight trajectory and the predicted goal location will be far from the actual hand position. The maximum height reached by the object is determined by the  $X_{WP}$  coordinate. This value joined with the increment of the  $X$  coordinate denotes the range of the shot but, as well, the flight trajectory duration.

Table 55 Manipulation active surprise evaluation

Trial	X <sub>Hand</sub>	Y <sub>WP</sub>	X <sub>WP</sub>	SA <sub>x</sub>	Surprise Elicited
1	0,077	0,167	0,225	0,1	Low
2	0,141	0,165	0,093	0,2	Low
3	-0,277	-0,216	0,167	3,5	Medium
4	-0,740	-0,594	0,245	8,6	High

In conclusion, this active surprise module helps to decide reaction triggering thanks to predictions. It is no necessary a high accuracy of the prediction because the goal of this estimation is the activation and parameterization of a movement pattern to accomplish the manipulation task. Therefore, this mechanism will be the first one to be involved in the reaction process.

#### 7.2.3.2.2 Locomotion Tasks

The performance success of a locomotion task depends mainly on the evaluation of the balance during all walking process. Therefore, the prediction of future balance evolution can be very useful to avoid possible balance lost. Due to the fast dynamics of the locomotion tasks, the prediction about future should be achieved as fast and precise as possible. This prediction is based on the use of well-known reference point like the Zero Moment Point which constitutes a good indicator of the robot balance.

The robot has two ways of ZMP measurement. The first one based on force/torque sensors computes the actual location of this point by means of the measurement of the reaction forces. The second one can be performed using the information coming from the Inertial Measurement Unit regarding dynamics of movement. Meanwhile the first source gives the actual ZMP location the second source can be used to predict the evolution ZMP, within a prediction horizon in which environmental conditions are considered invariables. The computation of the perceptual sources outputs the input dataset for the FIS regarding ZMP (Figure 137).

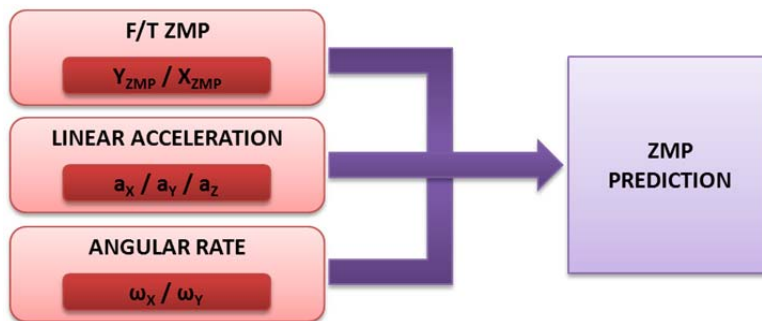


Figure 137 Locomotion active surprise inference system ZMP input dataset

As well, balance control is based on the knowledge of the ZMP position respecting the support base convex hull. Therefore, the prediction must be related as well with the computation of this convex hull. Its relation with the ZMP has been denoted by means of the determination of one point through which the ZMP could go outside the support

base. The so called Leak Point (LP) will be the means through which surprise is related with the actual and the future ZMP location. The result of the computation of the LP constitutes another input for the FIS module (Figure 138).

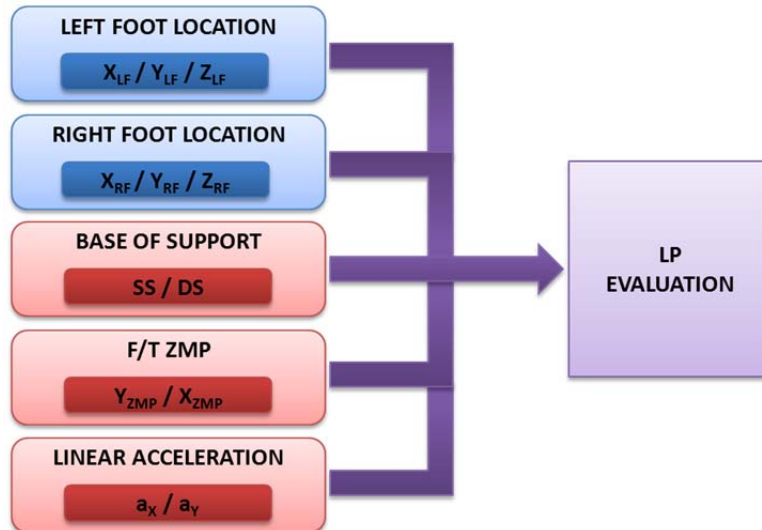


Figure 138 Locomotion active surprise inference system LP input dataset

Then, the inference system developed to produce the locomotion active surprise event is based on the determination of a couple distance relations (Figure 139): LP- Actual ZMP and LP-Future ZMP.

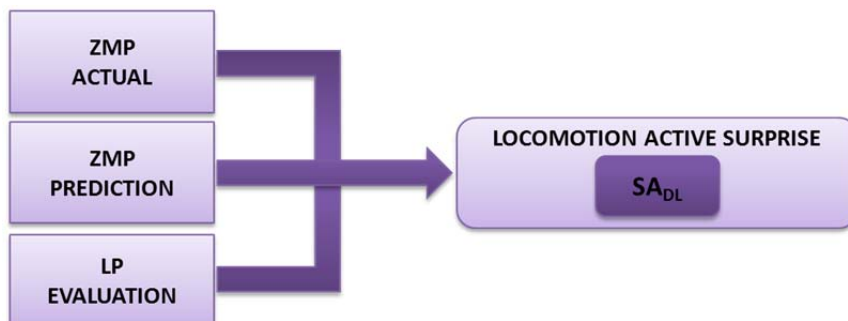


Figure 139 Locomotion active surprise inference system scheme

Figure 140 shows the means used to perform the surprise event computation during the double support phase. This evaluation has been performed considering the following constraints:

- 1) The prediction has been performed over the Virtual Horizontal Plane (VHP) defined in Section 6.3.4.2. It enables to perform the prediction in any kind of terrain independently of its irregularities.
- 2) Feet angles can be used for adjusting the footprint shape. This has been simplified considering always circular footprints for each foot on the ground.
- 3) The future ZMP locations are predicted taking in account the pre-established latencies from Section 6.3.4.2.

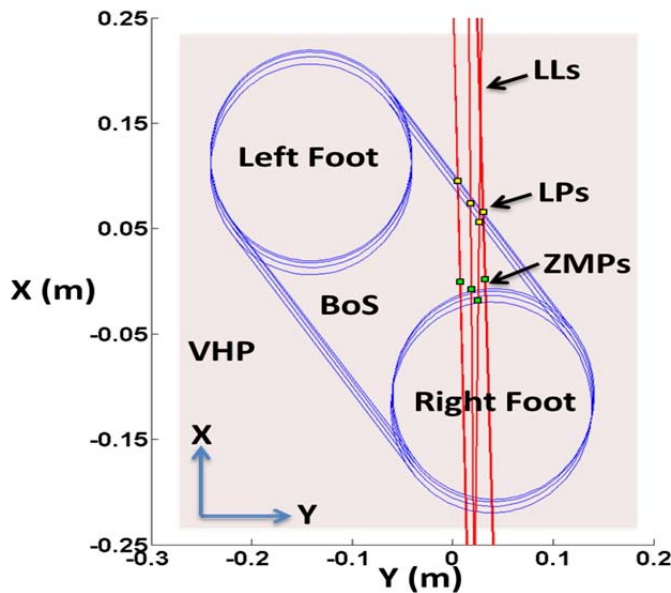


Figure 140 BoS on VHP for double support phase

The surprise event has been graded linearly taking in account predicted ZMP evolution. In this case, the neither task is driven by surprise nor the reaction does and, hence, the surprise event doesn't depend on the mechanical characteristics of the available synergies. Figure 141 shows the linear function for locomotion active surprise generation. The minimum value has been established in two situations: when the distance LP-future ZMP is long or when the ZMP is outside the BoS. In the second case, robot balance cannot be ensured and it will depend on dynamical conditions. As well, Table 56 exposes the graded values for predicted ZMP evolution

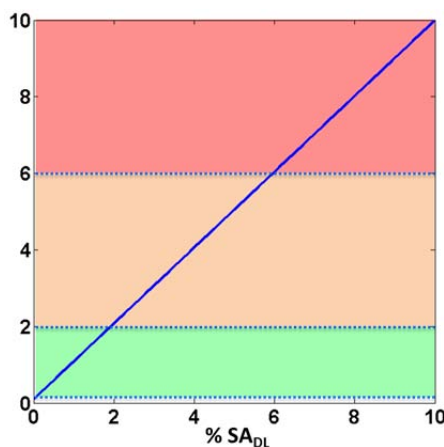


Figure 141 Linear law for locomotion synergies

Table 56 Manipulation active surprise levels

Locomotion Active Surprise Level	
Low	0 - 2
Medium	2 - 6
High	> 6

Based on the foundations explained until now, the development of the surprise module consisted of training the fuzzy inference system that maps the input from stability indicators with the surprise output. Figure 142 presents some of the inference surface that performs this mapping. Each one of these inference surfaces outputs one component of the final surprise value.

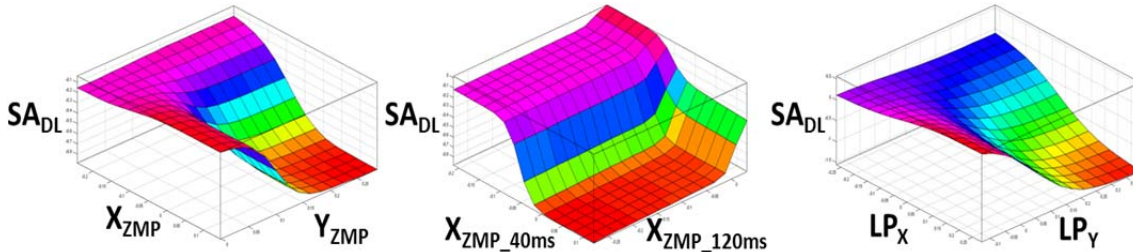


Figure 142 Locomotion surprise inference surfaces

Once the FIS development was concluded, its performance was evaluated with data extracted from the steps of the performed by the robot. Specifically, Table 57 exposes data from a right step which follows the sequence of support phases: DS1-SSL-DS2. At the very beginning of the movement (DS1), the acceleration produced leads a prediction of an unstable ZMP future location and the surprise elicited reaches a medium level ( $SA_{DL}=2,7$ ). In the single support phase with the left foot (SSL), the level of surprise is low but equal to zero. It means that ZMP is outside the BoS. This situation is not necessarily unstable because dynamical conditions domains the balance status. In this case, the ZMP location meets the definition of the Fictitious ZMP (FZMP). The last phase (DS2) is a double support situation with the right foot moved forward the left foot. In this case, ZMP is inside the BoS and the CoM deceleration leads a change on the ZMP movement tendency, producing a low surprise level.

Table 57 Locomotion active surprise evaluation

Phase	$X_{ZMP}$	$Y_{ZMP}$	$X_{ZMP}$ (40ms)	$Y_{ZMP}$ (40ms)	$X_{ZMP}$ (120ms)	$Y_{ZMP}$ (120ms)	$X_{LP}$	$Y_{LP}$	$SA_{DL}$
<b>DS1</b>	0,002	0,032	-0,01	0,0326	-0,012	0,033	0,06	0,03	Med.
<b>SS_L</b>	0,01	0,218	0,001	0,22	-0,018	0,225	0	0	Low
<b>DS2</b>	0,15	0,07	0,113	-0,104	-0,019	-0,366	0,40	-0,3	Low

In summary, the surprise events elicited by this predictive system can help to select the best strategy to anticipate motor reactions against possible balance loss.

## 7.2.4 Decision System Development

The last module integrating the human inspired TEO postural control architecture is the surprise driven decision system. This module is in charge of surprise events analysis and the generation of a reactive action or a recommendation for producing higher level reactions.

Because the output of this postural control system is produced in anticipation to the consequences, it will be necessary to track the evolution of the prediction. As well, the decision is highly influenced by the task because, for instance, the level of alert necessary for running is higher than the same level for walking.

Therefore, the development of this module follows the same structure of the previous subsystems of the postural control architecture. The decision system has been divided as well into manipulative and locomotive parts depending on each kind of task. Each one is composed by an inference system developed by means of the neuro-fuzzy bio-inspired technique. The inputs of the decision system will be the surprise events that will be weighted depending on:

- 1) The goal of the task. A surprise driven task (i.e. catch the ball) needs the highest levels of intervention of the developed postural control system for achieving the task and its goal can be anticipated.
- 2) The dynamics of the task. The faster one task is carried out the higher should be the alert level, giving more importance to the final decision.
- 3) The consequences of actions producing surprise events. Sometimes, it is necessary to give more importance to lesser surprise events than others because the sensorial information producing them informs about some adverse effect against correct task achievement.
- 4) The level of anticipation required. For instance, the robot body integrity can be put at risk during task performance whether a fast reaction is not deployed when some perturbation is detected. In this case, it should be necessary higher level of anticipation than in other kind of tasks.

Taking in account all these premises, the decision system has been developed for the manipulation and locomotion tasks proposed in this Thesis. Following this development is described.

#### **7.2.4.1 Manipulation Tasks**

The manipulation tasks decision module developed in Chapter 6 presented the evaluation of surprises as a sequential process, which output is a numeric parameter used to fulfil the reactive movement pattern.

This decision system evaluates the surprise inputs and generates an output according to the combination of the surprise values ( $K_{MR}$ ). The basic scheme representing this I/O relation is exposed in Figure 143.

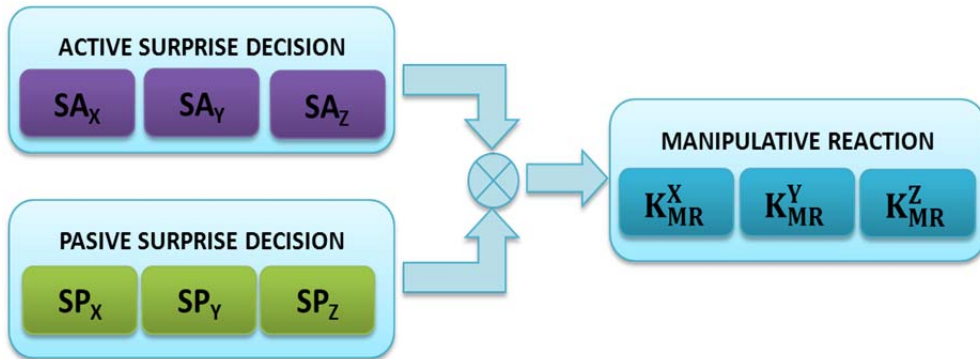


Figure 143 I/O Scheme for manipulative reaction generation

According to Figure 98 from Section 6.4.1, the sequential process to produce the decision parameter is a combination of the values from each kind of surprise. This combination as well depends on the surprise ‘intensity’.

The whole range for each surprise has been divided in sub-groups of low, medium or high ‘intensities’. Table 58 exposes the combination of surprise intensities (Low/Medium/High) with the ranges of aggregated surprise values.

These ranges of decision parameters were obtained by multiplication of the active and passive surprise values exposed in Section 7.2.3. It can be observed that there exists an overlapping among decision ranges. The value selected for the decision output parameter will be the corresponding to the highest active surprise level.

Table 58 Manipulative decision output chart

Active Surprise	Passive Surprise	Decision Output Parameter ( $K_{MR}$ )				
		Low	Medium	High	Low	Medium
Low	Low	0	0,4			
	Medium	0		0,8		
	High	0			2	
Medium	Low		0,4	0,94		
	Medium			0,8	1,88	
	High				2	4,70
High	----				4	10

The process flow exposed in Figure 98 has been modelled by a neuro-fuzzy inference system that evaluates the surprise inputs and generates the parameter to fulfil the corresponding synergy. Representing the modules developed, Figure 144 presents one inference surface for obtaining the decision parameters  $K_{MR}^X$  and  $K_{MR}^Y$ . These parameters can be used to create a complete movement sequence from the synergies X\_MOVE and Y\_MOVE established (see Figure 99).

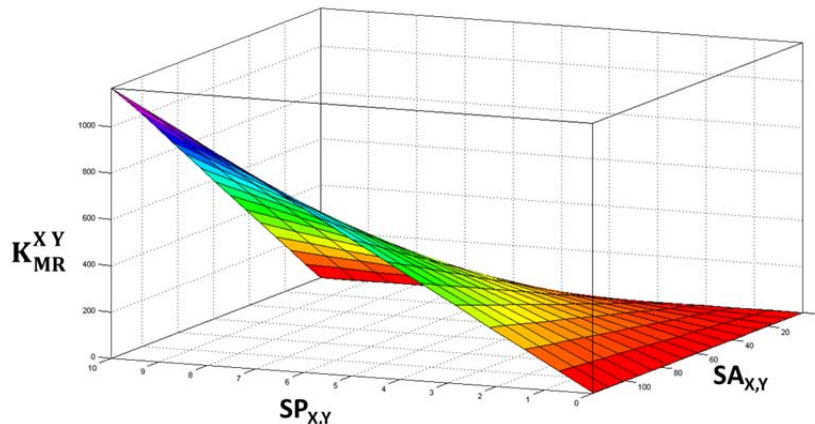


Figure 144 Inference surface for manipulative decision parameters  $K_{MR}^X$  and  $K_{MR}^Y$

Once the inference systems were obtained, they were checked using the input from the trials performed during surprise systems evaluation. Figure 145 exposes the results of the decision evaluation for three of those trajectories. Trajectory  $T_1$  is a vertical trajectory which both active and passive surprise levels remain at zero level.

$T_2$  trajectory corresponds to a trial in which the active surprise has a medium level. In this case, the initial surprise level determines an initial value of the decision parameter equal to the surprise intensity ( $K_{MR}^X = 1,84$ ). If no reaction is triggered and the hand keeps its initial location, the decision parameter changes depending on the passive surprise level detected (Figure 145 right). This evaluation process is performed until the task stops when the ball falls down the hand height.

The last trajectory ( $T_3$ ) corresponds to a ball shot in which the goal location is predicted outside the manipulation range. Then, it is generated a high active surprise event. The initial value is also equal to the active surprise intensity ( $K_{MR}^X = 6,87$ ). It can be observed saturation in the top level of the decision parameter graph because of the saturation of the passive surprise level (Figure 145 right).

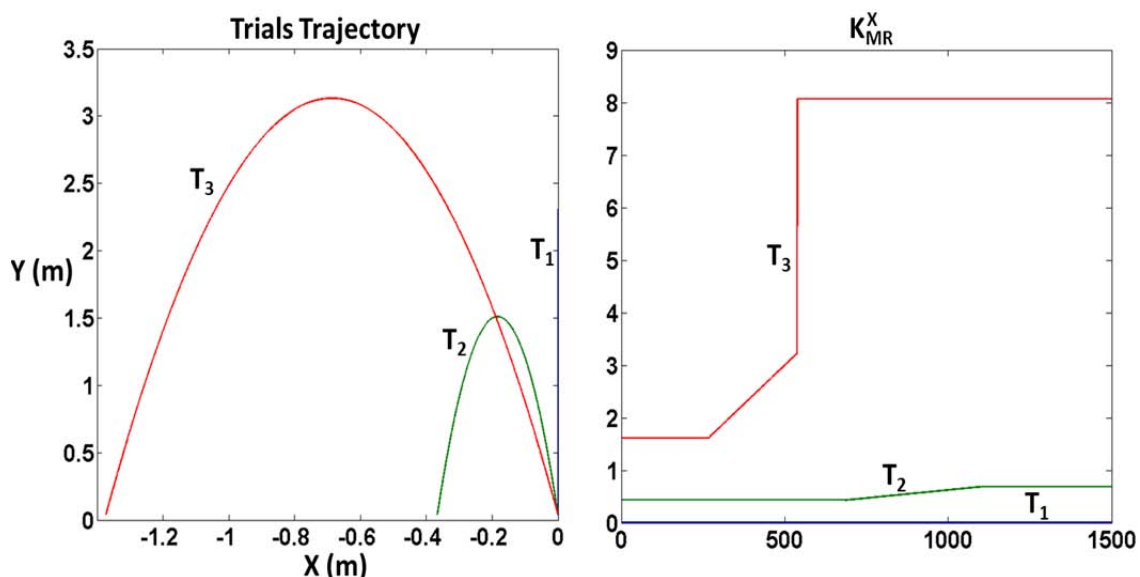


Figure 145 Trials trajectory and decision parameter (X coordinate component)

Then, the numeric values of  $K_{MR}^X$  can be used to perform a proportional reaction movement through the activation of the X\_MOVE synergy.

### 7.2.4.2 Locomotion Tasks

The locomotion tasks decision module exposed in Chapter 6 has one important difference from the one presented for manipulation tasks. The process exposed only finishes when the task is over but not when some kind of surprise is elicited. This difference is determined by the surprise driven nature of the execution of the proposed manipulation task. This locomotion decision system is composed by two modules working in parallel to evaluate sagittal and frontal plane surprise. Nevertheless, both processes have the active surprise value in common. The output of the decision making system is a numeric value ( $K_{LR}$ ) used to fulfil the locomotion synergies established as anticipative motor responses. The inputs and the outputs scheme of this module is represented in Figure 146.

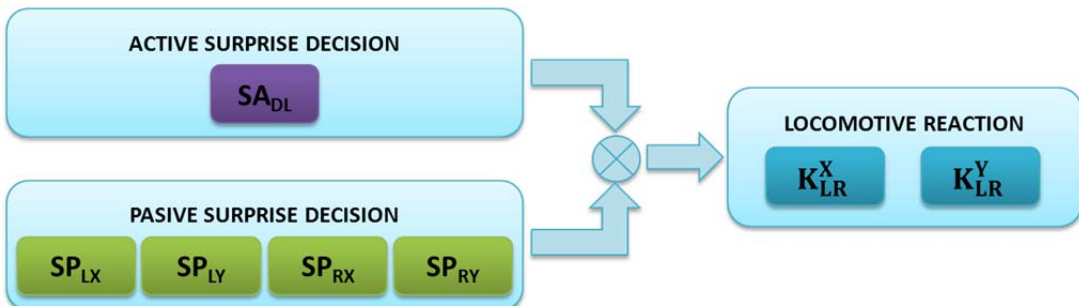


Figure 146 I/O Scheme for locomotive reaction generation

Following the same philosophy than the manipulative decision case, the output of this module is the combination of the passive surprise level with the active surprise intensity. Due to the existence of two different kinds of passive surprise, the decision process uses the maximum value obtained after their comparison. Table 59 presents the decision ranges for the sagittal plane, according to surprise levels and the process flow established.

Table 59 Locomotive decision output chart (X coordinate)

	Passive Surprise	Active Surprise	Decision Output Parameter ( $K_{LR}$ )			
SP <sub>LX</sub>	Low	ANY	0	1,8		
	Medium			1,8	15,2	
	High				15,2	43,8
SP <sub>RX</sub>	Low	ANY	0	2		
	Medium			2	23,5	
	High				23,5	98,1

As well, Table 60 exposes the same kind of chart than previous one but it considers the frontal plane movement. These ranges of decision parameters were obtained by multiplication of the active and passive surprise values exposed in Section 7.2.3. It can

be observed that values influenced by linear movement tendency ( $SP_L$ ) produces higher decision output values. It is produced because the linear acceleration has usually more influence in balance loss and ZMP computations.

Table 60 Locomotive decision output chart (Y coordinate)

Passive Surprise		Active Surprise	Decision Output Parameter ( $K_{LR}$ )			
$SP_{LY}$	Low	ANY	0	2,1		
	Medium			2,1	17,5	
	High				17,5	52,5
$SP_{RY}$	Low	ANY	0	0,6		
	Medium			0,6	7,3	
	High				7,3	30,3

Then, the neuro-fuzzy system designed for locomotion decision making processes all the locomotive surprise inputs and produces a decision parameter  $K_{LR}$  according to the charts exposed in Table 59 and Table 60. The inference surfaces presented in Figure 147 represents the evaluation of surprise events for the sagittal plane (X coordinate). The decision parameters produced fulfil the movement patterns established depending on the current locomotive task (see Figure 101).

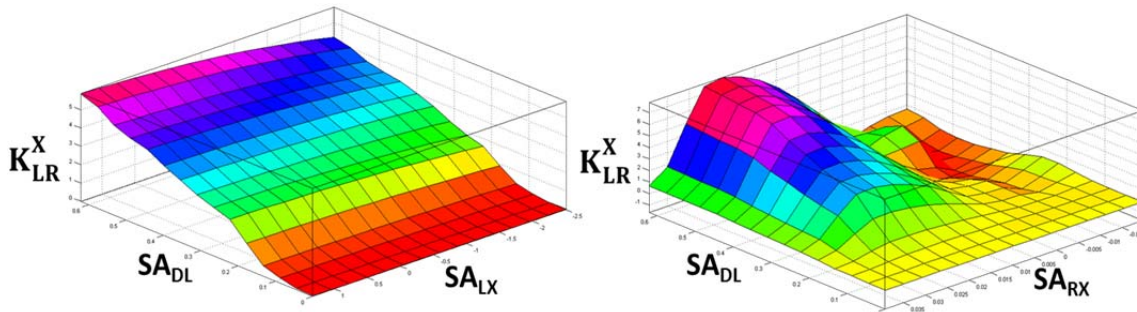


Figure 147 Inference surface for locomotive decision parameters  $K_{LR}^X$

The trained inference systems have been tested with the data obtained from the locomotion trials performed during the development. Figure 148 presents the results obtained during the performance of one right foot step. This task consists of moving forward the right foot from a double support phase and ending with the right foot in an advanced position respecting the left foot. Figure 148 left represents the absolute values of the inputs for the neuro-fuzzy decision system. It can be observed the highest levels of predictive surprise are produced when the robot changes from double support to single support phase. This value of surprise leads the medium value decision parameter ( $K_{MR}^X = 7,12$ ), according to Table 59.

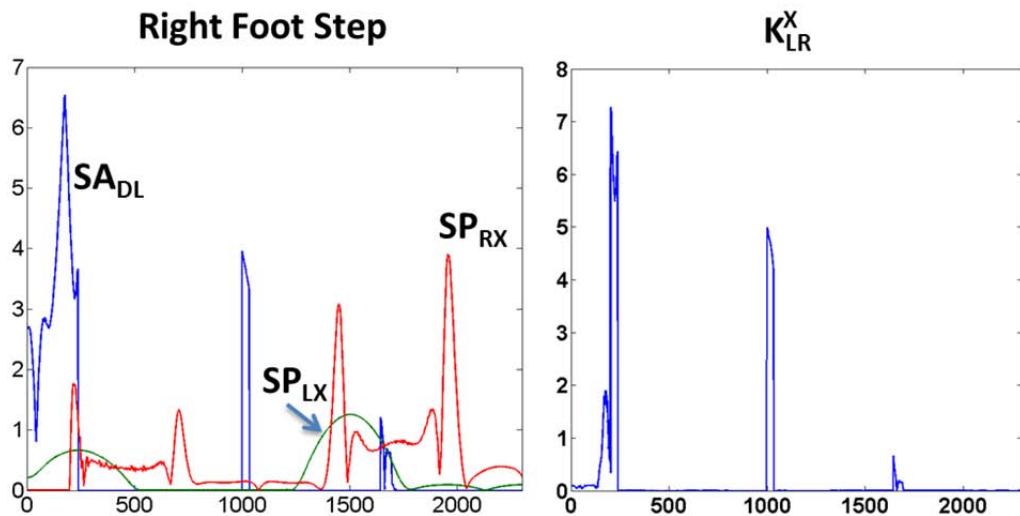


Figure 148 Step surprise levels (left) and decision parameter (right)

Depending on the task conditions, the decision value can lead the selection and execution of a movement pattern to keep posture and balance under control.





## CHAPTER 8

# Conclusions and Future Works

## 8.1 Conclusions

This PhD Thesis has been motivated by one of the most challenging of the humanoid robotics field: the human behaviour mimicked by humanoid robots. Because of this, the development of this Thesis has been performed trying to not forget three main premises:

- As the whole postural architecture as each one of its parts should be developed using human inspired principles.
- The architecture and its components should operate according to the human systems that accomplish the same function.
- The robot behaviour should be inspired in human behaviour. That is, the development should be task oriented and human tasks should be extrapolated to humanoid tasks that TEO humanoid robot could perform.

Taking in account these premises, a group of general conclusions can be extracted from the overall work carried out. These conclusions are:

- There has been performed a top-down study of the human postural control system. This study has stated the existence of two main subsystems integrating the high level control architecture with different modus operandi: reactive and anticipative. The study has concluded with the description of the features and functions of all subsystems and organs involved in the human postural control architecture operation.
- It has been established a novel humanoid postural control architecture based on the human case studied. Because there was pre-existing reactive balance control architecture for TEO humanoid robot, the development of this PhD Thesis has been centred in the anticipative subsystem integration, following the human inspiration's premise.
- To enable the human inspired architecture, it has been also studied each one of the artificial systems available in the humanoid robot TEO with the aim of comparing its features with the human systems performing the same function.

- The novel humanoid postural control architecture and subsystems have been developed applying state-of-the-art bio-inspired soft computing techniques and according to the premise of task orientation. After development completion, all components have been proved in simulated environments and, as well, validated performing different test with the full size humanoid robot TEO.

All these accomplished goals fit with the general guidelines proposed at the beginning of this work. As well, each general goal has been supported by the achievement of wide variety of sub-objectives which have been introduced along the process of development. They have been established and described mainly inside the specific sections related to them. Therefore, there are a series of specific conclusions that can be extracted from the development carried out.

The operation of the postural control system proposed has been inspired in the anticipative system identified in the human case. The anticipative postural action starts with the evaluation of any kind of disturbance that could put at risk the correct task performance.

Therefore, the first stage of postural control is the detection of stimuli from diverse external or internal sources. The result obtained from each sensor device is a set of raw information. Each set of data is not useful independently and it must be processed to compose appropriate input information for the postural control system. These processed sets are called perceptions and they are classified depending on the origin of the stimuli in proprioception (physical self-consciousness) and exoception (environmental consciousness).

There has been studied all sensorial sources, the effects they produce, and the devices that captures each stimulus. Then, each perception has been developed by means of the application of the bio-inspired neuro-fuzzy methodology. The perception systems deal with a huge amount of imprecise sensorial information to produce a well-defined and complex perceptual output. The capacity of performing this function as well as the ability to model each perceptual subsystem after a training process using sensed data has favoured the use of the neuro-fuzzy method. The resulting perceptions developed depend on many parameters: the task being performed, the level and nature of disturbances, the systems in which the sensations are processed, and the motor response required. This number of parameters influencing the perception generation shows its complexity.

The second stage carried out by the postural control system is the evaluation of the complex perceptions generated. Perceptual outputs provide information to the control system about the perturbations detected. But perceptions don't give information about the consequences each sensed disturbance can provoke. Due to this, it has been developed an evaluation system that analyses perceptual inputs and relates them with their possible effects over robot posture. This evaluation process has been based on psychophysical principles and, specifically, in the 'Theory of the Surprise'. A surprise event is elicited when the intensity or duration of a perturbation, characterized by the outputs from perceptions, reaches some pre-established limit. The evaluation of perceptual outputs is carried out by bio-inspired neuro-fuzzy systems that interpret

perceptions and output a graded surprise. In this way, this human inspired methodology mimics the human behaviour processing unexpected events.

The last stage achieved during the development of this Thesis is the establishment of a surprise driven decision system. The graded surprise events are evaluated to take a decision about the execution of postural corrections to keep the task inside its performance limits. These corrections or reactions are based on the fulfilment of movement patterns called synergies. The parameters used to fill in each pattern are usually proportional to the grade of the surprise event and the resulting motor response can be considered similar to the reflex and automatic human reactions. All these motor responses can be anticipated thanks to a predictive component enabled and introduced by the surprise generation.

The performance modules developed in the exposed stages have been tested and some conclusions have been obtained:

- 1) The use of neuro-fuzzy technique speeds the development process up considerably. The use of accurate data for system training enables it.
- 2) The complex sensorial data analysis can be performed in the same way than the process carried out by the human Central Nervous System. The use of neuro-fuzzy modules reduces the latency of the evaluation, simplifies the operation, and performs in parallel the same operations carried out by classical sequential processes.
- 3) The error committed by the neuro-fuzzy modules can be correlated with the errors committed by humans during task performance. As in the human case, these errors can be reduced by training and experience.
- 4) The application of a determinate kind of surprise events, whose generation is based on predictions, governs the anticipatory nature of the postural control system developed.

The integration of each developed module fashions the novel TEO human inspired postural control system.

## 8.2 Future Works

The development carried out in this PhD Thesis has been concluded with the establishment of the novel TEO postural control architecture. But some minor issues have still pending and other questions have aroused during the development process.

The novel TEO postural control architecture development has been supported by the comparison performed between human and humanoid. It has been tried to apply directly the results extracted from the study of the human capabilities study but, as it was expected, these results must be adapted because of inherent TEO robot constraints. These limitations are not related to the performance of each individual device but the required output to accomplish with the same function than human systems.

Talking about hardware systems, the compositions of perceptions will gain the advantage of the integration of the neuro-fuzzy processing capabilities inside the own device. Then, the robot CPUs could be freed of perceptual composition.

Other important constraint of the robot is related to one of the basic principles of this PhD Thesis: the task orientation. Actuation systems based on rigid transmission with rotary motors limits the number of DoF and, therefore, the flexibility of the robot for task achievement. This issue joint with other mechanical limitations limits mostly the set of task the robot can perform. The use of linear actuator, more similar to human muscles regarding operation, could avoid some of these mechanical constraints (structural angular limits, etc.). As well, the integration of compliant actuators is recommended because they also can absorb perturbations, improving the postural control system operation.

These hardware improvements could lead the design of a humanoid robot with extended capabilities and enabling a better human inspired hardware design.

Regarding the software developed improvement, the future works can be oriented in two different ways. The first one is related to the design neuro-fuzzy modules and, the second one is related to the improvement of the system.

The design of each inference module has been oriented to the integration of its function in only one system neuro-fuzzy. This issue simplifies the overall system design but, as well, it has some disadvantages:

- 1) The number of inputs increases with the number of functions integrated in the inference system. The division of complex neuro-fuzzy evaluation system into smaller units would enable a better comprehension its operation. As well, this fragmentation could give a better understanding of the structure of the modelled system, which the system is inspired in.
- 2) The less is the number of system inputs the fastest is the training process. The design of neuro-fuzzy system with a low number of inputs speed up the tuning process, even increasing the number of member functions that evaluates the system inputs.
- 3) The error committed is reduced because of two reasons. The design of small inference systems allows a better understanding of the training data and this issue usually increases the accuracy of the datasets, which leads the error minimization.

Then, it would be possible to increase the overall system performance by designing multilayer inference modules in those with multiple inputs. Furthermore, this suggested multilayer structure is more similar to the human neural processing structures.

The second future work proposed is the implementation of online tuning for the neuro-fuzzy inference modules. The development of the neuro-fuzzy systems carried out in this PhD Thesis was supported by data acquired from TEO robot during a limited number of trials. The modelling capacity of the neuro-fuzzy methodology is not based on the amount of information but on its variance. The richest and different is the data

used in fuzzy training the best performance can be obtained. But, to get this kind of datasets depends on performing a great number of task from which data can be extracted.

One way to avoid this huge work is the integration of an online training system. Once the basic system has been developed, the implementation of online tuning algorithms would improve each neuro-fuzzy system performance.



## REFERENCES

- Agid, Y. (1990). From posture to initiation of movement. *Revue Neurologique*, 146(10), 536-542. Retrieved from <http://www.ncbi.nlm.nih.gov/pubmed/2263815>
- Alexandrov, A., Frolov, A., & Massion, J. (1998). Axial synergies during human upper trunk bending. *Experimental Brain Research*, 118(2), 210-220. Retrieved from <http://www.ncbi.nlm.nih.gov/pubmed/9547090>
- Allum, J. H., Bloem, B. R., Carpenter, M. G., Hulliger, M., & Hadders-Algra, M. (1998). Proprioceptive control of posture: a review of new concepts. *Gait & Posture*, 8(3), 214-242. Elsevier. doi:10.1016/S0966-6362(98)00027-7
- Allum, J. H., & Honegger, F. (1993). Synergies and strategies underlying normal and vestibular deficient control of balance: implication for neuroprosthetic control. *Progress in Brain Research*, 97, 331-348. Retrieved from <http://www.sciencedirect.com/science/article/pii/S0079612308622931>
- Allum, J. H. J., Bloem, B. R., Carpenter, M. G., Hulliger, M., & Hadders-Algra, M. (1998). Proprioceptive control of posture: a review of new concepts. *Gait & Posture*, 8(3), 214-242. doi:DOI: 10.1016/S0966-6362(98)00027-7
- Ambrose, R., & Ambrose, C. (2004). Primate anatomy, kinematics and the principles for humanoid design. *International Journal of Humanoid Robotics*, 1(1), 175–198. doi:10.1142/S0219843604000101
- Angelaki, D E, & Cullen, K. E. (2008). Vestibular System : The Many Facets of a Multimodal Sense. *Annual Review of Neuroscience*, 31(1), 125-150. doi:10.1146/annurev.neuro.31.060407.125555
- Angelaki, D E, McHenry, M. Q., Dickman, J. D., Newlands, S. D., & Hess, B. J. (1999). Computation of inertial motion: neural strategies to resolve ambiguous otolith information. *Journal of Neuroscience*, 19(1), 316-327. SOC NEUROSCIENCE. Retrieved from <http://www.ncbi.nlm.nih.gov/pubmed/9870961>
- Angelaki, Dora E, & Yakusheva, T. A. (2009). How vestibular neurons solve the tilt/translation ambiguity. Comparison of brainstem, cerebellum, and thalamus. *Annals Of The New York Academy Of Sciences*, 1164(Basic and Clinical Aspects of Vertigo and Dizziness), 19-28. doi:10.1111/j.1749-6632.2009.03939.x
- Anstis, S. . M. ., & Mackay, D. . M. . (1980). The Perception of Apparent Movement [ and Discussion ]. *Philosophical Transactions of the Royal Society of London*, 290(1038), 153-168. doi:10.1098/rstb.1980.0088
- Anstis, S., Verstraten, F. A., & Mather, G. (1998). The motion aftereffect. *Trends in Cognitive Sciences*, 2(3), 111-117. MIT Press. Retrieved from <http://linkinghub.elsevier.com/retrieve/pii/S1364661398011425>
- Arbib, M. A. (1987). *Brains, Machines and Mathematics* (Second., p. 202). New York, NY, USA: Springer.

- Arbulu, M., & Balaguer, C. (2010). Real-time gait planning for Rh-1 humanoid robot, using Local Axis Gait algorithm. In B. Miripour (Ed.), *Climbing and Walking Robots* (Vol. 6, pp. 445-508). InTech. doi:10.5772/10422
- Arbulu, M., Kaynov, D., Cabas, L. M., & Balaguer, C. (2009). The Rh-1 full-size humanoid robot: design, walking pattern generation and control. *Journal of Applied Bionics and Biomechanics*, 6(3), 301-344. doi:10.1080/11762320903123575
- Arbulú, M. R. (2009). *Stable Locomotion of Humanoid Robots Based on Mass Concentrated Model*. Universidad Carlos III de Madrid. Retrieved from <http://hdl.handle.net/10016/5623>
- Asimov, I. (1942). Runaround. *Astounding Science Fiction*, 29, 94-103.
- Augustsson, P., & Wolff, K. (2002). Creation of a learning, flying robot by means of evolution. *Proceedings of the Genetic and Evolutionary Computation Conference (GECCO 02)* (pp. 1279-1285). New York, NY, USA: Morgan Kaufmann Publishers. Retrieved from <http://www.cs.bham.ac.uk/~wbl/biblio/gecco2002/ROB196.pdf>
- Aw, S. T., Haslwanter, T., Halmagyi, G. M., Curthoys, I. S., Yavor, R. A., & Todd, M. J. (1996). Three-dimensional vector analysis of the human vestibuloocular reflex in response to high-acceleration head rotations. I. Responses in normal subjects. *Journal of Neurophysiology*, 76(6), 4009-4020. Retrieved from <http://www.ncbi.nlm.nih.gov/pubmed/8985896>
- Aznar-Casanova, J. A., Quevedo, L., & Sinnett, S. (2005). The effects of drift and displacement motion on Dynamic Visual Acuity. *Psicológica: International Journal of Methodology and Experimental Psychology*, 26(1), 105-119. Retrieved from <http://www.uv.es/psicologica/articulos1.05/7-AZNAR.pdf>
- Baldi, P., & Itti, L. (2010). Of bits and wows: A Bayesian theory of surprise with applications to attention. *Neural Networks*, 23(5), 649-666. Elsevier Ltd. Retrieved from <http://www.ncbi.nlm.nih.gov/pubmed/20080025>
- Baloh, R. W., & Honrubia, V. (2001). Clinical neurophysiology of the vestibular system. *Brain: A journal of neurology*, 125(4), 924-926. New York, NY, USA: Oxford University Press. doi:10.1093/brain/awf074
- Bardy, B. G., Warren, W. H., & Kay, B. A. (1999). The role of central and peripheral vision in postural control during walking. *Perception And Psychophysics*, 61(7), 1356-1368. Springer. Retrieved from <http://www.ncbi.nlm.nih.gov/pubmed/10572464>
- Bardy, B., Oullier, O., Bootsma, R. J., & Stoffregen, T. A. (2002). Dynamics of human postural transitions. *Journal of Experimental Psychology: Human Perception and Performance*, 28(3), 499 -514. doi:10.1037//0096-1523.28.3.499
- Behnke, S. (2008). Humanoid Robots – From Fiction to Reality? *Künstliche Intelligenz, Heft*, 4(December), 5-9.

- Benson, A. J. (1990). Sensory functions and limitations of the vestibular system. In R. Warren & A. H. Wertheim (Eds.), *Perception and control of self motion* (pp. 145-170). Hillsdale: Lawrence Erlbaum Associates.
- Benson, A. J., Spencer, M. B., & Stott, J. R. (1986). Thresholds for the detection of the direction of whole-body, linear movement in the horizontal plane. *Aviation space and environmental medicine*, 57(11), 1088-1096.
- Berg, K. (1989). Measuring balance in the elderly: preliminary development of an instrument. *Physiotherapy Canada*, 41(6), 304-311. UT Press. doi:10.3138/ptc.41.6.304
- Bernstein, N. (1968). The co-ordination and regulation of movements. *Neuropsychologia*, 6(1), 96. Oxford: Pergamon Press. doi:10.1016/0028-3932(68)90043-2
- Berthoz, A., Lacour, M., Soechting, J. F., & Vidal, P. P. (1979). The role of vision in the control of posture during linear motion. In R. Granit & O. Pompeiano (Eds.), *Progress in Brain Research. Reflex Control of Posture And Movement* (Vol. Volume 50, pp. 197-209). Elsevier/North-Holland. doi:10.1016/S0079-6123(08)60820-1
- Beyer, H.-georg, & Schwefel, H.-paul. (2002). Evolution strategies. *Evolutionary Computation*, 1(1), 3-52. Springer. doi:10.1023/A:1015059928466
- Bodensteiner, J. B. (2008). The evaluation of the hypotonic infant. *Seminars in pediatric neurology*, 15(1), 10-20. doi:10.1016/j.spen.2008.01.003
- Bouisset, S., & Zattara, M. (1981). A sequence of postural movements precedes voluntary movement. *Neuroscience Letters*, 22(3), 263-270. doi:10.1016/0304-3940(81)90117-8
- Brandt, T., Paulus, W., & Straube, A. (1986). Vision and posture. In W. Bles & T. Brandt (Eds.), *Disorders of posture and gait* (pp. 157-175). Amsterdam: Elsevier.
- Brandão, M. L. (2004). *As bases biológicas do comportamento: introdução neurociência* (First., p. 224). São Paulo: Editora Pedagógica Universitária (EPU).
- Brenière, Y., & Dietrich, G. (1992). Heel-off perturbation during gait initiation: biomechanical analysis using triaxial accelerometry and a force plate. *Journal of Biomechanics*, 25(2), 121-127. Retrieved from <http://www.ncbi.nlm.nih.gov/pubmed/1733988>
- Brooks, R., Aryananda, L., Edsinger, A., Fitzpatrick, P., Kemp, C., Torres-Jara, E., Varshavskaya, P., et al. (2004). Sensing and manipulating built-for-human environments. *International Journal of Humanoid Robotics*, 1(1), 1-28. Citeseer. doi:10.1142/S0219843604000022
- Bruce, V., Green, P. R., & Georgeson, M. A. (2003). *Visual Perception: Physiology, Psychology and Ecology* (Fourth., Vol. 3, p. 496). London, UK: Psychology Press.

Buschmann, T., Lohmeier, S., & Ulbrich, H. (2009). Humanoid robot Lola: design and walking control. *Journal of physiology, Paris*, 103(3-5), 141-148. Elsevier Ltd. doi:10.1016/j.jphysparis.2009.07.008

Büttner, U., & Waespe, W. (1981). Vestibular nerve activity in the alert monkey during vestibular and optokinetic nystagmus. *Experimental Brain Research*, 41(3-4), 310-315. doi:10.1007/BF00238888

Capó-Aponte, J. E., Temme, L. A., Task, H. L., Pinkus, A. R., Kalich, M. E., Pantle, A. J., & Rash, C. E. (2009). Visual perception and cognitive performance. In C. E. Rash, M. B. Russo, T. R. Letowski, & E. T. Schmeisser (Eds.), *Helmet-Mounted Displays: Sensation, Perception and Cognitive Issues* (First., pp. 335-390). Fort Rucker, AL, USA: U.S. Army Aeromedical Research Laboratory.

Carinena, P., Regueiro, C. V., Otero, A., Bugarin, A. J., & Barro, S. (2004). Landmark detection in mobile robotics using fuzzy temporal rules. *IEEE Transactions on Fuzzy Systems*, 12(4), 423-435. doi:10.1109/TFUZZ.2004.832534

Carr, J. H., & Shepherd, R. B. (2000). *Movement Science: Foundations for physical therapy in rehabilitation* (Second., p. 220). Pro-Ed Incorporated.

Chatzis, S. P., Korkinof, D., & Demiris, Y. (2012). A nonparametric Bayesian approach toward robot learning by demonstration. *Robotics and Autonomous Systems*, 60(6), 789-802. doi:10.1016/j.robot.2012.02.005

Chen, C. H., Pau, L. F., & Wang, P. S. P. (2005). *Handbook of Pattern Recognition and Computer Vision*. (C. H. Chen, L. F. Pau, & P. S. P. Wang, Eds.) *Signals* (Fourth., pp. 2-5). River Edge, NJ, USA: World Scientific. doi:10.1142/9789812775320

Ciaravella, G., Laschi, C., & Dario, P. (2006). Biomechanical modeling of semicircular canals for fabricating a biomimetic vestibular system. *Proceedings of the IEEE International Conference of Engineering in Medicine and Biology Society* (Vol. 1, pp. 1758-1761). New York, NY, USA: IEEE. doi:10.1109/IEMBS.2006.260248

Compaq, Hewlett-Packard, Intel, Lucent, Microsoft, NEC, & Philips. (2000). *Universal Serial Bus Specification*. Group (p. 650). Retrieved from <http://www.usb.org/developers/docs/>

Crenna, P., Frigo, C., Massion, J., & Pedotti, A. (1987). Forward and backward axial synergies in man. *Experimental Brain Research*, 65(3), 538-548. Springer. doi:10.1007/BF00235977

Day, B. L., Steiger, M. J., Thompson, P. D., & Marsden, C. D. (1993). Effect of vision and stance width on human body motion when standing: Implications for afferent control of lateral sway. *Journal of Physiology*, 469, 479-499. Retrieved from <http://www.ncbi.nlm.nih.gov/pmc/articles/PMC1143881/?tool=pubmed>

De Jong, K., Fogel, D. B., & Schwefel, H.-P. (1997). A history of evolutionary computation. In T. Bäck, D. B. Fogel, & Z. Michalewicz (Eds.), *Handbook of Evolutionary Computation*, (pp. 28-39). New York, NY, USA: Oxford University Press.

DeHart, R. L., & Davis, J. R. (2002). *Fundamentals of aerospace medicine* (Third., p. 720). New York, NY, USA: Lippincott Williams & Wilkins.

- Dekker, M. H. P. (2009). *Zero-moment point method for stable biped walking.* matetuenl (p. 62). Eindhoven. Retrieved from <http://www.mate.tue.nl/mate/pdfs/10796.pdf>
- Delaney, J. D. (1998). *The Human Balance Control System: A Therapeutic Aid and Mathematical Control Model. Construction.* University College Dublin.
- Dey, A. K. (2001). Understanding and using context. *Personal and Ubiquitous Computing*, 5(1), 4-7. Springer-Verlag. doi:10.1007/s007790170019
- Dichgans, J., Mauritz, K. H., Allum, J. H., & Brandt, T. (1976). Postural sway in normals and atactic patients: analysis of the stabilising and destabilizing effects of vision. *Agressologie: Revue internationale de physiobiologie et de pharmacologie appliquées aux effets de l'agression*, 17, 15-24.
- Diener, H. C., Dichgans, J., Bacher, M., & Guschlbauer, B. (1984). Characteristic alterations of long-loop "reflexes" in patients with Friedreich's disease and late atrophy of the cerebellar anterior lobe. *Journal of Neurology, Neurosurgery & Psychiatry*, 47(7), 679-685. Retrieved from <http://www.ncbi.nlm.nih.gov/pmc/articles/PMC1027894>
- Diener, H. C., Dichgans, J., Bruzek, W., & Selinka, H. (1982). Stabilization of human posture during induced oscillations of the body. *Experimental Brain Research*, 45(1-2), 126-132. doi:10.1007/BF00235771
- Dijkstra, T. M., Schöner, G., & Gielen, C. C. (1994). Temporal stability of the action-perception cycle for postural control in a moving visual environment. *Experimental Brain Research*, 97(3), 477-486. doi:10.1007/BF00241542
- Dozier, G. (2001). Evolving robot behavior via interactive evolutionary computation: From real-world to simulation. *Proceedings of the 2001 ACM symposium on Applied computing* (pp. 340-344). New York, NY, USA: ACM. doi:10.1145/372202.372359
- Drung, D., Assmann, C., Beyer, J., Kirste, A., Peters, M., Ruede, F., & Schurig, T. (2007). Highly sensitive and easy-to-use SQUID sensors. *IEEE Transactions on Applied Superconductivity*, 17(2), 699-704. IEEE. doi:10.1109/TASC.2007.897403
- Dubuc, B. (2011). The brain from top to bottom. Retrieved September 3, 2011, from <http://thebrain.mcgill.ca/avance.php>
- D'Avella, A., Fernandez, L., Portone, A., & Lacquaniti, F. (2008). Modulation of phasic and tonic muscle synergies with reaching direction and speed. *Journal of Neurophysiology*, 100(3), 1433-54. doi:10.1152/jn.01377.2007
- Eaton, D., & Murphy, K. (2007). Bayesian structure learning using dynamic programming and MCMC. In R. Parr & L. Van der Gaag (Eds.), *Proceedings of the Twenty-Third Conference on Uncertainty in Artificial Intelligence* (pp. 1-8). Vancouver, BC, Canada: AUAI Press. Retrieved from <http://www.cs.ubc.ca/~murphyk/Papers/eaton-uai07.pdf>
- Eaton, M. (2008). Evolving humanoids : Using artificial evolution as an aid in the design of humanoid robots. In H. Iba (Ed.), *Frontiers in Evolutionary Robotics* (pp. 127-138). InTech. Retrieved from

[http://www.intechopen.com/articles/show/title/evolving\\_humanoids\\_\\_using\\_artificial\\_evolution\\_as\\_an\\_aid\\_in\\_the\\_design\\_of\\_humanoid\\_robots](http://www.intechopen.com/articles/show/title/evolving_humanoids__using_artificial_evolution_as_an_aid_in_the_design_of_humanoid_robots)

Echegoyen, C., Lozano, J. A., Santana, R., & Larranaga, P. (2007). Exact Bayesian network learning in estimation of distribution algorithms. *2007 IEEE Congress on Evolutionary Computation* (pp. 1051-1058). Singapore: IEEE. doi:10.1109/CEC.2007.4424586

Edwards, A. S. (1946). Body sway and vision. *Journal of Experimental Psychology*, 36(6), 526-535. doi:10.1037/h0059909

Ehrenstein, W. H., & Ehrenstein, A. (1966). Psychophysical methods. In M. Bass & H. Johansson (Eds.), *Modern techniques in neuroscience research* (Vol. III, pp. 1211-1241). McGraw-Hill. Retrieved from <http://www.psy.ulaval.ca/~isp/history/texts/PSYPHY-M.PDF>

Eiben, A. E., & Schoenauer, M. (2002). Introduction to evolutionary computing. *Information Processing Letters*, 82(1), 1-6. doi:10.1016/S0020-0190(02)00204-1

Ernst, M. O., & Banks, M. S. (2002). Humans integrate visual and haptic information in a statistically optimal fashion. *Nature*, 415(6870), 429-33. Nature Publishing Group. doi:10.1038/415429a

Fechner, G. T. (1858). Ueber ein wichtiges Psycho-physisches Grundgesetz und dessen Bezie-hung der Sterngrossen. *Abhandl K Ges Wissensch MathPhys Kl*, 4, 3-64.

Fernández, C., & Goldberg, J. M. (1976a). Physiology of peripheral neurons innervating otolith organs of the squirrel monkey. I. Response to static tilts and to long-duration centrifugal force. *Journal of Neurophysiology*, 39(5), 970-984. Retrieved from <http://www.ncbi.nlm.nih.gov/pubmed/824412>

Fernández, C., & Goldberg, J. M. (1976b). Physiology of peripheral neurons innervating otolith organs of the squirrel monkey. II. Directional selectivity and force-response relations. *Journal of Neurophysiology*, 39(5), 985-995. Retrieved from <http://www.ncbi.nlm.nih.gov/pubmed/824413>

Fetsch, C. R., Deangelis, G. C., & Angelaki, D. E. (2010). Visual-vestibular cue integration for heading perception: applications of optimal cue integration theory. *European Journal of Neuroscience*, 31(10), 1721-1729. Wiley Online Library. doi:10.1111/j.1460-9568.2010.07207.x

Fitts, P. M. (1954). The information capacity of the human motor system in controlling the amplitude of movement. *Journal of Experimental Psychology*, 47(6), 381-391. doi:10.1037/h0055392

Fujimoto, Y., & Kawamura, A. (1995). Three dimensional digital simulation and autonomous walking control for eight-axis biped robot. *Proceedings of 1995 IEEE International Conference on Robotics and Automation* (Vol. 3, pp. 2877-2884). Nagoya , Japan: IEEE. doi:10.1109/ROBOT.1995.525692

Fukuoka, Y., Tanaka, K., Ishida, A., & Minamitani, H. (1999). Characteristics of visual feedback in postural control during standing. *IEEE transactions on Rehabilitation*

Engineering., 7(4), 427-434. Retrieved from  
<http://www.ncbi.nlm.nih.gov/pubmed/10609630>

Fuller, R. (1995). *Neural fuzzy systems. Integration The Vlsi Journal* (Vol. 71, p. 253). Abo: Åbo akademi. Retrieved from <http://users.abo.fi/rfuller/ln1.pdf>

Fuller, R. (1999). Fuzzy logic and neural nets in intelligent systems. In C. Carlsson (Ed.), *Information Systems Day* (Vol. 17, pp. 74-94). Turku Centre for Computer Science. Retrieved from <http://users.abo.fi/rfuller/is97.pdf>

Gage, W. H., Winter, D. A., Frank, J. S., & Adkin, A. L. (2004). Kinematic and kinetic validity of the inverted pendulum model in quiet standing. *Gait & Posture*, 19(2), 124-132. Retrieved from <http://www.ncbi.nlm.nih.gov/pubmed/15013500>

Gentilucci, M., Toni, I., Chieffi, S., & Pavesi, G. (1994). The role of proprioception in the control of prehension movements: a kinematic study in a peripherally deafferented patient and in normal subjects. *Experimental Brain Research*, 99(3), 483-500. doi:10.1007/BF00228985

Gescheider, G. A. (1997). *Psychophysics: the fundamentals* (Third., p. 435). Lawrence Erlbaum Associates. Retrieved from <http://www.amazon.ca/exec/obidos/redirect?tag=citeulike09-20&path=ASIN/080582281X>

Ghahramani, Z. (1995). *Computation and Psychophysics of Sensorimotor Integration*. Computer. University of Pennsylvania. Retrieved from <http://citeseerx.ist.psu.edu/viewdoc/download?doi=10.1.1.13.6653&rep=rep1&type=pdf>

Ghez, C., & Krakauer, J. (2000). The organization of movement. In E R Kandel, J. H. Schwartz, & T. M. Jessell (Eds.), *Principles of Neural Science* (Fourth., pp. 652-673). McGraw-Hill.

Gibb, R. W. (2007). Visual spatial disorientation: revisiting the black hole illusion. *Aviation space and environmental medicine*, 78(8), 801-808. Retrieved from <http://www.ncbi.nlm.nih.gov/pubmed/17760289>

Gienger, M., Janssen, H., & Goerick, C. (2005). Task-oriented whole body motion for humanoid robots. *Proceedings of the 5th IEEE/RAS International Conference on Humanoid Robots* (pp. 238-244). Tsukuba, Japan: IEEE. doi:10.1109/ICHR.2005.1573574

Gillingham, K. K., & Previc, F. H. (1993). *Spatial orientation in flight* (p. 138).

Goldstein, E. B. (2009). *Sensation and perception*. (Cengage Learning, Ed.) (Eighth., p. 459). Wadsworth Pub Co.

Gorce, P., Vanel, O., & Ribreau, C. (1995). Equilibrium study of "human" robot. *1995 IEEE International Conference on Systems, Man and Cybernetics. Intelligent Systems for the 21st Century* (pp. 1309-1314). Vancouver, BC , Canada: IEEE. doi:10.1109/ICSMC.1995.537953

- Gorce, Philippe, & Vanel, O. (1997). Behaviour synthesis of the erect stance for a biped control. *Journal of Intelligent and Robotic Systems*, 18(2), 127-145. doi:10.1023/A:1007990219631
- Granit, R., & Burke, R. E. (1973). The control of movement and posture. *Brain Research*, 53(1), 1-28. Wadsworth Publishing Co. doi:10.1016/0006-8993(73)90763-4
- Grigsby, S. S., & Tsou, B. H. (1994). Visual processing and partial-overlap head-mounted displays. *Journal of the Society for Information Display*, 2(2), 69-74. Society for Information Display. Retrieved from <http://cat.inist.fr/?aModele=afficheN&cpsidt=3485630>
- Groves, P. D. (2008). *Principles of GNSS, inertial, and multisensor integrated navigation systems. Technology* (Vol. 9, p. 505). Norwood, MA, USA: Artech House.
- Guedry, F. E. J. (1974). Psychophysics of vestibular sensation. In H. H. Kornhuber (Ed.), *Handbook of sensory physiology. The vestibular system* (Vol. 2, pp. 3-154). New York, NY, USA: Springer-Verlag.
- Hain, T. C., & Helminski, J. O. (2000). Anatomy and physiology of the normal vestibular system. In S. J. Herdman (Ed.), *Vestibular Rehabilitation* (2nd Editio., pp. 2-17). Philadelphia: FA Davis Company.
- Hartmann, F. (1972). Resonance magnetometers. *IEEE Transactions on Magnetics*, 8(1), 66 - 75. doi:10.1109/TMAG.1972.1067262
- Harvey, I., Husbands, P., & Cliff, D. (1992). Evolutionary robotics. In B. Siciliano & O. Khatib (Eds.), *Adaptative Behaviour* (Vol. 10, p. 1611). Springer. Retrieved from <http://sro.sussex.ac.uk/21989/>
- Hirose, M., Haikawa, Y., Takenaka, T., & Hirai, K. (2001). Development of humanoid robot ASIMO. *International Conference on Intelligent Robots and Systems - IROS* (Vol. 13, pp. 1-6). Maui: IEEE.
- Hodgins, J. K. (1991). Biped Gait Transitions. *Proceedings 1991 IEEE International Conference on Robotics and Automation* (pp. 2092-2097). IEEE. doi:10.1109/ROBOT.1991.131936
- Hodgins, J. K. (1994). Simulation of Human Running. *IEEE International Conference on Robotics and Automation* (Vol. 2, pp. 1320-1325). San Diego: IEEE. doi:10.1109/ROBOT.1994.351304
- Hoeman, R., & Van Der Vaart, J. C. (1978). *Vestibular models and thresholds of motion perception: Results of tests in a flight simulator* (p. 81). Delft: Delft University of Technology, Dept. of Aerospace Engineering. Retrieved from <http://repository.tudelft.nl/assets/uuid:72bb1e55-7304-459f-a47c-dae7984418e3/LR-265.pdf>
- Holland, J. H. (1992). *Adaptation in natural and artificial systems*. (J. H. Holland, Ed.) Ann Arbor MI University of Michigan Press (Vol. Ann Arbor, p. 228). Cambridge, MA, USA: MIT Press. Retrieved from <http://mitpress.mit.edu/catalog/item/default.asp?ttype=2&tid=7593>

Hong, Y. D., Kim, Y. H., & Kim, J. H. (2009). Evolutionary optimized footstep planning for humanoid robot. *2009 IEEE International Symposium on Computational Intelligence in Robotics and Automation - (CIRA)* (pp. 266-271). Daejon, Korea: IEEE. doi:10.1109/CIRA.2009.5423197

Horak, F B, & Macpherson, J. M. (2011). *Postural orientation and equilibrium. Supplement 29: Handbook of Physiology, Exercise: Regulation and Integration of Multiple Systems* (Online., pp. 255-292). Wiley-Blackwell. doi:10.1002/cphy.cp120107

Horak, F B, Nashner, L. M., & Diener, H. C. (1990). Postural strategies associated with somatosensory and vestibular loss. *Experimental Brain Research*, 82(1), 167-177. Retrieved from <http://www.springerlink.com/index/Q1G8P8295J01280Q.pdf>

Horak, Fay B. (2006). Postural orientation and equilibrium: what do we need to know about neural control of balance to prevent falls? *Age and Ageing*, 35(Supplement 2), ii7-ii11. doi:10.1093/ageing/afl077

Intel. (2008). Retrieved September 13, 2011, from <http://www.intel.com/products/processor/core2duo/index.htm?wapkw=core 2 duo>

Isotalo, E., Kapoula, Z., Feret, P.-H., Gauchon, K., Zamfirescu, F., & Gagey, P.-M. (2004). Monocular versus binocular vision in postural control. *Auris Nasus Larynx*, 31(1), 11-17. Retrieved from <http://www.ncbi.nlm.nih.gov/pubmed/15041048>

JR3. (2011). Retrieved September 1, 2011, from <http://www.jr3.com/>

Jacobs, R. A. (1999). Optimal integration of texture and motion cues to depth. *Vision Research*, 39(21), 3621-3629. Vision Research. Retrieved from <http://www.ncbi.nlm.nih.gov/pubmed/10746132>

Jang, J. S. R. (1993). ANFIS: adaptive-network-based fuzzy inference system. *IEEE Transactions On Systems Man And Cybernetics*, 23(3), 665-685. IEEE. doi:10.1109/21.256541

Jeka, J. J., & Lackner, J. R. (1994). Fingertip contact influences human postural control. *Experimental Brain Research*, 100(3), 495-502. doi:10.1007/BF00229188

Jones, G. M., & Young, L. R. (1976). Subjective detection of vertical acceleration: A velocity dependent response? *Acta otolaryngologica*, 85(1-2), 45-53. Informa UK Ltd UK. Retrieved from <http://informahealthcare.com/doi/abs/10.3109/00016487809121422>

Josin, G., Charney, D., & White, D. (1988). Robot control using neural networks. *Proceedings of the 1988 IEEE International Conference on Neural Networks* (pp. 625-631). San Diego, CA, USA: IEEE. doi:10.1109/ICNN.1988.23980

Kagami, S., Kitagawa, T., Nishiwaki, K., Sugihara, T., Inaba, M., & Inoue, H. (2002). A fast dynamically equilibrated walking trajectory generation method of humanoid robot. *Autonomous Robots*, 12(1), 71-82. Kluwer Academic Publishers. doi:10.1023/A:1013210909840

- Kajita, S., Kanehiro, F., Kaneko, K., Fujiwara, K., Harada, K., Yokoi, K., & Hirukawa, H. (2003). Biped walking pattern generation by using preview control of zero-moment point. *Proceedings of the 2003 IEEE International Conference on Robotics and Automation* (pp. 1620-1626). Taipei, Taiwan: IEEE. doi:10.1109/ROBOT.2003.1241826
- Kajita, S., Kanehiro, F., Kaneko, K., Yokoi, K., & Hirukawa, H. (2001). The 3D linear inverted pendulum mode: a simple modeling for a biped walking pattern generation. *Proceedings 2001 IEEE/RSJ International Conference on Intelligent Robots and Systems* (Vol. 1, pp. 239-246). Maui: IEEE. doi:10.1109/IROS.2001.973365
- Kajita, S., & Tani, K. (1995). Experimental study of biped dynamic walking in the linear inverted pendulum mode. *Proceedings of 1995 IEEE International Conference on Robotics and Automation* (pp. 2885-2891). Nagoya, Japan: IEEE. doi:10.1109/ROBOT.1995.525693
- Kajita, S., Yamaura, T., & Kobayashi, A. (1992). Dynamic walking control of a biped robot along a potential energy conserving orbit. *IEEE Transactions on Robotics and Automation*, 8(4), 431-438. IEEE. doi:10.1109/70.149940
- Kamm, K., Thelen, E., & Jensen, J. L. (1990). A dynamical systems approach to motor development. *Physical Therapy*, 70(12), 763-775. Retrieved from <http://www.ncbi.nlm.nih.gov/pubmed/2236220>
- Kandel, Eric R, Schwartz, J. H., & Jessell, T. M. (2000). *Principles of Neural Science*. (Eric R Kandel, J. H. Schwartz, & T. M. Jessell, Eds.) *Neurology* (Fifth., Vol. 3, p. 1414). McGraw-Hill. doi:10.1036/0838577016
- Kaneko, K., Harada, K., Kanehiro, F., Miyamori, G., & Akachi, K. (2008). Humanoid robot HRP-3. *Intelligent Robots and Systems 2008 IROS 2008 IEEE/RSJ International Conference on* (pp. 2471-2478). Nice: IEEE. doi:10.1109/IROS.2008.4650604
- Karlsson, A., & Frykberg, G. (2000). Correlations between force plate measures for assessment of balance. *Clinical Biomechanics*, 15(5), 365-369. Retrieved from <http://www.ncbi.nlm.nih.gov/pubmed/10758298>
- Kasabov, N. K., & Song, Q. S. Q. (2002). DENFIS: dynamic evolving neural-fuzzy inference system and its application for time-series prediction. *IEEE Transactions on Fuzzy Systems*, 10(2), 144-154. IEEE. doi:10.1109/91.995117
- Kato, I. (1973). The WABOT-1. *Bulletin of Science and Engineering Research Laboratory Waseda University special issue on WABOT*. Retrieved February 2, 2011, from [http://www.humanoid.waseda.ac.jp/booklet/kato\\_2.html](http://www.humanoid.waseda.ac.jp/booklet/kato_2.html)
- Kavounoudias, A., Roll, R., & Roll, J.-P. (2001). Foot sole and ankle muscle inputs contribute jointly to human erect posture regulation. *The Journal of Physiology*, 532(Pt 3), 869-878. Blackwell Science Inc. doi:10.1111/j.1469-7793.2001.0869e.x
- Kaynov, D. (2008). *Open Motion Control Architecture for Humanoid Robots*. Universidad Carlos III de Madrid. Retrieved from <http://hdl.handle.net/10016/5573>

- Kaynov, D., Souères, P., Pierro, P., & Balaguer, C. (2009). A practical decoupled stabilizer for joint-position controlled humanoid robots. *Proceedings 2009 IEEE/RSJ International Conference on Intelligent Robots and Systems* (pp. 3392-3397). St. Louis, MO, USA: IEEE. doi:10.1109/IROS.2009.5354431
- Kejonen, P. (2002). *Body Movements During Postural Stabilization. Medicine*. Cambridge University Press Cambridge. Retrieved from <http://herkules.oulu.fi/isbn9514267931/html/>
- Kelso, J. A. S., & Saltzman, E. L. (1982). Motor control: which themes do we orchestrate? *Behavioral and Brain Sciences*, 5, 554-557. doi:10.1017/S0140525X00013510
- Kent, J. L. (2010). *Psychedelic Information Theory: Shamanism in the Age of Reason. Review Literature And Arts Of The Americas* (First., p. 204). Seattle: PIT Press. Retrieved from <http://psychedelic-information-theory.com>
- Kiguchi, K., Watanabe, K., & Izumi, K. (2000). Application of multiple fuzzy-neuro force controllers in an unknown environment using genetic algorithms. *Proceedings of the 2000 IEEE International Conference on Robotics & Automation* (pp. 2106-2111). San Francisco, CA, USA: IEEE. doi:10.1109/ROBOT.2000.846340
- Kim, J.-Y., Park, I.-W., Lee, J., Kim, M.-S., Cho, B.-K., & Oh, J.-H. (2005). System Design and Dynamic Walking of Humanoid Robot KHR-2. *Proceedings of the 2005 IEEE International Conference on Robotics and Automation*, (April), 1431-1436. ieee. doi:10.1109/ROBOT.2005.1570316
- Kuo, A. D. (2007). The six determinants of gait and the inverted pendulum analogy: A dynamic walking perspective. *Human movement science*, 26(4), 617-56. doi:10.1016/j.humov.2007.04.003
- Kuo, A. D., Donelan, J. M., & Ruina, A. (2005). Energetic consequences of walking like an inverted pendulum: step-to-step transitions. *Exercise and sport sciences reviews*, 33(2), 88-97. Retrieved from <http://www.ncbi.nlm.nih.gov/pubmed/15821430>
- Latash, M. L., Krishnamoorthy, V., Scholz, J. P., & Zatsiorsky, V. M. (2005). Postural Synergies and Their Development. *Neural Plasticity*, 12(2-3), 119-130. Hindawi Publishing Corporation. doi:10.1155/NP.2005.119
- Lee, D. N., & Lishman, J. R. (1975). Visual proprioceptive control of stance. *Journal of Human Movement Studies*, 1(2), 87-95.
- Lee, S. H., & Goswami, A. (2009). The reaction mass pendulum (RMP) model for humanoid robot gait and balance control. In B. Choi (Ed.), *Humanoid Robots* (First., Vol. 71, pp. 169-186). InTech. Retrieved from [http://www.intechopen.com/books/humanoid\\_robots/the\\_reaction\\_mass\\_pendulum\\_rmp\\_model\\_for\\_humanoid\\_robot\\_gait\\_and\\_balance\\_control](http://www.intechopen.com/books/humanoid_robots/the_reaction_mass_pendulum_rmp_model_for_humanoid_robot_gait_and_balance_control)
- Leibowitz, H. W., Rodemer, C. S., & Dichgans, J. (1979). The independence of dynamic spatial orientation from luminance and refractive error. *Perception And Psychophysics*, 25(2), 75-79.

- Levine, W. S., Zajac, F. E., Belzer, M. R., & Zomlefer, M. R. (1983). Ankle controls that produce a maximal vertical jump when other joints are locked. *IEEE Transactions on Automatic Control*, 28(11), 1008-1016. doi:10.1109/TAC.1983.1103169
- Lippmann, R. P. (1989). Review of Neural Networks for Speech Recognition. *Neural Computation*, 1(1), 1-38. MIT. doi:10.1162/neco.1989.1.1.1
- Lorini, E., & Falcone, R. (2005). Modeling expectations in cognitive agents. In C. Castelfranchi, C. Balkenius, M. Butz, & A. Ortony (Eds.), *AAAI 2005 Fall Symposium From Reactive to Anticipatory Cognitive Embodied Systems* (pp. 114-121). Washington: AAAI Press.
- Macedo, L., Reisenzein, R., & Cardoso, A. (2004). Modeling forms of surprise in artificial agents: empirical and theoretical study of surprise functions. In K. Forbus, D. Gentner, & T. Regier (Eds.), *Proceedings of the 26th annual conference of the cognitive science society* (pp. 873-878). Chicago. Retrieved from <http://csjarchive.cogsci.rpi.edu/Proceedings/2004/CogSci04.pdf>
- Mahboobin, A., Beck, C. L., Moeinzadeh, M. H., & Loughlin, P. (2002). Analysis and validation of a human postural control model. *Proceedings of the 2002 American Control Conference* (pp. 4122-4128). Anchorage: IEEE. doi:10.1109/ACC.2002.1024576
- Makhoul, J. (1991). Pattern recognition properties of neural networks. In C. M. Bishop (Ed.), *Proceedings of the 1991 IEEE Workshop on Neural Networks for Signal Processing* (Vol. 92, p. 1642). Princeton, NJ, USA: Oxford University Press. doi:10.1109/NNSP.1991.239524
- Mamdani, E., & Assilian, S. (1975). An experiment in linguistic synthesis with a fuzzy logic controller. *International Journal of ManMachine Studies*, 7(1), 1-13. Elsevier. doi:10.1016/S0020-7373(75)80002-2
- Manctl. (2012). RGBDemo. Retrieved March 13, 2012, from <http://labs.manctl.com/rbgdemo/>
- Mann, M. D. (1997). The nervous system in action. Retrieved September 8, 2011, from <http://www.unmc.edu/physiology/Mann/index.html>
- Marcel, A. J. (1983). Conscious and unconscious perception: Experiments on visual masking and word recognition. *Cognitive Psychology*, 15(2), 197-237. Retrieved from <http://www.ncbi.nlm.nih.gov/pubmed/6617135>
- Marin, J. M., Pudlo, P., Robert, C. P., & Ryder, R. (2011). Approximate Bayesian computational methods. *Statistics and Computing*, 1, 1-26. doi:10.1007/s11222-011-9288-2
- Martin, J. P. (1967). *The basal ganglia and posture* (First., p. 152). Philadelphia: Lippincot.
- Martinez, S., Balaguer, C., Martin, R., Jardon, A., & Perez, C. (2011). Sensor Táctil de Tres Ejes.

- Massion, J. (1984). Postural changes accompanying voluntary movements. Normal and pathological aspects. *Human Neurobiology*, 2(4), 261-267. Retrieved from <http://view.ncbi.nlm.nih.gov/pubmed/6715210>
- Massion, J. (1998). Postural control systems in developmental perspective. *Neuroscience and Biobehavioral Reviews*, 22(4), 465-472. Retrieved from <http://www.ncbi.nlm.nih.gov/pubmed/9595556>
- Maurer, C., Mergner, T., Bolha, B., & Hlavacka, F. (2001). Human balance control during cutaneous stimulation of the plantar soles. *Neuroscience Letters*, 302(1), 45-48. Retrieved from <http://www.ncbi.nlm.nih.gov/pubmed/11278108>
- McCollum, G., & Leen, T. K. (1989). Form and exploration of mechanical stability limits in erect stance. *Journal of Motor Behavior*, 21(3), 225-244. Heldref. Retrieved from <http://cat.inist.fr/?aModele=afficheN&cpsidt=6611470>
- Mendel, J. M. (1995). Fuzzy logic systems for engineering: a tutorial. *Proceedings of the IEEE*, 83(3), 345-377. IEEE. doi:10.1109/5.364485
- Merfeld, D. M., Zupan, L., & Peterka, R. J. (1999). Humans use internal models to estimate gravity and linear acceleration. *Nature*, 398(6728), 615-8. MACMILLAN MAGAZINES LTD. doi:10.1038/19303
- Mergner, T., & Glasauer, S. (1999). A simple model of vestibular canal-otolith signal fusion. *Annals Of The New York Academy Of Sciences*, 871(Otolith function in spatial orientation and movement), 430-434. John Wiley & Sons. Retrieved from <http://www3.interscience.wiley.com/journal/119081968/abstract>
- Merkle, R. C. (1988). How Many Bytes in Human Memory? *Foresight Update* 4. Retrieved from <http://www.merkle.com/humanMemory.html>
- Merkle, R. C. (1989). Energy limits to the computational power of the human brain. *Foresight Update* 6. Retrieved from <http://www.merkle.com/brainLimits.html>
- Meyer, J. R. (2006). Elements of Behavior. Retrieved from <http://www.cals.ncsu.edu/course/ent425/tutorial/Behavior/index.html>
- Meyer, W. U., Reisenzein, R., & Schützwohl, A. (1997). Toward a process analysis of emotions: The case of surprise. *Motivation and Emotion*, 21(3), 251-274. doi:10.1023/A:1024422330338
- Mihajlovic, V., & Petkovic, M. (2001). *Dynamic bayesian networks: A state of the art*. (U. of T. Centre for Telematics and Information Technology, Ed.) (p. 37). Twente. Retrieved from <http://doc.utwente.nl/36632/1/0000006a.pdf>
- Mittelstaedt, M. L., & Mittelstaedt, H. (2001). Idiothetic navigation in humans: estimation of path length. *Experimental Brain Research*, 139(3), 318-332. doi:10.1007/s002210100735
- Monje, C. A., Martinez, S., Jardon, A., Pierro, P., Balaguer, C., & Muñoz, D. (2011). Full-Size humanoid robot TEO: Design attending mechanical robustness and energy consumption. *Proceedings of the 2011 IEEE/RAS International*

*Conference on Humanoid Robots* (pp. 325-330). Bled: IEEE. doi:978-1-61284-868-6/11

Monje, C. A., Pierro, P., & Balaguer, C. (2009a). Pose control of the humanoid robot RH-1 for mobile manipulation. *International Conference on Advanced Robotics - ICAR* (pp. 1-6). Munich: IEEE. Retrieved from <http://ieeexplore.ieee.org/ielx5/5166725/5174665/05174765.pdf?tp=&arnumber=5174765&isnumber=5174665>

Monje, C. A., Pierro, P., & Balaguer, C. (2009b). Humanoid robot RH-1 for collaborative tasks: a control architecture for human-robot cooperation. *Applied Bionics and Biomechanics*, 5(4), 225-234. Taylor and Francis. doi:10.1080/11762320902789863

Nagata, T., Fukuoka, Y., Ishida, A., & Minamitani, H. (2001). Analysis of role of vision in human upright posture control. *Proceedings of the 23rd Annual International Conference of the IEEE Engineering in Medicine and Biology Society* (Vol. 2, pp. 1155-1158). Istanbul, Turkey: IEEE. doi:10.1109/IEMBS.2001.1020396

Nashner, L. M. (1985). Strategies for organization of human posture. In M. Igarashi & O. F. Black (Eds.), *Vestibular and Visual Control of Posture and Locomotor Equilibrium* (pp. 135-150). Houston: Karger Pub.

Nashner, L. M. (1993). Computerized dynamic posturography. In P. J. Gary, W. N. Craig, & M. K. Jack (Eds.), *Handbook of Balance Function Testing* (pp. 280-334). San Diego: Mosby.

Nashner, L. M., & Berthoz, A. (1978). Visual contribution to rapid motor responses during postural control. *Brain Research*, 150(2), 403-407. Retrieved from <http://www.ncbi.nlm.nih.gov/pubmed/678978>

Nashner, L. M., & McCollum, G. (1985). The organization of human postural movements: A formal basis and experimental synthesis. *Behavioral and Brain Sciences*, 8(01), 135-172. doi:10.1017/S0140525X00020008

Nawrot, M., & Sekuler, R. (1990). Assimilation and contrast in motion perception: explorations in cooperativity. *Vision Research*, 30(10), 1439. doi:10.1016/0042-6989(90)90025-G

Nishiwaki, K., Murakami, Y., Kagami, S., Kuniyoshi, Y., Inaba, M., & Inoue, H. (2002). A six-axis force sensor with parallel support mechanism to measure the ground reaction force of humanoid robot. *Proceedings of the 2002 IEEE International Conference on Robotics and Automation* (pp. 2277-2282). Washington, DC, USA: IEEE. doi:10.1109/ROBOT.2002.1013571

Oh, J.-H., Hanson, D., Kim, W.-S., Han, I. Y., Kim, J.-Y., & Park, I.-W. (2006). Design of Android type Humanoid Robot Albert HUBO. *Proceedings of the IEEE/RSJ International Conference on Intelligent Robots and Systems* (pp. 1428-1433). IEEE. doi:10.1109/IROS.2006.281935

Oman, C. M., & Young, L. R. (1969). Model for vestibular adaptation to horizontal rotation. *Aerospace Medicine*, 40(10), 1076-1080.

OpenKinect. (2012). Retrieved January 18, 2012, from [http://openkinect.org/wiki/Main\\_Page](http://openkinect.org/wiki/Main_Page)

Ortony, A., & Partridge, D. (1987). Surprisingness and expectation failure: what's the difference? In J. P. McDermott (Ed.), *Proceedings of the 10th International joint conference on Artificial intelligence-Volume 1* (pp. 106-108). Milan: Morgan Kaufmann Publishers.

Patane, F., Laschi, C., Miwa, H., Guglielmelli, E., Dario, P., & Takanishi, A. (2004). Design and development of a biologically-inspired artificial vestibular system for robot heads. *Proceedings 2004 IEEE/RSJ International Conference on Intelligent Robots and Systems* (pp. 1317-1322). Sendai, Japan: IEEE. doi:10.1109/IROS.2004.1389578

Paulus, W. M., Straube, A., & Brandt, T. H. (1984). Visual estabilization of posture. *Brain*, 107(4), 1143-1163. doi:10.1093/brain/107.4.1143

Pazul, K. (1999). *Controller Area Network (CAN) Basics. Technology* (Vol. 1939, p. 9). Retrieved from [http://moderncontroltechnology.com/docs/Engineering\\_Topics/CAN/AN713\\_Basics\\_00713a.pdf](http://moderncontroltechnology.com/docs/Engineering_Topics/CAN/AN713_Basics_00713a.pdf)

Pearn, J. (1999). Artificial Brains - The quest to build sentient machines. Retrieved April 18, 2012, from <http://www.artificialbrains.com/>

Peterka, R. J., Manor, B., Costa, M. D., Hu, K., Newton, E., Starobinets, O., Kang, H. G., et al. (2002). Sensorimotor integration in human postural control. *Journal of Neurophysiology*, 88(3), 1097-1118. Retrieved from <http://jn.physiology.org/content/88/3/1097.full.pdf>

Pierro, P., Monje, C. A., & Balaguer, C. (2008). Modelling and control of the humanoid robot RH-1 for collaborative tasks. *Proceedings of the 8th IEEE/RAS International Conference on Humanoid Robots* (pp. 125-131). Daejon: IEEE. doi:10.1109/ICHR.2008.4755942

Pierro, P., Monje, C. A., & Balaguer, C. (2009). The virtual COM joints approach for whole-body RH-1 motion. *Proceedings of the 18th IEEE International Symposium on Robot and Human Interactive Communication* (pp. 285-290). Toyama: IEEE. doi:10.1109/ROMAN.2009.5326259

Pollock, A. S., Durward, B. R., Rowe, P. J., & Paul, J. P. (2000). What is balance? *Clinical Rehabilitation*, 14(4), 402-406. Retrieved from <http://www.ncbi.nlm.nih.gov/pubmed/10945424>

Popovic, M., Goswami, A., & Herr, H. (2005). Ground reference points in legged locomotion: Definitions, biological trajectories and control implications. *The International Journal of Robotics Research*, 24(12), 1013-1032. doi:10.5772/4686

Previc, F., & Ercoline, W. (2004). *Spatial disorientation in aviation*. (P. Zarchan, Ed.) *Spatial disorientation in aviation* (First., p. 555). American Institute of Aeronautics and Astronautics, Inc.

Price, K. V., Storn, R. M., & Lampinen, J. A. (2005). *Differential Evolution: A Practical Approach to Global Optimization (Natural Computing Series)*. New York (First.,

- Vol. 28, p. 558). Secaucus, NJ, USA: Springer-Verlag New York, Inc. Retrieved from [http://books.google.com/books?hl=en&lr=&id=YRsq-PzOkAAC&oi=fnd&pg=PA1&dq>New+optimization+techniques+in+engineering&ots=8mtiDL8MHm&sig=Xkhwet\\_6-0JvTAi6Y-411gb4tY8](http://books.google.com/books?hl=en&lr=&id=YRsq-PzOkAAC&oi=fnd&pg=PA1&dq>New+optimization+techniques+in+engineering&ots=8mtiDL8MHm&sig=Xkhwet_6-0JvTAi6Y-411gb4tY8)
- Primdahl, F. (2002). The fluxgate magnetometer. *Journal of Physics E Scientific Instruments*, 12(4), 1-9. Institute of Physics Publishing. doi:10.1109/TIM.1978.4314723
- Purves, D., Brannon, E. M., Cabeza, R., Huettel, S. A., LaBar, K. S., Platt, M. L., & Woldorff, M. (2008). *Principles of cognitive neuroscience*. Appleton Lange Norwalk Connecticut (Vol. 83, p. 757). Sunderland, MA, USA: Sinauer Associates. doi:10.1086/592635
- Quek, C., Wahab, A., & Aarit, S. (2000). POP-Yager: A novel self-organizing fuzzy neural network based on the Yager inference. In B. Bosacchi, D. B. Fogel, & J. C. Bezdek (Eds.), *Proceedings of SPIE The International Society for Optical Engineering* (Vol. 4120, pp. 14-25). Society of Photo-Optical Instrumentation Engineers. doi:10.1117/12.403624
- Ra, S., Park, G., Kim, C., & You, B.-J. (2008). PCA-based genetic operator for evolving movements of humanoid robot. *2008 IEEE Congress on Evolutionary Computation (IEEE World Congress on Computational Intelligence)* (pp. 1219-1225). Hong Kong: IEEE. doi:10.1109/CEC.2008.4630952
- Raiert, M. H. (1986). Running with symmetry. *International Journal of Robotics Research*, 5(4), 3-19. Thousand Oaks, CA, USA: Sage Publications, Inc. doi:10.1177/027836498600500401
- Ribot-Ciscar, E., Bergenheim, M., Albert, F., & Roll, J.-P. (2003). Proprioceptive population coding of limb position in humans. *Experimental Brain Research*, 149(4), 512-519. Retrieved from <http://www.ncbi.nlm.nih.gov/pubmed/12677332>
- Rogers, M. W., Wardman, D. L., Lord, S. R., & Fitzpatrick, R. C. (2001). Passive tactile sensory input improves stability during standing. *Experimental Brain Research*, 136(4), 514-522. doi:10.1007/s002210000615
- Rojas, R. (1996). Neural Networks. A Systematic Introduction. (Springer-Verlag, Ed.) *Neural Networks*, 7(1), 509. Springer. doi:10.1016/S0893-6080(11)00301-7
- Roll, R., Kavounoudias, A., & Roll, J.-P. (2002). Cutaneous afferents from human plantar sole contribute to body posture awareness. *NeuroReport*, 13(15), 1957-1961. Retrieved from <http://www.ncbi.nlm.nih.gov/pubmed/12395099>
- Rosheim, M. E. (1994). *Robot evolution: the development of anthrobotics* (First., p. 423). Hoboken: Wiley-Interscience.
- Rothwell, J., & Lennon, S. (1994). Control of Human Voluntary Movement. *Physiotherapy*, 80(12), 869. doi:10.1016/S0031-9406(10)60176-9
- Ruina, A., & Pratap, R. (2010). *Introduction to statics and dynamics*. Power (p. 1033). Oxford University Press.

- Safiotti, A. (1997). Fuzzy logic in autonomous robotics: behavior coordination. *Proceedings of 6th International Fuzzy Systems Conference*, 1(july), 573-578. Ieee. doi:10.1109/FUZZY.1997.616430
- Seifert, R. (2001). Gigabit Ethernet. *Proceedings of the 26th Annual IEEE International Conference on Local Computer Networks (LCN'01)* (First., Vol. 00, p. 3). Tampa, FL, USA: IEEE. doi:10.1109/LCN.2001.10018
- Sensr. (2011). *Practical guide to accelerometers* (pp. 1-3). Elkader: Sensr. Retrieved from <http://www.sensr.com/pdf/practical-guide-to-accelerometers.pdf>
- Sherrington, C. S. (1907). The integrative action of the nervous system. *Nature*, 76(1962), 122-122. Yale University Press. doi:10.1038/076122a0
- Shumway-Cook, A., & Woollacott, M. (2000). *Motor control: Theory and practical applications* (Second., p. 614). Lippincott Williams & Wilkins.
- Si, X., Angelaki, D. E., & Dickman, J. D. (1997). Response properties of pigeon otolith afferents to linear acceleration. *Experimental Brain Research*, 117(2), 242-250. doi:10.1007/s002210050219
- Sipes, W. E., & Lessard, C. S. (1999). Spatial disorientation- A survey of incidence. *Proceedings of the 10th International Symposium on Aviation Psychology* (pp. 910-915). Columbus, OH, USA.
- Slijper, H., & Latash, M. (2000). The effects of instability and additional hand support on anticipatory postural adjustments in leg, trunk, and arm muscles during standing. *Experimental Brain Research*, 135(1), 81-93. doi:10.1007/s002210000492
- Smith, G., & Atchison, D. A. (1997). *The eye and visual optical instruments* (First., p. 828). Cambridge University Press. doi:10.1017/CBO9780511609541
- Song, K. T., & Sheen, L. H. (2000). Heuristic fuzzy-neuro network and its application to reactive navigation of a mobile robot. *Fuzzy Sets and Systems*, 110(3), 331-340. Elsevier Sci B.V. doi:10.1016/S0165-0114(97)00401-6
- Spirduso, W. W., Francis, K. L., & Macrae, P. G. (1995). *Physical dimensions of aging* (Second., p. 374). Human Kinetics.
- Spitz, D. L. (2011). *A computational model of surprise*. Worcester Polytechnic Institute.
- Stapleford, R. L. (1968). Multimodality pilot model for visual and motion cues. *Proceedings of 4th Annual NASA-University Conference on Manual Control (NASA SP-192)* (pp. 47-56). Ann Arbor, MI, USA: National Aeronautics and Space Administration, Office of Technology Utilization, Scientific and Technical Information Division. Retrieved from [http://www.archive.org/details/nasa\\_techdoc\\_19700005576](http://www.archive.org/details/nasa_techdoc_19700005576)
- Stephens, B. (2007). Integral control of humanoid balance. *Proceedings 2007 IEEE/RSJ International Conference on Intelligent Robots and Systems* (pp. 4020-4027). San Diego, CA, USA: IEEE. doi:10.1109/IROS.2007.4399407

Su, J., Zhang, H., Ling, C. X., & Matwin, S. (2008). Discriminative parameter learning for Bayesian networks. *Proceedings of the 25th International Conference on Machine Learning* (pp. 1016 - 1023). Helsinki: ACM Press. doi:10.1145/1390156.1390284

Sugihara, T., & Nakamura, Y. (2003). Variable impedance inverted pendulum model control for a seamless contact phase transition on humanoid robot. *Proceedings of the 2003 IEEE/RAS International Conference on Humanoid Robots* (pp. 51-56). Karlsruhe & Munich: IEEE. doi:10.1109/ROBOT.2003.1241572

Sugihara, T., Nakamura, Y., & Inoue, H. (2002). Real-time humanoid motion generation through ZMP manipulation based on inverted pendulum control. *Proceedings 2002 IEEE International Conference on Robotics and Automation* (Vol. 2, pp. 1404-1409). Washington, DC, USA: IEEE. doi:10.1109/ROBOT.2002.1014740

Sun, H. J., Campos, J. L., & Chan, G. S. W. (2004). Multisensory integration in the estimation of relative path length. *Experimental Brain Research*, 154(2), 246-254(9). doi:10.1007/s00221-003-1652-9

Takagi, H. (1997). Introduction to fuzzy systems, neural networks, and genetic algorithms. In D. Ruan (Ed.), *Intelligent Hybrid Systems: Fuzzy Logic, Neural Networks, and Genetic Algorithms* (First., pp. 1-33). Norwell, MA, USA: Kluwer Academic Publishers. Retrieved from <http://www.teleamerica.net/reference/Software/IntroToFuzzySystemsNuralNetsGeneticAlgorithms.pdf>

Takagi, T., & Sugeno, M. (1985). Fuzzy identification of systems and its applications to modeling and control. *IEEE Transactions On Systems Man And Cybernetics*, 15(1), 116-132. Institute of Electrical and Electronics Engineers. Retrieved from <http://takagiken.com/takagi-sugeno-modeling.pdf>

Takanishi, A., Takeya, T., Karaki, H., & Kato, I. (1990). A control method for dynamic biped walking under unknown external force. *IEEE International Workshop on Intelligent Robots and Systems Towards a New Frontier of Applications* (Vol. 2, pp. 795-801). Ibaraki: IEEE. doi:10.1109/IROS.1990.262498

Ting, L. H. (2007). Dimensional reduction in sensorimotor systems: a framework for understanding muscle coordination of posture. (P. Cisek, T. Drew, & J. F. Kalaska, Eds.) *Progress in Brain Research*, 165, 299–321. Elsevier. doi:10.1016/S0079-6123(06)65019-X

Ting, L. H., & McKay, J. L. (2007). Neuromechanics of muscle synergies for posture and movement. *Current opinion in neurobiology*, 17(6), 622-8. doi:10.1016/j.conb.2008.01.002

Tokumaru, O., Kaida, K., Ashida, H., Mizumoto, C., & Tatsuno, J. (1998). Visual influence on the magnitude of somatogravitational illusion evoked on advanced spatial disorientation demonstrator. *Aviation space and environmental medicine*, 69(2), 111-116.

Travis, R. C. (1945). An experimental analysis of dynamic and static equilibrium. *Journal of Experimental Psychology*, 35(3), 216-234. doi:10.1037/h0059788

Tung, W. L., & Quek, C. (2010). eFSM - A Novel Online Neural-Fuzzy Semantic Memory Model. *IEEE Transactions on Neural Networks*, 21(1), 136-57. doi:10.1109/TNN.2009.2035116

Tzafestas, S. (1995). Neural networks in robotics: state of the art. *Proceedings of the IEEE International Symposium on Industrial Electronics (ISIE '95)* (pp. 12-20). Athens, Greece: IEEE. doi:10.1109/ISIE.1995.497311

Vallbo, A. B., & Johansson, R. S. (1984). Properties of cutaneous mechanoreceptors in the human hand related to touch sensation. *Human Neurobiology*, 3(1), 3-14. Retrieved from <http://www.ncbi.nlm.nih.gov/pubmed/6330008>

Van Asten, W. N., Gielen, C. C., & Van Der Gon, J. J. (1988). Postural movements induced by rotations of visual scenes. *Journal of the Optical Society of America A Optics and image science*, 5(10), 1781-1789. doi:10.1364/JOSAA.5.001781

Van Beers, R. J., Sittig, A. C., & Denier Van Der Gon, J. J. (1999). Integration of proprioceptive and visual position-information. *Journal of Neurophysiology*, 81(3), 1355-1364. Retrieved from <http://eprints.ucl.ac.uk/4458/>

Van Der Helm, F. C. T., & Rozendaal, L. A. (2000). Musculoskeletal systems with intrinsic and proprioceptive feedback. In J. M. Winters & P. Crago (Eds.), *Biomechanics and neural control of posture and movement* (First., pp. 164-174). New York, NY, USA: Springer-Verlag. Retrieved from <http://e.guigon.free.fr/rsc/incoll/vanderHelmRozendaal00.pdf>

Veltink, P. H., Luinge, H. J., Kooi, B. J., Baten, C. T. M., & Slycke, P. (2001). The artificial vestibular system-design of a tri-axial inertial sensor system and its application in the study of human movement. *Proceedings of the Symposium of the International Society for Postural and Gait Research (ISPG 2001)* (pp. 1-4). Maastrich, The Netherlands: ISPG. Retrieved from <http://www.xsens.us/images/stories/PDF/ISPG2001.pdf>

Vincent, J. F. V., Bogatyreva, O. A., Bogatyrev, N. R., Bowyer, A., & Pahl, A.-K. (2006). Biomimetics: its practice and theory. *Journal of the Royal Society Interface the Royal Society*, 3(9), 471-482. The Royal Society. doi:10.1098/rsif.2006.0127

Vukobratovic, M., & Borovac, B. (2004). Zero-moment point — thirty five years of its life. *International Journal of Humanoid Robotics*, 1(1), 157-173. Citeseer. doi:10.1142/S0219843604000083

Vukobratovic, M., Frank, A. A., & Juricic, D. (1970). On the stability of biped locomotion. *IEEE Transactions on Biomedical Engineering*, 17(1), 25-36. IEEE. doi:10.1109/TBME.1970.4502681

Vukobratović, M., Hugh, M., Borovac, B., Raković, M., Popovic, M., Hofmann, A., Jovanovic, M., et al. (2008). Biological principles of control selection for a humanoid robot's dynamic balance preservation. *International Journal of Humanoid Robotics (IJHR)*, 5(4), 639-678. doi:10.1142/S0219843608001601

Welch, R. B., Widawski, M. H., Harrington, J., & Warren, D. H. (1979). An examination of the relationship between visual capture and prism adaptation. *Perception Psychophysics*, 25(2), 126-132. doi:10.3758/BF03198798

Whiteside, T. C., Graybel, A., & Niven, J. I. (1965). Visual illusions of movement. *Brain: A journal of neurology*, 88, 193-210.

Winter, D. A. (1995). Human balance and posture control during standing and walking. *Gait Posture*, 3(4), 193-214. Elsevier. doi:10.1016/0966-6362(96)82849-9

Winter, D. A., Prince, F., Frank, J. S., Powell, C., & Zabjek, K. F. (1996). Unified theory regarding A/P and M/L balance in quiet stance. *Journal of Neurophysiology*, 75(6), 2334-2343. Am Physiological Soc. Retrieved from <http://www.ncbi.nlm.nih.gov/pubmed/8793746>

Xia, Z., Liu, L., Xiong, J., Yi, Q., & Chen, K. (2007). Design aspects and development of humanoid robot THBIP-2. *Robotica*, 26(01), 109-116. doi:10.1017/S0263574707003645

Xsens. (2009). *MTi and MTx User Manual and Technical Documentation* (p. 60). Enschede: Xsens Technologies B.V. Retrieved from <http://www.xsens.com/en/general/mti>

Zadeh, L. A. (1962). A critical view of our research in automatic control. *IREE Transactions on Automatic Control*, 7(3), 74-75. doi:10.1109/TAC.1962.1105445

Zadeh, L. A. (1965). Fuzzy sets. (R. R. Yager, S. Ovchinnikov, R. M. Tong, & H. T. Nguyen, Eds.) *Information and Control*, 8(3), 338-353. Prentice Hall PTR Upper Saddle River, NJ, USA. doi:10.1016/S0019-9958(65)90241-X

Zadeh, L. A. (1994). Fuzzy logic, neural networks, and soft computing. *Communications of the ACM*, 37(3), 77-84. doi:10.1145/175247.175255

Zhang, W., Huang, Q., Du, P., Li, J., & Li, K. (2005). Compliance control of a humanoid arm based on force feedback. *Proceedings of the 2005 IEEE International Conference on Information Acquisition* (pp. 528-531). doi:10.1109/ICIA.2005.1635145

Zilouchian, A., & Jamshidi, M. (Eds.). (2001). *Intelligent control systems using soft computing methodologies*. *Control Engineering* (First., p. 493). CRC Press. doi:10.1201/9781420058147

Čapek, K. (1923). *Rossum's Universal Robots*. (N. Playfair, P. Selver, & W. A. Landes, Eds.) (p. 58). Garden City, NY, USA: Doubleday, Page & Company.